Hans Sverre Smalø

# Modeling Molecular Properties of Interest for Streamer Studies

Thesis for the degree of Philosophiae Doctor

Trondheim, December 2010

Norwegian University of Science and Technology
Faculty of Natural Sciences and Technology
Department of Chemistry

**NTNU – Trondheim**
Norwegian University of
Science and Technology

**NTNU**
Norwegian University of Science and Technology

Thesis for the degree of Philosophiae Doctor

Faculty of Natural Sciences and Technology
Department of Chemistry



ISBN 978-82-471-2499-4 (printed ver.)
ISBN 978-82-471-2500-7 (electronic ver.)
ISSN 1503-8181

Doctoral theses at NTNU, 2010:25

Printed by NTNU-trykk

# Acknowlegements

I would like to thank all people working with me in these years. My supervisor Per-Olof Åstrand has been patient with me, and especially during the writing process. Øystein Hestad and Stian Ingebrigtsens experimental knowledge has been of invaluable importance. Without them my contact with the experimental community would have been limited, and this thesis would not have been the same. Please believe me when I say, I'm not an experimentalist. Further, I would like to thank Magnus Ringholm for his work in his master thesis. If you meet him someday, you will momentarily know I'm telling the truth when I say he is a person which is really enjoyable to work with.

I would like to thank Terje Bruvoll for funding prior to the thesis work, general support and for organizing the tea breaks, which are of tremendous importance for our group. In this respect, I'm also grateful for all the nice social events organized by my fellow PhD employees.

I would also like to thank my all friends, Torunn Stranden Davidsen, Andreas Westermoen, Eirik Mo for support whenever I needed it, Norvald H. Ryeng for his fantastic sense of humor, *akademisk radio klubb* for showing me the enjoyable side of life, Odne S. Burheim et. al. for trying to take care of my health, all my computer nerds available at irc answering any stupid question immediately, etc. etc.

My research was funded by the Research Council of Norway, via a strategic institute program at SINTEF Energy research. I am grateful for their economical support.

# Contents

# Summary

If an insulating material is stressed by sufficiently large electric field, a plasma channel may be created which destroys the materials insulating properties. The processes involved are complicated and the field of research pushes into the boundaries of the unknown. Attempting to understand the processes involved from a fundamental point of view reveals many problems, and maybe that is what makes this field so interesting.

Two of the properties of interest which can be calculated from standard quantum chemical methods is the polarizability and the ionization potential. Therefore it is these two properties which have been studied further.

The molecules first order response to an electric field is given by the polarizability, and thus is an important property when a material is stressed by an electric field. In addition, the interaction between a charged and a neutral molecule is given by the polarizability. In the two first works (paper 1 and 2) a model based on atomic parameters for the polarizability is given. The third work (paper 3) is an attempt to link the polarizability model to a force field which is capable of simulating a plasma phase, which contains both neutral and charged particles.

Ionization potential is the energy required to ionize a neutral system, and is the most important molecular descriptor for all ionization mechanisms. In paper 4 we use standard quantum mechanical software to calculate the ionization potential and results in good agreement to experimental values are obtained. It is realized that there are a lot of other interesting molecular properties which also could have been studied, but many of these are difficult to calculate. A discussion regarding some of these properties are given in paper 4.

In paper 5 the ionization potential and ionization mechanism are studied in greater detail. Specifically it is found that the ionization potential of a molecule change in an electric field, and that the reduction in ionization potential due to the field cannot be ignored when studying high-field phenomena.

# List of papers

- H. S. Smalø and P.-O. Åstrand and L. Jensen, *Nonmetallic electronegativity equalization and point-dipole interaction model including exchange interactions for molecular dipole moments and polarizabilities*, J. Chem. Phys. **131**, 044100, (2009)
- H. S. Smalø, Per-Olof Åstrand, A. Mayer, *Combined nonmetallic electronegativy equalization and point-dipole interaction model for the frequency-dependent polarizability*, J. Phys. Chem. Submitted
- H. S. Smalø and Per-Olof Åstrand, *Interaction model for the argon atom, argon cation and a free electron at moderate separation distances*, J. Chem. Phys. Submitted
- H. S. Smalø Per-Olof Åstrand and S. Ingebrigtsen *Calculation of Ionization Potentials and Electron Affinities for Molecules Relevant for Streamer Initiation and Propagation*, IEEE Trans. Dielect. Electr. Insul. **17** 733-741 (2010)
- H. S. Smalø, Ø. Hestad, S. Ingebrigtsen and Per-Olof Åstrand, *Field dependence on the molecular ionization potential and excitation energies compared to conductivity models for insulation materials at high electrical fields*, J. Appl. Phys. Submitted

**Not included in thesis**:

- S. Ingebrigtsen, H. S. Smalø, P.-O. Åstrand and L. E. Lundgaard *Effects of electron-attaching and electron releasing additives in liquid cyclohexane*, IEEE Trans. Dielect. Electr. Insul. **16** 1511, (2009).
- Ø. L. Hestad, S. Ingebrigtsen, H. S. Smalø, P.-O. Åstrand and L. E. Lundgaard, *Effects of N,N-dimethylaniline and trichloroethene on prebreakdown phenomena in liquid and solid n-tridecane*, IEEE Trans. Dielect. Electr. Insul. submitted

# Chapter 1

# Introduction

If an insulation material is stressed by a sufficiently large electric field, a plasma channel may be created which destroys the materials insulating properties. These plasma channels are known as streamers. If the streamer bridges the gap between two electrodes, a sudden increase in current is observed which indicates a dielectric breakdown. Thus it is of great interest to gain insight into the transition between liquid/solid phase and a plasma phase. To study these phenomena experimentally, a high voltage is often applied to a needle-plane geometry, and thus the electric field is highly inhomogeneous [1–5]. The main reason for using this geometry experimentally is that higher electric fields is easier to obtain if the field is not homogeneous. Inhomogeneous fields may also be more realistic in many situations. The electric field around a tiny piece of metal, injected into the insulating material by accident, is an example of an inhomogeneous field. Further, in an inhomogeneous field, the background electric field will decrease as the streamer propagates towards the other electrode, typically limiting streamer growth. When two parallel plane electrodes are used, the electric field is more or less homogeneous, and it is difficult to stop streamers from bridging the gap between the two electrodes.

In general inhomogeneous fields are needed to study pre-breakdown phenomena. However, using this needle plane geometry instead of two plane electrodes has the disadvantage that the electric field at any given point is dependent on the material properties, and especially the conductivity, which in general is field dependent. The electric field between two parallel plane electrodes is also dependent on the material properties of the medium, but to a smaller degree. Thus the magnitude of the electric field in a needle-plane geometry, is uncertain even if the applied voltage is known.

The system studied has multiple typical length scales. One typical length

scale is the distance between the needle and the plane typically being around a few millimeters. However, the most interesting physics/chemistry occurs around the tip of the electrode, or the tip of a growing plasma chancel, which can have a radius of the order of a few $\mu$m [1–7]. The smallest of these length scales are within the magnitude where typical molecular dynamic (MD) simulation could be applied (one $\mu$m might be somewhat large for MD simulations, but will be achievable in the future). The transition from a liquid to a plasma occurs in this region, and thus it is important to understand the details around the behavior of the molecules in this region. Questions to be answered are;

- How strong are the intermolecular forces. These forces determines the boiling point and other properties.
- What is the energy required to ionize a molecule and how can it be done?
- How does the neutral molecules interact with free electrons? What is the energy transfer between free electrons and neutral molecules? Can neutral molecules capture free electrons and create stable negative ions?

Molecular modeling is useful for this purpose . However, the electric field in this interesting area (which is obliviously important) is dependent on the charge distribution in the entire system, and the entire system would be too large for an MD simulation. In the future one may therefore envisage a model where molecular dynamics is applied to the most important areas, and a combination of regular fluid dynamics and electrostatics are applied to the other areas.

Streamers are said to propagate in different modes. In the first mode streamer growth is slow, while in the 4th mode streamers can have the speed of several hundred km per second [8]. The different modes are believed to be governed by different mechanisms. The higher modes can be achieved by, for example, the application of higher voltages. The results are also dependent on the time development of the applied voltage. A step voltage which have a long rise time will give different results than a step voltage with short rise time. The streamers originating from a negative electrode will be different than a streamer originating from a positive electrode. Thus the results are dependent on the polarity of the high-field electrode. One of the reasons why the results differs, is that extracting charge in the form of electrons from a metal electrode is easier than extracting electrons from the medium. In addition, the interpretation of experimental results for streamer

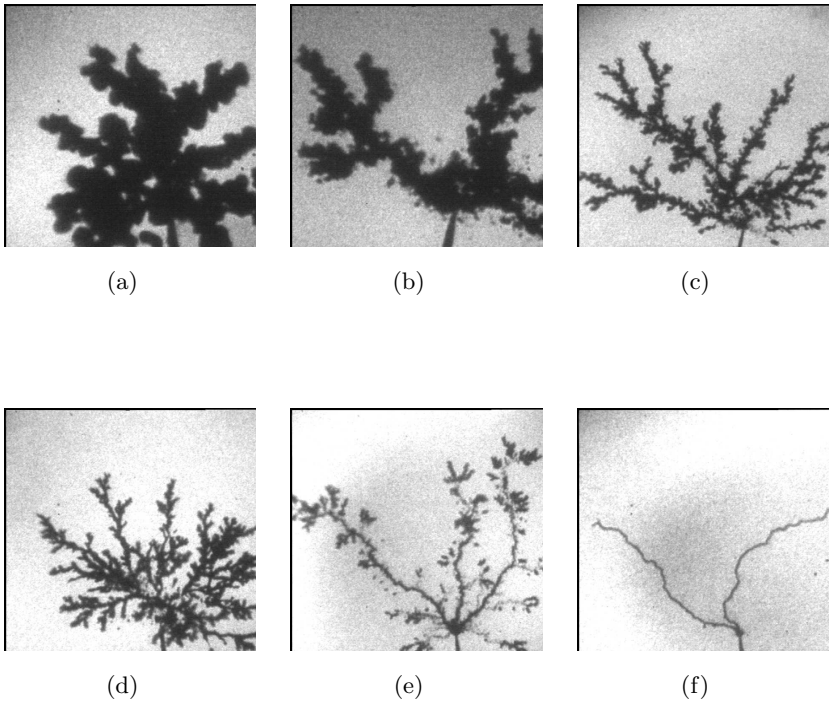


Figure 1.1: Typical pictures of streamers. All are taken from Ref. [9]; (a), (b) and (c) is taken from figure 2 while (d) (e) and (f) is taken from figure 6.

growth and propagation is difficult due to the highly stochastic nature of this phenomena.

Streamers comes in many different, irregular shapes. The shape of the streamer is highly dependent on the base material, additives and applied voltage. Some streamers are bush-like and other are more filamentary (see Figure 1.1 for typical examples). One reason for wanting a model on the molecular level is to understand the degree of branching, which is highly dependent on the chemical properties of the molecules involved. In macroscopic models, the streamer will typically grow spherically from the point needle with no branching, or like an extension of the needle. To understand branching and the highly stochastic nature of streamers, a model on the molecular level is needed.

The plasma channel is composed of neutral molecules, ions and free

electrons. The free electrons may either come from an electrode, or by ionization of a neutral molecule in the insulation. To be able to describe the system by MD simulation, the force field must be able to describe free electrons in addition to ions and neutral molecules.

Plasma models do exist [10], however these are typically for high temperatures, with a high degree of ionization and where electron and nucleus are in equilibrium. However, the plasma of interest here, is not caused by high temperature, but rather high electric fields, and the conditions are very different. Here, the degree of ionization is low. Based on spectroscopy analysis, it has been estimated that in typical streamers only about 0.1-1% of the molecules are ionized [11–13]. Thus, the most important interactions are those between ions/free electron and neutral molecules, and a plasma model which only takes into consideration singly ionized molecules should be a good approximation. In addition, since the electrons are much lighter than the heavy nucleus, electronic processes react much faster to an increase in electric field. In general an equilibrium between the free electrons and the ions/molecules cannot be expected. Lastly, since the transition between a liquid and a plasma phase is of interest, the model needs to be able to describe both phases.

The presented papers do not involve MD simulations of streamers, but the work should be read in the light of this goal. I hope to lay the fundamental building blocks which are required to develop a force field required to run MD simulations on streamers. It is especially interesting to combine the work here with the electron force field (eFF) [14] which is a force field where all electrons and nucleus are treated as classical particles. However, it must be clear that several important question are still unanswered, and a few years of development is probably required before any MD simulation of this type could be run. It shall also be noted that part of this work can be applied to force fields in general and thus has a wide range of applications beyond modeling streamers.

In the next section the quantum mechanical analogue to Newtons law is given. The main motivation behind discussing this equation is to understand in which cases Newtonian physics can be applied. Then a short introduction to different types of intermolecular forces is given. It is interesting to note that all interaction types; exchange, electrostatic, induction and dispersion forces, are of high importance in this study. At large separation distances, the models of interaction between molecules can, to a large extend also be applied to the interaction between a free electron (or another charged particle) and neutral molecule. The remaining question is how a molecule is ionized into a cation and a free electron, which is discussed in chapter 3.

Finally, presentation of papers, future work and a conclusion is given.

# Chapter 2

# Intermolecular forces

In all force fields, the basic idea is to replace the complicated quantum mechanics with a simpler model. Quantum mechanics is replaced with simple Newtonian physics, by calculating the force between the different particles. Thus, some accuracy is sacrificed to make large scale calculation involving millions of molecules possible. The goal is not only to describe the interaction between neutral molecules, but also include the interaction between charged systems in the same way. Therefore, an analogue to Newtons law of physics in quantum mechanics is examined, to understand when Newtonian physics can be applied.

In quantum mechanics (non-relativistic and without magnetic field) a Hamiltonian operator $\hat{H}$ may be written as

$$\hat{H} = \frac{\hat{p}^2}{2m} + V \tag{2.1}$$

where in atomic units[1] $\hat{p} = -i\partial/\partial x$ is the momentum operator, $m$ is the mass and $V$ is the potential. The Schrödinger equation may be written as

$$\hat{H}\psi = i\frac{\partial \psi}{\partial t} \tag{2.2}$$

where $\psi$ is the wavefunction. From the wavefunction, averages may be calculated by

$$\langle f \rangle = \int \psi^* \hat{f} \psi d\tau \tag{2.3}$$

where $f$ is some property and $\hat{f}$ is the corresponding operator. For a complete *introduction* to quantum mechanics and quantum chemistry the reader

[1] Atomic units (au) are defined by $|e| = 1$, $\hbar = 1$, $m_e = 1$, $1/4\pi\epsilon_0 = 1$. Energy in au is 1 hartree which is given by $E_h = m_e e^4/(4\pi\epsilon_o\hbar)^2 \approx 4.36 \times 10^{-18} J$.

is referred to Ref. [15] and [16]. Here it is just concluded that Ehrenfets theorem is obtained from Eqs. (2.2) and Eqs. (2.3) and can be written as [15]

$$\frac{d\langle p\rangle}{dt} = \langle -\nabla V\rangle \ . \tag{2.4}$$

This is an important equation, as it shows, that an analog to Newtons laws of physics can be obtained from Quantum Mechanics. Under the approximation that the average force, $\langle F(r)\rangle = \langle -\nabla V\rangle \approx F(\langle r\rangle)$, Eq. (2.4) is identical to Newtons law. In a one particle problem, this approximation is valid as long as the force is slowly varying over the volume spanned by the wavefunction.

The forces between the molecules can be calculated from quantum mechanics if the wavefunction is known. However, in practical application, simple models for the forces are used, and all such models include a set of parameters. A typical approach, is to use quantum mechanics to obtain the molecular properties, and thus use these properties to parametrize the model. This approach has been used in this work. An alternative is to find the parameters in the model by comparing to experimental results. One argument for using quantum mechanics instead of experimental results, is that a QM calculation can often be done faster and cheaper. Besides, the errors involved are often well documented, and it is easier to get a set of reference data where all data have the same level of accuracy.

The start point for most quantum chemistry approaches is the Hatree Fock equation [16]. In Hatree Fock theory the energy is found using the variation principle and a many electron wavefunction is written as a single determinant of one-particle wavefunctions. Further the one-particle wavefunction is expanded in terms of a basis functions. In practical applications the basis set is finite, but it is important that the basis set is large enough to describe the interesting region. Thus, when calculating properties where the *diffuse* region is of importance, a larger basis set is needed.

The Hatree Fock approximation generally gives fairly good total energies. However, to describe energy differences a better accuracy is desired. The Møller-Plesset or couple cluster approximations are a systematic improvement of the Hatree Fock solution [16]. Density functional theory (DFT) on the other hand can be seen as an ad-hoc modification of the Hatree Fock approximation. The benefit of using DFT is that it often gives good results at lower computational cost. However it is important to note that there exist many DFT functionals (version of DFT) and it is important to check the accuracy of the method for the property of interest. Since this work is not suppose to be a study in DFT, we try to apply standard, well known and well documented functionals in all our work.

However to apply Eq. (2.4) on large scale simulations, classical models for the different types of intermolecular forces are needed. As already mentioned, intermolecular forces can be grouped into, exchange, electrostatic, induction and dispersion forces.

## 2.1 Exchange

In many particle problems, the Pauli principle needs to be taken into account, and Eq. (2.4) becomes slightly more complicated to interpret. Examine a two electron wavefunction of the form

$$\psi(r_1, m_1, r_2, m_2) = N\left(\psi_1(r_1, m_1)\psi_2(r_2, m_2) - \psi_2(r_1, m_1)\psi_1(r_2, m_1)\right) \quad (2.5)$$

where $r_1$ and $r_2$ is the coordinate of particle one and two respectively, $m_1$ and $m_2$ is the spin (either + or -) of particle one and two respectively and $N$ is the norming constant. Let $\psi_1$ and $\psi_2$ describe two normalized functions, which are not necessarily orthogonal, and their overlap is given by

$$\int \psi_1^* \psi_2 d\tau = S \quad (2.6)$$

from which one finds the norming constant,

$$N = \frac{1}{\sqrt{2(1 - S^2)}} \, . \quad (2.7)$$

If $\psi_1(r, +) = 0$ and $\psi_2(r, -) = 0$ (or vice versa), the two particles have opposite spin and the overlap in Eq. (2.6) is automatically zero. The overlap $S$ is also zero at large separation distances, and in both these cases the regular $N = 1/\sqrt{2}$ is obtained. Thus $\psi_1$ and $\psi_2$ can be treated as independent states, and how they move can be determined by Eq. (2.4), by identifying $\psi_1$ as one classical particle and $\psi_2$ as another.

However if $\psi_1$ and $\psi_2$ describes particles with the same spin, $S$ is not zero and the normalizing constant diverges as $S \to 1$. In the case with two particles with the same spin, there is a large difference between the energy obtained using an antisymmetric wavefunction and the energy obtained using simpler product $\psi(r_1, r_2) = \psi_1(r_1)\psi_2(r_2)$. Effectively the antisymmetrization of the wavefunction leads to an increased energy which increases with increasing overlap $S$. In this work, exchange will be used as a term which includes all energy contributions which arises due to the Pauli principle and the anti-symmetrization of the wavefunction. However, it is confusing that in quantum chemistry the name exchange is used as the effect of the Pauli-principle on the electron-electron Coulomb repulsion only.

In quantum chemistry the other effects of the anti-symmetrization of the wavefunction is more or less trivial, and thus often not mentioned. However it must be clear that there is exchange on all energy contributions [17] and in a Newtonian model it is important that also these effects are included.

In interaction between two atoms or two molecules, exchange will be more difficult. However in the interaction between two closed shell systems, exchange will lead to a strong repulsive force at low separation distances. This is because no two electrons can be in the same electronic state and for for closed shell systems extra electrons are forced into a more energetic state. In force fields and MD simulation exchange between two closed shell systems is added by adding an potential with strong repulsion at low separation distances. For example, in the van der Waals forces the repulsion is modeled as proportional to $r^{-12}$.

Applied for the problem in this work, it is important to note that Eq. (2.4) means that not only molecules, but also free electrons move according to Newtonian Physics as long as the distance between the free electrons and molecules are large. Then the overlap between the electrons in the molecule and the free electron is small and the forces between them are varying slowly. At short separation distance it is more problematic. However Eq. (2.4) has been exploited in the electronic force field (eFF) [14]. By modeling the exchange between two electrons with a repulsive potential, the electrons are treated as classical particles. Similar model based on the propagation of quantum waves also exist [18].

However, treating free electrons with a fixed spin may cause problems. To illustrate this point, examine the case

$$\psi_1 = \psi_1(r, +) \tag{2.8}$$

and

$$\psi_2 = a_+\psi_2(r, +) \ + a_-\psi_2(r, -) \tag{2.9}$$

where $a_+^2 + a_-^2 = 1$. Then the overlap $S$ is give by $S = a_-S'$ where $S' = \int \psi_1(r, +)\psi_2(r, +)d\tau$. Under the assumption that $a_- \neq 0$, the combined antisymmetric wavefunction, in the limit $S' \to 0$, can be written as

$$\psi = \frac{1}{\sqrt{2}} \left(\psi_1(r_1, +)\psi_2(r_2, -) - \psi_1(r_2, +)\psi_2(r_1, -)\right) \tag{2.10}$$

and thus a singlet state is obtained and only the spin down part of $\psi_2$ survives. Since it is unlikely that two systems far apart are in the exact same spin state, the spin of a free electron change when it interacts with other systems.

In the quest of modeling a streamer, taking inspiration from the work done on intermolecular forces is helpful, as they may be formulated generally and thus have a wide range of use. Many of the models used for intermolecular forces can be applied to the study of the interaction between molecules and free electrons at large separation distances, and this especially apply to the electrostatic interactions and polarization.

## 2.2 Electrostatic interaction

At long separation distances, electrostatic interactions are usually dominant. In first order perturbation theory, the energy of a perturbed system is calculated using the wavefunction of the unperturbed system. Thus, the first order perturbation energy can be calculated by the electrostatic interaction between two static charge distributions, $\rho_A$ and $\rho_B$. For this purpose the multipole expansion may be applied

$$V^{elec} = \sum \frac{(-1)^m}{m!n!} M^{(m)}_{A,\alpha\beta\ldots} T^{(m+n)}_{AB,\alpha\beta\ldots} M^{(n)}_{B,\alpha\beta\ldots} \tag{2.11}$$

where $M^{(n)}$ are the multipole moments given by

$$M^{(m)}_{A,\alpha\beta\ldots} = \int \rho_a(r) \Pi_i^m r_{i\alpha_i} d\tau \tag{2.12}$$

and $T^{(n)}$ are the multipole interaction energies given by

$$T^{(n)} = \nabla^n R^{-1} \tag{2.13}$$

The zero-order multipole expansion is the charge, which for neutral molecules is zero, while the first order multipole expansion is the dipole moment, $\mu_\alpha$. Using quantum mechanics to find the unperturbed charge distributions, one can use Eq. (2.12) to calculate the multipole moments of the molecule. Note that only the lowest non-zero multipole moment is independent of the origin. Thus, for molecules with a non-zero dipole moment, the quadrupole moment is not independent of the origin. The total energy is independent of the choice of origin as long as the origin of the molecules used to calculate the multipole moments are the same as the origin between the two systems used to calculate $T^{(n)}$.

For charged systems, the charge (or zeroth order moment) gives the dominating interaction terms. For neutral molecules, the dipole moment is the first leading term (given that the dipole moment is not zero). Thus, at large separation distances, the electrostatic interaction is fairly simple.

However, when two molecules are close the multipole expansion may experience convergence problems [19], and this is obviously more problematic for larger molecules.

An attractive alternative is to assign multipoles to each individual atom. Thus obtaining atomic charges $q_I$ is one of the main concerns in molecular modeling. Sadly there is no unique way of obtaining atomic point charges $q_I$ from a charge distribution $\rho(r)$. Therefore there exist multiple schemes to calculate the charge on each atom. One of the most frequently used is the Mulliken charges [20], which can be written as

$$q_I = Z_I - \sum D_{ij} S_{ij} \tag{2.14}$$

where $Z_I$ is the nucleus charge, $D_{ij}$ is a density matrix element, $S_{ij}$ is the overlap of the basis function $i$ and $j$. The sum runs over all basis functions $j$ and over all basis functions $i$ associated with atom $I$. It has been demonstrated that these charges are highly dependent on the basis set, see for example [21]. It must also be clear that the point charges has one and only one objective, which is to reproduce the electrostatic interaction between two molecules. Mulikken charges indicate the value of the charges, but it is dangerous to use them as reference data, as they are not guaranteed to reproduce the molecular multipole moments.

It is important that the obtained atomic charges gives the correct molecular multipole moments, and of course especially the dipole moment. For a set of point charges the multipole moments can be written as

$$M^{(m)}_{A,\alpha\beta\ldots} = \sum q_I \Pi^m_i r_{i\alpha_i} \tag{2.15}$$

which can be compared to Eq. (2.12). In our work (paper 1) we have optimized the parameters of the model to reproduce the molecular dipole moments. However it is realized that using data for higher multipole moments might be necessary, as there might be many sets of charges which gives the same dipole moment.

In polar molecules which have a high dipole moment, electrostatic interaction are important. However, the multipole expansion is a general concept, and therefore may be applied to charged systems as well as neutral systems. High field phenomena of a polar medium are interesting in for example energy storage in capacitors, but insulating materials are made up of mostly non-polar molecules where the molecular dipole moment is zero. This is because if using polar systems the energy lost in the insulator will be to large. Therefore the induction and dispersion energy are more important than the electrostatic when modeling an insulating medium.

## 2.3 Induction energy (polarization)

In second order perturbation theory the energy is calculated by using the perturbed (to first order) wavefunction. In this case the charge distribution in a molecule may be modified by the presence of other molecules. The dipole moment of atom $I$ is modified by the presence of an electric field at the molecule $E_I$, which can be caused by another molecule or by an external electric field. Using a Taylor expansion of the electric field, the energy of a molecule in an electric field can be written as[2]

$$V = -\mu_\alpha E_\alpha + M^{(2)}_{\alpha\beta} E_{\alpha\beta} + \cdots + V^{self} \tag{2.16}$$

where $\alpha$ and $\beta$ indexes denotes the Cartesian coordinates, $E_{\alpha\beta} = \partial E_\alpha / \partial x_\beta$, $\mu$ is the dipole moment and $M^{(2)}$ is the quadrupole moment of the system. Here $V^{self}$ is the self interaction energy, which is the energy required to induce the multipole moments. It should be noted that Eq. (2.16) assumes a neutral system. For a charged system the monopole term $q^{tot} r_\alpha E_\alpha$ must be added (this energy is not independent of the choice of origin). The dipole moment is dependent on the electric field, and using a Taylor expansion it can be written as

$$\begin{aligned} \mu_\alpha &= \mu^0_\alpha + \alpha_{\alpha\beta} E_\beta + \frac{1}{2}\beta_{\alpha\beta\gamma} E_\gamma E_\beta + \frac{1}{6}\gamma_{\alpha\beta\gamma\delta} E_\delta E_\gamma E_\beta + \cdots \\ &\quad + A_{\alpha,\beta\gamma} E_{\beta\gamma} + \frac{1}{3} B_{\alpha\beta,\gamma\delta} E_{\gamma\delta} E_\beta + \cdots \\ &\quad + \cdots \end{aligned} \tag{2.17}$$

where $\mu^{(0)}_{I,\alpha}$ is the permanent dipole moment, $\alpha_{\alpha\beta}$ is the regular dipole-dipole polarization, $\beta_{\alpha\beta\gamma}$ is the first hyperpolarizability, $\gamma_{\alpha\beta\gamma\delta}$ is the second hyperpolarizzability, $A_{\alpha,\beta\gamma}$ is the dipole-quadrupole polarizability and $B_{\alpha\beta,\gamma\delta}$ is the dipole-quadrupole hyperpolarizability. Note that the coefficients of a corresponding Taylor expansion of $M^2$ would in general be dependent on the choice of origin. Likewise, the energy in an electric field is in general dependent on the choice of origin, but energy differences are not.

For the dipole-dipole polarizability, the self interaction energy cancels half the corresponding induction energy term, and to the lowest order the induction (or polarization) energy between two molecules $I$ and $J$ can be written as

$$V^{pol} = -\sum_I \frac{1}{2} \alpha^{mol}_{\alpha\beta} E_{I,\alpha} E_{I,\beta} \tag{2.18}$$

[2] using the Einsteins summing convention

Where $E_{I,\alpha}$ is the electric field at atom $I$. At large separation distances this is the main interaction between a charged and a neutral system. Thus, the polarizability, $\alpha$ of the neutral molecules are important.

The polarizability can be divided into two different types: The electronic polarization, which is the distortion of the electronic charge concentration, and polarization due to the movement of the nucleus. In the later the bond distances is tweaked due to the presence of an electric field. In our work (paper 1 and 2) we have concentrated on the electronic polarization.

In many force fields the polarizability is neglected, and the atomic charges are kept constant. In many situations this is a good approximation, however, if studying reactions of any kind, a different approach is needed, and including polarizability into the force field is important. Further, for obvious reasons, a force field capable of describing reactions cannot be based upon molecular parameters. In reactive force fields the atomic charges cannot be constant, and the charge needs to be able to move during the reaction. Even though the molecular polarizability in gas phase can be calculated fairly easily using quantum mechanics, it is beneficial to have a classical model which is capable of predicting the changes in the polarizability due to perturbation of either the molecule itself or or its surroundings.

Polarizability models can basically be grouped into two main categories, models based on the point dipole interaction (PDI) model [22–26], and models based on the electronegativity equalization model (EEM) [27–31]. In EEM charge is moved from one atom to another. Each atom $I$ is assigned an electronegativity, $\chi_I$, a hardness $\eta_I$ and a potential is written as

$$V = \sum \chi_I q_I + \eta_I q_I^2 + V_I^{ext} q_I \tag{2.19}$$

where $V_I^{ext}$ is an external potential at atom $I$, and the atomic charges are obtained by minimizing this potential (with a restriction that the total charge is zero). Thus in water the oxygen atom, with a higher electronegativity, will have a negative charge while the hydrogen will be positively charged. The charge transfer between atoms may either be due to different electronegativity between the atoms, or due to the presence of an external electric field. The first give permanent charges, while the second gives induced charges. EEM is applied in many force field [32–35], and among them the reactive force field Reax [36].

In the standard PDI model each atom is assigned a point dipole moment which interacts with an external electric field and the other point dipoles in the system,

$$V = \sum \alpha_I \mu_I^2 - \mu_I T_{IJ}^{(2)} \mu_J \tag{2.20}$$

where $\alpha_I$ is the isotropic polarization of atom $I$, and $T_{IJ}^{(2)}$ is the dipole-dipole interaction term. The standard PDI model give no permanent dipole moments.

The advantage of EEM is that it can also be used to describe the permanent charges, and EEM is necessary for a good description of metallic systems. However, the polarizability of EEM has been shown to scale as $N^3$ [37], which is not realistic for nonmetallic system. In paper one it is shown that the permanent dipole moment of a molecule with a polar end increases linearly with the size of the system in EEM. Thus using standard EEM for nonmetallic systems is extremely risky, as it is known that both the polarizability and the dipole moment scale incorrectly with the size of the system (see for example paper 1). Another drawback with EEM is that it cannot give any polarization out of the molecular plane of planar molecules. The PDI on the other hand works better for nonmetallic systems, and can better describe the polarization of planar molecules.

Thus both models have been used for different kinds of systems and purposes. In paper 1 the EEM and PDI model has been merged. To be able to do so, a nonmetallic extension of the EEM has been developed. An alternative formulation of a nonmetallic EEM model is the split charge model [38–42]. Except for a difference in formulation, there is no major difference between the split charge model and the model developed here. The biggest difference with our nonmetallic EEM model and the split charge model is a difference in design philosophy regarding parameters. The split charge model depends on a set of atom pair parameters, while our model is based purely on atomic parameters. A benefit of the model developed in paper one is that the way the model scales with the size of the system can be modeled using one single function. The split charge model is tuned by two independent parameters [37]

The interaction between a neutral and a charged system at long separation distance is dominated by the polarization energy. In paper 3 we study the interaction between argon, argon cation and free electrons. We show that the interactions at moderate separation distances may be modeled using simple models, and that the induction energy is indeed important. There are several reason for studying argon. The polarizability model developed in paper 1 is dependent on charge neutrality, while in a cation the total charge is equal to +1. To expand the polarizability model for charge systems, a model for placing the extra charge among the atoms are needed. In a mono atomic molecule this problem is avoided, since all the charge is centered around the single atom. This makes argon a particularly simple system to study. Further, argon has a reachable boiling point of -189.3$^0$C, and

streamer propagation studies in liquid argon have been performed [43, 44].

## 2.4 Frequency dependent polarizability

The frequency dependent polarizability of a system give the response to a time-dependent electric field, and is thus one of the fundamental properties in optics and construction of electronic devices. Streamers emit light [1, 8, 45], and the amount of emitted light is dependent on the medium and the mode of the streamer. Thus the study of frequency dependent polarizability might also be useful for the problem at hand.

For low frequencies, the Unsõld approximation may be applied, and can be written as [46]

$$\alpha(\omega) = \frac{\alpha}{\overline{\omega}^2 - \omega^2} \tag{2.21}$$

where $\omega$ is the frequency and $\bar{\omega}$ can be seen as an molecular excitation energy. Without a damping term, the polarization has a pole at this excitation frequency and above this frequency, the Unsõld approximation cannot be applied.

In paper 2 we combine the polarizability model developed in paper 1, with a model for the frequency dependent polarizability described in Ref. [47]. Here, a polarization similar to Eq. (2.21) is obtained, but $\overline{\omega}$ is described using atomic parameters. To obtain good results for the polarizability at high frequencies an accurate value for $\overline{\omega}$ is needed.

One of the more subtle advantage with the frequency dependent polarization model, is that it helps parametrize the static polarizability. The reason is that the frequency dependent polarizability is dependent on how the static polarizability is divided into the EEM part and the PDI part. If the static polarizability is not divided properly, large errors in the frequency dependent polarizability are seen.

In paper 4 the excitation energy of molecules typically relevant for streamer studies are calculated as a function of the electric field. For most molecules the excitation energies are independent of the electric fields for fields below 10 *MV/cm*. However, for tridecane, the excitation energy is dependent on the electric field (see paper 5). A drawback with the frequency dependent polarizability model developed in paper 2 is that the excitation energy will not under any circumstances be dependent on the static electric field. The reason is that all frequencies are completely independent of the presence of other frequencies, including the limit where $\omega \to 0$. For high intensities, or high electric fields, this is questionable, and as the result of paper 4 show, the excitation energy may be dependent on the static electric

field. However for most molecules and for small fields, the first excitation energy is independent of the external electric field, and thus modeling the frequency responses as independent of each other should be adequate for most purposes.

## 2.5 Dispersion Forces

Calculating dispersion forces quantum mechanically requires methods which go beyond the Hatree Fock level of theory [16], and is thus problematic for many density function theory approximations [48]. However the concept is fairly easy to understand. If one molecule gets a temporary dipole moment $\mu^{tmp}$, it will induce a temporary dipole moment in the other molecule. This leads to an attractive force which is proportional to $R^{-6}$. If the polarization and electrostatic interactions are zero due to the symmetry of the molecules, dispersion forces are important. This is typically the case for non-polar organic liquids [49], such as cyclohexane which is often used as model system for transformer oil.

For our case, the dispersion forces are important to model the liquid before it is transformed into a plasma. Thus, when developing molecular models for streamers, both the short range dispersion force and the long ranged Coulomb forces have to be included. Needless to say, the addition of long range interactions will complicate numerical computation.

# Chapter 3

# Ionization Processes

The liquid phase should be possible to simulate using MD simulations, and as shown in paper 3, for moderate separation distances the interaction between a free electron and a neutral molecule may be modeled using rather simple models. The remaining problem arise due to the interaction at short separation distances. How can the transition between a bound and a free state be modeled in a force field?

Thus, questions on how a neutral molecule is ionized arises. How large must the electric field be to ionize a molecule by tunneling? What determines photoionization probabilities, and how can the different ionization mechanism be modeled? In theory these question may be answered by the Schrödinger equation. However, many of these questions are challenging for the typical quantum chemistry approach, where a wavefunction is expanded in terms of a basis set. Free electron may be incorporated in the basis set, by for example adding sin and cos functions. Simulating free electrons by adding one extremely diffuse function to the basis set have been used to calculate the IP [50]. However, if a specific free state is needed, such that the same level of accurate description of the free states as for the bound state are required, it will be far more problematic to apply the standard quantum chemistry approach. In this case the approach would require an extremely large basis set.

In chemistry it is usually ground state energies and the properties of stable systems which are interesting. However, in this case, we are interested in a transition from a stable to an unstable system. Thus, it might be necessary to use time dependent quantum mechanics, which is significantly more difficult. Therefore obtaining desired reference quantum chemical data, such as for example different cross sections, may be difficult. However, all ionization processes are dependent on the ionization potential (IP), which may

be defined as

$$IP = U_{A^+} - U_A \tag{3.1}$$

where $U_A$ is the energy of the neutral molecule and $U_{A^+}$ is the energy of the corresponding cation. Thus, the IP give the energy required to ionize the molecule.

The IP of a molecule in vacuum may be calculated accurately by using standard quantum chemistry [51–54]. In paper 4 we show that the ionization potential is straight forward to calculate, and give good results when compared to experiments. We also show that the IP is an important parameter for streamer initiation and propagation. The effect of additives in pure cyclohexane has been shown to be dependent on the difference in IP between the additive and cyclohexane [9].

As discussed in paper 4 electron capture processes are more difficult to study. The electron affinity, EA, defined as

$$EA = U_A - U_{A^-} \tag{3.2}$$

give a measure of the stability of a negative ion, but contrary to ionization processes, it is not a potential barrier that is needed to be crossed before an electron is captured. This is illustrated as the electron capture cross sections may be nonzero for electrons with zero energy [53, 55, 56]. Thus it is unclear how important the EA is for electron capture processes.

In addition, quantum mechanically it may be difficult to distinguish between a negative ion $A^-$ and a molecule $A$ plus a free electron $e^-$. Stable molecules seldom create stable negative ions, and if they do the electron affinity is often low compared to the IP. (see for example paper 4). This means that electrons captured by neutral molecules are usually not very stable. The calculation of the EA can be performed, however typically only for complexes such as $OH$ where the negative ion is stable, but the neutral system is a radical [53, 55, 56]. Electron capture processes by neutral molecules may be dependent on breaking chemical bonds, as for example in creating a stable chloride by electron impact with a chlorinated hydrocarbon.

For this reason we focused mainly on ionization processes in paper 5. The obvious question to answer is how the IP depend on an electric field. The Coulomb potential in an electric field is illustrated in Figure 3.1, and can be written as (setting $E = -|E|$),

$$V = -1/r - |E|r \tag{3.3}$$

and has a maximum at $V^{max} = -2\sqrt{E}$. Based on this potential the IP of a system in an electric field can be modeled as

$$IP = IP_0 - 2\sqrt{E} \tag{3.4}$$

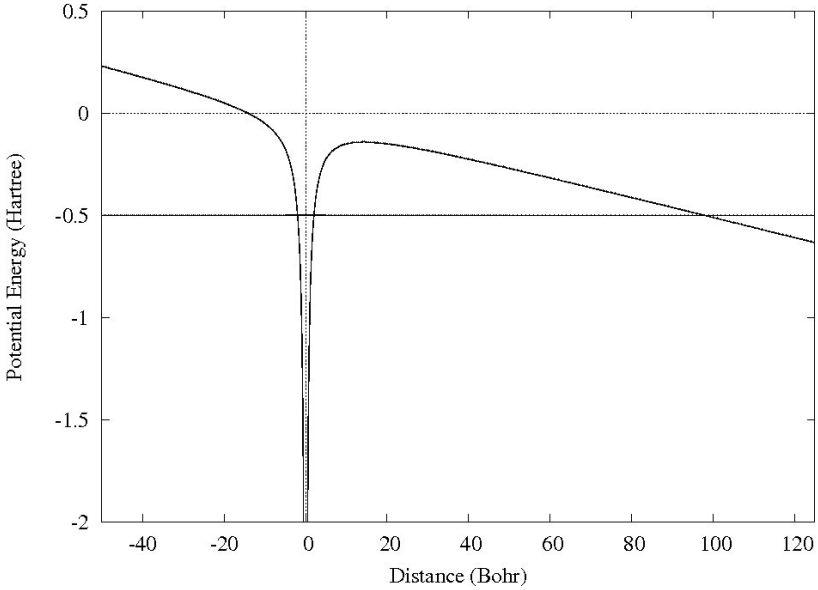


Figure 3.1: Illustration of the Coulomb potential in an electric field. Taken from paper 5

and this is the basis for the Poole-Frenkel conduction model [57]. In the Poole-Frenkel model, the conductivity increases exponentially with the field,

$$\sigma(E) \propto e^{-\frac{\beta_{PF}\sqrt{E}}{k_b T}} \quad . \tag{3.5}$$

Using a model based on an interaction between a negative point charge and a cation described by density functional theory, it is shown (in paper 5) that Eq. (3.4) is surprisingly accurate also for more complicated system.

Further, in paper 5, three different fundamental ionization processes are discussed: impact ionization, photoionization and field ionization (or tunneling). A field dependent IP gives insight into all these possible processes, but do not determine ionization probabilities uniquely. Streamers are assumed to have 4 modes of propagation, and different propagation mechanisms dominate for different modes. For example for 4th mode streamers (fast event), photoionization is believed to be the main ionization mechanism [8]. Therefore it is important to study all three ionization processes and not only determine the energy required to ionize a system, but also study the dynamics of the process.

# Chapter 4

# Presentation of papers and future work

Before proceeding to future work, a short recap of the papers are given.

- In paper 1 a model of the electrostatic and induction energy is developed. Both the polarizability and the dipole moment of molecules scale correctly with the size of the molecule, which has been the main problem with the EEM model. In this paper, analytical results for the linear chain is obtained, which helps understand the role of each parameter in the model.

- In paper 2, the model in paper 1 is expanded to include a frequency dependent response. Good results are obtained for both nonmetallic carbon systems and carbon systems with metallic properties, as for example systems based on benzene rings.

- Paper 3 is an attempt to apply the ideas in paper 1 and paper 2 to a model relevant for streamer initiation and propagation. The interaction between $Ar$, $Ar^+$ and $e^-$ at moderate separation distances can be described using surprisingly simple models.

- Paper 4 describes how the IP may be calculated using standard quantum mechanical tools, and how it can be related to streamer studies. In this paper a short discussion about the limitations of standard quantum mechanical calculations are given.

- Paper 5 presents a way to calculate the field dependent IP, which is applied to calculate the field dependence of the IP for a handful of molecules. The results are compared to classical conductivity models.

The main conclusion in this paper is that the IP is a field dependent property and that the field dependence cannot be ignored in high field phenomena.

## 4.1 Future work

The polarization model developed in paper 1 has mainly been tested on carbon-hydrogen systems. In order to apply the polarization model in force fields, thought has to be given to how to generalize the model to a generic set of atoms. Another aspect is that it is desirable to be able to model the dipole moment and the polarizability using the same set of parameters. In this respect it is satisfying that the polarization model given in paper 2 uses reasonable atomic sizes.

In paper 4 we use a polarizable continuum model (PCM) to calculate the IP in a medium. Without an electric field, a sharp division between the medium and molecule can be applied as the free electron is at infinite separation. However, the model used in paper 5 for the calculation of the IP in an electric field, includes an interaction with a point charge some distance from the QM system. Thus with an electric field a sharp boundary may be problematic and the result of PCM might be to dependent on where the boundary is placed. However, an alternative is to apply the model for Argon developed in paper 3 for a hybrid quantum mechanical/molecular mechanics (QM/MM) model which would give a softer boundary between the QM region and the classical region. Thus developing a QM/MM model to calculate the field dependence of the IP in a medium may be interesting. A remaining question is whether the effect of the medium is the same for high electric fields as for low. One could expect that the medium has less effect on IP if the potential (see Figure 3.1) has a maximum close to the molecule.

For understanding streamers it would be very helpful to include ionization processes in a molecular model. With the basis of the ideas in paper 3 and 5, simple models for ionization could be incorporated into molecular force field, and free electrons could be modeled using quantum wave package similar to the eFF force field [14]. An argon atom may be modeled as an argon cation and a single electron, and some parameters (associated with the core electrons of argon) can be adjusted such that the minimum energy of the single electron corresponds to the IP of argon. Thus, with the single electron as a classical particle, ionization processes could be modeled in an MD simulation.

However, one of the main obstacle is to obtain further reference data to

test a model. The IP of a molecule can be calculated, but ionization probabilities are also desired. For argon it is therefore interesting that impact ionization has recently been studied, both theoretically and experimentally. However it is problematic that these studies use very large electron energies (of the order 100eV) [58]. For modeling streamers in liquids or solids, electron energies of the order 10-20eV for the incoming electron is of far greater interest. Another interesting topic regarding obtaining reference data is the field dependence of photoionization probabilities, which is briefly discussed in paper 5. If the problem with obtaining reference data could be solved, a combination of solving Poisson's equation by the finite element method and using MD simulation on the interesting area should be investigated.

# Chapter 5

# Conclusion

The main result of this work is the development of a polarization model. Based on a modified version of EEM, a charge-transfer model has been merged with the PDI model, allowing both metallic and nonmetallic systems to be modeled. The model has been solved analytically for a linear chain, with regards to a dipole moment, static and frequency dependent polarizability. An analytical solution aids the understanding of the different pieces and how they interact. Thus the analytical solution for the linear chain is very helpful in the development stages of the model. Specifically it is found that the degree of metallicity in the system can be described using one single function, which we have called $\epsilon$, and this is an attractive feature of this model.

A model for the permanent and the induced atomic charges and point dipole moments is a key ingredient in any force field, and thus the model can be applied to force fields in general. However the general approximations in the model may also be used to develop a force field capable of describing a liquid to plasma transition (streamer initiation and propagation). Monoatomic molecules such as argon are particularly simple, and are thus nice model systems. In an argon streamer, the interaction between the different species at moderate separation distances may be described based on models for the exchange, dispersion and the polarization energy.

The important interaction at short separation distances are mainly those that describes the different ionization mechanism; impact ionization, photoionization and field ionization. Calculating different ionization probabilities from quantum mechanics is difficult, but all ionization processes are strongly dependent on the IP, which for molecules in gas phase may be calculated fairly easily with good accuracy.

Representing an electron as a negative point charge, allows the calcula-

tion of the IP in an electric field using standard quantum chemistry. Representing an electron as a point charge should be a good approximation as long as the electron is far from the molecule. Based on the calculation of the field dependence of the IP, it is important to stress that it is not a field independent property. The classical form of the field dependence of IP is

$$IP = IP_0 - 2\sqrt{E} \tag{5.1}$$

and is surprisingly accurate also for molecular systems. Further, the field dependence of the IP can be used to aid the interpretation of experimental results on streamer initiation and propagation. Thus it is concluded that Eq. (5.1) is very important in all high field phenomena.

The main obstacle in developing a force field capable of describing streamers is to obtain reference data for both impact and photoionization probabilities (preferable in high electric fields).

# Bibliography


[1] A. Denat, N. Bonifaci, and M. Nur. IEEE Trans. Dielect. Elect. Insul., **5**, 382–387, (1998).

[2] L. Dumitrescu, O. Lesaint, N. Bonifaci, A. Denat, and P. Notingher. J. Electrostat., **53**, 135–146, (2001).

[3] P. Gournay and O. Lesaint. J. Phys. D: Appl. Phys., **26**, 1966–74, (1993).

[4] S. Ingebrigtsen, L. E. Lundgaard, and P.-O. Åstrand. J. Phys. D: Appl. Phys., **40**, 5161–5169, (2007).

[5] S. Ingebrigtsen, L. E. Lundgaard, and P.-O. Åstrand. J. Phys. D: Appl. Phys., **40**, 5624–5634, (2007).

[6] Ø. L. Hestad, L. E. Lundgaard, and D. Linhjell. IEEE Trans. Dielect. Elect. Insul., **17**, 767-777, (2010).

[7] Ø. L. Hestad, L. E. Lundgaard, and P.-O. Åstrand. Submitted, (2010).

[8] L. Lundgaard, D. Linhjell, G. Berg, and S. Sigmond. IEEE Trans. Dielect. Elect. Insul., **5**, 388–395, (1998).

[9] S. Ingebrigtsen, H. S. Smalø, P.-O. Åstrand, and L. E. Lundgaard. IEEE Trans. Dielect. Electr. Insul., **16**, 1511, (2009).

[10] J. M. Dawson. Rev. Mod. Phys., **55**, 403, (2000).

[11] S. Ingebrigsten, N. Bonifaci, A. Denat, and O. Lesaint. J. Phys. D. Appl. Phys., page 235204, (2008).

[12] N. Bonifaci, A. Denat, and P. E. Frayssines. J. Electrostat., **64**, 445-449, (2006).

[13] P. E. Frayssines, N. Bonifaci, A. Denat, and O. Lesaint. J. Phys. D: Appl. Phys., **35**, 369-377, (2002).

[14] J. T. Su and W. A. Goddard III. J. Chem. Phys, **131**, 244501, (2009).

[15] P. C. Hemmer. *Kvantemekanikk*. Tapir akdemisk forlag, (2000).

[16] T. Helgaker, P. Jørgensen, and J. Olsen. *Molecular electronic-structure theory*. Wiley, Chichester, (2000).

[17] A. J. Stone. *The Theory of Intermolecular Forces*. Clarendon Press, Oxford, (1996).

[18] D. Klakow, C. Toepffer, and P. G. Reinhard. J. Chem. Phys, **101**, 10766, (1994).

[19] A. D. Buckingham, P. W. Fowler, and J. M. Hutson. Chem. Rev., **88**, 963-988, (1988).

[20] R. S. Mulliken. J. Chem. Phys., **23**, 1833-1840, (1955).

[21] P.-O. Åstrand, K. Ruud, K. V. Mikkelsen, and T. Helgaker. J. Phys. Chem. A, **102**, 7686-7691, (1998).

[22] L. Silberstein. Phil. Mag., **33**, 92-128, (1917).

[23] L. Silberstein. Phil. Mag., **33**, 215-222, (1917).

[24] L. Silberstein. Phil. Mag., **33**, 521-533, (1917).

[25] J. Applequist, J. R. Carl, and K.-F. Fung. J. Am. Chem. Soc., **94**, 2952-2960, (1972).

[26] J. Applequist. Acc. Chem. Res., **10**, 79-85, (1977).

[27] R. T. Sanderson. Science, **114**, 670-672, (1951).

[28] W. J. Mortier, K. van Genechten, and J. Gasteiger. J. Am. Chem. Soc., **107**, 829-835, (1985).

[29] A. K. Rappé and W. A. Goddard III. J. Phys. Chem., **95**, 3358-3363, (1991).

[30] J. Cioslowski and B. B. Stefanov. J. Chem. Phys., **99**, 5151-5162, (1993).

[31] D. M. York and W. Yang. J. Chem. Phys., **104**, 159-172, (1996).

[32] A. C. T. van Duin, J. M. A. Baas, and B. van de Graaf. J. Chem. Soc., Faraday Trans., **90**, 2881-2895, (1994).

[33] H. A. Stern, G. A. Kaminski, J. L. Banks, R. Zhou, B. J. Berne, and R. A. Friesner. J. Phys. Chem. B, **103**, 4730-4737, (1999).

[34] H. A. Stern, F. Rittner, B. J. Berne, and R. A. Friesner. J. Chem. Phys., **115**, 2237-2251, (2001).

[35] G. A. Kaminski, H. A. Stern, B. J. Berne, R. A. Friesner, Y. X. Cao, R. B. Murphy, R. Zhou, and T. A. Halgren. J. Comput. Chem., **23**, 1515-1531, (2002).

[36] A. C. T. van Duin, S. Dasgupta, F. Lorant, and W. A. Goddard III. J. Phys. Chem. A, **105**, 9396-9409, (2001).

[37] G. L. Warren, J. E. Davis, and S. Patel. J. Chem. Phys., **128**, 144110, (2008).

[38] R. Chelli, P. Procacci, R. Righini, and S. Califano. J. Chem. Phys., **111**, 8569-8575, (1999).

[39] R. A. Nistor, J. G. Polihronov, M. H. Müser, and N. J. Mosey. J. Chem. Phys., **125**, 094108, (2006).

[40] D. Mathieu. J. Chem. Phys., **127**, 224103, (2007).

[41] J. Chen, D. Hundertmark, and T. J. Martínez. J. Chem. Phys., **129**, 214113, (2008).

[42] J. Chen and T. J. Martínez. Chem. Phys. Lett., **438**, 315-320, (2007).

[43] H. M. Jones and E. E. Kunhardt. J. phys. D. Appl. Phys., **28**, 178-188, (1995).

[44] N. Bonifaci, A. Denat, and V Atrazhev. J. phys. D. Appl. Phys., **39**, (1997).

[45] N. Bonifaci and A. Denat. IEEE Trans. Dielectr. Electr. Insul., **26**, 610-614, (1991).

[46] A. Unsöld. Z. Phys., **43**, 563-574, (1927).

[47] A. Mayer, Ph. Lambin, and P.-O. Åstrand. Nanotechnology, **19**, 025203, (2008).

[48] M. J. Allen and D. J. Tozer. jcp, **113**, 11113-11120, (2002).

[49] S. Grimme, J. Antony, T. Schwabe, and C. Mück-Lichtenfeld. Org. Biomol. Chem., **5**, 741-758, (2007).

[50] J. F. Stanton and J. Gauss. J. Chem. Phys., **111**, 8785-8788, (1999).

[51] C. Zhan, J. A. Nichols, and D. A. Dixon. J. Phys. Chem. A., **107**, 4184-4194, (2003).

[52] V. Lemierre, A. Chrostowska, A. Dargelos, and H. Chermette. J. Phys. Chem. A., **109**, 8348-8355, (2005).

[53] L. A. Curtiss, P. C. Redfern, K. Raghavachari, and J. A. Pople. J. Chem. Phys., **109**, 42-55, (1998).

[54] A. D. Becke. J. Chem. Phys, **98**, 5648-5652, (1993).

[55] Y. Takahata and D. P. Chong. J. Braz. Chem. Soz., **10**, 354-358, (1999).

[56] M. Meunier, N. Quirke, and D. Binesti. Mol. Simulat., **23**, 109-125, (1999).

[57] L. A. Dissado and J. C. Fothergill. *Electrical Degradation and Breakdown in Polymers*. Material and Devices Series 9. The Institution of Engineering and Technology, London, United Kingdom, (1992).

[58] D. A. Biava, H. P. Saha, E. Engel, R. M. Dreizler, R. P. McEachran, M. A. Haynes, B. Lohmann, C. T Whelan, and B. H. Madison. J. Phys. B, **35**, 293-307, (2002).

# Paper 1:

*Nonmetallic electronegativity equalization and point-dipole interaction model including exchange interactions for molecular dipole moments and polarizabilities*

Hans S. Smalø, P.-O. Åstrand and L. Jensen

J. Chem. Phys. **131** 044101 (2009)

# Nonmetallic electronegativity equalization and point-dipole interaction model including exchange interactions for molecular dipole moments and polarizabilities

Hans S. Smalø,[1] Per-Olof Åstrand,[1,a)] and Lasse Jensen[2]
[1]*Department of Chemistry, Norwegian University of Science and Technology (NTNU), N-7491 Trondheim, Norway*
[2]*The Pennsylvania State University, University Park, Pennsylvania 16802, USA*

(Received 16 April 2009; accepted 10 June 2009; published online 22 July 2009)

The electronegativity equalization model (EEM) has been combined with a point-dipole interaction model to obtain a molecular mechanics model consisting of atomic charges, atomic dipole moments, and two-atom relay tensors to describe molecular dipole moments and molecular dipole-dipole polarizabilities. The EEM has been phrased as an atom-atom charge-transfer model allowing for a modification of the charge-transfer terms to avoid that the polarizability approaches infinity for two particles at infinite distance and for long chains. In the present work, these shortcomings have been resolved by adding an energy term for transporting charges through individual atoms. A Gaussian distribution is adopted for the atomic charge distributions, resulting in a damping of the electrostatic interactions at short distances. Assuming that an interatomic exchange term may be described as the overlap between two electronic charge distributions, the EEM has also been extended by a short-range exchange term. The result is a molecular mechanics model where the difference of charge transfer in insulating and metallic systems is modeled regarding the difference in bond length between different types of system. For example, the model is capable of modeling charge transfer in both alkanes and alkenes with alternating double bonds with the same set of carbon parameters only relying on the difference in bond length between carbon $\sigma$- and $\pi$-bonds. Analytical results have been obtained for the polarizability of a long linear chain. These results show that the model is capable of describing the polarizability scaling both linearly and nonlinearly with the size of the system. Similarly, a linear chain with an end atom with a high electronegativity has been analyzed analytically. The dipole moment of this model system can either be independent of the length or increase linearly with the length of the chain. In addition, the model has been parametrized for alkane and alkene chains with data from density functional theory calculations, where the polarizability behaves differently with the chain length. For the molecular dipole moment, the same two systems have been studied with an aldehyde end group. Both the molecular polarizability and the dipole moment are well described as a function of the chain length for both alkane and alkene chains demonstrating the power of the presented model. © *2009 American Institute of Physics*. [DOI: 10.1063/1.3166142]

## I. INTRODUCTION

Molecular mechanics force fields are in most cases used as an alternative to *ab initio* quantum chemical methods in the calculation of intra- and intermolecular energies in simulations of condensed phases.[1] The reason is basically that the energy calculations using a force field only take a fraction of the time as compared to quantum chemical calculations, and the energy needs to be calculated repeatedly for relatively large systems in a molecular simulation.[2] A prominent exception is the Car–Parrinello method,[3] where the electron density in terms of density functional theory (DFT) is propagated in time but presently it is limited to relatively small systems and short times.

A force field relies on a set of atom-type parameters that represents the molecular charge distribution, as for example, atomic charges to describe the electrostatics and Lennard-Jones parameters to model van der Waals interactions. The transferability of these atom-type parameters from one type of molecular system to another thus becomes a central issue.[4] The major difficulty is most probably the electrostatics. It has been demonstrated that atomic charges are not transferable,[5] which obviously causes problems since the electrostatic energy is the dominating term in most cases. An attractive approach to overcome these problems is the electronegativity equalization model (EEM),[6–11] which is related to concepts of DFT as electronegativity and chemical hardness.[12] In the EEM, an atom in a molecule is represented by an atomic electronegativity and an atomic chemical hardness and charge is allowed to flow between the atoms such as the molecular electronegativity (chemical potential) is equalized over the molecule. The EEM has been employed in several force fields to obtain atomic charges,[13–17] and it has also been demonstrated that the EEM reproduces atomic

a)Author to whom correspondence should be addressed. Electronic mail: per-olof.aastrand@chem.ntnu.no.

 

charges as calculated by other methods.[18–20] The EEM has also been used to calculate molecular polarizabilities.[21]

Based on atom-atom charge transfer (AACT) variables,[22] several models have been developed to address the problems with the EEM.[22–26] The behavior of the EEM in the dissociation limit has been investigated by either introducing a distance-dependent electronegativity[25,26] or a distance-dependent chemical hardness.[23,24] To be able to calculate the polarizability for large nonmetallic materials, bond-type parameters have been introduced,[22,23] and how these models scale with the size of the system have been analyzed.[27] The split-charge model demonstrates the correct scaling of the polarizability with the EEM and the AACT model as limiting cases.[23,27] The split-charge model has also been used to analyze the dielectric properties of crystal structures.[28]

It has also become more common to include electronic polarization explicitly in force fields in terms of atomic polarizabilities.[4,29–32] The transferability of atomic polarizabilities is satisfactory as long as the model is restricted to isotropic polarizabilities. In fact, over the years it has been common to model the isotropic part of the molecular polarizability in terms of additive atom-type contributions.[33,34] It is difficult, however, to construct an additive model for polarizability tensors, apart from highly symmetric systems, as for example, fluoro- and chlorobenzenes where ellipsoidal carbon polarizabilities may be adopted.[35]

In the point-dipole interaction (PDI) model, molecular polarizability tensors are obtained from isotropic atomic polarizabilities coupled to each other by the interactions of atomic induced dipole moments in an external electric field.[36–40] The PDI model has been improved by regarding the interaction between two charge distributions instead of between two point particles.[41–45] The model has been used for studying polarizabilities of a variety of molecular systems including carbon fullerenes and nanotubes,[44,46–49] boron nitride tubes,[50] molecular clusters,[51–53] amino acids[45] and proteins,[54] and in force fields for water.[55] The PDI model has also been extended to hyperpolarizabilities,[56–60] optical rotation,[61–64] absorption,[65] molecular crystals,[66] and Raman intensities.[67–72]

If a molecule is divided into subsystems, there is in principle two distinct contributions to molecular polarization: a charge-transfer contribution arising from that charge is flowing from one subsystem to another and a polarization contribution arising from internal polarization within a subsystem. In addition to a polarizability term, the charge-transfer contribution may be modeled in terms of capacitance models,[73–76] EEM,[15,16,77,78] and monopole polarizabilities.[79,80] A combined capacitance and PDI model has also been extended to electronic absorption.[81]

In this work, we have investigated a modification of a combined EEM and PDI model. It includes interatomic damping terms according to the overlap of two Gaussian charge distributions.[44] Furthermore, the self-exchange term is included,[82] and the interatomic exchange term is approximated as the overlap between two charge distributions.[83] The reformulation of the EEM into AACT terms[22] allows an energy term for transporting charges to be included and is needed for the polarizability to scale correctly with the size of the system for nonmetallic systems. The charge transport term can be introduced by a modification of the chemical hardness to be dependent on interatomic distances, which allows for a unified model for metallic and nonmetallic systems. The model is tested analytically for long linear chains, and it has been parametrized for some model systems including both alkane and alkene chains.

## II. THEORY

### A. A combined AACT and PDI model

The starting point of the presented model is a combination of the EEM and the PDI model. Thus each atom $I$ has a charge $q_I$ and an atomic dipole moment $\mu_{I,\alpha}$. The molecular energy may be written as

$$V = V^{qq} + V^{q\mu} + V^{\mu\mu}, \tag{1}$$

where $V^{qq}$ is the charge-charge interaction energy, $V^{q\mu}$ is the charge-dipole interaction energy, and $V^{\mu\mu}$ is the dipole-dipole interaction energy, respectively. The EEM is contained within $V^{qq}$ and the PDI model within $V^{\mu\mu}$, while $V^{q\mu}$ couples the two models. The energy is then minimized to find the optimal $q_I$ and $\mu_{I,\alpha}$.

A molecule is regarded as a set of $N$ atoms that interacts and exchanges charge as in both the capacitance model[73,76] and in the EEM.[6,7,10] The main difference between a capacitance model and the EEM is that the EEM also adopts an atomic electronegativity $\chi_I^*$ that gives an inherent potential difference between different elements. The charge-charge contribution to the molecular energy $V^{qq}$ is given as[8,15]

$$V^{qq} = \sum_I^N \left( V_I^0 + (\chi_I^* + \varphi_I^{\text{ext}})q_I + \frac{1}{2}\eta_I^* q_I^2 + \frac{1}{2}\sum_{J\neq I}^N q_I T_{IJ}^{(0)} q_J \right) - \mu\left( q^{\text{mol}} - \sum_I^N q_I \right), \tag{2}$$

where $V_I^0$ is the energy of atom $I$ in an unperturbed and uncharged state, $q_I$ is an atomic charge created by the charge flow between the atoms, and $\eta_I^*$ is an atomic chemical hardness. The term including a sum over atom pairs is the Coulomb electrostatic interaction, and in classical electrostatics $T_{IJ}^{(0)} = \frac{1}{R_{IJ}}$ (for $I \neq J$), where $R_{IJ}$ is the distance between particles $I$ and $J$. An interaction with an external electrostatic potential $\varphi_I^{\text{ext}}$ is also included. The last term on the right-hand side of Eq. (2) is a constraint to keep the molecular charge $q^{\text{mol}}$ preserved, where $\mu$ (identified as the chemical potential) is a regular Lagrange multiplier. If the notation $T_{II}^{(0)} = \eta_I^*$ is adopted and the constant term $V_I^0$ is ignored,

$$V^{qq} = \sum_I^N \left( (\chi_I^* + \varphi_I^{\text{ext}})q_I + \frac{1}{2}\sum_J^N q_I T_{IJ}^{(0)} q_J \right) - \mu\left( q^{\text{mol}} - \sum_I^N q_I \right). \tag{3}$$

For a system of $N$ particles with an atomic charge and an atomic dipole moment, the charge-dipole energy $V^{q\mu}$ becomes

$$V^{q\mu} = \sum_{I,J}^{N} q_I T^{(1)}_{IJ,\alpha} \mu_{J,\alpha}, \tag{4}$$

where $T^{(1)}_{IJ,\alpha}$ is the charge-dipole interaction term given by the gradient of $T^{(0)}_{IJ}$. The dipole-dipole energy $V^{\mu\mu}$ term is the same as in the capacitance model[73,76]

$$V^{\mu\mu} = \frac{1}{2}\sum_{J}^{N} \mu_{J,\alpha}\alpha^{-1}_{J,\alpha\beta}\mu_{J,\beta} - \frac{1}{2}\sum_{J}^{N}\sum_{K\neq J}^{N} \mu_{J,\alpha} T^{(2)}_{JK,\alpha\beta}\mu_{K,\beta} - \sum_{J}^{N} E^{\mathrm{ext}}_{J,\alpha}\mu_{J,\alpha}, \tag{5}$$

where $\alpha_{J,\alpha\beta}$ is an atomic polarizability, $T^{(2)}_{JK,\alpha\beta}$ is the dipole-dipole interaction term given by the gradient of $T^{(1)}_{IJ,\alpha}$, and $E^{\mathrm{ext}}_{J,\alpha}$ is an external electric field at atom $J$.

To easily identify problems associated with charge transfer over large distances, the AACT approach is adopted.[22,23] The charge transfer $q_{IJ}$ is defined as the charge transfer from atom $J$ to atom $I$ such as[22]

$$q_I = \sum_{J}^{N} L_{IJ} q_{IJ}. \tag{6}$$

For neutral molecules, the conservation of the molecular charge may be included by imposing $q_{JI}=-q_{IJ}$ and $q_{II}=0$ and may be used instead of the Lagrange multiplier. A topology matrix $L_{IJ}$ is introduced where its elements are 1 if charge transfer is allowed between atoms $I$ and $J$ and otherwise it is 0.[22] The model is independent of how the variables are represented, and therefore, as long as the entire system is connected by at least one $L_{IJ}\neq 0$, the model will be mathematically identical to the original model regardless of how the variable substitution in Eq. (6) is written. In terms of the new variables, the equations needed are given by

$$\frac{\partial V}{\partial q_{SP}} = \frac{\partial V^{qq}}{\partial q_{SP}} + \frac{\partial V^{q\mu}}{\partial q_{SP}} = 0 \tag{7}$$

and

$$\frac{\partial V}{\partial \mu_{I,\alpha}} = \frac{\partial V^{q\mu}}{\partial \mu_{I,\alpha}} + \frac{\partial V^{\mu\mu}}{\partial \mu_{I,\alpha}} = 0. \tag{8}$$

By using Eqs. (3) and (6), the charge-charge energy $V^{qq}$ may be rewritten as

$$V^{qq} = \sum_{I,J}^{N} (\chi^*_I + \varphi^{\mathrm{ext}}_I) L_{IJ} q_{IJ} + \frac{1}{2}\sum_{I,J,K,M}^{N} L_{IK} q_{IK} T^{(0)}_{IJ} L_{JM} q_{JM}. \tag{9}$$

Since trivially,

$$\sum_{I,J}^{N} (\chi^*_I + \varphi^{\mathrm{ext}}_I) L_{IJ} q_{IJ} = \sum_{I,J}^{N} (\chi^*_J + \varphi^{\mathrm{ext}}_J) L_{JI} q_{JI}, \tag{10}$$

and since $q_{II}=0$,

$$\begin{aligned}\sum_{I,J}^{N} (\chi^*_I + \varphi^{\mathrm{ext}}_I) L_{IJ} q_{IJ} &= \frac{1}{2}\sum_{I,J}^{N} (\chi^*_I + \varphi^{\mathrm{ext}}_I) L_{IJ} q_{IJ} + (\chi^*_J + \varphi^{\mathrm{ext}}_J) L_{JI} q_{JI} \\ &= \frac{1}{2}\sum_{I,J}^{N} (\chi^*_{IJ} + \varphi^{\mathrm{ext}}_{IJ}) L_{IJ} q_{IJ} \\ &= \sum_{I,J>I}^{N} (\chi^*_{IJ} + \varphi^{\mathrm{ext}}_{IJ}) L_{IJ} q_{IJ},\end{aligned} \tag{11}$$

and since $L_{IJ}=L_{JI}$ and $q_{IJ}=-q_{JI}$,

$$\chi^*_{IJ} = \chi^*_I - \chi^*_J \tag{12}$$

and

$$\varphi^{\mathrm{ext}}_{IJ} = \varphi^{\mathrm{ext}}_I - \varphi^{\mathrm{ext}}_J. \tag{13}$$

The energy in Eq. (9) is thus rewritten in terms of electronegativity and potential differences as

$$V^{qq} = \sum_{I,J>I}^{N} (\chi^*_{IJ} + \varphi^{\mathrm{ext}}_{IJ}) L_{IJ} q_{IJ} + \frac{1}{2}\sum_{I,J,K,M}^{N} L_{IK} q_{IK} T^{(0)}_{IJ} L_{JM} q_{JM}, \tag{14}$$

which is minimized with respect to an atom-atom charge-transfer $q_{SP}$, where $S>P$, leading to

$$\frac{\partial V^{qq}}{\partial q_{SP}} = L_{SP}\left(\chi^*_{SP} + \varphi^{\mathrm{ext}}_{SP} + \sum_{J,M}^{N} (T^{(0)}_{SJ} - T^{(0)}_{PJ}) L_{JM} q_{JM}\right), \tag{15}$$

where we have used that $\partial V/\partial q_{SP} = -\partial V/\partial q_{PS}$ and $T^{(0)}_{IJ} = T^{(0)}_{JI}$. It is noted that if $L_{SP}=0$, $\partial V^{qq}/\partial q_{SP}$ is automatically zero. Therefore, only pairs $S$ and $P$ such that $L_{SP}=1$ are relevant. Equation (15) is further rewritten as

$$\begin{aligned}\frac{\partial V^{qq}}{\partial q_{SP}} &= \chi^*_{SP} + \varphi^{\mathrm{ext}}_{SP} + \sum_{J,M}^{N} (T^{(0)}_{SJ} - T^{(0)}_{PJ}) L_{JM} q_{JM} \\ &= \chi^*_{SP} + \varphi^{\mathrm{ext}}_{SP} + \sum_{J,M>J}^{N} ((T^{(0)}_{SJ} - T^{(0)}_{PJ}) - (T^{(0)}_{SM} - T^{(0)}_{PM})) L_{JM} q_{JM}.\end{aligned} \tag{16}$$

Defining

$$T^{(0)}_{SP,JM} = (T^{(0)}_{SJ} - T^{(0)}_{PJ}) - (T^{(0)}_{SM} - T^{(0)}_{PM}), \tag{17}$$

an equation is obtained for each atom pair, where $L_{SP}\neq 0$, as

$$\frac{\partial V^{qq}}{\partial q_{SP}} = \chi^*_{SP} + \varphi^{\mathrm{ext}}_{SP} + \sum_{J>M}^{N} T^{(0)}_{SP,JM} L_{JM} q_{JM}. \tag{18}$$

$T^{(0)}_{SP,JM}$ has the following properties:

$$T^{(0)}_{SP,JM} = -T^{(0)}_{PS,JM}; \quad T^{(0)}_{SP,JM} = -T^{(0)}_{SP,MJ}, \tag{19}$$

which are obtained from Eq. (17). Because of these symmetries, the resulting charge obeys $q_{JM}=-q_{MJ}$ automatically, and only the cases where $S<P$ and $J<M$ have to be included. Thereby the charge neutrality condition is fulfilled. For the charge-dipole energy, inserting Eq. (6) into Eq. (4) gives

$$V^{q\mu} = \sum_{I,K,J} L_{IK} q_{IK} T^{(1)}_{IJ,\alpha} \mu_{J,\alpha}$$
$$= \sum_{I,K>I,J} L_{IK} q_{IK} (T^{(1)}_{IJ,\alpha} - T^{(1)}_{KJ,\alpha}) \mu_{J,\alpha} \quad (20)$$

where again $q_{JK}=-q_{KJ}$ has been used. The charge-dipole energy is also minimized with respect to the charge transfer $q_{SP}$ as

$$\frac{\partial V^{q\mu}}{\partial q_{SP}} = L_{SP} \sum_{J}^{N} (T^{(1)}_{SJ,\alpha} - T^{(1)}_{PJ,\alpha}) \mu_{J,\alpha}. \quad (21)$$

Introducing the notation

$$T^{(1)}_{SP,J,\alpha} = T^{(1)}_{SJ,\alpha} - T^{(1)}_{PJ,\alpha}, \quad (22)$$

we obtain

$$\frac{\partial V^{q\mu}}{\partial q_{SP}} = L_{SP} \sum_{J}^{N} T^{(1)}_{SP,J,\alpha} \mu_{J,\alpha}. \quad (23)$$

Analogously

$$\frac{\partial V^{q\mu}}{\partial \mu_{J,\alpha}} = \sum_{S,P>S} (T^{(1)}_{SJ,\alpha} - T^{(1)}_{PJ,\alpha}) L_{SP} q_{SP}$$
$$= -\sum_{S,P>S} (T^{(1)}_{JS,\alpha} - T^{(1)}_{JP,\alpha}) L_{SP} q_{SP}, \quad (24)$$

where it is used that $T^{(1)}_{JS,\alpha}=-T^{(1)}_{SJ,\alpha}$. Introducing the notation

$$T^{(1)}_{J,SP,\alpha} = T^{(1)}_{SJ,\alpha} - T^{(1)}_{PJ,\alpha} = -(T^{(1)}_{JS,\alpha} - T^{(1)}_{JP,\alpha}) = (T^{(1)}_{SP,J,\alpha})^T \quad (25)$$

leads to

$$\frac{\partial V^{q\mu}}{\partial \mu_{J,\alpha}} = \sum_{S,P>S} T^{(1)}_{J,SP,\alpha} L_{SP} q_{SP}. \quad (26)$$

Finally, the differentiation of $V^{\mu\mu}$ with respect to $\mu_{J,\alpha}$ gives

$$\frac{\partial V^{\mu\mu}}{\partial \mu_{J,\alpha}} = \alpha^{-1}_{J,\alpha\beta} \mu_{J,\beta} - \sum_{K\neq J}^{N} T^{(2)}_{JK,\alpha\beta} \mu_{K,\beta} - E^{\text{ext}}_{J,\alpha}. \quad (27)$$

The entire model is put together by inserting Eqs. (18), (23), (26), and (27) into Eqs. (7) and (8) and may be written as a matrix equation,

$$\begin{pmatrix} T^{(0)}_{SP,JM} & T^{(1)}_{SP,J,\alpha} \\ T^{(1)}_{I,JM,\alpha} & T^{(2)}_{IJ,\alpha\beta} \end{pmatrix} \begin{pmatrix} q_{JM} \\ \mu_{J,\beta} \end{pmatrix} = \begin{pmatrix} -\chi^*_{SP} - \varphi^{\text{ext}}_{SP} \\ E^{\text{ext}}_{I,\alpha} \end{pmatrix}, \quad (28)$$

where $T^{(2)}_{II,\alpha\beta}=\alpha^{-1}_I \delta_{\alpha\beta}$. Only atom pairs where $L_{SP}=1$ and $L_{JM}=1$ are included in the matrix, since the matrix elements are zero if either $L_{SP}$ or $L_{JM}$ is zero. The number of equations is thus reduced, but the model is unchanged as long as all atoms in the system are connected by at least one $L_{IJ}\neq 0$. The reason is simply that Eq. (28) gives the optimal distribution of the charges, and it does not care about how the charges are transferred in the system. In the remainder of this work the topology matrix is not given explicitly. Instead a sum of the type $\Sigma_{I,J}$ indicates a sum over all pairs $I$ and $J$ such that $L_{IJ}=1$, and likewise $\Sigma_{I,J>I}$ indicates a sum over all pairs $I$ and $J$ such that $J>I$ and $L_{IJ}=1$.

The total size of the matrix in Eq. (28) is $(3N+SP \times 3N+SP)$, where $N$ is the number of atoms and $SP$ is the number of atom pairs considered in the topology matrix $L_{SP}$. If $L_{SP}=1$ for bonded atoms and is zero otherwise, $SP$ is simply the number of chemical bonds in the system. As long as the number of bonds is approximately equal to the number of atoms in the system, the size of the matrix to be inverted is almost the same as in formulation of the combined EEM and PDI model in terms of point charges and point-dipole moments.

This model is so far identical to a combined EEM and PDI model as long as all atoms are connected by at least one $L_{IJ}\neq 0$. The combined EEM and PDI model thus depends on three atom-type parameters $\chi^*_I$, $\eta^*_I$, and $\alpha_I$ which have to be specified. The method is in analogy to DFT where the energy functional is minimized with respect to the electron charge distribution.[11,12] An advantage with the energy expressions given above is that all energy terms are either linear or quadratic in $q_I$ (and thus also in terms of $q_{IJ}$) and $\mu_{J,\alpha}$ which leads to a linear set of equations to obtain the atomic charges and dipole moments which can be solved by regular matrix techniques.

The field-independent quantities $q^0_{JM}$ and $\mu^0_{J,\alpha}$ are governed by

$$\begin{pmatrix} T^{(0)}_{SP,JM} & T^{(1)}_{SP,J,\alpha} \\ T^{(1)}_{I,JM,\beta} & T^{(2)}_{IJ,\beta\alpha} \end{pmatrix} \begin{pmatrix} q^0_{JM} \\ \mu^0_{J,\alpha} \end{pmatrix} = \begin{pmatrix} -\chi^*_{SP} \\ 0 \end{pmatrix} \quad (29)$$

and give atomic charges as well as atomic and molecular dipole moments. The molecular dipole moment $\mu^{\text{mol}}_\alpha$ is given as

$$\mu^{\text{mol}}_\alpha = \sum_I R_{I,\alpha} q^0_I + \sum_I \mu^0_{I,\alpha}$$
$$= \sum_{I,M} R_{I,\alpha} q^0_{IM} + \mu^0_{I,\alpha}$$
$$= \sum_{I,M>I} R_{IM,\alpha} q^0_{IM} + \sum_I \mu^0_{I,\alpha}. \quad (30)$$

A homogeneous electric field $E^{\text{ext}}_\alpha$ is assumed such that the electrostatic potential at atom $I$ is $\varphi^{\text{ext}}_I=-R_{I,\alpha}E^{\text{ext}}_\alpha$ (plus an arbitrary constant). By taking the derivative with respect to the electric field on both sides of Eq. (28), an equation for the quantities $\partial q_{JM}/\partial E^{\text{ext}}_\gamma$ and $\partial \mu_{J,\alpha}/\partial E^{\text{ext}}_\gamma$ is obtained as

$$\begin{pmatrix} T^{(0)}_{SP,JM} & T^{(1)}_{SP,J,\alpha} \\ T^{(1)}_{I,JM,\beta} & T^{(2)}_{IJ,\beta\alpha} \end{pmatrix} \begin{pmatrix} \partial q_{JM}/\partial E^{\text{ext}}_\gamma \\ \partial \mu_{J,\alpha}/\partial E^{\text{ext}}_\gamma \end{pmatrix} = \begin{pmatrix} R_{SP,\gamma} \\ \delta_{\beta\gamma} \end{pmatrix}, \quad (31)$$

where $R_{JM,\gamma}=R_{J,\gamma}-R_{M,\gamma}$ and $R_{J,\gamma}$ is the position of atom $J$. The molecular polarizability $\alpha^{\text{mol}}_{\alpha\beta}$ may thus be calculated as

$$\alpha^{\text{mol}}_{\alpha\beta} = \frac{\partial \mu^{\text{ind}}_\alpha}{\partial E^{\text{ext}}_\beta} = \sum_I R_{I,\alpha} \frac{\partial q_{IM}}{\partial E^{\text{ext}}_\beta} + \frac{\partial \mu_{I,\alpha}}{\partial E^{\text{ext}}_\beta}$$
$$= \sum_{I,M>I} R_{IM,\alpha} \frac{\partial q_{IM}}{\partial E^{\text{ext}}_\beta} + \sum_I \frac{\partial \mu_{I,\alpha}}{\partial E^{\text{ext}}_\beta}. \quad (32)$$

From Eq. (31) it is noted that the polarizability is independent of the atomic electronegativities.

### B. Damping of electrostatic interactions and exchange terms

In our previous work on the PDI model,[44] Gaussian distributions have been employed for atomic charges,

$$q_I\left(\frac{\Phi_I^*}{\pi}\right)^{3/2} e^{-\Phi_I^* r_I^2}, \tag{33}$$

where the width of the distribution $\Phi_I^*$ is an additional atom-type parameter. Note that the total atomic charge is $q_I$. The electrostatic interaction energy between two Gaussian charge distributions $V_{IJ}$ is given as[84]

$$V_{IJ} = q_I q_J \frac{\mathrm{erf}(\sqrt{a_{IJ}} R_{IJ})}{R_{IJ}}, \tag{34}$$

where

$$a_{IJ} = \frac{\Phi_I^* \Phi_J^*}{\Phi_I^* + \Phi_J^*}. \tag{35}$$

In our previous work,[44] we have regarded a "scaled distance" $R_{IJ}^s$,

$$R_{IJ}^s = \frac{R_{IJ}}{\mathrm{erf}(\sqrt{a_{IJ}} R_{IJ})}, \tag{36}$$

such that

$$V = \frac{q_I q_J}{R_{IJ}^s}. \tag{37}$$

The scaled distance may be approximated as[85]

$$R_{IJ}^s = \sqrt{R_{IJ}^2 + \frac{\pi}{4a_{IJ}}}, \tag{38}$$

which has the same limiting behavior as Eq. (36) at $R_{IJ} \to \infty$ and $R_{IJ} \to 0$. In our model, we differentiate with respect to $R_{IJ}^s$ instead of $R_{IJ}$ in the calculation of electric fields and electric field gradients.[44]

To add exchange terms to the molecular energy in Eq. (9), an analogy is made to the Hartree–Fock approximation, where the energy $V$ may be written as[86]

$$V = H_i + J_{ii} + J_{ij} + K_{ii} + K_{ij}, \tag{39}$$

where $H_i$ is the one-electron term, $J_{ii}$ and $J_{ij}$ are the self-Coulomb and Coulomb terms, respectively, and $K_{ii}$ and $K_{ij}$ are the self-exchange and exchange terms, respectively. It is noted that the self-exchange term exactly cancels half of the self-Coulomb term, and the self-exchange is thus trivially included by modifying Eq. (2),[82]

$$V^{qq} = \sum_{I=1}^{N} \left( V_I^0 + (\chi_I^* + \varphi_I^{\mathrm{ext}}) q_I + \frac{1}{4}\eta_I^* q_I^2 + \frac{1}{2}\sum_{J \neq I}^{N} q_I T_{IJ}^{(0)} q_J \right) - \mu\left(q^{\mathrm{mol}} - \sum_I^N q_I\right). \tag{40}$$

In practice, it only results in a scaling of the $\eta_I^*$ with a factor of 2 unless $\eta_I^*$ also contribute to other energy terms. This can be achieved by including the condition that the Coulomb term in the limit of $R_{IJ} \to 0$ in Eq. (38) is equal to the self-Coulomb term in line with the work by Mayer.[77] This condition leads to the following relation between the $\eta_I^*$ and $\Phi_I^*$ parameters,

$$\eta_I^* = \lim_{R_{IJ} \to 0} \frac{1}{R_{IJ}^s} = \sqrt{\frac{2\Phi_I^*}{\pi}}. \tag{41}$$

At an intermediate range, the interparticle exchange energy may be approximated as being proportional to the square of the overlap of the particle wave functions $\psi_I$,[87]

$$V_{IJ}^{\mathrm{exch}} = C\langle \psi_I | \psi_J \rangle^2, \tag{42}$$

where $C$ is a prefactor to be determined. In this model, Eq. (42) is approximated by the overlap of charge distributions,[83,88]

$$V_{IJ}^{\mathrm{exch}} = C \int \rho_I \rho_J d\tau. \tag{43}$$

At this stage, the atomic charge is partitioned into a nuclear $Z_I$ and an electronic $n_I$ contribution since the overlap only refers to the electronic charge distribution,

$$q_I = n_I + Z_I. \tag{44}$$

It might be useful to include the core electrons in an effective nuclear charge $Z_I^{\mathrm{eff}}$ and only regard the overlap of the valence electrons $n_I^{\mathrm{val}}$,

$$q_I = n_I^{\mathrm{val}} + Z_I^{\mathrm{eff}}. \tag{45}$$

If a Gaussian distribution of the valence electrons is assumed, analogous to Eq. (33),

$$n_I^{\mathrm{val}}\left(\frac{\Phi_I^*}{\pi}\right)^{3/2} e^{-\Phi_I^* r_I^2}, \tag{46}$$

the interatomic exchange energy becomes

$$V_{IJ}^{\mathrm{exch}} = C n_I^{\mathrm{val}} n_J^{\mathrm{val}} \left(\frac{a_{IJ}}{\pi}\right)^{3/2} e^{-a_{IJ} R_{IJ}^2}, \tag{47}$$

where the Gaussian product rule has been used and $a_{IJ}$ is defined in Eq. (35). To determine the prefactor $C$, we again use the limiting behavior, i.e., that the interparticle exchange term should approach the self-exchange term at short distances,

$$-\frac{1}{2}\eta_I^* = -\sqrt{\frac{\Phi_I^*}{2\pi}}. \tag{48}$$

The following relation fulfils this condition,

$$V_{IJ}^{\mathrm{exch}} = -\sqrt{\frac{a_{IJ}}{\pi}} e^{-a_{IJ} R_{IJ}^2} n_I^{\mathrm{val}} n_J^{\mathrm{val}}. \tag{49}$$

To be consistent with the model for the electrostatics, this energy term is written as a function of the charge transfer $q_{IM}$, and the charge is therefore rewritten as

$$q_I = Z_I^{\mathrm{eff}} + n_I^{\mathrm{val}} = Z_I^{\mathrm{eff}} + n_I^{(0)} + \sum_K q_{IK}, \tag{50}$$

where $n_I^{(0)} = -Z_I^{\mathrm{eff}}$ is the number of valence electrons in the unperturbed atom. Thus,

$$n_I^{\mathrm{val}} = n_I^{(0)} + \sum_K q_{IK}. \tag{51}$$

The total number of valence electrons in the atom is $n_I^{(0)}$ modified by the total amount of electrons given or received from other atoms through the variables $q_{IK}$. Equation (49) is rewritten as

$$V^{\mathrm{exch}} = -\sum_{I,K,J,M} \sqrt{\frac{a_{IJ}}{\pi}} e^{-a_{IJ}R_{IJ}^2} q_{IK} q_{JM} - 2\sum_{I,J,M} \sqrt{\frac{a_{IJ}}{\pi}} e^{-a_{IJ}R_{IJ}^2} n_I^{(0)} q_{JM} - \sum_{I,J} \sqrt{\frac{a_{IJ}}{\pi}} e^{-a_{IJ}R_{IJ}^2} n_I^{(0)} n_J^{(0)}. \tag{52}$$

The last term in Eq. (52) is independent of $q_{IK}$ and can therefore be ignored. Comparing with Eq. (9), the exchange terms modify $\chi_I^*$ as

$$\chi_I^* \rightarrow \chi_I^* - 2\sum_I \sqrt{\frac{a_{IJ}}{\pi}} e^{-a_{IJ}R_{IJ}^2} n_I^{(0)} \tag{53}$$

and $T_{IJ}^{(0)}$ as

$$T_{IJ}^{(0)} \rightarrow T_{IJ}^{(0)} - \sqrt{\frac{a_{IJ}}{\pi}} e^{-a_{IJ}R_{IJ}^2}. \tag{54}$$

Thus the exchange terms can be included by simply modifying the atomic electronegativity and the Coulomb interaction terms. An exchange repulsion energy as a modification of the Coulomb term has also been presented elsewhere.[89]

### C. Charge transport energy and distance-dependent chemical hardness

In the EMM, charge transfer occurs between two infinitely separated particles either because of a difference in electronegativity, which is the case if the two particles are different, or because of a difference in the external electrostatic potential, for example caused by a homogeneous external electric field.[76] Likewise, it can be realized that the EEM has a similar problem for infinitely long chains. The polarizability becomes infinite by charge transfer in infinitely long chains, thus the EEM may be referred to as a *metallic* model.

Consider a two-atom system, 1 and 2, where point-dipole terms are ignored. In this system there is only one bond $SP=12$ and thus Eq. (7) gives one equation to be solved,

$$(\eta_1^* + \eta_2^* - 2T_{12}^{(0)})q_{12} = -(\chi_{12}^* + \varphi_{12}^{\mathrm{ext}}). \tag{55}$$

In this case $q_1 = -q_2 = q_{12}$, which results in

$$q_1 = -q_2 = \frac{-\chi_{12}^*}{(\eta_1^* + \eta_2^*) - 2T_{12}^{(0)}} + \frac{-\varphi_{12}^{\mathrm{ext}}}{(\eta_1^* + \eta_2^*) - 2T_{12}^{(0)}}, \tag{56}$$

where the first term on the right-hand side gives the permanent atomic charges and the second term gives a contribution to the polarizability in the case of a homogeneous external electric field. For very long distances, $T_{12}^{(0)} \approx 0$, and Eq. (56) is reduced to

$$q_1 = -q_2 = \frac{-\chi_{12}^*}{\eta_1^* + \eta_2^*} + \frac{-\varphi_{12}^{\mathrm{ext}}}{\eta_1^* + \eta_2^*}, \tag{57}$$

which illustrates the shortcomings of the EEM.

The atom-pair charge $q_{IJ}$ in the Mulliken approach[90] may be written as

$$q_{IJ} = \sum_{i\in I}\sum_{j\in J} D_{ij}S_{ij}, \tag{58}$$

where $D_{ij}$ is a density matrix element, $S_{ij}$ is an overlap matrix element, and $i$ and $j$ are sums over basis functions restricted to atoms $I$ and $J$, respectively. The overlap between two basis functions $S_{ij}$ declines exponentially with the distance between atoms $I$ and $J$ (assuming $I \neq J$), and thus the charge transfer approaches zero at large interatomic distances.

It may be argued that an orbital overlap term of the form $S_{ij}$ is missing in Eq. (56). One may consider to add an overlap term to the electronegativity difference,[25,26]

$$\chi_{12}^* = (\chi_1^* - \chi_2^*)S_{12}, \tag{59}$$

such that a nonzero overlap of the orbitals of atoms 1 and 2 is required for a charge transfer. This modification would, however, only affect the permanent atomic electric moments and not the polarizability. Instead, we have chosen to modify the chemical hardness term as

$$(\eta_1^* + \eta_2^*)S_{12}^{-1}, \tag{60}$$

such that the required work for charge transfer increases exponentially with the distance between two atoms. Thus the energy terms in Eq. (9) of the form

$$\frac{1}{2}\eta_I^* q_{IK} q_{IM} \tag{61}$$

are modified as

$$\frac{1}{2}\eta_I^* S_{IK}^{-1/2} S_{IM}^{-1/2} q_{IK} q_{IM}. \tag{62}$$

Based on the Gaussian charge distribution in Eq. (33) a functional form for the overlap $S_{IJ}$ may be chosen as

$$S_{IJ} = e^{-a_{IJ}R_{IJ}^2}. \tag{63}$$

This scheme will solve the two-atom problem in Eq. (56) as the charge transfer will decline exponentially with the distance between two atoms. A distance-dependent chemical hardness has also been proposed elsewhere to get the correct dissociation behavior.[24] Assuming that $S_{IJ}=0$ for atom pairs $I$ and $J$ which are not neighbors, the charge transfer $q_{IJ}$ may be ignored for these pairs, which justify the use of a topology matrix $L_{IJ}$. However, if all atoms in the system are connected by a nonzero $S_{IJ}$ the model is in practice unmodified in the sense that charge transfer is allowed from one end of the molecule to the opposite end without an energy cost.

To investigate the problem with infinitely long chains a linear three-particle system is considered. If an electrical field is applied along the chain, charge will flow as

$$\overset{q_{KI}}{\bullet_K} \leftarrow \overset{q_{IM}}{\bullet_I} \leftarrow \bullet_M, \tag{64}$$

and charge are transported from atom $M$ through atom $I$ to atom $K$. Note that the charge on atom $I$ is given as $q_I = q_{IM} + q_{IK} = q_{IM} - q_{KI}$. A simple way of adding an energy for transporting charge through atom $I$ is

$$\epsilon \eta_I^* q_{KI} q_{IM}, \tag{65}$$

where $K \neq M$ and $\epsilon$ is an additional parameter larger than zero. The chemical hardness terms of the charge-charge energy for the three-particle system become

$$V^\eta = \frac{1}{2}\eta_K^* q_{KI}^2 + \frac{1}{2}\eta_I^*(q_{KI}^2 - 2(1-\epsilon)q_{KI}q_{IM} + q_{IM}^2) + \frac{1}{2}\eta_M^* q_{IM}^2. \tag{66}$$

The differentiation with respect to $q_{KI}$ and $q_{IM}$ gives

$$\frac{\partial V^\eta}{\partial q_{KI}} = (\eta_K^* + \eta_I^*)q_{KI} - (1-\epsilon)\eta_I^* q_{IM} \tag{67}$$

and

$$\frac{\partial V^\eta}{\partial q_{IM}} = (\eta_M^* + \eta_I^*)q_{IM} - (1-\epsilon)\eta_I^* q_{KI}. \tag{68}$$

If $\epsilon > 1$, the effective chemical hardness for atom $I$ will be negative. Therefore, $\epsilon$ must obey the following condition:

$$0 \leq \epsilon \leq 1. \tag{69}$$

In larger systems, charge will flow through many atoms, and the energy transport term in Eq. (65) is applied repeatedly. The idea is that the energy for transporting charge through atoms by Eq. (65) leads to a *nonmetallic* model when $\epsilon$ is close to 1, and a metallic model in the case $\epsilon = 0$. If $\epsilon = 0$ the EEM[8,15] is obtained and if $\epsilon = 1$ the AACT model[22] is obtained. Thus this model is similar to the split-charge model[23] in the sense that both EEM and AACT are obtained as limiting cases.

The $\epsilon$ parameter should be adjusted automatically depending on the character of the chemical bond. For example carbon-carbon $\pi$-bonds behave differently than carbon-carbon $\sigma$-bonds. Therefore, the correction in Eq. (65) is introduced by modifying Eq. (62) as

$$\frac{1}{2}\eta_I^* S_{IK}^{-1/2} S_{IM}^{-1/2} g_{I,KM}(R_{KI}, R_{IM}) q_{KI} q_{IM}, \tag{70}$$

where $g_{I,KM}(R_{KI}, R_{IM})$ is a function of the distances $R_{KI}$ and $R_{IM}$. The different charge-transfer characteristics of $\sigma$- and $\pi$-bonds will therefore rely on the small differences in the bond length between $\sigma$- and $\pi$-bonds.

To obtain Eq. (62) in the two-atom case we set $g_{I,KM} = 1$ when $K = M$. Furthermore, the energy expression in Eq. (70) becomes equivalent to Eq. (66) if $S_{IK} = S_{IM}$,

$$\eta_I^* \rightarrow \eta_I^* S_{IK}^{-1}, \tag{71}$$

and if

$$\epsilon = 1 - g_{I,KM}(R_{KI}, R_{IM}). \tag{72}$$

TABLE I. Bond distances for alkene molecules (atomic unit).

| No. C[a] | $\langle R_{I,I+1}\rangle$[b] | $S_{R_{I,I+1}}$[c] | $\langle R_{I-1,I}+R_{I,I+1}\rangle$[d] | $S_{R_{I-1,I}+R_{I,I+1}}$[e] |
|---|---|---|---|---|
| 2 | 2.5255 | ⋯ | ⋯ | ⋯ |
| 4 | 2.6175 | 0.1230 | 5.3060 | ⋯ |
| 6 | 2.6314 | 0.0999 | 5.3025 | 0.0112 |
| 8 | 2.6368 | 0.0876 | 5.3009 | 0,0111 |
| 10 | 2.6396 | 0.0795 | 5.2999 | 0.0106 |
| 14 | 2.6424 | 0.0689 | 5.2989 | 0.0096 |
| 18 | 2.6437 | 0.0623 | 5.2982 | 0.0088 |
| 22 | 2.6443 | 0.0573 | 5.2973 | 0.0080 |
| 26 | 2.6448 | 0.0536 | 5.2968 | 0.0074 |
| 48 | 2.6458 | 0.0418 | 5.2953 | 0.0056 |

[a] C is the number of carbon atoms.
[b] $R_{I,I+1}$ is the distance between two neighboring carbon atoms, while $\langle R_{I,I+1}\rangle$ is the average of $R_{I,I+1}$ for a given molecule.
[c] $S_{R_{I,I+1}}$ is the standard deviation of $R_{I,I+1}$ within the given molecule.
[d] $\langle R_{I-1,I}+R_{I,I+1}\rangle$ is the average of the sum of these two distances.
[e] $S_{R_{I-1,I}+R_{I,I+1}}$ is the standard deviation of $R_{I-1,I}+R_{I,I+1}$ within the given molecule

In an ideal linear chain, all distances between neighbors are equal, $R_{I-1,I} = R_{I,I+1}$. However, in alkene molecules with alternating double bonds, this is not the case. The distance between the carbons alternates, which makes it difficult to define a function $g_{I,KM}$ giving an $\epsilon$ small enough for the alkenes while being large enough for alkane molecules.

This is illustrated in Table I where bond-distance standard deviations are given for some alkene molecules. The standard deviation in bond distances for carbon in alkenes should be compared to the difference in the average bond distance in alkene and the average bond distance in alkane chains. A simple Gaussian function for each atom pair would not work as the small variation in bond distances will determine how close to 1 the function $g_{I,KM}$ can be, if it is also required that $g_{I,KM}$ should be close to zero for the alkane systems.

However, for alkene molecules with alternating double bonds, the sum $R_{I-1,I} + R_{I,I+1}$ varies much less compared to the bond distances $R_{I,I+1}$. From Table I, it is noted that the variation in $R_{I-1,I} + R_{I,I+1}$ is an order of magnitude smaller. Therefore the following form of $g_{I,KM}$ is adopted:

$$g_{I,KM}(R_{IK}, R_{IM}) = e^{-C(R_{IK} + R_{IM} - 2R_I^* - R_K^* - R_M^*)^2}, \tag{73}$$

where $C$ is a global parameter and $R_I^*$ is an additional atom-type parameter.

It is noted that the form of $g_{I,KM}$ used here has been designed for carbon single and double bonds. In Eq. (73), it is assumed that the sum of the distances $R_{IM}$ and $R_{IK}$ is less than the sum of the parameters $2R_I^* + R_K^* + R_M^*$. For example for carbon triple bonds, this assumption is not true and therefore the functional form in Eq. (73) would need some adjustments in this case.

In molecular systems where all atoms are bonded to at least one other atom the function $S_{IK}$ is of less importance. Since $S_{IK}$ should be close to one when $R_{IK} = R_{IK}^{\text{bond}}$, the parameter $R_I^*$ can be used to modify Eq. (63) as

$$S_{IK} = e^{-a_{IK}(R_{IK} - R_I^* - R_K^*)^2} \tag{74}$$

if $R_{IK} > R_I^* + R_K^*$ and $S_{IK} = 1$ otherwise. This form has the advantage that the model will be closer to the original EEM for molecular systems, while Eq. (63) is still obtained in the limit when $R_{IK}$ becomes large.

The modification in Eq. (70) only modifies $T^{(0)}_{SP,JM}$ in Eq. (17) when $S=J$, $P=M$, $K=J$, or $K=M$, or a combination of these. The modified $T^{(0)}_{SP,JM}$ tensor becomes, assuming all indexes $J$, $M$, $S$, and $P$ are different,

$$\begin{aligned}
T^{(0)}_{SP,SM} &= T^{(0)}_{SS} S^{-1}_{SP} S^{-1}_{SM} g_{S,PM} - T^{(0)}_{PS} - T^{(0)}_{SM} + T^{(0)}_{PM}, \\
T^{(0)}_{SP,JS} &= T^{(0)}_{SJ} - T^{(0)}_{PJ} - T^{(0)}_{SS} S^{-1}_{SP} S^{-1}_{JS} g_{S,PJ} + T^{(0)}_{PS}, \\
T^{(0)}_{SP,PM} &= T^{(0)}_{SP} - T^{(0)}_{PP} S^{-1}_{PS} S^{-1}_{PM} g_{P,SM} - T^{(0)}_{SM} + T^{(0)}_{PM}, \\
T^{(0)}_{SP,JP} &= T^{(0)}_{SJ} - T^{(0)}_{PJ} - T^{(0)}_{SP} + T^{(0)}_{PP} S^{-1}_{PS} S^{-1}_{PJ} g_{P,SJ}, \\
T^{(0)}_{SP,SP} &= T^{(0)}_{SS} S^{-1}_{SP} S^{-1}_{SP} - T^{(0)}_{PS} - T^{(0)}_{SP} + T^{(0)}_{PP} S^{-1}_{SP} S^{-1}_{SP}, \\
T^{(0)}_{SP,PS} &= T^{(0)}_{PS} - T^{(0)}_{SS} S^{-1}_{SP} S^{-1}_{SP} - T^{(0)}_{PP} S^{-1}_{SP} S^{-1}_{SP} + T^{(0)}_{SP}, \\
T^{(0)}_{SP,JM} &= T^{(0)}_{SJ} - T^{(0)}_{PJ} - T^{(0)}_{SM} + T^{(0)}_{PM}.
\end{aligned} \tag{75}$$

This tensor still has the symmetries in Eq. (19) and only the cases $S>P$ and $J>M$ need to be considered in the final equations.

Without the additional charge transport energy term, the total energy is only determined by the charge $q_I$, and the charge transfers $q_{JM}$ are not necessarily uniquely determined by minimizing the energy. For example, in ring structures there are many sets of charge transfers which give the same set of charges $q_I$, and therefore the final matrix governing $q_{JM}$ will be singular.[25] However, the introduction of a charge transport energy takes care of this problem. Consider a ring structure of $K$ identical atoms with hardness $\eta^*$ and $\epsilon = 1 - g_{I,KM}$. Each atom gives a charge $q_{IK}$ to the next atom in the ring, at the same time as each atom receives the same amount of charge from the previous atom. In this system, the atomic charges are zero, so the Coulomb energy and the unmodified hardness energy are also zero. The only nonzero energy is the cost of transporting charge, which can be written as

$$K \epsilon \eta^* q_{IK}^2. \tag{76}$$

When $\epsilon > 0$, this energy is at minimum when $q_{IK}=0$, while $q_{IK}$ cannot be uniquely determined if $\epsilon = 0$.

## III. CALCULATIONS AND PARAMETRIZATION

It is advantageous to use quantum chemical calculations for the parametrization of a molecular mechanics model since a consistent data set may be obtained. In our previous work, we have used Hartree–Fock calculations for the parametrization.[50,54,59,91] In principle, DFT gives an improved description of molecular properties over Hartree–Fock, but for polarizabilities of large systems many functionals present problems and several improvements have been suggested.[92–100] We therefore use current-DFT (c-DFT) for the calculation of the polarizability with the AUG/ATZP basis set, which gives improved results for the polarizability for large systems.[101] For the dipole moment and geometry optimization, the BLYP functional and the TZP basis set were employed. The ADF software[102–104] was used for all quantum chemical calculations. DFT calculations have previously been used to parametrize the PDI model for amino acids.[45]

To test the model, a parametrization has been carried out for alkanes and alkenes with alternating double bonds, where both the molecular polarizability and the dipole moment behave differently as a function of the chain length. In the calculations of the dipole moment, an aldehyde group has been added to the end of the molecule to obtain a nonzero dipole moment. It is also advantageous that the alkene systems are planar. Since the charge-transfer term only gives contributions to the in-plane components of the polarizability, planar molecules are useful to establish the correct balance between charge and dipole terms to the polarizability.

In addition to parametrizing the model for molecules, the model is analyzed analytically for model chains in Appendices A and B. The two different types of results serve two different purposes. Calculations on molecules show that the model is capable of reproducing realistic data, while analytical results provide a deeper understanding of the model. However, both types of results prove that the model is capable of predicting the correct scaling of both the dipole moment and the polarizability.

The topology element $L_{IK}$ was set to 1 if the atoms $I$ and $K$ are bonded and zero otherwise. When determining if two atoms are bonded or not, the distance $R_{IK}$ was compared to known bond distances. If $R_{SP} \leq 1.3 R_{SP}^{\text{bond}}$, $L_{SP}$ is one and otherwise it is zero. The bond distances are chosen as $R_{\text{CH}}^{\text{bond}} = 1.09$ Å, $R_{\text{CC}}^{\text{bond}} = 1.54$ Å, $R_{\text{CO}}^{\text{bond}} = 1.36$ Å, and $R_{\text{OH}}^{\text{bond}} = 0.96$ Å, respectively.

The following parameters have thus been used: the atomic polarizability $\alpha_I$, a width of a Gaussian $\Phi_I^*$, which describes the damping of electrostatics, exchange interactions and the overlap $S_{IK}$, the electronegativity $\chi_I^*$, and the chemical hardness $\eta_I^*$, and to describe the function $g_{I,KM}$ we have $R_I^*$ and a global parameter $C$. It is assumed that hydrogen atoms only get a charge transfer from neighboring atoms, thus $g_{I,KM}=0$ when one of the involved atoms is a hydrogen.

Different atom-type parameters have been used for the dipole moment and the polarizability. For the response to an external electric field the bandgap is important, while the dipole moment may be regarded as a result of the formation of chemical bonds and molecules. However, for each property, the same parameters have been used for all molecules.

Molecular dipole moments and polarizabilities were calculated using the model and compared to data obtained from DFT and c-DFT respectively, and in both cases, the parameters were optimized to minimize the absolute root mean square deviation (RMSD). In this respect, molecules with a large dipole moment/polarizability are more important than molecules with small values of the properties.

### A. Dipole moment

In Fig. 1, the molecular dipole moment of the alkenal and alkanal molecules is given as a function of the number of

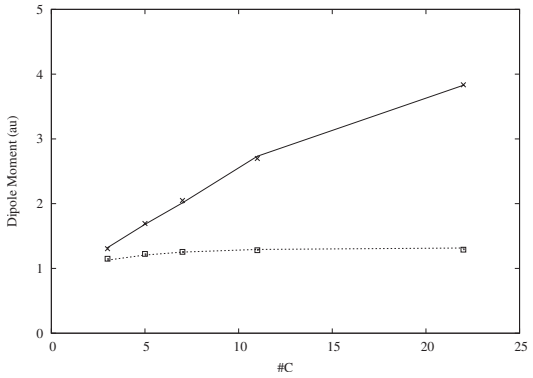


FIG. 1. The dipole moment as a function of the number of carbon atoms in alkenal and alkanal chains, respectively. Alkenal: model —, DFT ×; Alkanal: model ·····, DFT □.

carbon atoms, while the optimized parameters are presented in Table II. The RMSD is 0.05 a.u., which is satisfyingly low compared to the magnitude of the molecular dipole moment. Figure 1 shows that the model is capable of modeling the dipole moment for both the alkanal and alkenal molecules for various chain lengths. Note that the total dipole moment is almost constant for the alkanal systems, which had not been possible to obtain with the EEM without introducing an extra energy term for transporting charge.

The analysis of the dipole moment is presented in Appendix A. A linear chain composed of identical atoms apart from one atom with higher electronegativity at one end of the chain is studied. The atomic dipole moments are only nonzero due to interactions with atomic charges, and therefore it is assumed that the atomic dipole moments are of less importance for all systems. In the case $\epsilon \approx 0$, the molecular dipole moment is given by Eq. (A11), and in the case $\epsilon \approx 1$ the dipole moment is given by Eq. (A7), where in both cases the Coulomb interactions are neglected. In the first case ($\epsilon = 0$), the electronegative atom receives charge from the entire system, while in the latter case ($\epsilon = 1$) the electronegative atom receives charge only from its nearest neighbor. Thus when $\epsilon = 0$ the effect of the electronegative atom is global, while when $\epsilon = 1$ the effect is local. As a direct consequence of this fact, the Coulomb interaction becomes small for large systems in the case $\epsilon \approx 0$ but noticeable when $\epsilon \approx 1$. An approximation of the effect of the Coulomb interaction for the latter case is obtained in Eq. (A30).

The dipole moments of the alkanals are almost constant while the dipole moment for the alkenals increases with the length of the molecule as found in Fig. 1. Thus Eqs. (A11) and (A7) are good approximations for the two different systems, and the differences can be explained in terms of the differences in $\epsilon$.

TABLE II. Parameters for dipole moment model (atomic unit).

| Atom | $\alpha_I$ | $\Phi_I^*$ | $\chi_I^*$ | $R_I^*$ | $\eta_I^*$ |
|---|---|---|---|---|---|
| H | 0.9601 | 5.3712 | 0.0[a] | ··· [b] | 0.4 |
| C | 8.0700 | 0.0824 | 0.0649 | 1.313 | 1.0 |
| O | 3.7000 | 0.0038 | 0.8353 | 0.775 | 1.1 |
| | | $C=5.0$ | | | |

[a]The electronegativity of hydrogen is chosen to be zero.
[b]$g_{I,KM}=0$ when at least one of the atoms $I$, $K$, or $M$ is hydrogen.

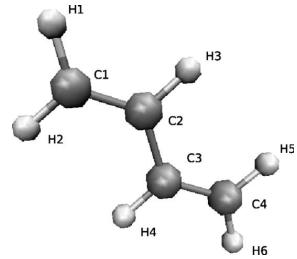


(a)Butadiene

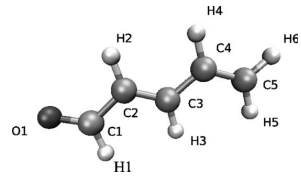


(b)Pentadienal

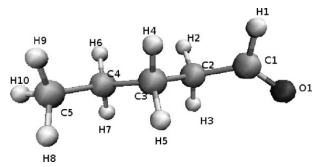


(c)Pentanal

FIG. 2. Atom labels for butadiene, pentadienal, and pentanal. For the alkane and alkanal molecules, the $x$-axis is along the alkane chain, the $y$-axis is in the carbon-carbon plane, and the $z$-axis is perpendicular to the carbon-carbon plane. The alkene and alkenal molecules are planar molecules, and for these systems the $z$-axis is the out-of-plane axis, the $x$-axis is along one C–C double bond (along the bond between C2 and C3 in pentadienal and along the bond between C1 and C2 in butadiene), and the $y$-axis is the other in-plane axis.

The molecular coordinate systems and the atomic labels for some molecules are given in Fig. 2. The molecular dipole moment can be divided into a charge-transfer part and a contribution from atomic dipole moments. For pentadienal, the charge-transfer part is $\mu_x = 1.47$ a.u., while the total dipole moment is 1.56 a.u. For $\mu_y$, the same trend is found where the charge-transfer part alone gives a dipole moment of 0.52 a.u. of the total moment of 0.62 a.u. The major part of the molecular dipole moment is therefore given by the charge-transfer term as expected.

From Table III it is found that the atomic dipole moments are small. Furthermore, the main difference between the charge distribution in pentanal and pentadienal is that the charge on the first carbon (C1) is higher in pentanal than in pentadienal. However the charges on the other carbon atoms (C2–C5) are higher in pentadienal as compared to pentanal. These charges are also higher when compared to the carbon

TABLE III. Atomic charges and dipole moments (atomic unit).

| | Pentanal | | | | | Pentadienal | | | | Butadiene | | |
|---|---|---|---|---|---|---|---|---|---|---|---|---|
| Atom | $q$ | $\mu_x$ | $\mu_y$ | $\mu_z$ | Atom | $q$ | $\mu_x$ | $\mu_y$ | Atom | $q$ | $\mu_x$ | $\mu_y$ |
| O1 | −0.382 | −0.005 | −0.001 | −0.002 | O1 | −0.399 | −0.006 | −0.001 | | | | |
| C1 | 0.329 | −0.007 | 0.001 | −0.007 | C1 | 0.270 | −0.020 | −0.003 | | | | |
| C2 | −0.035 | 0.059 | 0.055 | −0.025 | C2 | 0.003 | 0.036 | 0.047 | C1 | −0.132 | 0.042 | −0.005 |
| C3 | −0.104 | 0.050 | 0.048 | −0.016 | C3 | −0.017 | 0.037 | 0.049 | C2 | −0.064 | −0.015 | −0.032 |
| C4 | −0.118 | 0.040 | −0.008 | −0.030 | C4 | −0.029 | 0.040 | 0.006 | C3 | −0.064 | 0.015 | 0.032 |
| C5 | −0.193 | −0.013 | 0.007 | 0.009 | C5 | −0.097 | −0.003 | 0.006 | C4 | −0.132 | −0.042 | 0.005 |
| H1 | 0.011 | 0.009 | −0.016 | 0.008 | H1 | 0.016 | 0.008 | −0.015 | H1 | 0.066 | 0.004 | −0.005 |
| H2 | 0.041 | 0.005 | 0.005 | 0.004 | H2 | 0.040 | −0.003 | 0.008 | H2 | 0.065 | 0.004 | 0.004 |
| H3 | 0.041 | −0.001 | 0.008 | −0.004 | H3 | 0.045 | 0.004 | 0.001 | H3 | 0.065 | −0.003 | −0.006 |
| H4 | 0.052 | 0.004 | 0.004 | −0.002 | H4 | 0.052 | 0.002 | 0.001 | H4 | 0.065 | 0.003 | 0.006 |
| H5 | 0.051 | 0.004 | 0.003 | −0.002 | H5 | 0.057 | 0.001 | 0.002 | H5 | 0.065 | −0.004 | −0.004 |
| H6 | 0.058 | 0.003 | >−0.001 | −0.004 | H6 | 0.060 | <0.001 | <0.001 | H6 | 0.066 | −0.004 | 0.005 |
| H7 | 0.058 | 0.004 | −0.002 | −0.001 | | | | | | | | |
| H8 | 0.063 | −0.002 | 0.003 | −0.001 | | | | | | | | |
| H9 | 0.063 | 0.001 | 0.001 | 0.003 | | | | | | | | |
| H10 | 0.067 | −0.002 | −0.002 | <0.001 | | | | | | | | |

charges in butadiene. As expected, the charge transfer to the carbon atom in the carbonyl group is redistributed to the neighboring carbon atoms in a $\pi$-system, whereas it is almost localized to the carbonyl group for the alkanes. Except for the charge on the first hydrogen atom (H1), which is slightly lower in pentadienal and pentanal compared to butadiene, the hydrogen charges are similar in all three cases. Thus the charge transfer between hydrogen and carbon is not significantly altered by the carbonyl group.

The charge distribution in alkanal and alkenal is not as simple as in the analysis of the model chain, mainly due to the small charge transfer between hydrogen and carbon. However, the main result that the charge transfer is more localized in pentanal as compared to pentadienal is in agreement with the analytical results in Appendix A.

### B. Polarizability

In Table IV, the parameters for the polarizability model are presented. In Figs. 3 and 4, the model is compared to c-DFT calculations by presenting the polarizability per carbon atom versus the number of carbon atoms. Presenting the polarizability per carbon atom makes the transition from metallic behavior (polarizability scale as the number of atom $K^2$ or higher) to nonmetallic behavior (polarizability proportional to the number of atom $K$) clearer in the figures since the polarizability per carbon atom approaches a constant in the latter case. The RMSD is 21 a.u., which is small compared to the size of the polarizabilities. Since the errors are small both for the alkane and the alkene molecules, we find that the model is capable of describing the molecular polarizability in both cases. Comparing Figs. 3 and 4, it is noted that the polarizabilities for alkene and alkane behave differently. The polarizability for the alkenes varies more both with respect to length and the orientation of the molecule.

TABLE IV. Parameters for the polarizability model (atomic unit).

| Atom | $\alpha_I$ | $\Phi_I^*$ | $R_I^*$ | $\eta_I^*$ |
|---|---|---|---|---|
| H | 0.9601 | 0.0736 | ··· [a] | 0.4 |
| C | 8.0700 | 0.1080 | 1.2996 | 1.0 |
| | | $C$=6.0 | | |

[a] $g_{I,KM}$=0 when at least one of the atoms $I$, $K$ or $M$ is hydrogen.

In Appendix B, the polarizability is calculated for a linear chain of identical atoms in two different cases. When $K\epsilon \ll 1$, where $K$ is the number of atoms and $\epsilon = 1 - g_{I,KM}$, it is argued that the polarizability along the linear chains scales as at least $K^2$. In the other case, where $K\epsilon \gg 1$, the polarizability is given in Eqs. (B43) and (B44). It is found that the polarizability is proportional to the number of atom $K$ and therefore scales with the length of the chain as a nonmetallic system should. Also in this case, both the Coulomb and the charge-dipole interactions become negligible. Thus the charge-transfer terms of the polarizability are independent of the point-dipole term when $K\epsilon \gg 1$. In the other case $K\epsilon \ll 1$, neither the Coulomb interaction nor the charge-dipole interactions are necessarily small.

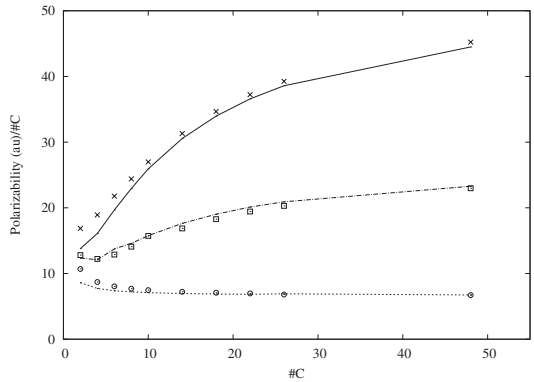


FIG. 3. The polarizability per carbon atom for alkene chains with alternating double bonds. $xx$-component: model —, c-DFT ×; $yy$-component: model −·−, c-DFT □; $zz$-component: model ···, c-DFT ○.

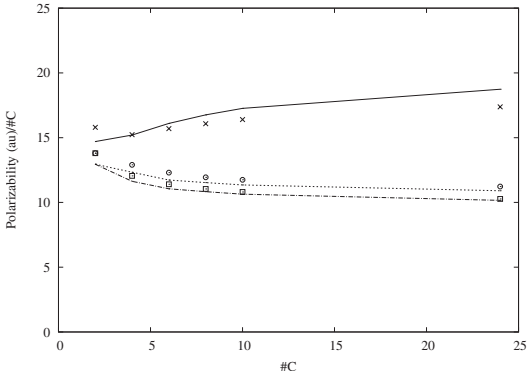


FIG. 4. The polarizability per carbon atom for alkanes. *xx*-component: model —, c-DFT ×; *yy*-component: model –·–, c-DFT □; *zz*-component: model ···, c-DFT ○.

The similarities between a linear chain composed of identical atoms and the alkane and alkene chains are evident. The polarizability for both the alkane and alkene chains scales linearly with the length of the chain for long chains. Therefore, for long chains Eq. (B43) is valid for both cases, where the differences between the systems may be explained only in terms of $\epsilon=1-g_{I,KM}$. The analytical results also predict that the scaling of the polarizability changes from quadratic (or higher) to linear when going from a case where $K\epsilon \ll 1$ to $K\epsilon \gg 1$. For alkene chains this is exactly what both the model and c-DFT calculations give (see Fig. 3). Alkene chains start to scale linearly at ~20 carbon atoms, and it is noted that putting $20\epsilon=1$ gives a good starting point for determining the parameters in $g_{I,KM}$ in Eq. (73). For alkane chains, $\epsilon$ is large enough such that $K\epsilon$ is never much smaller than 1. Therefore it scales linearly with the length of the chain for all $K$. This shows how important it is to get the right form of $g_{I,KM}$. An $\epsilon=1-g_{I,KM}$ of 0.05 is very different from 0.01, since the latter will start to scale linearly with the number of carbons atoms at $K=100$ instead of at $K=20$. Small differences in $\epsilon$ may lead to huge differences in the polarizability for large systems.

In Fig. 5, the charge-transfer and the point-dipole contributions to the polarizability are presented. For all systems, the point-dipole term per carbon atom is constant, which is in agreement with Eq. (B43). For short alkene chains, the charge-transfer part of the polarizability per carbon atom increases for the in-plane components but approaches a constant for longer chains. In these cases, the charge-transfer term dominates. The out-of-plane component for the alkene chains obviously has no charge-transfer component. For alkane systems, the point-dipole terms dominate for all components. This illustrates that charge-transfer may or may not be important for the molecular polarizability depending on what kind of system that is studied.

In Eq. (B43), it is seen that it is a combination of $\epsilon=1-g_{I,KM}$ and $\eta^*$ that determines how large the charge-transfer term is. Thus $\epsilon$ describes both when the polarizability starts to scale linearly with the system and the relative importance of the charge-transfer term in the model. This illustrates that systems behave qualitatively differently when $\epsilon \approx 0$ and when $\epsilon \approx 1$, and $\epsilon$ can be regarded as the most important descriptor of the system.

### C. Small Φ-parameters

When calculating the dipole moment, we excluded the electronegativity modification due to exchange terms in Eq. (53), since the contribution becomes too dominant. This is partly because the parameter $\Phi_I^*$ is used to describe both the damping in the electrostatics and the exchange contribution is too small (see Tables II and IV), since the Gaussian function describing the charge distribution for a single carbon atom spans over several atoms. This is a shortcoming of the present model. If applying Eq. (41) to link $\eta_I^*$ to $\Phi_I^*$, small $\Phi_I^*$ parameters would likewise lead to small $\eta_I^*$. Therefore separate parameters for $\eta_I^*$ and $\Phi_I^*$ were applied.

The term $S_{IJ}$ in Eq. (70) is only included for $I$ and $J$ if $L_{IJ}=1$. Since we choose to set $L_{IJ}=1$ when the two atoms $I$ and $J$ are bonded and zero otherwise, $S_{IJ}$ is more or less a constant. Therefore this term may seem less important and indeed when doing calculations on molecules where all atoms are bonded to each other, it is. However if the model is used for intermolecular complexes, it may be critical to be able to gradually turn off or on the ability of transferring charge between the atoms involved. It is therefore useful for further work that the two-atom problem in Eq. (57) has been solved. Therefore, an additional potential problem with the small $\Phi_I^*$ parameters is that the overlap $S_{IK}$ declines too slowly with the distances between the subsystems (molecules). Since only molecules and not molecular complexes are studied this issue is not critical here.

The main reason that the $\Phi_I^*$ parameters become small in the parametrization of the polarizability is that for alkenes this parameter is used to correct the relative size of the in-plane components versus the out-of-plane components. To fix this problem it is possible to do a modification of the spherically symmetric atomic polarizability parameter according to its chemical neighborhood.[42] This might be used to balance the in-plane components versus the out-of-plane components of the polarizability for planar molecules, and then hopefully the $\Phi_I^*$ parameters are not required to be small. This will be examined in a future publication.

## IV. CONCLUSIONS

We have shown through both analytical calculations on model chains and numerically on molecules that in adopting a charge-transfer model and adding a charge transport term, the polarizability scales correctly with the size of the system. We have seen that the model is capable of describing both systems where charge transfer is important and where it is unimportant, and that the model is capable of predicting a smooth transition between the different cases. Similarly, the correct scaling for the molecular dipole moment is achieved. One advantage of the model is that the scaling of the dipole moment and polarizability with system size can be characterized by a single function, $\epsilon=1-g_{I,KM}$. The model also

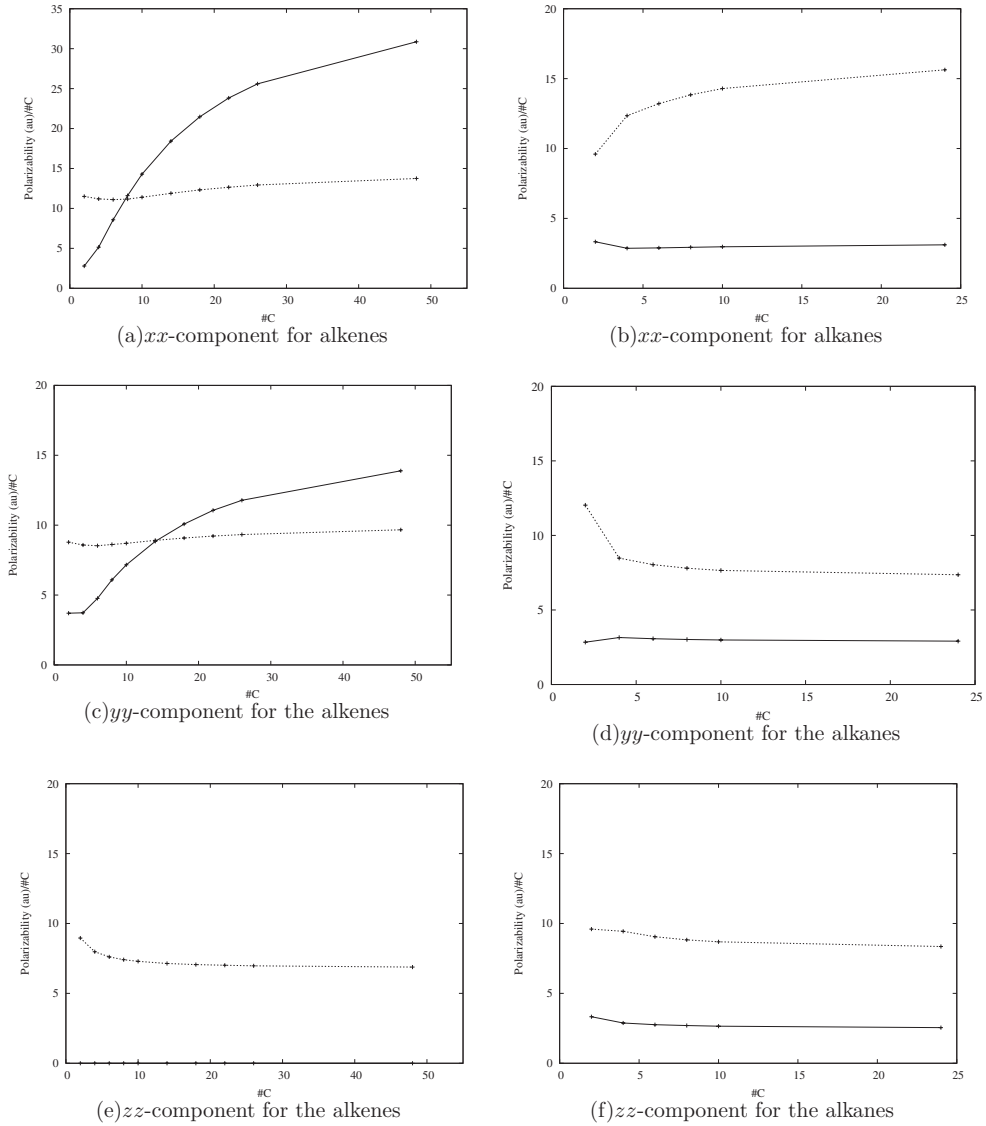


FIG. 5. Charge-transfer (—) and point-dipole (···) contributions to the polarizability.

solves the two-atom problem, since the model gives a charge transfer between two atoms which decays exponentially with the distance between them.

## ACKNOWLEDGMENTS

We would like to thank Gaétan Weck for fruitful discussions. Support from the Norwegian Research Council through a Strategic Industry Program (Grant No. 164603/I30), from a NANOMAT program (Grant No 158538/431), and a grant of computer time are acknowledged.

## APPENDIX A: DIPOLE MOMENT OF LINEAR CHAIN

The system considered is a linear chain composed of identical atoms except for one atom at the end which has a much higher electronegativity. Except for a higher electronegativity, this atom has the same characteristics as the other atoms.

Let the chemical hardness for all atoms be $\eta^*$, the distance between neighboring atoms be $R_0$, and let $\epsilon=1-g(R_0,R_0)$ be a parameter of the model. Let the electronegative atom be atom number zero at the right end of the chain, such that the position of atom $I$ is given by $R_I=-IR_0$. Furthermore let the number of atoms in the chain be $K+1$. The

topology elements in Eq. (6) are $L_{IK}=1$ when $K=I\pm 1$ and zero otherwise, thus only a charge transfer between nearest neighbors is considered. Let us assume that all atoms are within a bonding distance such that $S_{SP}=1$ for neighboring atoms.

### 1. Point-dipole model

The point-dipole model without an external electric field and without any interactions with charges is simply

$$T^{(2)}_{IJ,\alpha\beta}\mu_{J,\beta}=0. \tag{A1}$$

Since the matrix $T^{(2)}_{IJ,\alpha\beta}$ is not singular, all $\mu_{J,\beta}=0$. Therefore the atomic point dipoles will only be nonzero due to the interaction with atomic charges. It is assumed that atomic point dipoles are small and that the main contribution to the molecular dipole moment will arise from the charge-transfer terms.

### 2. Charge-transfer model without Coulomb interaction

For simplicity let us assume that all atoms have an electronegativity equal to zero apart from the first atom which has the electronegativity $\chi^*$. In a chain of $K+1$ atoms, the model gives the following set of equations when ignoring Coulomb interactions and point-dipole terms:

$$2\eta^* q_{01}-\eta^*(1-\epsilon)q_{12}=-\chi^* \quad N=0, \tag{A2}$$

$$-\eta^*(1-\epsilon)q_{N-1,N}+2\eta^* q_{N,N+1}-\eta^*(1-\epsilon)q_{N+1,N+2}=0 \quad 1\le N\le K-2, \tag{A3}$$

$$-\eta^*(1-\epsilon)q_{K-2,K-1}+2\eta^* q_{K-1,K}=0 \quad N=K-1. \tag{A4}$$

The sum of all $K$ equations above gives

$$2\epsilon\eta^*\left(\sum_I q_{I,I+1}\right)+\eta^*(1-\epsilon)(q_{01}+q_{K-1,K})=-\chi^*. \tag{A5}$$

This equation is useful for some special cases. If $\epsilon=1$, the last term on the left-hand side becomes zero,

$$\sum_I q_{I,I+1}=-\frac{\chi^*}{2\epsilon\eta^*}, \tag{A6}$$

which gives that

$$\mu^{\mathrm{mol}}=-\frac{\chi^* R_0}{2\epsilon\eta^*}. \tag{A7}$$

In this case the dipole moment is independent of the length of the chain, which for a nonmetallic system is reasonable.

In the case where $\epsilon=0$ and by assuming that $q_{01}$ is much larger than the last $q_{K-1,K}$, it is realized from Eq. (A5) that $q_{01}$ is found directly and gives the charge on the electronegative atom. However, to find the dipole moment, the distribution of all other charges also has to be known. Let us treat the charge on the electronegative atom given as $q_0$, and the potential energy for all other charges $q_I$ is obtained as

$$V=\sum_I \eta^* q_I^2+\lambda\left(\sum_I q_I-(-q_0)\right), \tag{A8}$$

where $\lambda$ is a Lagrangian multiplier. In this system the charge is distributed evenly among all atoms and therefore,

$$q_I=-\frac{q_0}{K}=-\frac{q_{01}}{K}. \tag{A9}$$

From this calculation it is seen that $q_I=q_{I-1,I}-q_{I,I+1}=q_0/K$ and that the approximation $q_{01}\gg q_{K-1,K}$ should be valid for large $K$. Specifically $q_{K-1,K}=q_{01}/K$ and from Eq. (A5),

$$q_0=q_{01}=-\frac{K}{K+1}\frac{\chi^*}{\eta^*}. \tag{A10}$$

Thus for large $K$, $q_0$ simply becomes $\chi^*/\eta^*$. From the charge distribution in Eq. (A9) the molecular dipole moment $\mu^{\mathrm{mol}}$ is calculated as

$$\mu^{\mathrm{mol}}=\sum_I^K \frac{q_o}{K}IR_0=\left(\frac{q_0R_0}{K}\right)\sum_I^K I=-(K+1)\frac{\chi^* R_0}{2\eta^*}. \tag{A11}$$

The model is now analyzed in two special cases. The first is the case where $\epsilon=1$ and the other is the case where $\epsilon=0$. But what about the case where $\epsilon\ll 1$ but $K$ is so large such that $K\epsilon$ is small but not negligible? In the case where $K\to\infty$ and $\epsilon=0$, Eq. (A9) gives

$$q_{I-1,I}-q_{I,I+1}=-q_0/K=0, \tag{A12}$$

and therefore for a general charge transfer term,

$$q_{I,I+1}=-\frac{\chi^*}{\eta^*}. \tag{A13}$$

Let us take this solution as the starting point for the case where $1\gg\epsilon>0$ and for large $K$. In an infinite chain there is no last atom, and therefore Eq. (A5) becomes

$$2\epsilon\eta^*\left(\sum_I q_{I,I+1}\right)+\eta^*(1-\epsilon)q_{01}=-\chi^*. \tag{A14}$$

In the case $1\gg\epsilon>0$ the charge distribution in Eq. (A13) is incorrect for large $K$, since the term $2\epsilon\eta^*(\Sigma_I q_{I,I+1})=2\eta^* K\epsilon\langle q_{I,I+1}\rangle$ would not be negligible. Specifically for the first charge transfer $q_{01}$, by setting $1-\epsilon\approx 1$,

$$q_0=q_{01}=-\frac{\chi^*}{\eta^*}-2K\epsilon\langle q_{I,I+1}\rangle\equiv-\left(\frac{\chi^*}{\eta^*}-\delta\right), \tag{A15}$$

where $\delta$ is positive and equal to $-2K\epsilon\langle q_{I,I+1}\rangle$. Using Eq. (A2) the second charge transfer $q_{12}$ is obtained as

$$q_{12}=-\left(\frac{\chi^*}{\eta^*}-2\delta-2q_{01}\epsilon+O(\epsilon^2)\right), \tag{A16}$$

and in general from Eq. (A3),

$$q_{N-1,N}=-\left(\frac{\chi^*}{\eta^*}-N\delta+O(\epsilon)\right), \tag{A17}$$

which can be shown by induction. As we increase $N$ and go further and further away from the first charge transfer, the value of the charge transfer drops steadily down to a point where the terms of order $\epsilon$ cannot be neglected. Thus in this

model the effect of a high electronegative atom will have a limited range as long as $\epsilon > 0$.

Now, consider the charge of the atom with the high electronegativity. From Eq. (A15),

$$\delta = -2\epsilon\left(\sum_I q_{I,I+1}\right), \tag{A18}$$

and since all $q_{I,I+1}$ are assumed to be negative, the sum increases with the number of terms in the sum. Therefore for small $\epsilon$, the charge on the electronegative atom, which is given by $q_{01}$ in Eq. (A15), will be smaller for larger chains. But since $q_{N,N+1}$ drops to zero as $N$ increases, $\delta$ will reach a point where it is practically independent of the large number of atoms in the system.

From Eq. (A2) it is realized that for the case $\epsilon \approx 1$, the charge on the electronegative atom is independent of the number of atoms and is given by

$$q_0 = -\frac{\chi^*}{2\eta^*}. \tag{A19}$$

Note that there is a factor of one half between this and the case where we have a long chain and $\epsilon = 0$.

### 3. Coulomb perturbation

The charge distribution in Eq. (A9) is now used to calculate a Coulomb perturbation to the energy of the system for the case where $\epsilon = 0$. As previously, the large number of atoms is large. If $\epsilon = 0$, for atom $I \geq 1$,

$$q_I = -\frac{q_0}{K}. \tag{A20}$$

The Coulomb interaction is given as

$$\frac{1}{2}\sum_{I,J} q_I T_{IJ}^{(0)} q_J = \sum_{I,J>I} q_I T_{IJ}^{(0)} q_J. \tag{A21}$$

For the interaction between the electronegative atom and all the other atoms,

$$\sum_J^K q_0 T_{0J}^{(0)} q_J = -\frac{q_0^2}{R_0}\frac{\sum_J^K 1/J}{K}, \tag{A22}$$

where we have used that $1/R_{0J} = 1/(JR_0)$. By using the right-hand side of Eq. (A21), the Coulomb interaction for atom $I$ can be calculated as

$$\sum_{J=I+1}^K q_I T_{IJ}^{(0)} q_J = \frac{q_0^2}{R_0}\frac{\sum_{J=1}^{K-I} 1/J}{K^2}. \tag{A23}$$

When $K \to \infty$ this term will be independent of which atom $I$ we are looking at. Furthermore, since there are $K$ terms similar to Eq. (A23), the total Coulomb interaction is

$$\sum_{I,J>I}^K q_I T_{IJ}^{(0)} q_J = \sum_J^K q_0 T_{0J}^{(0)} q_J + K\sum_{J=I+1}^K q_I T_{IJ}^{(0)} q_J$$
$$= -\frac{q_0^2}{R_0}\frac{\sum_J^K 1/J}{K} + \frac{q_0^2}{R_0}\frac{\sum_J^K 1/J}{K} = 0. \tag{A24}$$

Since $\Sigma_J^K 1/J \sim \ln K$,

$$\frac{1}{K}\sum_J^K \frac{1}{J} \sim \frac{\ln K}{K}, \tag{A25}$$

which approaches zero as $K$ becomes large, and the two terms in Eq. (A24) thus go to zero individually. It does not go fast to zero, but still goes to zero, and becomes negligible compared to the energies $\eta^* q_0^2$ and $\chi^* q_0$. In the case where $\epsilon = 0$ and the number of atom $K$ is large, the Coulomb interaction becomes small. This is because all atoms apart from the electronegative atom will have practically no charge.

In the case where $\epsilon = 1$, the starting charge distribution is the following:

$$q_0 = -q_1, \tag{A26}$$

$$q_I = 0 \quad I \geq 2, \tag{A27}$$

In this case, the perturbative Coulomb energy becomes

$$q_0 T_{01}^{(0)} q_1, \tag{A28}$$

which is a trivial perturbation to the energy but not negligible. Assuming that Eqs. (A26) and (A27) are approximately true also when including the Coulomb interaction terms, a two particle problem is obtained, which has the solution

$$q_0 = -q_1 = -\frac{\chi^*}{2(\eta^* - T_{01})}, \tag{A29}$$

which again gives the dipole moment as

$$\mu^{\text{mol}} = -\frac{R_0 \chi^*}{2(\eta^* - T_{01})}. \tag{A30}$$

As a conclusion, for the case where $\epsilon \approx 1$ the problem becomes local, and the main charge transfer is between the electronegative atom and its closest neighbor. When $\epsilon \approx 0$ the problem becomes nonlocal and the electronegative atom receives charge from the entire system. The charge will be distributed evenly among all other atoms and the Coulomb interaction becomes negligible.

## APPENDIX B: POLARIZABILITY OF A LINEAR CHAIN

The polarizability is calculated for a long linear chain of identical atoms by calculating it term by term. In the first case only chemical hardness terms are included. Then it is demonstrated that the Coulomb interaction becomes negligible as long as periodic boundary conditions can be applied. After that, the polarizability within the PDI model is calculated. Finally, it is shown that charge-transfer and point-dipole terms are independent of each other in long chains.

### 1. Charge transfer without Coulomb interactions

The topology elements in Eq. (6) are $L_{IK}=1$ when $K=I\pm 1$ and zero otherwise, thus only the charge transfer between the nearest neighbors is considered. In a long linear chain, all equations are equal, apart from the equations for the first and last atom pairs. Let us assume that all atoms are within a bonding distance such that $S_{SP}=1$ for neighboring atoms. Let the chemical hardness be $\eta^*$, the distance between neighboring atoms be $R_0$, and let $\epsilon=1-g(R_0,R_0)$ be a parameter of the model. Let the electrical field be uniform and point in the direction of the chain, such that

$$-\frac{d(\varphi_{I+1}-\varphi_I)}{dE}=R_0. \tag{B1}$$

Let the number of atoms be $K+1$ and the allowed charge transfers be $dq_{I,I+1}/dE=y_I$. Then the chemical hardness terms of Eq. (31) can be written as

$$2\eta^* y_1-\eta^*(1-\epsilon)y_2=R_0 \quad N=1, \tag{B2}$$

$$-\eta^*(1-\epsilon)y_{N-1}+2\eta^* y_N-2\eta^*(1-\epsilon)y_{N+1}=R_0 \quad 2\geq N\leq K-1, \tag{B3}$$

$$-\eta^*(1-\epsilon)y_{K-1}+2\eta^* y_K=R_0 \quad N=K. \tag{B4}$$

The sum of all $K$ equations becomes

$$\eta^*(1-\epsilon)(y_1+y_{k-1})+2\epsilon\eta^*\left(\sum_N^K y_N\right)=\eta^*(1-\epsilon)(y_1+y_K)+2K\epsilon\eta^*\langle y_N\rangle=KR_0, \tag{B5}$$

where $\langle y_I\rangle$ is the average charge transfer. All the charge transfers have the same sign, so therefore the average charge transfer $\langle y_I\rangle$ is of the same magnitude as the individual charge transfer terms, and in the limit of periodic boundary conditions all charge transfers $y_I$ are equal. Therefore, if $K\epsilon\gg 1$, the first term of Eq. (B5) is negligible and $\langle y_N\rangle$ is given as

$$\langle y_N\rangle=\left\langle\frac{dq_{N,N+1}}{dE}\right\rangle=\frac{R_0}{2\epsilon\eta^*}. \tag{B6}$$

The molecular polarizability is given by Eq. (32). For the linear chain, the only nontrivial part is the $\alpha_{xx}^{\mathrm{mol}}$ component. Furthermore, $R_{I+1,I}=R_0$ and $\partial q_{IK}/\partial E=y_I$, leading to

$$\alpha_{xx}^{\mathrm{mol}}=\sum_N R_0 y_N=R_0K\langle y_N\rangle=\frac{KR_0^2}{2\epsilon\eta^*}. \tag{B7}$$

In the case $K\epsilon\ll 1$, Eq. (B5) gives

$$(y_1+y_K)=\frac{KR_0}{\eta^*(1-\epsilon)}=\frac{KR_0}{\eta^*}. \tag{B8}$$

Using equations that are symmetric around the center of the chain leads to $y_1=y_K$, which gives the charge transfer for the end atoms. From Eq. (B2), $y_2$ is obtained as $(\epsilon\to 0)$,

$$y_2=2y_1-R_0/\eta^*, \tag{B9}$$

and from Eq. (B3) a recursive formula for $y_N$ is obtained as

$$y_{N+1}=2y_N-y_{N-1}-\frac{R_0}{\eta^*}. \tag{B10}$$

By induction it can be shown that

$$y_N=Ny_1-N(N-1)\frac{R_0}{2\eta^*}=(NK-N(N-1))\frac{R_0}{2\eta^*}. \tag{B11}$$

This formula is symmetric around the center $N=K/2$. The charge transfer increases toward the center of the system, although the total amount of induced charge on each atom $q_I=dq_I/dE\ E=(y_I-y_{I-1})E$ decreases. For simplicity let $E=1$, and then the induced charge on atom $N$ is given by

$$q_N=y_N-y_{N-1}=(K-2(N-1))\frac{R_0}{2\eta^*}. \tag{B12}$$

Thus the induced charge decreases linearly. To calculate the polarizability it is, however, easier to use $y_N$ in Eqs. (B11) and (32) as

$$\alpha_{xx}^{\mathrm{mol}}=\sum_N^K R_0y_N=\frac{R_0^2}{2\eta^*}(K+1)\sum_N^K N-\frac{R_0^2}{2\eta^*}\sum_N^K N^2. \tag{B13}$$

Using that

$$\sum_N^K N=\frac{1}{2}K(K+1) \tag{B14}$$

and

$$\sum_N^K N^2=\frac{1}{6}K(K+1)(2K+1), \tag{B15}$$

the polarizability is obtained as

$$\alpha_{xx}^{\mathrm{mol}}=\left(\frac{1}{6}K^3+\frac{1}{2}K^2+\frac{1}{3}K\right)\frac{R_0^2}{2\eta^*}. \tag{B16}$$

The polarizability in the case $\epsilon K\ll 1$ scales as $K^3$. This derivation assumes that Coulomb interaction terms are negligible. However, intuitively the Coulomb interaction causes any charge to be pushed to the surface, and therefore actually increasing the polarizability further. Therefore it is concluded that the polarizability scales as at least $K^2$ when $\epsilon=0$. Since the EEM is identical to our model when $\epsilon=0$, the polarizability in the EEM scales in a metallic way, whereas for large nonmetallic systems the polarizability should scale linearly with the size of the system.

### 2. Charge transfer with Coulomb interactions

The Coulomb interaction is now included in the limit of $K\to\infty$ by using periodic boundary conditions. However letting the size of the system $K\to\infty$ may not be applied in a system where $\epsilon$ is exactly zero, since both the charge-transfer terms in Eq. (B11) and the induced charges in Eq. (B12) increase with the length of the chain $K$. This may be interpreted as that surface effects are not negligible.

In the case where $\epsilon=1$, Eq. (B3) gives a constant charge transfer

$$y_N = \frac{R_0}{\epsilon \eta^*}, \tag{B17}$$

and the charge will be zero on all atoms except the atom at each end. In this case, it is obvious that the Coulomb interaction terms would not modify the results for large systems. In the case $K\epsilon \gg 1$, the energy of transporting charge dominates, and therefore one can argue that periodic boundary condition is a good approximation.

The only topology elements $L_{IJ}$ different from zero are those where $I=J\pm 1$. Therefore $P=S+1$ and $M=J+1$ in Eq. (18). Using periodic boundary conditions all equations in the system are equal (separating $\eta^*$ from $T_{IJ}^{(0)}$ such that $T_{II}^{(0)}=0$),

$$-\eta^*(1-\epsilon)y_{S-1} + 2\eta^* y_S - 2\eta^*(1-\epsilon)y_{S+1} + \sum_I (T_{S,I}^{(0)} - T_{S,I+1}^{(0)} - T_{S+1,I+1}^{(0)} + T_{S+1,I}^{(0)})y_I = R_0, \tag{B18}$$

which is valid for all $S$. Let $K$ be the periodicity of the system and let all atom sums go from $-K/2$ to $K/2$, assuming that Coulomb interaction terms are negligible for atoms $S$ and $N$ if $|S-N|>K/2$.

The Coulomb interaction is only dependent on the distance between the atoms, which in the linear chain is proportional to the difference between the indices

$$T_{SI}^{(0)} = T_{S+1,I+1}^{(0)} = \frac{1}{(S-I)R_0}, \tag{B19}$$

which give the relation $T_{SI}=T_{S+1,I+1}$. By taking the sum over all equations as in Eq. (B5), the Coulomb modification to Eq. (B5) becomes

$$\begin{aligned}\sum_{S=-K/2}^{K/2} \sum_I (T_{S,I}^{(0)} - T_{S,I+1}^{(0)} - T_{S+1,I+1}^{(0)} + T_{S+1,I}^{(0)})y_I &= \sum_I \sum_{S=-K/2}^{K/2} (T_{S,I+1}^{(0)} - T_{S+1,I}^{(0)})y_I \\ &= \sum_I \left( \sum_{S=-(K/2+1)}^{K/2-1} T_{S+1,I+1}^{(0)} - \sum_{S=-(K/2-1)}^{K/2+1} T_{S,I}^{(0)} \right) y_I. \end{aligned} \tag{B20}$$

Since periodic boundary conditions are applied, atom number $K/2+1$ is the same as atom $-K/2$, and thus

$$\sum_{S=-(K/2+1)}^{K/2-1} \cdots = \sum_{S=-(K/2-1)}^{K/2+1} \cdots = \sum_{S=-K/2}^{K/2} \cdots. \tag{B21}$$

Using this trick and that $T_{S+1,I+1}^{(0)}=T_{S,I}^{(0)}$, the sum of all Coulomb terms becomes

$$\begin{aligned}\sum_I \left( \sum_{S=-(K/2+1)}^{K/2-1} T_{S,I}^{(0)} - \sum_{S=-(K/2-1)}^{K/2+1} T_{S,I}^{(0)} \right) y_I &= \sum_I \left( \sum_{S=-K/2}^{K/2} T_{S,I}^{(0)} - \sum_{S=-K/2}^{K/2} T_{S,I}^{(0)} \right) y_I = 0. \end{aligned} \tag{B22}$$

Thus, the Coulomb interaction is negligible for large chains when $K\epsilon \gg 1$.

The three atom linear chain is a $2\times 2$ matrix problem and is solved exactly as

$$\langle y_N \rangle = \frac{R_0}{\eta^*(1+\epsilon) - T_{13}^{(0)}}, \tag{B23}$$

which in this case does not depend on the Coulomb interaction between the neighbors $T_{12}^{(0)}$. In the case $\epsilon=1$ the three atom problem gives a similar average charge transfer as the two-particle problem in Eq. (56), where the only difference is the Coulomb interaction term.

### 3. Point-dipole model

We now proceed by calculating the polarizability for a long linear chain in the PDI model. Let the $x$-axis lie in the direction of the linear chain and let the $y$- and $z$-axes be perpendicular to the $x$-axis. Then the $T_{IJ,\alpha\beta}^{(2)}$ tensor between the two atoms is $T_{IJ,xx}^{(2)}=T_{JI,xx}^{(2)}=-2/R_{IJ}^3$, $T_{IJ,yy}^{(2)}=T_{JI,yy}^{(2)}=1/R_{IJ}^3$, $T_{IJ,zz}^{(2)}=T_{JI,zz}^{(2)}=1/R_{IJ}^3$, and all other components are zero. As usual $R_{IJ}$ is the distance between atom $I$ and atom $J$ given as $R_{IJ}=|I-J|R_0$. Therefore there are three independent sets of equations, one for each component, and we proceed by calculating the $xx$-component of the polarizability.

The dipole-dipole interactions are short range, and if only $T_{IJ,\alpha\beta}^{(2)}$ for nearest neighbors are included, the only difference between periodic boundary conditions and a finite chain length would be the interaction between two virtual atoms after the end and before the start of the chain. For long chains these corrections are negligible, and for long chains periodic boundary conditions should be a good approximation for the PDI model.

Let the atomic polarizability be $\alpha$ and let $\mu'_{J,xx}=d\mu_{J,x}/dE_x$. With periodic boundary conditions,

$$-\frac{2}{R_0^3}\left( \sum_{N=1}^{K/2} \frac{1}{N^3} \mu'_{J-N,xx} \right) + \alpha^{-1}\mu'_{J,xx} - \frac{2}{R_0^3}\left( \sum_{N=1}^{K/2} \frac{1}{N^3} \mu'_{J+N} \right) = 1, \tag{B24}$$

which is valid for all $J$. By taking the sum over all equations,

$$\left( \alpha^{-1} - \frac{4}{R_0^3}\left( \sum_N^{K/2} \frac{1}{N^3} \right) \right) \sum_J^K \mu'_{J,xx} = K. \tag{B25}$$

For large systems,

$$\sum_{N=1}^{K/2} \frac{1}{N^3} \approx 1.2. \tag{B26}$$

Using the average induced dipole moment $\langle \mu'_J \rangle = (\Sigma \mu'_J)/K$, the polarizability becomes

$$\alpha_{xx}^{\mathrm{mol}} = K\langle \mu'_{J,xx} \rangle = K\left( \frac{\alpha}{1 - 4.8R_0^{-3}\alpha} \right). \tag{B27}$$

The $yy$- and $zz$-components of the polarizability become

$$\alpha_{yy}^{\mathrm{mol}} = \alpha_{zz}^{\mathrm{mol}} = K\langle \mu'_{J,yy} \rangle = K\langle \mu'_{J,zz} \rangle = K\left( \frac{\alpha}{1 + 2.4R_0^{-3}\alpha} \right). \tag{B28}$$

The interaction between two different dipole moments, here included as $R_0^{-3}$ dependence, increases the polarizability

along the chain but decreases it on the components perpendicular to the chain. Thus, by introducing damping as in Eq. (38) by setting

$$R_0 \to \sqrt{R_0^2 + \frac{a_{IJ}}{4\pi}}, \tag{B29}$$

the polarizability component along the linear chain decreases but the components perpendicular to the chain increase.

#### 4. Combined charge-transfer and point-dipole models

We now proceed by showing that for a long linear chain in a system with $K\epsilon \gg 1$ the charge-transfer and point-dipole terms are independent of each other.

An expression for the average variables $\langle \mu'_{I,xx} \rangle$ and $\langle y_I \rangle$ has been obtained, given that these two properties are independent. It would therefore be nice if an equation of the form (where a large number of atoms is assumed)

$$K\begin{pmatrix} 2\epsilon\eta^* & b \\ B & \dfrac{1-4.8R_0^{-3}\alpha}{\alpha} \end{pmatrix}\begin{pmatrix} \langle y_N \rangle \\ \langle \mu'_{J,x} \rangle \end{pmatrix} = K\begin{pmatrix} R_0 \\ 1 \end{pmatrix} \tag{B30}$$

could be obtained, where $b$ is given by the $T^{(1)}_{IJ,\alpha}$ tensor and the variables $\mu'_{I,\alpha}$ and $B$ is given by $T^{(1)}_{IJ,\alpha}$ and the variables $y_n$. The strategy for finding the unknown $b$ is to set (note that we have $K-1$ bonds)

$$bK\langle \mu'_{J,x} \rangle = \sum_J \sum_S^{K-1} (T^{(1)}_{SJ} - T^{(1)}_{S+1J,\alpha})\mu'_{J,\alpha}, \tag{B31}$$

which is the sum over all $dV^{q\mu}/dq_{SP}$ terms in the equations (note that once again only $P=S+1$ are considered as the allowed charge-transfer terms).

Let us first look at the sum over $S$ and divide the sum into two parts and consider them separately,

$$\sum_{S=1}^{K-1} T^{(1)}_{SJ,\alpha}\mu'_{J,\alpha} = \sum_{S=1}^{K-1} T^{(1)}_{SJ,\alpha}\mu'_{J,\alpha} + T^{(1)}_{KJ,\alpha}\mu'_{J,\alpha} - T^{(1)}_{KJ}\mu'_{J,\alpha}$$

$$= \left(\sum_{S=1}^{K} T^{(1)}_{SJ,\alpha}\mu'_{K,\alpha}\right) - T^{(1)}_{KJ}\mu'_{J,\alpha}, \tag{B32}$$

and similarly,

$$\sum_{S=1}^{K-1} T^{(1)}_{S+1J,\alpha}\mu'_{J,\alpha} = \sum_{S=2}^{K} T^{(1)}_{SJ}\mu'_{J,\alpha} + T^{(1)}_{1J,\alpha}\mu'_{J,\alpha} - T^{(1)}_{1J,\alpha}\mu'_{J,\alpha}$$

$$= \left(\sum_{S=1}^{K} T^{(1)}_{SJ}\mu'_{K}\right) - T^{(1)}_{1J}\mu'_{J}. \tag{B33}$$

Inserting Eqs. (B32) and (B33) into Eq. (B31),

$$\sum_J (T^{(1)}_{1J,\alpha} - T^{(1)}_{KJ,\alpha})\mu'_{J,\alpha}. \tag{B34}$$

With a linear chain of identical atoms where the electric field points along the chain, only point dipoles in the direction of the field $E_x$ are relevant. Since we have the same distance $R_0$ between all atoms,

$$T^{(1)}_{KJ,x} = -T^{(1)}_{JK,x} = -\frac{1}{(K-J)^2 R_0^2} = -T^{(1)}_{1,K-J+1,x} \tag{B35}$$

and

$$\sum_J (T^{(1)}_{1J,\alpha} - T^{(1)}_{KJ})\mu'_{J,\alpha} = \sum_J (T^{(1)}_{1J,x} + T^{(1)}_{1K-J+1,x})\mu'_{J,x} \tag{B36}$$

which gives

$$b = \frac{\sum_J (T^{(1)}_{1J,x} + T^{(1)}_{1K-J+1,x})\mu'_{J,x}}{K\langle \mu'_{I,x} \rangle}. \tag{B37}$$

Since

$$T^{(1)}_{1J} \propto \frac{1}{J^2}, \tag{B38}$$

the sum must be finite even for very large systems. However since it can be assumed that all $\mu'_{J,x}$ has the same sign and the same order of magnitude, $K\langle \mu'_{I,x} \rangle \to \infty$ as $K \to \infty$, and

$$\lim_{K\to\infty} b = 0. \tag{B39}$$

Finding $B$ is done similarly and the answer is

$$B = \frac{\sum_N (T^{(1)}_{1,N+1,x} + T^{(1)}_{NK,x})y_N}{K\langle y_N \rangle}. \tag{B40}$$

In the case $K\epsilon \gg 1$ the average charge transfer $\langle y_I \rangle$ has the same sign and magnitude as any individual induced charge transfer and therefore

$$\lim_{K\to\infty} B = 0. \tag{B41}$$

To summarize for large systems with $K\epsilon \gg 1$,

$$K\begin{pmatrix} 2\epsilon\eta^* & 0 \\ 0 & \dfrac{1-4.8R_0^{-3}\alpha}{\alpha} \end{pmatrix}\begin{pmatrix} \langle y_N \rangle \\ \langle \mu'_{J,x} \rangle \end{pmatrix} = K\begin{pmatrix} R_0 \\ 1 \end{pmatrix}, \tag{B42}$$

and it has been shown that the average induced charge transfer is independent on the average induced point-dipole moments for large systems when $K\epsilon \gg 1$. The total polarizability along the linear chain is therefore given by

$$\alpha^{\mathrm{mol}}_{xx} = K\left(\frac{R_0^2}{2\epsilon\eta^*} + \frac{\alpha}{1-4.8R_0^{-3}\alpha}\right), \tag{B43}$$

and thus the polarizability scales linearly with the size of the system as long as $K\epsilon \gg 1$. For the out-of-plane component the average charge transfer term is zero by symmetry arguments,

$$\alpha^{\mathrm{mol}}_{yy} = \alpha^{\mathrm{mol}}_{zz} = K\left(\frac{\alpha}{1+2.4R_0^{-3}\alpha}\right). \tag{B44}$$

It is more complicated in the case $K\epsilon \ll 1$. In this case the entire upper part of a matrix similar to Eq. (B30) will be small and thus $b$ will not necessarily be negligible. In the same manner, since $R_0\langle y_i \rangle \gg \langle \mu'_{N,x} \rangle$, $B$ would not be negligible either. Specifically, if it is assumed that $\langle y_i \rangle \propto K$ in the charge-transfer part of the model, the upper left of the matrix must be proportional to $1/K$, and thus the same magnitude as

*b*. Within this assumption, it is obvious that the interaction between a charge-transfer model and the PDI model cannot be neglected. Since *b* is not negligible and dependent on the variables of the individual atoms, Eq. (B37) is in this case not useful.


[1] A. K. Rappé and C. J. Casewit, *Molecular Mechanics Across Chemistry* (University Science Books, Sausalito, 1997).
[2] M. P. Allen and D. S. Tildesley, *Computer Simulations of Liquids* (Clarendon, Oxford, 1987).
[3] R. Car and M. Parrinello, Phys. Rev. Lett. **55**, 2471 (1985).
[4] O. Engkvist, P.-O. Åstrand, and G. Karlström, Chem. Rev. (Washington, D.C.) **100**, 4087 (2000).
[5] S. L. Price and A. J. Stone, J. Chem. Soc., Faraday Trans. **88**, 1755 (1992).
[6] R. T. Sanderson, Science **114**, 670 (1951).
[7] R. T. Sanderson, *Chemical Bonds and Bond Energy*, 2nd ed. (Academic, New York, 1976).
[8] W. J. Mortier, K. van Genechten, and J. Gasteiger, J. Am. Chem. Soc. **107**, 829 (1985).
[9] A. K. Rappé and W. A. Goddard III, J. Phys. Chem. **95**, 3358 (1991).
[10] J. Cioslowski and B. B. Stefanov, J. Chem. Phys. **99**, 5151 (1993).
[11] D. M. York and W. Yang, J. Chem. Phys. **104**, 159 (1996).
[12] P. Geerlings, F. De Proft, and W. Langenaeker, Chem. Rev. (Washington, D.C.) **103**, 1793 (2003).
[13] A. C. T. van Duin, J. M. A. Baas, and B. van de Graaf, J. Chem. Soc., Faraday Trans. **90**, 2881 (1994).
[14] A. C. T. van Duin, S. Dasgupta, F. Lorant, and W. A. Goddard III, J. Phys. Chem. A **105**, 9396 (2001).
[15] H. A. Stern, G. A. Kaminski, J. L. Banks, R. Zhou, B. J. Berne, and R. A. Friesner, J. Phys. Chem. B **103**, 4730 (1999).
[16] H. A. Stern, F. Rittner, B. J. Berne, and R. A. Friesner, J. Chem. Phys. **115**, 2237 (2001).
[17] G. A. Kaminski, H. A. Stern, B. J. Berne, R. A. Friesner, Y. X. Cao, R. B. Murphy, R. Zhou, and T. A. Halgren, J. Comput. Chem. **23**, 1515 (2002).
[18] P. Bultinck, W. Langenaeker, P. Lahorte, F. De Proft, P. Geerlings, M. Waroquier, and J. P. Tollenaere, J. Phys. Chem. A **106**, 7887 (2002).
[19] P. Bultinck, W. Langenaeker, P. Lahorte, F. De Proft, P. Geerlings, C. van Alsenoy, and J. P. Tollenaere, J. Phys. Chem. A **106**, 7895 (2002).
[20] P. Bultinck, R. Vanholme, P. L. A. Popelier, F. De Proft, and P. Geerlings, J. Phys. Chem. A **108**, 10359 (2004).
[21] U. Dinur, J. Phys. Chem. **97**, 7894 (1993).
[22] R. Chelli, P. Procacci, R. Righini, and S. Califano, J. Chem. Phys. **111**, 8569 (1999).
[23] R. A. Nistor, J. G. Polihronov, M. H. Müser, and N. J. Mosey, J. Chem. Phys. **125**, 094108 (2006).
[24] D. Mathieu, J. Chem. Phys. **127**, 224103 (2007).
[25] J. Chen, D. Hundertmark, and T. J. Martínez, J. Chem. Phys. **129**, 214113 (2008).
[26] J. Chen and T. J. Martínez, Chem. Phys. Lett. **438**, 315 (2007).
[27] G. Lee Warren, J. E. Davis, and S. Patel, J. Chem. Phys. **128**, 144110 (2008).
[28] R. A. Nistor and M. H. Müser, Phys. Rev. B **79**, 104303 (2009).
[29] T. A. Halgren and W. Damm, Curr. Opin. Struct. Biol. **11**, 236 (2001).
[30] P. Ren and J. W. Ponder, J. Comput. Chem. **23**, 1497 (2002).
[31] P. Ren and J. W. Ponder, J. Phys. Chem. B **107**, 5933 (2003).
[32] J. W. Ponder and D. A. Case, Adv. Protein Chem. **66**, 27 (2003).
[33] K. G. Denbigh, Trans. Faraday Soc. **36**, 936 (1940).
[34] B. C. Vickery and K. G. Denbigh, Trans. Faraday Soc. **45**, 61 (1949).
[35] K. O. Sylvester-Hvid, P.-O. Åstrand, M. A. Ratner, and K. V. Mikkelsen, J. Phys. Chem. A **103**, 1818 (1999).
[36] L. Silberstein, Philos. Mag. **33**, 92 (1917).
[37] L. Silberstein, Philos. Mag. **33**, 215 (1917).
[38] L. Silberstein, Philos. Mag. **33**, 521 (1917).
[39] J. Applequist, J. R. Carl, and K.-F. Fung, J. Am. Chem. Soc. **94**, 2952 (1972).
[40] J. Applequist, Acc. Chem. Res. **10**, 79 (1977).
[41] B. T. Thole, Chem. Phys. **59**, 341 (1981).
[42] R. R. Birge, J. Chem. Phys. **72**, 5312 (1980).
[43] R. R. Birge, G. A. Schick, and D. F. Bocian, J. Chem. Phys. **79**, 2256 (1983).
[44] L. Jensen, P.-O. Åstrand, A. Osted, J. Kongsted, and K. V. Mikkelsen, J. Chem. Phys. **116**, 4001 (2002).
[45] M. Swart, J. G. Snijders, and P. Th. van Duijnen, J. Comput. Methods Sci. Eng. **4**, 419 (2004).
[46] L. Jensen, O. H. Schmidt, K. V. Mikkelsen, and P.-O. Åstrand, J. Phys. Chem. B **104**, 10462 (2000).
[47] L. Jensen, P.-O. Åstrand, and K. V. Mikkelsen, J. Phys. Chem. B **108**, 8226 (2004).
[48] L. Jensen, P.-O. Åstrand, and K. V. Mikkelsen, J. Phys. Chem. A **108**, 8795 (2004).
[49] L. Jensen, A. L. Esbensen, P.-O. Åstrand, and K. V. Mikkelsen, J. Comput. Methods Sci. Eng. **6**, 353 (2006).
[50] J. Kongsted, A. Osted, L. Jensen, P.-O. Åstrand, and K. V. Mikkelsen, J. Phys. Chem. B **105**, 10243 (2001).
[51] C. J. Burnham, J. Li, S. S. Xantheas, and M. Leslie, J. Chem. Phys. **110**, 4566 (1999).
[52] M. Guillaume and B. Champagne, Struct. Chem. **15**, 385 (2004).
[53] M. Guillaume and B. Champagne, Phys. Chem. Chem. Phys. **7**, 3284 (2005).
[54] T. Hansen, L. Jensen, P.-O. Åstrand, and K. V. Mikkelsen, J. Chem. Theory Comput. **1**, 626 (2005).
[55] J. A. C. Rullmann and P. Th. van Duijnen, Mol. Phys. **63**, 451 (1988).
[56] K. R. Sundberg, J. Chem. Phys. **66**, 114 (1977).
[57] K. R. Sundberg, J. Chem. Phys. **66**, 1475 (1977); **67**, 4314 (E) (1977).
[58] A. D. Buckingham, E. P. Concannon, and I. D. Hands, J. Phys. Chem. **98**, 10455 (1994).
[59] L. Jensen, K. O. Sylvester-Hvid, K. V. Mikkelsen, and P.-O. Åstrand, J. Phys. Chem. A **107**, 2270 (2003).
[60] L. Jensen, P.-O. Åstrand, and K. V. Mikkelsen, Nano Lett. **3**, 661 (2003).
[61] J. Applequist, J. Am. Chem. Soc. **95**, 8255 (1973).
[62] J. Applequist, J. Am. Chem. Soc. **95**, 8258 (1973).
[63] J. Applequist, J. Chem. Phys. **58**, 4251 (1973).
[64] K. R. Sundberg, J. Chem. Phys. **68**, 5271 (1978).
[65] J. Applequist, K. R. Sundberg, M. L. Olson, and L. C. Weiss, J. Chem. Phys. **70**, 1240 (1979); J. Chem. Phys. **71**, 2330 (E) (1979).
[66] R. W. Munn, Mol. Phys. **64**, 1 (1988).
[67] J. Applequist and C. O. Quicksall, J. Chem. Phys. **66**, 3455 (1977).
[68] D. F. Bocian, G. A. Schick, and R. R. Birge, J. Chem. Phys. **74**, 3660 (1981).
[69] D. F. Bocian, G. A. Schick, and R. R. Birge, J. Chem. Phys. **75**, 2626 (1981).
[70] D. F. Bocian, G. A. Schick, and R. R. Birge, J. Chem. Phys. **75**, 3215 (1981).
[71] D. F. Bocian, G. A. Schick, J. K. Hurd, and R. R. Birge, J. Chem. Phys. **76**, 4828 (1982).
[72] D. F. Bocian, G. A. Schick, J. K. Hurd, and R. R. Birge, J. Chem. Phys. **76**, 6454 (1982).
[73] M. L. Olson and K. R. Sundberg, J. Chem. Phys. **69**, 5400 (1978).
[74] J. Applequist, J. Phys. Chem. **97**, 6016 (1993).
[75] B. Shanker and J. Applequist, J. Phys. Chem. **100**, 10834 (1996).
[76] L. Jensen, P.-O. Åstrand, and K. V. Mikkelsen, Int. J. Quantum Chem. **84**, 513 (2001).
[77] A. Mayer, Phys. Rev. B **71**, 235333 (2005).
[78] A. Mayer, Appl. Phys. Lett. **86**, 153110 (2005).
[79] A. J. Stone, Mol. Phys. **56**, 1065 (1985).
[80] A. J. Stone, J. Chem. Theory Comput. **1**, 1128 (2005).
[81] B. Shanker and J. Applequist, J. Chem. Phys. **104**, 6109 (1996).
[82] J. R. Reimers and N. S. Hush, J. Phys. Chem. B **105**, 8979 (2001).
[83] R. J. Wheatley, Chem. Phys. Lett. **294**, 487 (1998).
[84] T. Helgaker, P. Jørgensen, and J. Olsen, *Molecular Electronic-Structure Theory* (Wiley, New York, 2000).
[85] H. J. C. Berendsen and G. A. van der Velde, in *MD and MC on Water*, CECAM Workshop Report, edited by H. J. C. Berendsen (CECAM, Orsay, 1972), pp. 63–76.
[86] A. R. Leach, *Molecular Modelling: Principles and Applications*, 2nd ed. (Prentice-Hall, Englewood Cliffs, NJ, 2001).
[87] M. Margenau and N. R. Kestner, *Theory of Intermolecular Forces* (Pergamon, New York, 1969).
[88] R. J. Wheatley and W. J. Meath, Mol. Phys. **79**, 253 (1993).
[89] S. Brdarski and G. Karlström, J. Phys. Chem. A **102**, 8182 (1998).
[90] R. S. Mulliken, J. Chem. Phys. **23**, 1833 (1955).
[91] L. Jensen, P.-O. Åstrand, K. O. Sylvester-Hvid, and K. V. Mikkelsen, J. Phys. Chem. A **104**, 1563 (2000).
[92] B. Champagne, E. A. Perpte, D. Jacquemin, S. J. A. van Gisbergen, E.-J. Baerends, C. Soubra-Ghaoui, K. A. Robins, and B. Kirtman, J. Phys. Chem. A **104**, 4755 (2000).

[93] B. Champagne, E. A. Perpéte, S. J. A. van Gisbergen, E.-J. Baerends, J. G. Snijders, S. Soubra-Ghaoui, K. A. Robins, and B. Kirtman, J. Chem. Phys. **109**, 10489 (1998).
[94] M. van Faassen, P. L. de Boeij, R. van Leeuwen, J. A. Berger, and J. G. Snijders, Phys. Rev. Lett. **88**, 186401 (2002).
[95] M. van Faassen, P. L. de Boeij, R. van Leeuwen, J. A. Berger, and J. G. Snijders, J. Chem. Phys. **118**, 1044 (2003).
[96] P. Sałek, T. Helgaker, O. Vahtras, H. Ågren, D. Jonsson, and J. Gauss, Mol. Phys. **103**, 439 (2005).
[97] M. J. G. Peach, T. Helgaker, P. Sałek, T. W. Keal, O. B. Lutns, D. J. Tozer, and N. C. Handy, Phys. Chem. Chem. Phys. **8**, 558 (2006).
[98] B. Champagne, F. A. Bulat, W. Yang, S. Bonness, and B. Kirtman, J. Chem. Phys. **125**, 194114 (2006).
[99] O. A. Vydrov and G. E. Scuseria, J. Chem. Phys. **125**, 234109 (2006).
[100] H. Sekino, Y. Maeda, M. Kamiya, and K. Hirao, J. Chem. Phys. **126**, 014107 (2007).
[101] M. van Faassen, L. Jensen, J. A. Berger, and P. L. de Boeij, Chem. Phys. Lett. **395**, 274 (2004).
[102] G. te Velde, F. M. Bickelhaupt, S. J. A. van Gisbergen, C. F. Guerra, F. M. Bickelhaupt, C. Fonseca Guerra, E. J. Baerends, J. G. Snijders, and T. Ziegler, J. Comput. Chem. **22**, 931 (2001).
[103] C. Fonseca Guerra, J. G. Snijders, G. te Velde, and E. J. Baerends, Theor. Chem. Acc. **99**, 391 (1998).
[104] SCM, Theoretical Chemistry, Vrije Universiteit, Amsterdam, The Netherlands, ADF2008.01.

## List of corrections

- Eq. (28) should read:

$$\begin{pmatrix} T^{(0)}_{\mathrm{SP,JM}} & T^{(1)}_{\mathrm{SP,J},\beta} \\ T^{(1)}_{\mathrm{I,JM},\alpha} & T^{(2)}_{\mathrm{IJ},\alpha\beta} \end{pmatrix} \begin{pmatrix} q_{\mathrm{JM}} \\ \mu_{\mathrm{J},\beta} \end{pmatrix} = \begin{pmatrix} -\chi^{*}_{\mathrm{SP}} - \varphi^{\mathrm{ext}}_{\mathrm{SP}} \\ E^{\mathrm{ext}}_{\mathrm{I},\alpha} \end{pmatrix}$$

- Upper part of Eq. (32) should read:

$$\alpha^{\mathrm{mol}}_{\alpha\beta} = \frac{\partial \mu^{\mathrm{ind}}_{\alpha}}{\partial E^{\mathrm{ext}}_{\beta}} = \sum_{\mathrm{I,M}} R_{\mathrm{I},\alpha} \frac{\partial q_{\mathrm{IM}}}{\partial E^{\mathrm{ext}}_{\beta}} + \sum_{\mathrm{I}} \frac{\partial \mu_{\mathrm{I},\alpha}}{\partial E^{\mathrm{ext}}_{\beta}}$$

- Eq. (B3) should read:

$$-\eta^{*}(1-\epsilon) y_{\mathrm{N\text{-}1}} + 2\eta^{*} y_{\mathrm{N}} - \eta^{*}(1-\epsilon) y_{\mathrm{N+1}} = R_0 \quad 2 \leq N \leq K-1$$

# Paper 2:

*Combined nonmetallic electronegativy equalization and point-dipole interaction model for the frequency-dependent polarizability*

Hans S. Smalø, P.-O. Åstrand and A. Mayer

J. Phys. Chem.

**Submitted**

# Combined nonmetallic electronegativy equalization and point-dipole interaction model for the frequency-dependent polarizability

Hans S. Smalø ,[†] Per-Olof Åstrand,[*,†] and Alexandre Mayer[‡]

*Department of Chemistry, Norwegian University of Science and Technology (NTNU), N-7491 Trondheim, Norway, and FUNDP-University of Namur, Rue de Bruxelles 61, B-5000 Namur, Belgium*

E-mail: per-olof.aastrand@chem.ntnu.no

**Abstract**

A molecular mechanics model for the frequency-dependent polarizability is presented. It is a combination of a recent model for the frequency-dependence in a charge-dipole model [Nanotechnology 19, 025203, 2008] and a nonmetallic modification of the electronegativity equalization model rephrased as atom-atom charge-transfer terms [J. Chem. Phys. 131, 044101, 2009]. An accurate model for the frequency-dependent polarizability requires a more accurate partitioning into charge and dipole contributions than the static polarizability which has resulted in several modification of the charge-transfer model. Results are presented for hydrocarbons including among others alkanes, polyenes and aromatic systems. Although their response to an electric field are quite different in terms of the importance of charge-transfer contributions, it is demonstrated that their frequency-dependent polarizabilities can be described with the same set of atom-type parameters.

[*]To whom correspondence should be addressed
[†]NTNU
[‡]FUNDP-University of Namur

# Introduction

The frequency-dependent polarizability gives the response at the microscopic level to a time-dependent electric field and is one of the fundamental properties in optics and in the construction of electric and optical devices on the molecular scale.[1,2] To understand both the relation between structure and property and how a molecular material can be manipulated to optimize the property of interest, an understanding at the atomistic scale becomes a central issue. Here modeling and calculations play a prominent role. The frequency-dependent polarizability is in quantum chemistry obtained through response theory,[3] and it is available in most general-purpose quantum-chemical program packages at different levels of theory. Quantum chemical calculations are, however, still expensive, although the efficiency is improved continuously, and is in most cases restricted to relatively small molecules in the gas phase.

Force-field or molecular-mechanics models are on the other hand used in molecular dynamics simulations where the forces between thousands of atoms are calculated repeatedly.[4] Although the energy expression is much simpler than in quantum chemical calculations, it contains the essence of intermolecular interactions in particular for the electrostatics which in most cases is the most important energy contribution. Furthermore, electronic polarization has been included in force fields, for example by using atomic polarizabilities,[5–7] charge equilibration schemes,[8,9] and charges-on-spring models.[10–12]

In the point-dipole interaction (PDI) model,[13–17] a set of native (in the sense that the atomic polarizabilities do not sum up to the molecular polarizability) atomic polarizabilities are used as atom-type parameters, and the molecular polarizabilities are obtained from solving a set of linear equations for a set of atomic polarizabilities interacting in an external electric field. The usefulness of the model has been improved by parametrization to quantum chemical data,[18] and the inclusion of short-ranged damping of the interactions.[18–21] The model has been used extensively for the study of polarization in large systems such as carbon nanotubes and fullerenes,[21,22] boron nitride tubes[23] and proteins,[24] and the model has been extended for example to optical rotation,[25–28] hyperpolarizabilities,[29–36] Raman intensities,[37,38] and in force fields.[39,40]

The PDI model has also been combined with the capacitance model[41–45] and with the electronegativity equalization model (EEM).[46–51] Both the capacitance model and the EEM suffer from that it is in principal a metallic model, i.e. charge is allowed to flow freely in the molecule,[44,52] and modifications have been suggested to cure this problem.[52–61] In our contribution, we suggest a model that in the limits behaves as a metallic and a completely insulating model with a smooth transition dependent only on variations in bond lengths.[60]

The inclusion of the frequency-dependence in a force-field model for the polarizability is a nontrivial task. It has been included in an Unsöld-type of approximation by regarding atom-type excitation frequencies,[18,22–24,36] or a set of oscillators with Lorentzian band-shape associated with each atom.[62–64] In a recent work,[65] we associated the time-dependence of the atomic charges and the induced dipole moments with their respective kinetic energies and with bond currents. Solving the Lagrangian equations for the system leads to a relatively simple frequency-dependent modification of of the standard charge-dipole model. This model has subsequently been used for silver clusters and the interaction between molecules and silver clusters.[66,67]

In this work we combine our recent models for the frequency-dependence with the nonmetallic charge-transfer/point-dipole interaction (CT/PDI) model.[60,65] It is demonstrated that the frequency-dependence for the charge term is described in a more realistic way for molecular systems since, in contrast to metallic systems, its excitation energy is nonvanishing for nonmetallic systems. With computations, it is shown that the frequency-dependent polarizability of alkanes, polyenes, and aromatic systems can be described with the same set of atom-type parameters.

# Theory

## Frequency-dependence for a combined charge-transfer and point-dipole model

In this work two previous models[60,65] are combined to give a nonmetallic electronegativity equalization and point-dipole interaction model for the frequency-dependent polarizability. Each atom is associated with a time-dependent charge $q_I(t)$ and a time-dependent dipole moment $\mu_{I,\alpha}(t)$, so

that the Lagrangian may be written as[65]

$$L = K^q + K^\mu - V \tag{1}$$

where $K^q$ is the kinetic energy for the atomic charges, $K^\mu$ is the kinetic energy for the atomic dipole moments and $V$ is the potential energy. For a system of $N$ particles, the charge is rewritten in terms of charge-transfer variables $q_{IK}(t)$ as[52,60]

$$q_I(t) = \sum_K^N L_{IK} q_{IK}(t) \ , \tag{2}$$

where $L_{IK}$ is a topology matrix which is one if charge transfer is allowed between atoms $I$ and $K$ and zero otherwise. The time-derivative of the charge-transfer, $\dot{q}_{IK}$, is viewed as a current $I_{IK}$ going from atom $K$ to atom $I$. Thus, the kinetic energy $K^q$ for the oscillation of charges is[65]

$$K^q = \frac{1}{2} \sum_{I,K>I}^N \left(c_I^q + c_K^q\right) R_{IK}^2 \left(\dot{q}_{IK}\right)^2 \tag{3}$$

where $R_{IK}$ is the bond distance between atoms $I$ and $K$, and $c_I^q$ is an atom-type parameter. Here atomic units are used.[68] The kinetic energy $K^\mu$ for the oscillating atomic dipole moments is[65]

$$K^\mu = \frac{1}{2} \sum_I^N c_I^\mu \left(\dot{\mu}_I\right)^2 \tag{4}$$

where $\dot{\mu}_I$ is the time-derivative of $\mu_I$ and $c_I^\mu$ is an additional atom-type parameter.

With the extension that the atomic charges, atomic dipole moments and the external electric field can be time-dependent, the potential energy $V$ in Eq. (1) is[60,65]

$$V = V^{qq} + V^{q\mu} + V^{\mu\mu} \tag{5}$$

where $V^{qq}$ is the charge-charge interaction, $V^{q\mu}$ is the charge-dipole interaction, and $V^{\mu\mu}$ is the dipole-dipole interaction energy, respectively. The starting point for $V^{qq}$ is the standard electroneg-

ativity equalization model (EEM)[69,70]

$$V^{qq} = \sum_{I}^{N} \left( \left( \chi_I^* + \varphi_I^{\text{ext}} \right) q_I + \frac{1}{2} \eta_I^* q_I^2 + \frac{1}{2} \sum_{J \neq I}^{N} q_I T_{IJ}^{(0)} q_J \right) \tag{6}$$

where $\chi_I^*$ is the atomic electronegativity, $\eta_I^*$ is the atomic chemical hardness, $\varphi_I^{\text{ext}}$ is the external electrostatic potential at atom $I$, $q_I T_{IJ}^{(0)} q_J$ is the Coulomb interaction, and in classical electrostatics $T_{IJ}^{(0)} = 1/R_{IJ}$ where $R_{IJ}$ is the distance between atoms $I$ and $J$. Furthermore, let $T_{II}^{(0)} = \eta_I^*$ and insert Eq. (2) into Eq. (6) to obtain[60]

$$V^{qq} = \sum_{I,J>I}^{N} \left( \chi_{IJ} + \varphi_{IJ}^{\text{ext}} \right) q_{IJ} + \frac{1}{2} \sum_{I,K>I,J,M>J}^{N} q_{IK} T_{IK,JM}^{(0)} q_{JM} \tag{7}$$

where $\chi_{IJ} = \chi_I^* - \chi_J^*$, $\varphi_{IJ}^{\text{ext}} = \varphi_I^{\text{ext}} - \varphi_J^{\text{ext}}$ and $T_{IK,JM}^{(0)} = T_{IJ}^{(0)} - T_{KJ}^{(0)} - T_{IM}^{(0)} + T_{KM}^{(0)}$. The topology matrix elements $L_{IK}$ in Eq. (2) are omitted here, but it is implied that only atom-pairs with $L_{IK} = 1$ are included in the summations. So far this is nothing but a reformulation of the EEM not changing the physics of the model. However, several modifications of the tensor $T_{IK,JM}^{(0)}$ are applied. Instead of point-charges for each atom, a Gaussian distribution is applied[21]

$$\rho_I(r_i) = q_I \left( \frac{\Phi_I^*}{\pi} \right)^{\frac{3}{2}} e^{-\Phi_I^* r_i^2} \tag{8}$$

where the width of the Gaussian, $\Phi_I^*$, is an additional atom-type parameter of the model. Note that Eq. (8) is normalized so that the atomic charge is $q_I$. The interaction between two Gaussian charge distributions is approximated as[21]

$$V = \frac{q_I q_J}{\widetilde{R}_{IJ}} \tag{9}$$

where $\widetilde{R}_{IJ}$ is a scaled distance given by[71]

$$\widetilde{R}_{IJ} = \sqrt{R_{IJ}^2 + \frac{\pi}{4 a_{IJ}}} \tag{10}$$

where

$$a_{IJ} = \frac{\Phi_I^* \Phi_J^*}{\Phi_I^* + \Phi_J^*} \, . \tag{11}$$

Eq. (9) has the correct limiting behavior at $R_{IJ} \to 0$ and at $R_{IJ} \to \infty$. In earlier work the distances $R_{IJ}$ was replaced by the scaled distances $\widetilde{R}_{IJ}$ also when considering the charge-dipole interaction $T^{(1)}_{IJ,\alpha}$ and the dipole-dipole interaction $T^{(2)}_{IJ,\alpha\beta}$. However, this damping model resulted in too small damping for the dipole-dipole interaction, and unphysically small $\Phi_I^*$-parameters were needed to avoid a polarization catastrophe. Therefore $T^{(1)}_{IJ,\alpha}$ is here written as

$$T^{(1)}_{IJ,\alpha} = \frac{\partial T^{(0)}_{IJ}}{\partial R_{IJ,\alpha}} = -\frac{R_{IJ,\alpha}}{\widetilde{R}^3_{IJ}} \tag{12}$$

and

$$T^{(2)}_{IJ,\alpha\beta} = \frac{\partial T^{(1)}_{IJ,\alpha}}{\partial R_{IJ,\beta}} = \frac{3R_{IJ,\alpha}R_{IJ,\beta}}{\widetilde{R}^5_{IJ}} - \frac{\delta_{\alpha\beta}}{\widetilde{R}^3_{IJ}} \, , \tag{13}$$

where Greek subscripts, $\alpha$, $\beta$, ..., denote one of the Cartesian coordinates, $x$, $y$ or $z$, and the Einstein summation convention is used for repeated Greek subscripts. Still $T^{(1)}_{IJ,\alpha} \to 0$ when $R_{IJ} \to 0$, but the $T^{(2)}_{IJ,\alpha\beta}$ tensor in Eq. (13) is not traceless. Therefore care should be taken before expanding the model to quadrupole moments, where a traceless formalism is normally adoped.[72]

For the static polarizability to scale correctly with the size of the system both for metallic and nonmetallic systems, an energy for transporting charge through atoms have been added of the form[60]

$$\varepsilon \eta_I^* q_{KI} q_{IM} \; ; \; K \neq M \tag{14}$$

where $\varepsilon$ is a dimensionless quantity between 0 and 1. This term describes an energy cost for transporting charge from atom $M$ through atom $I$ to atom $K$. If $\varepsilon = 0$, the system behaves metallically and if $\varepsilon = 1$ the system behaves as an insulating system. The charge transport energy in Eq. (14) has been incorporated by modifying the chemical hardness terms in the potential energy $V^{qq}$ as[60]

$$\frac{1}{2}\eta_I^* q_{KI} q_{IM} \to \frac{1}{2}\eta_I^* S_{IK}^{-\frac{1}{2}} S_{IM}^{-\frac{1}{2}} g_{I,KM} q_{KI} q_{IM} \tag{15}$$

where $g_{I,KM}$ is a function of the two distances $R_{IK}$ and $R_{IM}$, and $g_{I,KM} = 1$ if $K = M$. For a two-atom system ($K = M$) this becomes $\eta_I \to \eta_I S_{IK}^{-1}$, where $S_{IK}$ is the overlap between atoms $I$ and $K$. Thus, $q_{IK} \propto S_{IK}$ and $q_{IK}$ approaches zero when $R_{IK} \to \infty$. Furthermore if $S_{IK} = S_{IM}$, the following relation holds

$$\varepsilon = 1 - g_{I,KM} \, . \tag{16}$$

Thus, $g_{I,KM}$ describes the resistance against charge-flow within the molecule. For some molecules included here, the previously used functional form of $g_{I,KM}$[60] gave a too drastic change in $g_{I,KM}$ with the bond length. For example, if $R_{IK} + R_{IM}$ is increased from 2.8 Å to 2.9 Å, $\varepsilon$ increased from 0.05 to 0.4. This lead to problems describing molecules as stilbene where key junctions in the system with atypical bond lengths had a too high $\varepsilon$ and thus a too low charge transfer. For this reason, $g_{I,KM}$ is here rewritten as

$$g_{I,KM} = g_{0,I}^{*\,2} g_{0,K}^{*} g_{0,J}^{*} H_{I,KM}(\Delta_{I,KM}) + g_{1,I}^{*\,2} g_{1,K}^{*} g_{1,J}^{*} \left(1 - H_{I,KM}(\Delta_{I,KM})\right) \tag{17}$$

where $g_{0,I}^{*}$ and $g_{1,I}^{*}$ are atom-type parameters. To ensure that $g_{I,KM}$ is between 0 and 1, these parameters must also be between 0 and 1. Furthermore, $H_{I,KM}$ is a smooth step function (dependent on atoms $I$, $K$ and $M$) given as

$$H_{I,KM}(\Delta) = \frac{1}{2}\left(1 + \tanh(C_{I,KM}\Delta_{I,KM})\right) \tag{18}$$

where $C_{I,KM} = (C_I^*)^2 C_K^* C_M^*$ and $C_I^*$ is an atom-type parameter. Furthermore,

$$\Delta_{I,KM} = R_{IK} + R_{IM} - 2R_I^* - R_K^* - R_M^* \tag{19}$$

where also $R_I^*$ is an atom-type parameter. For carbon, $g_{0,I}^{*}$ describes $\varepsilon$ for $sp^3$-carbon and $g_{1,I}^{*}$ describes $\varepsilon$ for $sp^2$-carbon, respectively, and a smooth step function is added for the transition between the two cases. The $R_I^*$ parameter govern where the transition between the two cases occurs, while $C_I^*$ governs how steep the transition is.

For double bonds and a system involving only carbon, $\varepsilon$ is described by $\varepsilon = 1 - g_{1,C}^{*\,4}$. Since $0 \leq g_{1,I}^{*} \leq 1$ for all atoms, if replacing one carbon with another atom (not the central carbon),

$$1 - g_{1,C}^{*\,3} \leq \quad \varepsilon \quad \leq 1\,. \tag{20}$$

Thus, there exist a lower limit for the modified $\varepsilon$ given by the parameters for pure carbon, but the connection could be made as nonmetallic as desired by setting $g_{1,K}^{*} = 0$. For simplicity, and to avoid a large amount of parameters for hydrogen that does not play any significant role, in this work $g_{I,KM}$ is set equal to $g_{0,C}^{*3} g_{0,H}^{*}$ (where $g_{0,C}^{*}$ is the parameter for carbon) when at least one of the atoms is a hydrogen atom. Thus Eq. (17) is used here only for carbon.

With the $R_I^*$ parameters, $S_{IK}$ is given as

$$S_{IK} = e^{-a_{IK}(R_{IK} - R_I^* - R_K^*)^2} \tag{21}$$

where $a_{IK}$ is given by Eq. (11). $S_{IK} \approx 1$ when atoms $I$ and $K$ are within typical bonding distances, but for large $R_{IK}$ it is an exponentially decaying function given by the overlap of two Gaussian distributions. Simplified, $S_{IK}$ describes charge transfer between molecules, while $g_{I,KM}$ describes charge transfer within the molecule.

In earlier work, the out-of-plane polarizability for planar molecules tends to be too low, which has been compensated by low values of the $\Phi_I^*$-parameters,[60] or different atomic polarizabilities for the out-of-plane and in-plane components of the carbon atoms.[51,65] One may modify the atomic polarizability parameter so that it depends on the chemical surroundings, for example as,[73]

$$\alpha_{I,\alpha\beta} = \alpha_I \left(\delta_{\alpha\beta} + x_I^* \left(1 - G_{I,\alpha\beta}\right)\right) \tag{22}$$

where $\alpha_I$ is an isotropic atomic polarizability and $x_I^*$ is an additional atom-type parameter and $G_{I,\alpha\beta}$ is

$$G_{I,\alpha\beta} = \frac{3}{Tr(\Gamma_I)} \Gamma_{I,\alpha\beta} \tag{23}$$

where $\Gamma_{I,\alpha\beta}$ in this work is given as

$$\Gamma_{I,\alpha\beta} = \sum_{J\neq I}^{N} \alpha_J S_{IJ} \frac{R_{IJ,\alpha} R_{IJ,\beta}}{R_{IJ}^2} \,. \tag{24}$$

In Eq (24), $R_{IJ,\alpha}R_{IJ,\beta}/R_{IJ}^2$ gives the correct rotational properties of $\alpha_{I,\alpha\beta}$, $S_{IJ}$ is an exponentially decaying function given by Eq. (21) to include a distance dependence, and the atom-type polarizability $\alpha_J$ serves as a measure of the size of the neighboring atom. The sum is restricted to atom-pairs where $L_{IJ} = 1$. For planar molecules, $R_{IJ,\alpha}$ is zero for $\alpha = z$. In this case, $\Gamma_{I,zz} = 0$, and Eq. (22) simplifies to

$$\alpha_{I,zz} = \alpha_I \left(1 + x_I^*\right) \tag{25}$$

for $\alpha = \beta = z$. Since the trace of $G_{I,\alpha\beta}$ is normalized to 3, the polarizability of the other components decreases. Thus the out-of-plane component of the polarizability increases without increasing the in-plane components, which is the main purpose of introducing the anisotropic modification to the atomic polarizability. For the linear case, $G_{I,xx} = 3$, $G_{I,yy} = G_{I,zz} = 0$, and the *xx*-component of the atomic polarizability becomes

$$\alpha_{I,xx} = \alpha_I \left(1 - 2x_I^*\right) \tag{26}$$

To avoid the possibility of negative atomic polarizabilities, it is therefore required that $x_I^* < 0.5$. In this work, the PDI model is extended with this modification.

An exchange term according to our earlier work[60] is not included here. It has a relatively small impact on the molecular polarizability and a refined model for the exchange energy is developed elsewhere with argon as a model system.[74]

Rewritten in terms of charge-transfer variables, the charge-dipole interaction energy, $V^{q\mu}$ is given by[60]

$$V^{q\mu} = \sum_{I,K,J}^{N} q_{IK} T_{IJ,\alpha}^{(1)} \mu_{J,\alpha} = \sum_{I,K>I,J}^{N} q_{IK} \left(T_{IJ,\alpha}^{(1)} - T_{KJ,\alpha}^{(1)}\right) \mu_{J,\alpha} \,. \tag{27}$$

The dipole-dipole interaction energy $V^{\mu\mu}$ is given by the point-dipole interaction (PDI) model[41]

$$V^{\mu\mu} = \frac{1}{2}\sum_{J}^{N} \mu_{J,\alpha} \left(\alpha_{J,\beta\alpha}\right)^{-1} \mu_{J,\beta} - \frac{1}{2}\sum_{J}^{N}\sum_{K\neq J}^{N} \mu_{J,\alpha} T^{(2)}_{JK,\alpha\beta} \mu_{K,\beta} - \sum_{J}^{N} E^{\text{ext}}_{J,\alpha} \mu_{J,\alpha} \tag{28}$$

where $\alpha_{J,\alpha\beta}$ is given by Eq. (22), $T^{(2)}_{IJ,\alpha\beta}$ is given in Eq. (13) and $E^{\text{ext}}_{J,\alpha}$ is an external electric field at atom $J$.

The Lagrangian equations to be solved are written as[65]

$$\frac{\partial}{\partial t}\left(\frac{\delta L}{\delta \dot{q}_{IK}}\right) - \frac{\delta L}{\delta q_{IK}} = 0 \;\; ; \;\; \frac{\partial}{\partial t}\left(\frac{\delta L}{\delta \dot{\mu}_{I,\alpha}}\right) - \frac{\delta L}{\delta \mu_{I,\alpha}} = 0 \tag{29}$$

If an external electric field and electrostatic potential at atom $J$ with frequency $\omega$ is assumed,

$$E^{\text{ext}}_{J,\alpha} = E^{(\omega)}_{J,\alpha}\, Re\, e^{i\omega t} \;\; ; \;\; \varphi^{\text{ext}}_{IJ} = \varphi^{(\omega)}_{IJ}\, Re\, e^{i\omega t}, \tag{30}$$

and the charge transfer and atomic dipole moments also oscillate with the same frequency

$$q_{IK} = Re\, \left(q^{(0)}_{IK} + q^{(\omega)}_{IK} e^{i\omega t}\right) \;\; ; \;\; \mu_{I,\alpha} = Re\, \left(\mu^{(0)}_{I,\alpha} + \mu^{(\omega)}_{I,\alpha} e^{i\omega t}\right) \; . \tag{31}$$

where $q^{(0)}_{IK}$ and $\mu^{(0)}_{I,\alpha}$ are the static charge transfers and the static atomic dipole moments respectively. With these definitions,[65]

$$\frac{\partial}{\partial t}\left(\frac{\partial L}{\partial \dot{q}_{SP}}\right) = -\left(c^{q}_{S} + c^{q}_{P}\right) R^{2}_{SP}\, \omega^{2}\, Re\left(q^{(\omega)}_{SP} e^{i\omega t}\right) \; . \tag{32}$$

and for the dipole moments,[65]

$$\frac{\partial}{\partial t}\left(\frac{\partial L}{\partial \dot{\mu}_{I,\alpha}}\right) = \frac{\partial}{\partial t}\left(\frac{\partial K^{\mu}}{\partial \dot{\mu}_{I,\alpha}}\right) = -c^{\mu}_{I}\, \omega^{2} Re\left(\mu^{(\omega)}_{I,\alpha}\, e^{i\omega t}\right) \tag{33}$$

The remaining terms of the Lagrangian in Eqs. (29) yield[60]

$$\frac{\partial L}{\partial q_{IK}} = -\frac{\partial V}{\partial q_{IK}} = -\sum_{J<M}^{N} T^{(0)}_{IK,JM} q_{JM} - \sum_{J}^{N} T^{(1)}_{IK,J,\alpha} \mu_{J,\alpha} - \left(\chi_{IK} + \varphi^{\text{ext}}_{IK}\right) \tag{34}$$

$$\frac{\partial L}{\partial \mu_{I,\alpha}} = -\frac{\partial V}{\partial \mu_{I,\alpha}} = -\sum_{J<M}^{N} T^{(1)}_{I,JM,\alpha} q_{JM} + \sum_{J}^{N} T^{(2)}_{IJ,\alpha\beta}\, \mu_{J,\beta} + E^{\text{ext}}_{I,\alpha} \tag{35}$$

where $T^{(1)}_{IK,J,\alpha} = T^{(1)}_{IJ,\alpha} - T^{(1)}_{KJ,\alpha}$, $T^{(1)}_{I,JM,\alpha} = -\left(T^{(1)}_{IJ,\alpha} - T^{(1)}_{IM,\alpha}\right)$ and $T^{(2)}_{II,\alpha\beta} = -(\alpha_{I,\beta\alpha})^{-1}$. Using Eqs. (31), the final Lagrangian equation can be divided into a field-independent part,

$$\sum_{J>M}^{N} T^{(0)}_{IK,JM} q^{(0)}_{JM} + \sum_{J}^{N} T^{(1)}_{IK,J,\alpha} \mu^{(0)}_{J,\alpha} = -\chi_{IK} \tag{36}$$

$$\sum_{J>M}^{N} T^{(1)}_{I,JM,\alpha} q^{(0)}_{JM} - \sum_{J}^{N} T^{(2)}_{IJ,\alpha\beta} \mu^{(0)}_{J,\beta} = 0 \tag{37}$$

and a field-dependent part

$$\sum_{J>M}^{N} T^{(0)}_{IK,JM} q^{(\omega)}_{JM} + \sum_{J}^{N} T^{(1)}_{IK,J,\alpha}\, \mu^{(\omega)}_{J,\alpha} - \omega^2 \left(c^q_I + c^q_K\right)\, R^2_{IK} q^{(\omega)}_{IK} = -\varphi^{(\omega)}_{IK} \tag{38}$$

$$\sum_{J>M}^{N} T^{(1)}_{I,JM,\alpha} q^{(\omega)}_{JM} - \sum_{J}^{N} T^{(2)}_{IJ,\alpha\beta} \mu^{(\omega)}_{J,\beta} - \omega^2\, c^{\mu}_I\, \mu^{(\omega)}_{I,\alpha} = E^{(\omega)}_{I,\alpha} \tag{39}$$

It is noted that the terms $\omega^2 \left(c^q_I + c^q_K\right)\, R^2_{IK} q^{(\omega)}_{IK}$ and $\omega^2\, c^{\mu}_I \mu^{(\omega)}_{I,\alpha}$ can be viewed as a frequency-dependent modification of a static model ($\omega = 0$). Dissipation may be introduced by replacing $\omega^2$ with $\omega^2 - i\frac{1}{2}\left(\gamma^q_I + \gamma^q_K\right)\omega$ in Eq. (38) and with $\omega^2 - i\gamma^{\mu}_I \omega$ in Eq. (39), where $\gamma^q_I$ and $\gamma^{\mu}_I$ are additional atom-type parameters.[65]

In matrix form the field-dependent equations, including non-zero dissipation, are given as

$$\left( \begin{pmatrix} T^{(0)}_{SP,JM} & T^{(1)}_{SP,K,\beta} \\ T^{(1)}_{I,JM,\alpha} & -T^{(2)}_{IK,\alpha\beta} \end{pmatrix} - \omega^2 \begin{pmatrix} \tau_{JM}\, \delta_{SJ}\delta_{PM} & 0 \\ 0 & c^{\mu}_K \left(1 - i\gamma^{\mu}_K/\omega\right) \delta_{IK}\delta_{\alpha\beta} \end{pmatrix} \right) \begin{pmatrix} q^{(\omega)}_{JM} \\ \mu^{(\omega)}_{K,\beta} \end{pmatrix} = \begin{pmatrix} -\varphi^{(\omega)}_{SP} \\ E^{(\omega)}_{I,\alpha} \end{pmatrix} \tag{40}$$

where $\tau_{JM} = \left(c^q_J + c^q_M\right) R^2_{JM} \left(1 - i/2\left(\gamma^q_J + \gamma^q_M\right)/\omega\right)$ and thus the modification to the static model is obtained by subtracting a diagonal matrix. If the wavelength $\lambda$ is much larger than the size

of the system/molecule, the external electric field may be regarded as homogeneous. In this case, $E^{(\omega)}_{I,\alpha} = E^{(\omega)}_{\alpha}$ and $\phi^{(\omega)}_{SP} = -\left(R_{S,\alpha} - R_{P,\alpha}\right) E^{(\omega)}_{\alpha}$. For a homogeneous electric field, $\partial q^{(\omega)}_{JM}/\partial E^{(\omega)}_{\gamma}$ and $\partial \mu^{(\omega)}_{J,\alpha}/\partial E^{(\omega)}_{\gamma}$ are obtained by solving the following set of linear equations,

$$\left( \begin{pmatrix} T^{(0)}_{SP,JM} & T^{(1)}_{SP,K,\beta} \\ T^{(1)}_{I,JM,\alpha} & -T^{(2)}_{IK,\alpha\beta} \end{pmatrix} - \omega^2 \begin{pmatrix} \tau_{JM}\, \delta_{SJ}\delta_{PM} & 0 \\ 0 & c^{\mu}_{K}\left(1 - i\gamma^{\mu}_{K}/\omega\right)\delta_{IK}\delta_{\alpha\beta} \end{pmatrix} \right) \begin{pmatrix} \partial q^{(\omega)}_{JM}/\partial E^{(\omega)}_{\gamma} \\ \partial \mu^{(\omega)}_{K,\beta}/\partial E^{(\omega)}_{\gamma} \end{pmatrix} = \begin{pmatrix} R_{SP,\gamma} \\ \delta_{\alpha\gamma} \end{pmatrix} \tag{41}$$

The induced molecular dipole moment $\mu^{\mathrm{ind}}_{\alpha}$ oscillates with frequency $\omega$ and thus $\mu^{(\omega)}_{\alpha}$ may be defined as $\mu^{\mathrm{ind}}_{\alpha} = Re\left(\mu^{(\omega)}_{\alpha} e^{i\omega t}\right)$. With this definition, the molecular polarizability $\alpha^{\mathrm{mol}}_{\alpha\beta}(\omega)$ is given as

$$\begin{aligned} \alpha^{\mathrm{mol}}_{\alpha\beta}(\omega) &= \frac{\partial \mu^{\mathrm{ind}}_{\alpha}}{\partial E^{\mathrm{ext}}_{\beta}} = \frac{\partial \mu^{(\omega)}_{\alpha}}{\partial E^{(\omega)}_{\beta}} = \sum_{I,M}^{N} R_{I,\alpha} \frac{\partial q^{(\omega)}_{IM}}{\partial E^{(\omega)}_{\beta}} + \sum_{I}^{N} \frac{\partial \mu^{(\omega)}_{I,\alpha}}{\partial E^{(\omega)}_{\beta}} \\ &= \sum_{I,M>I}^{N} R_{IM,\alpha} \frac{\partial q^{(\omega)}_{IM}}{\partial E^{(\omega)}_{\beta}} + \sum_{I}^{N} \frac{\partial \mu^{(\omega)}_{I,\alpha}}{\partial E^{(\omega)}_{\beta}} \end{aligned} \tag{42}$$

Solving Eq. (41) gives $\partial q^{(\omega)}_{IM}/\partial E^{(\omega)}_{\beta}$ and $\partial \mu^{(\omega)}_{I,\alpha}/\partial E^{(\omega)}_{\beta}$ and thus also the frequency-dependent polarizability $\alpha^{\mathrm{mol}}_{\alpha\beta}(\omega)$. If including the dissipation terms $i\gamma^{q}_{I}$ and $i\gamma^{\mu}_{I}$, the polarizability $\alpha^{(\omega)}_{\alpha\beta}$ becomes imaginary. In this case, the molecular induced dipole moment $\mu^{\mathrm{ind}}_{\alpha}$ is given by

$$\mu^{\mathrm{ind}}_{\alpha} = E^{(\omega)}_{\beta} Re\ \alpha^{\mathrm{mol}}_{\beta\alpha} e^{i\omega t}. \tag{43}$$

and the amplitude of the induced dipole moment is given by the amplitude of the polarizability.

## The linear chain as a model system

The static model has previously been analyzed analytically for a linear chain composed of identical atoms,[60] which is here extended to the frequency-dependent polarizability. Let $N$ be the number of atoms in the chain, $\eta^{*}$ be the atomic chemical hardness, $\alpha$ be the atomic polarizability, let the distance between neighboring atoms be $R_0$, let $\varepsilon = 1 - g(R_0, R_0)$ be a parameter of the model, $c^{q}$

and $c^{\mu}$ be the parameters associated with $K^q$ and $K^{\mu}$, respectively. Dissipation is ignored for the moment. Furthermore, let the $x$-axis be along the linear chain, and $L_{IJ} = 1$ only if $J = I \pm 1$, such that only charge transfer between nearest neighbors is taken into account. In the case $N\varepsilon \gg 1$, an equation of the form[60]

$$N \begin{pmatrix} 2\varepsilon\eta^* & 0 \\ 0 & \frac{1-4.8R_0^{-3}\alpha}{\alpha} \end{pmatrix} \begin{pmatrix} < \partial q_{I,I+1}/\partial E_x > \\ < \partial \mu_{J,x}/\partial E_x > \end{pmatrix} = N \begin{pmatrix} R_0 \\ 1 \end{pmatrix} \tag{44}$$

is obtained, where $\langle \partial q_{I,I+1}/\partial E_x \rangle$ and $\langle \partial \mu_I/\partial E_x \rangle$ are the averages of $\partial q_{I,I+1}/\partial E_x$ and $\partial \mu_I/\partial E_x$, respectively. Here it is assumed that the electric field is uniform so that

$$-\frac{d\varphi_{I,I+1}}{dE_x} = R_0 \ . \tag{45}$$

Furthermore, the factor 4.8 in Eq. (44) comes from the Riemann zeta function with the argument 3 (multiplied by a factor 4) for the dipole-dipole interactions (without damping). For details about the approximations used to obtain Eq. (44), see the appendix in Ref. 60.

In the case of $\omega \neq 0$, Eq. (45) is a good approximation given that the wavelength, $\lambda$, is much larger than the length of the chain $NR_0$. The number of atoms $N$ must be large so that $N\varepsilon \gg 1$, but at the same time small so that $\lambda \gg NR_0$. Furthermore, Eq. (44) was obtained by setting $\omega = 0$ and taking the sum of all equations in Eq. (41). To obtain a similar equation for $\omega \neq 0$, all that is needed is adding the sum of all frequency-dependent terms to the static part. Since the frequency-dependence appears in the diagonal part of the matrix, the result becomes

$$N \begin{pmatrix} 2(\varepsilon\eta^* - \omega^2 R_0^2 c_I^q) & 0 \\ 0 & \frac{1-4.8R_0^{-3}\alpha}{\alpha} - \omega^2 c_J^{\mu} \end{pmatrix} \begin{pmatrix} \langle \partial q_{I,I+1}/\partial E_x \rangle \\ \langle \partial \mu_{J,x}/\partial E_x \rangle \end{pmatrix} = N \begin{pmatrix} R_0 \\ 1 \end{pmatrix} \ . \tag{46}$$

The frequency-dependent polarizability along the linear chain becomes

$$\begin{aligned}\alpha_{xx}^{\mathrm{mol}}(\omega) &= N\left(R_0\langle\partial q_{I,I+1}/\partial E_x\rangle + \langle\partial\mu_{J,x}/\partial E_x\rangle\right) \\ &= N\left(\frac{R_0^2}{2(\varepsilon\eta^* - c^q\omega^2 R_0^2)} + \frac{\alpha}{1-4.8R_0^{-3}\alpha - \omega^2\alpha c^\mu}\right)\end{aligned} \tag{47}$$

which has two poles, $\omega_1$ and $\omega_2$, one associated with charge-transfer at

$$\omega_1 = \sqrt{\frac{\varepsilon\eta^*}{c^q R_0^2}} \tag{48}$$

and another associated with atomic point-dipoles at

$$\omega_2 = \sqrt{\frac{1}{c^\mu}\left(\frac{1}{\alpha} - \frac{4.8}{R_0^3}\right)}\,. \tag{49}$$

The lowest of these two frequencies, $\omega_1$ and $\omega_2$, can be viewed as the first excitation energy. From Eq. (48), it is seen that the excitation energy decreases when $\varepsilon$ becomes smaller, which is consistent with the interpretation that $\varepsilon = 0$ corresponds to a metallic system. Furthermore, the poles of the frequency-dependent polarizability are dependent on a correct division of the polarizability into a charge-transfer part, $\langle\partial q_{I,I+1}/\partial E_\alpha\rangle$, and a point-dipole part, $\langle\partial\mu_I/\partial E_\alpha\rangle$.

Including non-zero dissipation, and using $\omega_1$ and $\omega_2$ given by Eqs. (48) and (49), the polarizability of the linear chain is

$$\alpha_{xx}^{\mathrm{mol}}(\omega) = N\left(\frac{1}{2c^q(\omega_1^2 - \omega^2 + i\gamma^q\omega)} + \frac{1}{c^\mu(\omega_2^2 - \omega^2 + i\gamma^\mu\omega)}\right) \tag{50}$$

where it is understood that the amplitude of the polarisability $\alpha_{xx}$, is real and given by the absolute value of this complex quantity. With dissipation, the polarizability is finite both at $\omega = \omega_1$ and $\omega = \omega_2$.

## Calculations and parametrization

It is advantageous to use quantum chemical calculations for the parametrization of a molecular mechanics model since a consistent data set is obtained.[18] In principle, density functional theory (DFT) gives an improved description of molecular properties over the Hartree-Fock approximation, but for polarizabilities of large systems many functionals present problems and several improvements have been suggested.[75–83] We therefore use current-DFT[84] with the AUG/ATZP[85,86] basis set, which gives improved results for the polarizability for large systems.[87] If the frequency is too close to an excitation energy (pole in the polarization), DFT calculations are unreliable and such data points were removed from the data set. For the geometry optimization, the BLYP[88,89] functional and the TZP[85] basis set were employed. It is noted that linear symmetry was used in the geometry optimization of the polyynes structures. The ADF software[90–92] was used for all DFT calculations.

To test the model, a parametrization has been carried out for a handful of molecules (see table Table 1) and tested for all molecules in tables Table 2. Even though only the isotropic polarizabilities are presented in some cases, the full polarizability tensor was included in the parametrization. Furthermore, the error for each molecule and each component of the polarizability was divided by the isotropic polarization of the molecule, in an effort to keep all molecules in the training set equally important. For the frequency-dependent terms, the difference between the static and the polarization at the given frequency was considered in the parametrization.

In the notation of graphenes, we refer to one type of chains of aromatic rings as armchair structures, whereas the zigzag structures correspond to the acenes. The notation $g(N,M)$ refers to an aromatic system with $N$ rings in the zigzag direction and $M$ rings in the armchair direction. The same set of parameters, given in table Table 3, is used for all molecules. Since dissipation was not included in the DFT calculations, it is also excluded in the parametrization.

The $\Phi_I^*$-parameter used here is equivalent to a Gaussian distribution with a standard-deviation of about 1.1 Bohr, which is more reasonable than a Gaussian with a standard-deviation of 2.6 Bohr obtained in earlier work.[60] Reasonable sizes for the $\Phi_I^*$ parameters are important when for

Table 1: Molecules in training set

| Group | Molecules |
|---|---|
| Alkanes | ethane, propane, dodecane |
| Polyenes | ethene, $C_{18}H_{22}$ |
| Acenes | benzene, octacene |
| Armchair | benzo[c]naphto[2,1-m]picene |
| Poly(p-phenylene vinylene) | 1,4-dicinnamyl-benzene |
| Other systems | g(4,3) |

Table 2: Molecules

| Group | Molecules |
|---|---|
| Alkanes | ethane, propane, octane and dodecane |
| Polyenes | ethene, hexatriene, $C_{14}H_{16}$, $C_{18}H_{20}$ $C_{22}H_{24}$ and $C_{26}H_{28}$ |
| Acenes | benzene, anthracene, pentacene, and octacene |
| Armchair | phenanthrene, chrysene, benzo[c]picene, benzo[c]naphto[2,1-m]picene |
| Poly(p-phenylene vinylene) | styrene, stilbene,1,4-dicinnamyl-benzene |
| Polyynes | ethyne, $C_8H_2$, $C_{16}H_2$, $C_{20}H_2$ |

example studying the interaction between two molecules, where the function $S_{IJ}$ is more important. The polarizability of carbon is within the expected range. It is noted that the model is sensitive to how close $g^*_{1,I}$ is to one, and it is therefore included with 4 digits here. To summarize, it is satisfying to have only one set of carbon parameters describing both $sp^3$ and $sp^2$-carbon atoms.

# Results

The polarizability of the alkane molecules, see Figure 1, is almost independent of the frequency. The out-of-plane component of the polyenes does not increase significantly with frequency, see Figure 2(a), while the in-plane component, defined as $\alpha_{in} = 1/2(\alpha_{xx} + \alpha_{yy})$, has a much stronger dependence on the frequency, especially for the larger molecules (see Figure 2(b)). Thus for systems with a low $\varepsilon$ as the polyenes, the critical frequency associated with charge transfer, exemplified in Eq. (48), gives the dominating contribution to the frequency dependence of the polarizability. The isotropic polarizability of the alkanes and the out-of-plane component for the polyenes increase both about 4% from $\omega = 0$ to $\omega = 0.1$ hartree. Thus the charge transfer contribution for

Table 3: Atom-type parameters (au)

| | $\alpha_I$ | $x_I^*$ | $\Phi_I^*$ | $g_{0,I}^*$ | $g_{1,I}^*$ | $C_I^*$ | $R_I^*$ | $\eta_I^*$ | $c_I^q$ | $c_I^\mu$ |
|---|---|---|---|---|---|---|---|---|---|---|
| H | 1.65 | 0.32 | 1.02 | 1.00 | - | - | - | 0.23 | 0.03 | 0.63 |
| C | 8.35 | 0.38 | 0.43 | 0.77 | 0.9957 | 4.13 | 1.41 | 1.03 | 0.61 | 0.59 |

alkanes behave differently from the charge transfer terms of the polyenes.

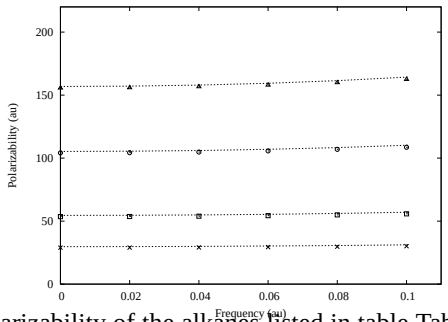


Figure 1: The isotropic polarizability of the alkanes listed in table Table 2 in order of increasing molecular size (from bottom to top), as a function of the frequency. The points represent c-DFT data while the lines represent the model.

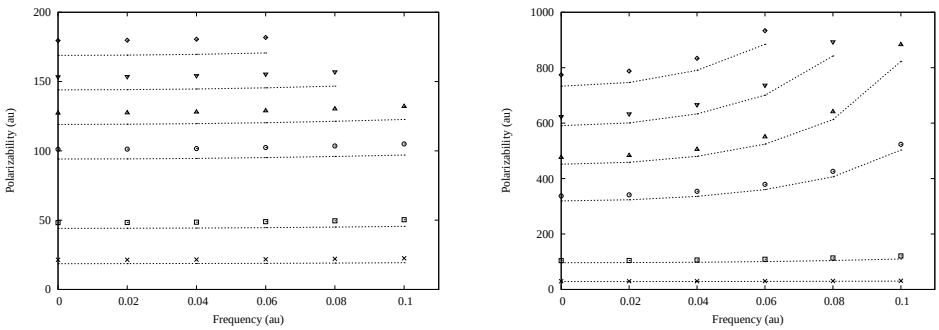


Figure 2: The out-of plane (a) and in-plane (b) components of the polarizability of the polyenes listed in table Table 2 in order of increasing molecular size (from bottom to top), as a function of the frequency. The points represent the c-DFT data while the lines represent the model.

The aromatic systems are presented in Figure 3(a), Figure 3(b), Figure 4(a) and Figure 4(b). For the polyenes and the aromatic systems, the out-of plane components behave similarly for all systems and are more or less constant as a function of the frequency. Therefore only the static polarizability is shown in Figure 3(a) and Figure 4(a). The out-of-plane contributions to the polarizability is adequately described for these systems.

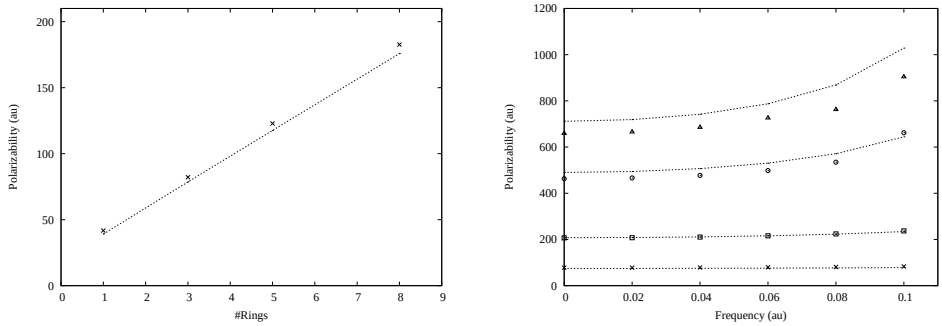


Figure 3: The out-of plane (a) and the in-plane (b) components of the polarizability of the acenes listed in table Table 2. (a) the static polarizability as a function of the number of rings in the system. (b) the polarizability in order of increasing molecular size (from bottom to top), as a function of the frequency. In both cases, the points represent the c-DFT data while the lines represent the model.

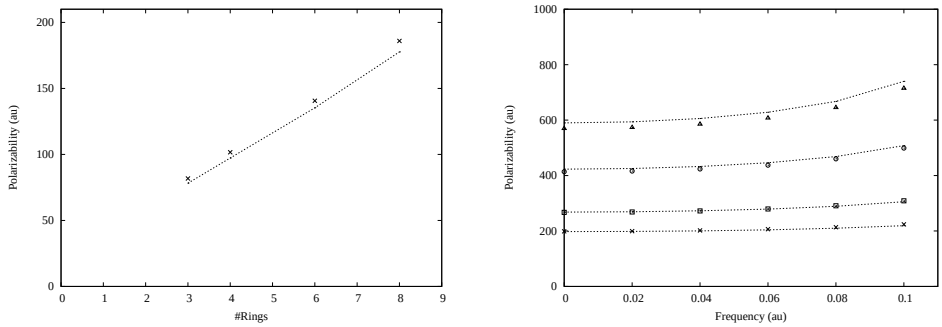


Figure 4: The out-of plane (a) and the in-plane (b) components of the polarizability of the armchair system listed in table Table 2. (a) static polarizability as a function of the number of rings in the system, (b) the polarizability in order of increasing molecular size (from bottom to top), as a function of the frequency. The points represent the c-DFT data while the lines represent the model.

Also the in-plane component behaves quantitatively similarly for these systems (polyenes, acenes and armchair structures). The static polarizability for these systems are larger than a corresponding alkane chain, and the increase in polarizability due to the frequency is higher. However, there are small differences within these systems, which appear both in the c-DFT data and in the data obtained from the model. The in-plane component of the polarizability of the polyenes increases more with length compared to the acenes (Figure 3(b)) which again has slightly higher polarizability than the armchair series (Figure 4(b)). The differences in polarizability can be explained by looking at the number of carbon atoms in the chain compared to the length of the chain.

In table Table 4, the size of the chains are reported both with respect to number of carbon atoms and distance. It is noted that although the polyene $C_{18}H_{20}$ and octacene have a similar number of carbon atoms in the chain, the polyene is about 7% longer. Thus with the same electric field, the polyene feels a larger potential difference between its ends as compared to octacene. The

Table 4: Chain length

| Name | Scaling[1] | #C[2] | Distance/Å[3] |
|---|---|---|---|
| $C_{18}H_{20}$ | 1.85 | 18 | 21.7 |
| octazene | 1.34 | 17 | 19.7 |
| benzo[c]naphto[2,1-m]picene | 1.25 | 18 | 18.0 |

same reasoning can be used to explain why octacene has a higher polarizability (both static and frequency-dependent) compared to benzo[c]naphto[2,1-m]picene. The latter is shorter in length but longer in terms of number of carbon atoms, both which according to the model should predict a lower polarizability. In addition, due to slightly different bond distances, octacene has a higher average $\varepsilon$ along the chain compared to benzo[c]naphto[2,1-m]picene. For both polyenes and aromatic molecules, the sum of the two distances describing $g_{I,KM}$ and $\varepsilon$ is usually about 2.8 Å. However, in a few cases where carbon is bonded to three other carbon atoms, this distance may increase to about 2.9 Å. In this case, $\varepsilon$ increases to around 0.15 (see Figure 5), which is a factor 3 larger than the value for the polyene chains, and which lead to the revised form of $g_{I,KM}$ in Eq. (17). This is the case both for the acenes and in the armchair series, but for the acenes it has less impact on the total polarizability. For the acenes, $\varepsilon$ becomes larger when connecting the two parallel carbon chains, and in this case the value of $\varepsilon$ is of less importance. For the armchair series, $\varepsilon$ becomes large for a few connections along the chain which have a larger impact.

In the poly(p-phenylene vinylene) systems, the key junctions between the benzene ring and the vinyl group has an $g_{I,KM}$ or $\varepsilon$ described by bond lengths which sum to about 2.9 Å, so also in this case, the revised form of $g_{I,KM}$ in Eq. (17) lead to a dramatic improvement of the description of the polarizability along the chain. Thus these systems are now well described (see Figure 6). From Figure 5 it is also noted that the $\varepsilon$ for $sp^3$-carbon is lower than in out previous work.[60] In addition, both the hardness for hydrogen and and $\varepsilon$ when one of the atoms is a hydrogen atom (given by

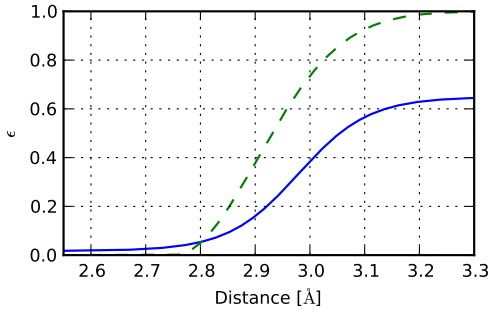


Figure 5: $\varepsilon$ for carbon as a function of the sum of two bond lengths ($R_{IK}+R_{IM}$), $-$ model and parameters used in this work, $--$ model and parameters used previously.[60] For $sp^3$ carbon the relevant distance is typically around 3.1 Å, while for $sp^2$-carbon it is typically about 2.8 Å, but can increase to about 2.9 Å in some situations. For $sp$-carbon the distance is about 2.6 Å.

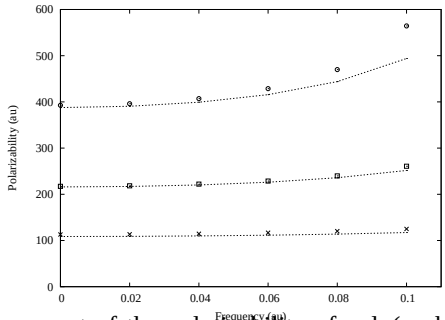


Figure 6: The in-plane component of the polarizability of poly(p-phenylene vinylene) systems listed in table Table 2, in order of increasing molecular size (from bottom to top), as a function of the frequency. The points represent the c-DFT data while the lines represent the model.

$\varepsilon = 1 - g^{*}_{0,C}{}^{3} g^{*}_{0,H} \approx 0.46$) is less than in previous works.[60] In combination, these effects give a larger charge transfer contribution compared to previous work (for dodecane the charge transfer contribution is currently of the same order of magnitude as the point dipole terms).[60] However since the charge transfer term of the polarizability in a long linear chain is proportional to $\varepsilon^{-1}$ (see Eq. (47)), the differences between the models are less critical for high values of $\varepsilon$.

The polarizability along linear polyyne chains (not included in the parametrization) are shown in Figure 7. For the longest chain at high frequencies, relatively larger errors are noted. However, these errors are associated with a high frequency, and small errors in the estimation of the critical frequency, approximately given by Eq. (49) for long chains, will have large impact on the result.

For these systems $\varepsilon$ approaches $1 - g_{I,C}^{*\,4}$ and is thus about 0.02 (see Figure 5), and since the model overestimates the frequency-dependent polarizability, this value is probably slightly too low. But, taken into consideration that the model was not parametrized with triple bonds, the polarizability of the smaller systems and the static polarizability of the larger systems are well described.

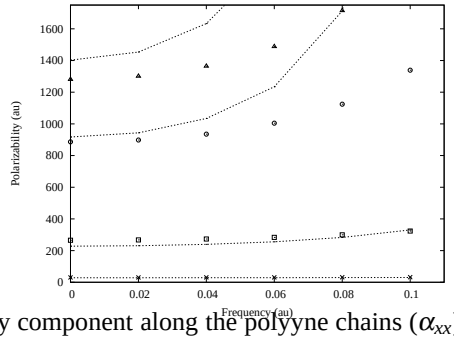


Figure 7: The polarizability component along the polyyne chains ($\alpha_{xx}$) listed in table Table 2, in order of increasing molecular size (from bottom to top), as a function of the frequency. The points represent the c-DFT data while the lines represent the model.

In addition, the model was tested for both the static and frequency-dependent polarizability for a large set of carbon-hydrogen systems not included in the parametrization, and the results of this test is given in supplementary material. With the exception of a few cases with high frequency close to a critical frequency, the model predicts the polarizability within 5-10% error for all molecules and all polarizability components in the test. This shows that the parameters obtained studying simple systems are indeed transferable to other more complex molecules. One reason for obtaining good static polarizability for many different systems, with parameters obtained from a small training set is that the frequency-dependent polarizability is critically dependent on how the static polarizability is divided into charge-transfer and point-dipole contributions.

# Conclusions

The differences between the c-DFT calculations and the model are in general small, and it is concluded that the presented model is capable of modeling the frequency-dependent polarizability for systems containing hydrogen and carbon. Investigating the frequency-dependent polarizability

also helps in parametrize the static polarizability, since the frequency-dependent polarizability is highly dependent on how the static polarizability is divided into a charge-transfer part and a point-dipole part. It is demonstrated that parameters for the polarizability yielding good result for many different systems could be obtained using a small training set.

## Acknowledgments

We would like to thank Magnus Ringholm for his contribution to the software development in his master thesis. Support from the Norwegian Research Council through a Strategic Industry Program (164603/I30), and a grant of computer time are acknowledged.

### Notes and References

(1) Prasad, P. N.; Williams, D. J. *Introduction to nonlinear optical effects in molecules and polymers*; Wiley: New York, 1991.

(2) Kanis, D. R.; Ratner, M. A.; Marks, T. J. *Chem. Rev.* **1994**, *94*, 195–242.

(3) Olsen, J.; Jørgensen, P. *J. Chem. Phys.* **1985**, *82*, 3235–3264.

(4) Allen, M. P.; Tildesley, D. S. *Computer Simulations of Liquids*; Clarendon: Oxford, 1987.

(5) Engkvist, O.; Åstrand, P.-O.; Karlström, G. *Chem. Rev.* **2000**, *100*, 4087–4108.

(6) Ponder, J. W.; Case, D. A. *Adv. Protein Chem.* **2003**, *66*, 27–85.

(7) Rick, S. W.; Stuart, S. J. *Rev. Comp. Chem.* **2002**, *18*, 89–146.

(8) Rappé, A. K.; III, W. A. G. *J. Phys. Chem.* **1991**, *95*, 3358–3363.

(9) van Duin, A. C. T.; Dasgupta, S.; Lorant, F.; III, W. A. G. *J. Phys. Chem. A* **2001**, *105*, 9396–9409.

(10) Lamoureux, G.; Roux, B. *J. Chem. Phys.* **2003**, *119*, 3025–3039.

(11) Yu, H.; van Gunsteren, W. F. *Comput. Phys. Commun.* **2005**, *172*, 69–85.

(12) Lopes, P. E. M.; Lamoureux, G.; Roux, B.; Jr., A. D. M. *J. Phys. Chem. B* **2007**, *111*, 2873–2885.

(13) Silberstein, L. *Phil. Mag.* **1917**, *33*, 92–128.

(14) Silberstein, L. *Phil. Mag.* **1917**, *33*, 521–533.

(15) Applequist, J. *Acc. Chem. Res.* **1977**, *10*, 79–85.

(16) Applequist, J.; Carl, J. R.; Fung, K.-F. *J. Am. Chem. Soc.* **1972**, *94*, 2952–2960.

(17) Applequist, J. *J. Chem. Phys.* **1985**, *83*, 809–826, Erratum in 98, 7664, 1993.

(18) Jensen, L.; Åstrand, P.-O.; Sylvester-Hvid, K. O.; Mikkelsen, K. V. *J. Phys. Chem. A* **2000**, *104*, 1563–1569.

(19) Thole, B. T. *Chem. Phys.* **1981**, *59*, 341–350.

(20) Birge, R. R. *J. Chem. Phys.* **1980**, *72*, 5312–5319.

(21) Jensen, L.; Åstrand, P.-O.; Osted, A.; Kongsted, J.; Mikkelsen, K. V. *J. Chem. Phys.* **2002**, *116*, 4001–4010.

(22) Jensen, L.; Schmidt, O. H.; Mikkelsen, K. V.; Åstrand, P.-O. *J. Phys. Chem. B* **2000**, *104*, 10462–10466.

(23) Kongsted, J.; Osted, A.; Jensen, L.; Åstrand, P.-O.; Mikkelsen, K. V. *J. Phys. Chem. B* **2001**, *105*, 10243–10248.

(24) Hansen, T.; Jensen, L.; Åstrand, P.-O.; Mikkelsen, K. V. *J. Chem. Theory Comput.* **2005**, *1*, 626–633.

(25) Applequist, J. *J. Chem. Phys.* **1973**, *58*, 4251–4259.

(26) Applequist, J. *J. Am. Chem. Soc.* **1973**, *95*, 8255–8258.

(27) Sundberg, K. R. *J. Chem. Phys.* **1978**, *68*, 5271–5276.

(28) Applequist, J. *J. Phys. Chem. A* **1998**, *102*, 7723–7724.

(29) Sundberg, K. R. *J. Chem. Phys.* **1977**, *66*, 114–118.

(30) Buckingham, A. D.; Concannon, E. P.; Hands, I. D. *J. Phys. Chem.* **1994**, *98*, 10455–10459.

(31) Jensen, L.; Sylvester-Hvid, K. O.; Mikkelsen, K. V.; Åstrand, P.-O. *J. Phys. Chem. A* **2003**, *107*, 2270–2276.

(32) Jensen, L.; Åstrand, P.-O.; Mikkelsen, K. V. *Nano Lett.* **2003**, *3*, 661–665.

(33) Jensen, L.; Åstrand, P.-O.; Mikkelsen, K. V. *J. Phys. Chem. B* **2004**, *108*, 8226–8233.

(34) Jensen, L.; Åstrand, P.-O.; Mikkelsen, K. V. *J. Phys. Chem. A* **2004**, *108*, 8795–8800.

(35) Jensen, L.; Esbensen, A. L.; Åstrand, P.-O.; Mikkelsen, K. V. *J. Comput. Meth. Sci. Engin.* **2006**, *6*, 353–364.

(36) Jensen, L.; Åstrand, P.-O.; Mikkelsen, K. V. *J. Comput. Theor. Nanosci* **2009**, *6*, 270–291.

(37) Applequist, J.; Quicksall, C. O. *J. Chem. Phys.* **1977**, *66*, 3455–3459.

(38) Bocian, D. F.; Schick, G. A.; Birge, R. R. *J. Chem. Phys.* **1981**, *74*, 3660–3667.

(39) Xie, W.; Pu, J.; Jr., A. D. M.; Gao, J. *J. Chem. Theory Comput.* **2007**, *3*, 1878–1889.

(40) Bernardo, D. N.; Ding, Y.; Krogh-Jespersen, K.; Levy, R. M. *J. Phys. Chem.* **1994**, *98*, 4180–4187.

(41) Olson, M. L.; Sundberg, K. R. *J. Chem. Phys.* **1978**, *69*, 5400–5404.

(42) Applequist, J. *J. Phys. Chem.* **1993**, *97*, 6016–6023.

(43) Shanker, B.; Applequist, J. *J. Phys. Chem.* **1994**, *98*, 6486–6489.

(44) Jensen, L.; Åstrand, P.-O.; Mikkelsen, K. V. *Int. J. Quant. Chem.* **2001**, *84*, 513–522.

(45) Jensen, L. L.; Jensen, L. *J. Phys. Chem. C* **2008**, *112*, 15697–15703.

(46) Stern, H. A.; Rittner, F.; Berne, B. J.; Friesner, R. A. *J. Chem. Phys.* **2001**, *115*, 2237–2251.

(47) Mayer, A. *Phys. Rev. B* **2005**, *71*, 235333.

(48) Mayer, A. *Appl. Phys. Lett.* **2005**, *86*, 153110.

(49) Mayer, A.; Lambin, P.; Langlet, R. *Appl. Phys. Lett.* **2006**, *89*, 063117.

(50) Mayer, A. *Phys. Rev. B* **2007**, *75*, 045407.

(51) Mayer, A.; Åstrand, P.-O. *J. Phys. Chem. A* **2008**, *112*, 1277–1285.

(52) Chelli, R.; Procacci, P.; Righini, R.; Califano, S. *J. Chem. Phys.* **1999**, *111*, 8569–8575.

(53) Shanker, B.; Applequist, J. *J. Phys. Chem.* **1996**, *100*, 10834–10836.

(54) Nistor, R. A.; Polihronov, J. G.; Müser, M. H.; Mosey, N. J. *J. Chem. Phys.* **2006**, *125*, 094108.

(55) Mathieu, D. *J. Chem. Phys.* **2007**, *127*, 224103.

(56) Chen, J.; Martínez, T. J. *Chem. Phys. Lett.* **2007**, *438*, 315–320.

(57) Lee Warren, G.; Davis, J. E.; Patel, S. *J. Chem. Phys.* **2008**, *128*, 144110.

(58) Chen, J.; Hundertmark, D.; Martínez, T. J. *J. Chem. Phys.* **2008**, *129*, 214113.

(59) Nistor, R. A.; Müser, M. H. *Phys. Rev. B* **2009**, *79*, 104303.

(60) Smalø, H. S.; Åstrand, P.-O.; Jensen, L. *J. Chem. Phys.* **2009**, *131*, 044101.

(61) Verstraelen, T.; Speybroeck, V. V.; Waroquier, M. *J. Chem. Phys.* **2009**, *131*, 044127.

(62) Applequist, J.; Sundberg, K. R.; Olson, M. L.; Weiss, L. C. *J. Chem. Phys.* **1979**, *70*, 1240–1246, Erratum in **71**, 2330, 1979.

(63) Shanker, B.; Applequist, J. *J. Chem. Phys.* **1996**, *104*, 6109–6116.

(64) Jensen, L. L.; Jensen, L. *J. Phys. Chem. C* **2009**, *113*, 15182–15190.

(65) Mayer, A.; Lambin, P.; Åstrand, P.-O. *Nanotechnology* **2008**, *19*, 025203.

(66) Mayer, A.; González, A. L.; Aikens, C. M.; Schatz, G. C. *Nanotechnology* **2009**, *20*, 195204.

(67) Mayer, A.; Schatz, G. C. *J. Phys.: Condens. Matter* **2009**, *21*, 325301.

(68) In atomic units, $|e| = 1$, $\hbar = 1$, $m_e = 1$, $1/4\pi\varepsilon_0 = 1$. The energy unit 1 hartree is given by $E_h = m_e e^4/(4\pi\varepsilon_0\hbar)^2 \approx 4.36 \times 10^{-18}$ J, distance unit is 1 bohr given by $a_0 = 4\pi\varepsilon_0/(m_e e^2) \approx 5.29 \times 10^{-11}$m, frequency is given by $E_h/\hbar \approx 4.13 \times 10^{16}$Hz and polarization is given by $a_0^3 \approx 0.15\text{Å}^3$.

(69) Mortier, W. J.; van Genechten, K.; Gasteiger, J. *J. Am. Chem. Soc.* **1985**, *107*, 829–835.

(70) Stern, H. A.; Kaminski, G. A.; Banks, J. L.; Zhou, R.; Berne, B. J.; Friesner, R. A. *J. Phys. Chem. B* **1999**, *103*, 4730–4737.

(71) van der Velde, G. A. A realistic Coulomb potential. *MD and MC on water. CECAM workshop report*, Orsay, France, 1972; pp 38–39.

(72) Buckingham, A. D. *Adv. Chem. Phys.* **1967**, *12*, 107–142.

(73) Birge, R. R.; Schick, G. A.; Bocian, D. F. *J. Chem. Phys.* **1983**, *79*, 2256–2264.

(74) Smalø, H. S.; Åstrand, P.-O. Submitted.

(75) Champagne, B.; PerpÃÍte, E. A.; Jacquemin, D.; van Gisbergen, S. J. A.; Baerends, E.-J.; Soubra-Ghaoui, C.; Robins, K. A.; Kirtman, B. *J. Phys. Chem. A* **2000**, *104*, 4755–4763.

(76) Champagne, B.; Perpéte, E. A.; van Gisbergen, S. J. A.; Baerends, E.-J.; Snijders, J. G.; Soubra-Ghaoui, S.; Robins, K. A.; Kirtman, B. *J. Chem. Phys.* **1998**, *109*, 10489–10498.

(77) van Faassen, M.; de Boeij, P. L.; van Leeuwen, R.; Berger, J. A.; Snijders, J. G. *Phys. Rev. Lett.* **2002**, *88*, 186401.

(78) van Faassen, M.; de Boeij, P. L.; van Leeuwen, R.; Berger, J. A.; Snijders, J. G. *J. Chem. Phys.* **2003**, *118*, 1044–1053.

(79) Sałek, P.; Helgaker, T.; Vahtras, O.; Ågren, H.; Jonsson, D.; Gauss, J. *Mol. Phys.* **2005**, *103*, 439–450.

(80) Peach, M. J. G.; Helgaker, T.; Sałek, P.; Keal, T. W.; Lutnæs, O. B.; Tozer, D. J.; Handy, N. C. *Phys. Chem. Chem. Phys.* **2006**, *8*, 558–562.

(81) Champagne, B.; Bulat, F. A.; Yang, W.; Bonness, S.; Kirtman, B. *J. Chem. Phys.* **2006**, *125*, 194114.

(82) Vydrov, O. A.; Scuseria, G. E. *J. Chem. Phys.* **2006**, *125*, 234109.

(83) Sekino, H.; Maeda, Y.; Kamiya, M.; Hirao, K. *J. Chem. Phys.* **2007**, *126*, 014107.

(84) Vignale, G.; Kohn, W. *Phys. Rev. Lett.* **1996**, *77*, 2037.

(85) van Lenthe, E.; Baerends, E. J. *Journal of Computational Chemistry* **2003**, *24*, 1142–1156.

(86) Chong, D. P. *Mol. Phys.* **2005**, *103*, 749–761.

(87) van Faassen, M.; Jensen, L.; Berger, J. A.; de Boeij, P. L. *Chem. Phys. Lett.* **2004**, *395*, 274–278.

(88) Becke, A. D. *Phys. Rev. A* **1988**, *38*, 3098.

(89) Lee, C.; Yang, W.; Parr, R. G. *Phys. Rev. B* **1988**, *37*, 785.

(90) te Velde, G.; Bickelhaupt, F. M.; Baerends, E. J.; Guerra, C. F.; van Gisbergen, S. J. A.; Snijders, J. G.; Ziegler, T. *J. Comput. Chem.* **2001**, *22*, 931–967.

(91) Guerra, C. F.; Snijders, J. G.; te Velde, G.; Baerends, E. J. *Theor. Chem. Acc.* **1998**, *99*, 391–401.

(92) *ADF2008.01*; SCM, Theoretical Chemistry: Vrije Universiteit, Amsterdam, The Netherlands, 2008, http://www.scm.com.

# Supplementary data

Table 1: Polarizability in au

| | $\omega$ | $\alpha_{xx}$ | | $\alpha_{yy}$ | | $\alpha_{zz}$ | | $\alpha_{xy}$ | | $\alpha_{xz}$ | | $\alpha_{yz}$ | |
|---|---|---|---|---|---|---|---|---|---|---|---|---|---|
| | | Mod. | DFT | Mod. | DFT | Mod. | DFT | Mod. | DFT | Mod. | DFT | Mod. | DFT |
| methane | 0.00 | 16.46 | 17.23 | 16.46 | 17.23 | 16.46 | 17.23 | 0.00 | 0.00 | 0.00 | 0.00 | -0.00 | 0.00 |
| ethane | 0.00 | 27.85 | 27.65 | 27.85 | 27.65 | 33.72 | 31.58 | -0.00 | 0.00 | -0.00 | 0.00 | -0.00 | 0.00 |
| ethane | 0.02 | 27.88 | 27.69 | 27.88 | 27.69 | 33.82 | 31.63 | -0.00 | 0.00 | -0.00 | 0.00 | -0.00 | 0.00 |
| ethane | 0.04 | 27.98 | 27.80 | 27.98 | 27.80 | 34.11 | 31.78 | -0.00 | 0.00 | -0.00 | 0.00 | -0.00 | 0.00 |
| ethane | 0.06 | 28.16 | 28.01 | 28.16 | 28.01 | 34.61 | 32.04 | -0.00 | 0.00 | -0.00 | 0.00 | -0.00 | 0.00 |
| ethane | 0.08 | 28.41 | 28.29 | 28.41 | 28.29 | 35.38 | 32.41 | -0.00 | 0.00 | -0.00 | 0.00 | -0.00 | 0.00 |
| ethane | 0.10 | 28.74 | 28.68 | 28.74 | 28.68 | 36.46 | 32.90 | -0.00 | 0.00 | -0.00 | 0.00 | -0.00 | 0.00 |
| propane | 0.00 | 46.24 | 45.28 | 38.06 | 38.01 | 41.92 | 40.27 | 0.00 | 0.00 | -0.00 | 0.00 | -0.00 | 0.00 |
| propane | 0.02 | 46.34 | 45.35 | 38.10 | 38.06 | 41.99 | 40.34 | 0.00 | 0.00 | -0.00 | 0.00 | -0.00 | 0.00 |
| propane | 0.04 | 46.64 | 45.57 | 38.24 | 38.23 | 42.22 | 40.52 | 0.00 | 0.00 | -0.00 | 0.00 | -0.00 | 0.00 |
| propane | 0.06 | 47.17 | 45.93 | 38.47 | 38.51 | 42.61 | 40.84 | 0.00 | 0.00 | -0.00 | 0.00 | -0.00 | 0.00 |
| propane | 0.08 | 47.95 | 46.46 | 38.80 | 38.92 | 43.19 | 41.30 | 0.00 | 0.00 | -0.00 | 0.00 | -0.00 | 0.00 |
| propane | 0.10 | 49.03 | 47.17 | 39.25 | 39.46 | 43.99 | 41.92 | 0.00 | 0.00 | -0.00 | 0.00 | -0.00 | 0.00 |
| butane | 0.00 | 62.31 | 61.24 | 53.38 | 51.27 | 48.05 | 48.16 | -2.41 | -1.43 | -0.00 | 0.00 | 0.00 | 0.00 |
| butane | 0.02 | 62.44 | 61.34 | 53.47 | 51.35 | 48.11 | 48.23 | -2.43 | -1.44 | 0.00 | 0.00 | -0.00 | 0.00 |
| butane | 0.04 | 62.86 | 61.64 | 53.76 | 51.59 | 48.27 | 48.44 | -2.51 | -1.45 | 0.00 | 0.00 | -0.00 | 0.00 |
| butane | 0.06 | 63.59 | 62.15 | 54.24 | 52.01 | 48.56 | 48.80 | -2.65 | -1.47 | 0.00 | 0.00 | -0.00 | 0.00 |
| butane | 0.08 | 64.66 | 62.88 | 54.95 | 52.61 | 48.97 | 49.32 | -2.86 | -1.50 | -0.00 | 0.00 | 0.00 | 0.00 |
| butane | 0.10 | 66.14 | 63.86 | 55.93 | 53.42 | 49.52 | 50.01 | -3.17 | -1.55 | 0.00 | 0.00 | -0.00 | 0.00 |
| pentane | 0.00 | 57.92 | 58.26 | 78.05 | 77.30 | 65.45 | 62.52 | 0.00 | 0.00 | -0.00 | 0.00 | 0.00 | 0.00 |
| hexane | 0.00 | 82.65 | 79.18 | 89.08 | 88.76 | 67.74 | 68.36 | -8.85 | -9.22 | -0.00 | 0.00 | 0.00 | 0.00 |
| hexane | 0.02 | 82.83 | 79.31 | 89.25 | 88.91 | 67.82 | 68.46 | -8.89 | -9.24 | 0.00 | 0.00 | 0.00 | 0.00 |
| hexane | 0.04 | 83.35 | 79.71 | 89.77 | 89.35 | 68.05 | 68.76 | -9.03 | -9.30 | -0.00 | 0.00 | -0.00 | 0.00 |
| hexane | 0.06 | 84.25 | 80.39 | 90.66 | 90.09 | 68.44 | 69.28 | -9.28 | -9.39 | 0.00 | 0.00 | 0.00 | 0.00 |
| hexane | 0.08 | 85.59 | 81.37 | 91.96 | 91.17 | 69.01 | 70.03 | -9.63 | -9.53 | -0.00 | 0.00 | -0.00 | 0.00 |
| hexane | 0.10 | 87.46 | 82.69 | 93.73 | 92.61 | 69.77 | 71.04 | -10.13 | -9.70 | 0.00 | 0.00 | -0.00 | 0.00 |
| heptane | 0.00 | 77.53 | 78.31 | 111.68 | 111.37 | 88.50 | 84.57 | -0.00 | 0.00 | -0.00 | 0.00 | -0.00 | 0.00 |
| octane | 0.00 | 129.23 | 128.80 | 99.62 | 95.36 | 87.30 | 88.26 | -0.68 | 0.57 | 0.00 | 0.00 | -0.00 | 0.00 |
| octane | 0.02 | 129.52 | 129.02 | 99.80 | 95.51 | 87.39 | 88.39 | -0.70 | 0.57 | 0.00 | 0.00 | -0.00 | 0.00 |
| octane | 0.04 | 130.40 | 129.68 | 100.32 | 95.98 | 87.68 | 88.79 | -0.76 | 0.57 | 0.00 | 0.00 | 0.00 | 0.00 |
| octane | 0.06 | 131.90 | 130.82 | 101.22 | 96.77 | 88.18 | 89.45 | -0.87 | 0.56 | -0.00 | 0.00 | -0.00 | 0.00 |
| octane | 0.08 | 134.11 | 132.45 | 102.54 | 97.93 | 88.90 | 90.42 | -1.05 | 0.55 | 0.00 | 0.00 | -0.00 | 0.00 |
| octane | 0.10 | 137.13 | 134.63 | 104.37 | 99.48 | 89.86 | 91.72 | -1.31 | 0.54 | -0.00 | 0.00 | 0.00 | 0.00 |
| decane | 0.00 | 164.02 | 164.05 | 122.57 | 117.49 | 106.78 | 108.13 | 0.39 | 1.75 | -0.00 | 0.00 | -0.00 | 0.00 |
| dodecane | 0.00 | 157.59 | 151.63 | 187.09 | 187.25 | 126.23 | 127.93 | -22.51 | -24.48 | -0.00 | 0.00 | 0.00 | 0.00 |
| dodecane | 0.02 | 157.90 | 151.89 | 187.48 | 187.57 | 126.36 | 128.12 | -22.60 | -24.53 | -0.00 | 0.00 | 0.00 | 0.00 |
| dodecane | 0.04 | 158.85 | 152.66 | 188.66 | 188.56 | 126.78 | 128.69 | -22.88 | -24.69 | -0.00 | 0.00 | 0.00 | 0.00 |
| dodecane | 0.06 | 160.48 | 153.98 | 190.68 | 190.23 | 127.48 | 129.67 | -23.37 | -24.95 | -0.00 | 0.00 | 0.00 | 0.00 |
| dodecane | 0.08 | 162.89 | 155.89 | 193.63 | 192.65 | 128.50 | 131.08 | -24.08 | -25.33 | -0.00 | 0.00 | 0.00 | 0.00 |
| dodecane | 0.10 | 166.23 | 158.47 | 197.65 | 195.89 | 129.88 | 132.98 | -25.05 | -25.82 | -0.00 | 0.00 | 0.00 | 0.00 |

Table 2: Polarizability in au

| | $\omega$ | $\alpha_{xx}$ | | $\alpha_{yy}$ | | $\alpha_{zz}$ | | $\alpha_{xy}$ | | $\alpha_{xz}$ | | $\alpha_{yz}$ | |
|---|---|---|---|---|---|---|---|---|---|---|---|---|---|
| | | Mod. | DFT | Mod. | DFT | Mod. | DFT | Mod. | DFT | Mod. | DFT | Mod. | DFT |
| ethene | 0.00 | 18.61 | 21.40 | 27.16 | 25.61 | 29.86 | 33.71 | 0.00 | 0.00 | 0.00 | 0.00 | -0.00 | 0.00 |
| ethene | 0.02 | 18.64 | 21.44 | 27.19 | 25.65 | 29.94 | 33.79 | 0.00 | 0.00 | 0.00 | 0.00 | -0.00 | 0.00 |
| ethene | 0.04 | 18.72 | 21.56 | 27.31 | 25.77 | 30.17 | 34.05 | 0.00 | 0.00 | 0.00 | 0.00 | 0.00 | 0.00 |
| ethene | 0.06 | 18.85 | 21.77 | 27.50 | 25.97 | 30.57 | 34.49 | 0.00 | 0.00 | 0.00 | 0.00 | 0.00 | 0.00 |
| ethene | 0.08 | 19.04 | 22.08 | 27.78 | 26.27 | 31.17 | 35.13 | 0.00 | 0.00 | 0.00 | 0.00 | 0.00 | 0.00 |
| ethene | 0.10 | 19.30 | 22.49 | 28.15 | 26.66 | 32.00 | 36.01 | 0.00 | 0.00 | 0.00 | 0.00 | 0.00 | 0.00 |
| butadiene | 0.00 | 63.12 | 75.70 | 50.98 | 48.86 | 31.47 | 34.83 | -5.33 | -9.01 | 0.00 | 0.00 | 0.00 | 0.00 |
| butadiene | 0.02 | 63.32 | 76.02 | 51.07 | 48.96 | 31.51 | 34.89 | -5.38 | -9.09 | 0.00 | 0.00 | 0.00 | 0.00 |
| butadiene | 0.04 | 63.94 | 76.99 | 51.35 | 49.27 | 31.64 | 35.06 | -5.51 | -9.33 | 0.00 | 0.00 | 0.00 | 0.00 |
| butadiene | 0.06 | 65.02 | 78.70 | 51.82 | 49.79 | 31.85 | 35.37 | -5.75 | -9.76 | 0.00 | 0.00 | 0.00 | 0.00 |
| butadiene | 0.08 | 66.63 | 81.31 | 52.52 | 50.57 | 32.15 | 35.81 | -6.12 | -10.42 | 0.00 | 0.00 | 0.00 | 0.00 |
| butadiene | 0.10 | 68.92 | 85.12 | 53.48 | 51.64 | 32.55 | 36.40 | -6.65 | -11.42 | 0.00 | 0.00 | 0.00 | 0.00 |
| hexatriene | 0.00 | 111.26 | 130.68 | 80.54 | 77.32 | 44.09 | 48.23 | -21.03 | -27.44 | 0.00 | 0.00 | 0.00 | 0.00 |
| hexatriene | 0.02 | 111.85 | 131.48 | 80.77 | 77.57 | 44.15 | 48.31 | -21.28 | -27.74 | 0.00 | 0.00 | 0.00 | 0.00 |
| hexatriene | 0.04 | 113.70 | 134.00 | 81.50 | 78.32 | 44.31 | 48.54 | -22.06 | -28.71 | 0.00 | 0.00 | 0.00 | 0.00 |
| hexatriene | 0.06 | 117.02 | 138.55 | 82.78 | 79.65 | 44.59 | 48.94 | -23.47 | -30.46 | 0.00 | 0.00 | 0.00 | 0.00 |
| hexatriene | 0.08 | 122.27 | 145.80 | 84.76 | 81.73 | 45.00 | 49.53 | -25.74 | -33.31 | 0.00 | 0.00 | 0.00 | 0.00 |
| hexatriene | 0.10 | 130.33 | 157.11 | 87.73 | 84.84 | 45.53 | 50.32 | -29.33 | -37.86 | 0.00 | 0.00 | 0.00 | 0.00 |
| polyene($C_8H_{10}$) | 0.00 | 169.89 | 195.34 | 116.58 | 112.68 | 56.63 | 61.53 | -45.61 | -54.79 | 0.00 | 0.00 | 0.00 | 0.00 |
| polyene($C_8H_{10}$) | 0.02 | 171.19 | 196.93 | 117.11 | 113.21 | 56.70 | 61.62 | -46.28 | -55.54 | 0.00 | 0.00 | 0.00 | 0.00 |
| polyene($C_8H_{10}$) | 0.04 | 175.30 | 201.93 | 118.77 | 114.86 | 56.91 | 61.91 | -48.42 | -57.90 | 0.00 | 0.00 | 0.00 | 0.00 |
| polyene($C_8H_{10}$) | 0.06 | 182.90 | 211.20 | 121.81 | 117.89 | 57.26 | 62.40 | -52.41 | -62.33 | 0.00 | 0.00 | 0.00 | 0.00 |
| polyene($C_8H_{10}$) | 0.08 | 195.56 | 226.61 | 126.79 | 122.84 | 57.77 | 63.11 | -59.17 | -69.80 | 0.00 | 0.00 | 0.00 | 0.00 |
| polyene($C_8H_{10}$) | 0.10 | 216.73 | 252.35 | 134.96 | 130.90 | 58.44 | 64.07 | -70.72 | -82.49 | 0.00 | 0.00 | 0.00 | 0.00 |
| polyene($C_{10}H_{12}$) | 0.00 | 238.62 | 269.78 | 155.69 | 150.72 | 69.14 | 74.72 | -75.70 | -87.18 | 0.00 | 0.00 | 0.00 | 0.00 |
| polyene($C_{10}H_{12}$) | 0.02 | 240.98 | 272.48 | 156.64 | 151.65 | 69.23 | 74.83 | -77.01 | -88.55 | 0.00 | 0.00 | 0.00 | 0.00 |
| polyene($C_{10}H_{12}$) | 0.04 | 248.52 | 281.08 | 159.67 | 154.59 | 69.48 | 75.17 | -81.22 | -92.96 | 0.00 | 0.00 | 0.00 | 0.00 |
| polyene($C_{10}H_{12}$) | 0.06 | 262.87 | 297.36 | 165.39 | 160.12 | 69.90 | 75.75 | -89.29 | -101.38 | 0.00 | 0.00 | 0.00 | 0.00 |
| polyene($C_{10}H_{12}$) | 0.08 | 287.89 | 325.53 | 175.22 | 169.57 | 70.51 | 76.59 | -103.55 | -116.15 | 0.00 | 0.00 | 0.00 | 0.00 |
| polyene($C_{10}H_{12}$) | 0.10 | 333.28 | 375.99 | 192.76 | 186.27 | 71.31 | 77.73 | -129.82 | -143.09 | 0.00 | 0.00 | 0.00 | 0.00 |
| polyene($C_{14}H_{16}$) | 0.00 | 394.93 | 438.47 | 241.95 | 236.08 | 94.12 | 101.07 | 148.32 | 165.27 | 0.00 | 0.00 | 0.00 | 0.00 |
| polyene($C_{14}H_{16}$) | 0.02 | 400.31 | 444.27 | 244.12 | 238.18 | 94.23 | 101.22 | 151.48 | 168.48 | 0.00 | 0.00 | 0.00 | 0.00 |
| polyene($C_{14}H_{16}$) | 0.04 | 417.80 | 463.07 | 251.15 | 244.99 | 94.56 | 101.67 | 161.80 | 178.93 | 0.00 | 0.00 | 0.00 | 0.00 |
| polyene($C_{14}H_{16}$) | 0.06 | 452.47 | 500.06 | 265.00 | 258.35 | 95.13 | 102.42 | 182.39 | 199.68 | 0.00 | 0.00 | 0.00 | 0.00 |
| polyene($C_{14}H_{16}$) | 0.08 | 517.79 | 568.94 | 290.81 | 283.17 | 95.93 | 103.52 | 221.54 | 238.85 | 0.00 | 0.00 | 0.00 | 0.00 |
| polyene($C_{14}H_{16}$) | 0.10 | 655.07 | 711.91 | 344.40 | 334.94 | 97.00 | 105.00 | 304.71 | 321.85 | 0.00 | 0.00 | 0.00 | 0.00 |

Table 3: Polarizability in au

| | $\omega$ | $\alpha_{xx}$ | | $\alpha_{yy}$ | | $\alpha_{zz}$ | | $\alpha_{xy}$ | | $\alpha_{xz}$ | | $\alpha_{yz}$ | |
|---|---|---|---|---|---|---|---|---|---|---|---|---|---|
| | | Mod. | DFT | Mod. | DFT | Mod. | DFT | Mod. | DFT | Mod. | DFT | Mod. | DFT |
| polyene($C_{18}H_{20}$) | 0.00 | 566.92 | 623.95 | 334.75 | 329.15 | 119.05 | 127.26 | 231.12 | 254.72 | 0.00 | 0.00 | 0.00 | 0.00 |
| polyene($C_{18}H_{20}$) | 0.02 | 576.21 | 633.78 | 338.51 | 332.84 | 119.19 | 127.44 | 236.71 | 260.38 | 0.00 | 0.00 | 0.00 | 0.00 |
| polyene($C_{18}H_{20}$) | 0.04 | 606.84 | 666.07 | 350.85 | 344.97 | 119.61 | 127.99 | 255.19 | 279.05 | 0.00 | 0.00 | 0.00 | 0.00 |
| polyene($C_{18}H_{20}$) | 0.06 | 669.42 | 731.65 | 375.92 | 369.70 | 120.31 | 128.92 | 293.14 | 317.37 | 0.00 | 0.00 | 0.00 | 0.00 |
| polyene($C_{18}H_{20}$) | 0.08 | 794.53 | 862.65 | 425.62 | 419.73 | 121.32 | 130.26 | 369.59 | 395.33 | 0.00 | 0.00 | 0.00 | 0.00 |
| polyene($C_{18}H_{20}$) | 0.10 | 1093.44 | 1206.59 | 543.19 | 559.96 | 122.65 | 132.08 | 553.79 | 609.88 | 0.00 | 0.00 | 0.00 | 0.00 |
| polyene($C_{22}H_{24}$) | 0.00 | 747.80 | 819.05 | 431.54 | 427.42 | 143.97 | 153.38 | 319.99 | 351.61 | 0.00 | 0.00 | 0.00 | 0.00 |
| polyene($C_{22}H_{24}$) | 0.02 | 761.61 | 833.56 | 437.14 | 433.02 | 144.14 | 153.60 | 328.40 | 360.17 | 0.00 | 0.00 | 0.00 | 0.00 |
| polyene($C_{22}H_{24}$) | 0.04 | 807.57 | 880.82 | 455.71 | 452.07 | 144.64 | 154.25 | 356.45 | 389.46 | 0.00 | 0.00 | 0.00 | 0.00 |
| polyene($C_{22}H_{24}$) | 0.06 | 903.61 | 982.44 | 494.29 | 491.13 | 145.48 | 155.35 | 415.33 | 449.25 | 0.00 | 0.00 | 0.00 | 0.00 |
| polyene($C_{22}H_{24}$) | 0.08 | 1104.74 | 1203.62 | 574.47 | 582.61 | 146.69 | 156.95 | 539.42 | 587.08 | 0.00 | 0.00 | 0.00 | 0.00 |
| polyene($C_{26}H_{28}$) | 0.00 | 933.80 | 1020.57 | 529.95 | 527.99 | 168.88 | 179.56 | 411.72 | 452.05 | 0.00 | 0.00 | 0.00 | 0.00 |
| polyene($C_{26}H_{28}$) | 0.02 | 952.50 | 1040.20 | 537.53 | 535.71 | 169.07 | 179.81 | 423.18 | 463.81 | 0.00 | 0.00 | 0.00 | 0.00 |
| polyene($C_{26}H_{28}$) | 0.04 | 1015.14 | 1105.99 | 562.86 | 561.78 | 169.65 | 180.56 | 461.64 | 503.49 | 0.00 | 0.00 | 0.00 | 0.00 |
| polyene($C_{26}H_{28}$) | 0.06 | 1148.26 | 1247.82 | 616.40 | 619.56 | 170.64 | 181.84 | 543.74 | 590.70 | 0.00 | 0.00 | 0.00 | 0.00 |
| benzene | 0.00 | 73.85 | 77.67 | 73.85 | 77.67 | 39.10 | 41.74 | 0.00 | 0.00 | 0.00 | 0.00 | 0.00 | 0.00 |
| benzene | 0.02 | 73.99 | 77.88 | 73.99 | 77.88 | 39.15 | 41.80 | 0.00 | 0.00 | 0.00 | 0.00 | 0.00 | 0.00 |
| benzene | 0.04 | 74.40 | 78.50 | 74.40 | 78.50 | 39.28 | 41.99 | 0.00 | 0.00 | 0.00 | 0.00 | 0.00 | 0.00 |
| benzene | 0.06 | 75.11 | 79.57 | 75.11 | 79.57 | 39.50 | 42.30 | 0.00 | 0.00 | 0.00 | 0.00 | 0.00 | 0.00 |
| benzene | 0.08 | 76.14 | 81.16 | 76.14 | 81.16 | 39.82 | 42.76 | 0.00 | 0.00 | 0.00 | 0.00 | 0.00 | 0.00 |
| benzene | 0.10 | 77.54 | 83.37 | 77.54 | 83.37 | 40.24 | 43.38 | 0.00 | 0.00 | 0.00 | 0.00 | 0.00 | 0.00 |
| anthracene | 0.00 | 78.59 | 82.16 | 156.59 | 158.29 | 255.92 | 255.07 | 0.00 | 0.00 | 0.00 | 0.00 | 0.00 | 0.00 |
| anthracene | 0.02 | 78.67 | 82.26 | 156.88 | 158.76 | 257.29 | 256.48 | 0.00 | 0.00 | 0.00 | 0.00 | 0.00 | 0.00 |
| anthracene | 0.04 | 78.93 | 82.59 | 157.76 | 160.21 | 261.53 | 260.84 | 0.00 | 0.00 | 0.00 | 0.00 | -0.00 | 0.00 |
| anthracene | 0.06 | 79.35 | 83.14 | 159.27 | 162.83 | 269.15 | 268.64 | 0.00 | 0.00 | 0.00 | 0.00 | 0.00 | 0.00 |
| anthracene | 0.08 | 79.96 | 83.95 | 161.52 | 167.08 | 281.18 | 280.88 | 0.00 | 0.00 | 0.00 | 0.00 | 0.00 | 0.00 |
| anthracene | 0.10 | 80.76 | 85.02 | 164.78 | 174.49 | 299.65 | 299.45 | 0.00 | 0.00 | 0.00 | 0.00 | 0.00 | 0.00 |
| naphtalene | 0.00 | 58.97 | 62.07 | 116.15 | 118.30 | 150.19 | 154.88 | 0.00 | 0.00 | 0.00 | 0.00 | 0.00 | 0.00 |
| naphtalene | 0.02 | 59.03 | 62.16 | 116.37 | 118.63 | 150.70 | 155.51 | 0.00 | 0.00 | 0.00 | 0.00 | -0.00 | 0.00 |
| naphtalene | 0.04 | 59.23 | 62.41 | 117.03 | 119.64 | 152.26 | 157.44 | 0.00 | 0.00 | 0.00 | 0.00 | -0.00 | 0.00 |
| naphtalene | 0.06 | 59.55 | 62.85 | 118.16 | 121.40 | 154.99 | 160.84 | 0.00 | 0.00 | 0.00 | 0.00 | -0.00 | 0.00 |
| naphtalene | 0.08 | 60.02 | 63.49 | 119.83 | 124.07 | 159.12 | 166.02 | 0.00 | 0.00 | 0.00 | 0.00 | 0.00 | 0.00 |
| naphtalene | 0.10 | 60.63 | 64.34 | 122.20 | 127.95 | 165.06 | 173.53 | 0.00 | 0.00 | 0.00 | 0.00 | 0.00 | 0.00 |

Table 4: Polarizability in au

| | $\omega$ | $\alpha_{xx}$ | | $\alpha_{yy}$ | | $\alpha_{zz}$ | | $\alpha_{xy}$ | | $\alpha_{xz}$ | | $\alpha_{yz}$ | |
|---|---|---|---|---|---|---|---|---|---|---|---|---|---|
| | | Mod. | DFT | Mod. | DFT | Mod. | DFT | Mod. | DFT | Mod. | DFT | Mod. | DFT |
| phenanthrene | 0.00 | 78.20 | 81.77 | 227.56 | 229.09 | 165.19 | 168.13 | 0.00 | 0.00 | 0.00 | 0.00 | -0.00 | 0.00 |
| phenanthrene | 0.02 | 78.28 | 81.88 | 228.55 | 230.20 | 165.53 | 168.64 | 0.00 | 0.00 | 0.00 | 0.00 | -0.00 | 0.00 |
| phenanthrene | 0.04 | 78.53 | 82.21 | 231.64 | 233.65 | 166.58 | 170.22 | 0.00 | 0.00 | 0.00 | 0.00 | -0.00 | 0.00 |
| phenanthrene | 0.06 | 78.95 | 82.77 | 237.17 | 239.83 | 168.38 | 173.01 | 0.00 | 0.00 | 0.00 | 0.00 | -0.00 | 0.00 |
| phenanthrene | 0.08 | 79.55 | 83.58 | 245.93 | 249.52 | 171.05 | 177.27 | 0.00 | 0.00 | 0.00 | 0.00 | -0.00 | 0.00 |
| phenanthrene | 0.10 | 80.34 | 84.67 | 259.67 | 264.27 | 174.90 | 183.57 | 0.00 | 0.00 | 0.00 | 0.00 | -0.00 | 0.00 |
| tetracene | 0.04 | 397.56 | 383.96 | 197.91 | 199.65 | 98.53 | 103.24 | 0.00 | 0.00 | 0.00 | 0.00 | 0.00 | 0.00 |
| tetracene | 0.06 | 413.64 | 398.68 | 199.79 | 203.24 | 99.06 | 103.92 | 0.00 | 0.00 | 0.00 | 0.00 | 0.00 | 0.00 |
| tetracene | 0.08 | 439.99 | 422.46 | 202.61 | 209.57 | 99.81 | 104.89 | 0.00 | 0.00 | 0.00 | 0.00 | 0.00 | 0.00 |
| tetracene | 0.10 | 482.90 | 460.51 | 206.75 | 228.90 | 100.80 | 106.21 | -0.00 | 0.00 | 0.00 | 0.00 | 0.00 | 0.00 |
| pentacene | 0.00 | 535.63 | 506.86 | 236.07 | 235.59 | 117.59 | 122.87 | 0.00 | 0.00 | 0.00 | 0.00 | 0.00 | 0.00 |
| pentacene | 0.02 | 540.42 | 511.03 | 236.49 | 236.30 | 117.71 | 123.03 | 0.00 | 0.00 | 0.00 | 0.00 | 0.00 | 0.00 |
| pentacene | 0.04 | 555.58 | 524.20 | 237.78 | 238.56 | 118.09 | 123.50 | 0.00 | 0.00 | 0.00 | 0.00 | 0.00 | 0.00 |
| pentacene | 0.06 | 583.94 | 548.59 | 240.02 | 242.77 | 118.71 | 124.29 | 0.00 | 0.00 | 0.00 | 0.00 | 0.00 | 0.00 |
| pentacene | 0.08 | 631.88 | 589.30 | 243.37 | 250.82 | 119.61 | 125.43 | 0.00 | 0.00 | 0.00 | 0.00 | 0.00 | 0.00 |
| pentacene | 0.10 | 714.25 | 660.25 | 248.39 | 273.75 | 120.78 | 126.97 | 0.00 | 0.00 | 0.00 | 0.00 | 0.00 | 0.00 |
| heptacene | 0.00 | 877.91 | 806.40 | 314.83 | 312.21 | 156.45 | 162.80 | -0.00 | 0.00 | 0.00 | 0.00 | 0.00 | 0.00 |
| heptacene | 0.02 | 888.24 | 814.91 | 315.38 | 313.24 | 156.62 | 163.00 | -0.00 | 0.00 | 0.00 | 0.00 | 0.00 | 0.00 |
| heptacene | 0.04 | 921.40 | 842.16 | 317.07 | 316.22 | 157.10 | 163.60 | -0.00 | 0.00 | 0.00 | 0.00 | 0.00 | 0.00 |
| heptacene | 0.06 | 985.22 | 894.43 | 319.99 | 322.18 | 157.93 | 164.64 | -0.00 | 0.00 | 0.00 | 0.00 | 0.00 | 0.00 |
| heptacene | 0.08 | 1098.90 | 988.94 | 324.37 | 337.51 | 159.10 | 166.13 | -0.00 | 0.00 | 0.00 | 0.00 | 0.00 | 0.00 |
| heptacene | 0.10 | 1313.23 | 1123.95 | 330.99 | 348.18 | 160.65 | 168.12 | -0.00 | 0.00 | 0.00 | 0.00 | 0.00 | 0.00 |

Table 5: Polarizability in au

| | $\omega$ | $\alpha_{xx}$ | | $\alpha_{yy}$ | | $\alpha_{zz}$ | | $\alpha_{xy}$ | | $\alpha_{xz}$ | | $\alpha_{yz}$ | |
|---|---|---|---|---|---|---|---|---|---|---|---|---|---|
| | | Mod. | DFT | Mod. | DFT | Mod. | DFT | Mod. | DFT | Mod. | DFT | Mod. | DFT |
| hexacene | 0.00 | 700.67 | 652.04 | 275.50 | 273.74 | 137.03 | 143.02 | 0.00 | 0.00 | 0.00 | 0.00 | 0.00 | 0.00 |
| hexacene | 0.02 | 707.99 | 658.20 | 275.99 | 274.56 | 137.18 | 143.20 | 0.00 | 0.00 | 0.00 | 0.00 | 0.00 | 0.00 |
| hexacene | 0.04 | 731.34 | 677.79 | 277.48 | 277.10 | 137.61 | 143.73 | 0.00 | 0.00 | 0.00 | 0.00 | 0.00 | 0.00 |
| hexacene | 0.06 | 775.69 | 714.70 | 280.06 | 281.81 | 138.33 | 144.64 | 0.00 | 0.00 | 0.00 | 0.00 | 0.00 | 0.00 |
| hexacene | 0.08 | 852.78 | 778.63 | 283.94 | 290.17 | 139.37 | 145.96 | -0.00 | 0.00 | 0.00 | 0.00 | 0.00 | 0.00 |
| hexacene | 0.10 | 991.79 | 1017.47 | 289.78 | 306.46 | 140.73 | 147.72 | -0.00 | 0.00 | 0.00 | 0.00 | 0.00 | 0.00 |
| octacene | 0.00 | 1064.45 | 967.60 | 354.08 | 351.30 | 175.86 | 182.66 | -0.00 | 0.00 | 0.00 | 0.00 | 0.00 | 0.00 |
| octacene | 0.02 | 1078.19 | 978.77 | 354.70 | 352.52 | 176.04 | 182.88 | -0.00 | 0.00 | 0.00 | 0.00 | 0.00 | 0.00 |
| octacene | 0.04 | 1122.55 | 1014.78 | 356.58 | 356.65 | 176.59 | 183.56 | -0.00 | 0.00 | 0.00 | 0.00 | 0.00 | 0.00 |
| octacene | 0.06 | 1208.90 | 1085.06 | 359.82 | 367.13 | 177.52 | 184.71 | -0.00 | 0.00 | 0.00 | 0.00 | 0.00 | 0.00 |
| octacene | 0.08 | 1366.05 | 1219.06 | 364.69 | 306.07 | 178.83 | 186.36 | 0.00 | 0.00 | 0.00 | 0.00 | 0.00 | 0.00 |
| octacene | 0.10 | 1674.59 | 1437.29 | 372.05 | 371.09 | 180.57 | 188.58 | 0.00 | 0.00 | 0.00 | 0.00 | 0.00 | 0.00 |
| styrene | 0.00 | 118.57 | 123.28 | 97.18 | 102.68 | 51.32 | 54.68 | -10.08 | -14.43 | 0.00 | 0.00 | 0.00 | 0.00 |
| styrene | 0.02 | 118.95 | 123.78 | 97.38 | 102.97 | 51.38 | 54.76 | -10.17 | -14.56 | 0.00 | 0.00 | 0.00 | 0.00 |
| styrene | 0.04 | 120.11 | 125.34 | 97.98 | 103.88 | 51.55 | 55.01 | -10.45 | -14.98 | 0.00 | 0.00 | 0.00 | 0.00 |
| styrene | 0.06 | 122.15 | 128.11 | 99.01 | 105.47 | 51.85 | 55.42 | -10.96 | -15.75 | 0.00 | 0.00 | 0.00 | 0.00 |
| styrene | 0.08 | 125.24 | 132.41 | 100.54 | 107.86 | 52.28 | 56.02 | -11.74 | -16.96 | 0.00 | 0.00 | 0.00 | 0.00 |
| styrene | 0.10 | 129.69 | 138.85 | 102.65 | 111.29 | 52.85 | 56.83 | -12.89 | -18.85 | 0.00 | 0.00 | 0.00 | 0.00 |
| stilbene | 0.00 | 203.95 | 210.23 | 225.39 | 224.13 | 83.25 | 87.77 | 58.95 | 57.62 | 0.00 | 0.00 | 0.00 | 0.00 |
| stilbene | 0.02 | 204.85 | 211.29 | 226.56 | 225.41 | 83.34 | 87.89 | 59.71 | 58.39 | 0.00 | 0.00 | 0.00 | 0.00 |
| stilbene | 0.04 | 207.65 | 214.61 | 230.23 | 229.41 | 83.61 | 88.25 | 62.13 | 60.81 | 0.00 | 0.00 | 0.00 | 0.00 |
| stilbene | 0.06 | 212.74 | 220.68 | 236.93 | 236.80 | 84.07 | 88.86 | 66.62 | 65.38 | 0.00 | 0.00 | 0.00 | 0.00 |
| stilbene | 0.08 | 220.95 | 230.59 | 247.82 | 249.10 | 84.72 | 89.75 | 74.12 | 73.23 | 0.00 | 0.00 | 0.00 | 0.00 |
| stilbene | 0.10 | 234.08 | 249.87 | 265.45 | 271.48 | 85.58 | 90.95 | 86.66 | 88.44 | 0.00 | 0.00 | 0.00 | 0.00 |
| 1,4-dicinnamyl-benzene | 0.00 | 528.57 | 533.06 | 243.55 | 252.28 | 127.07 | 133.39 | 51.69 | 59.07 | 0.00 | 0.00 | 0.00 | 0.00 |
| 1,4-dicinnamyl-benzene | 0.02 | 533.53 | 539.04 | 244.07 | 253.06 | 127.21 | 133.56 | 52.50 | 60.08 | 0.00 | 0.00 | 0.00 | 0.00 |
| 1,4-dicinnamyl-benzene | 0.04 | 549.34 | 558.51 | 245.67 | 255.49 | 127.62 | 134.10 | 55.10 | 63.39 | 0.00 | 0.00 | 0.00 | 0.00 |
| 1,4-dicinnamyl-benzene | 0.06 | 579.25 | 597.38 | 248.48 | 259.88 | 128.31 | 135.01 | 60.05 | 69.98 | 0.00 | 0.00 | 0.00 | 0.00 |
| 1,4-dicinnamyl-benzene | 0.08 | 630.95 | 672.71 | 252.82 | 266.98 | 129.29 | 136.32 | 68.71 | 82.68 | 0.00 | 0.00 | 0.00 | 0.00 |
| 1,4-dicinnamyl-benzene | 0.10 | 723.32 | 849.80 | 259.41 | 279.06 | 130.58 | 138.08 | 84.38 | 111.78 | 0.00 | 0.00 | 0.00 | 0.00 |
| 1,4-divinylbenzene | 0.00 | 178.31 | 190.63 | 114.89 | 119.37 | 63.46 | 67.71 | -13.41 | -22.99 | 0.00 | 0.00 | 0.00 | 0.00 |
| 1,4-divinylbenzene | 0.02 | 179.15 | 191.83 | 115.10 | 119.70 | 63.54 | 67.81 | -13.55 | -23.24 | 0.00 | 0.00 | 0.00 | 0.00 |
| 1,4-divinylbenzene | 0.04 | 181.73 | 195.61 | 115.74 | 120.69 | 63.76 | 68.11 | -13.99 | -24.05 | 0.00 | 0.00 | 0.00 | 0.00 |
| 1,4-divinylbenzene | 0.06 | 186.34 | 202.59 | 116.85 | 122.44 | 64.13 | 68.62 | -14.78 | -25.54 | 0.00 | 0.00 | 0.00 | 0.00 |
| 1,4-divinylbenzene | 0.08 | 193.50 | 214.15 | 118.48 | 125.11 | 64.67 | 69.36 | -16.01 | -28.02 | 0.00 | 0.00 | 0.00 | 0.00 |
| 1,4-divinylbenzene | 0.10 | 204.26 | 233.52 | 120.72 | 129.03 | 65.38 | 70.36 | -17.90 | -32.19 | 0.00 | 0.00 | 0.00 | 0.00 |

Table 6: Polarizability in au

| | $\omega$ | $\alpha_{xx}$ | | $\alpha_{yy}$ | | $\alpha_{zz}$ | | $\alpha_{xy}$ | | $\alpha_{xz}$ | | $\alpha_{yz}$ | |
|---|---|---|---|---|---|---|---|---|---|---|---|---|---|
| | | Mod. | DFT | Mod. | DFT | Mod. | DFT | Mod. | DFT | Mod. | DFT | Mod. | DFT |
| chrysene | 0.00 | 208.01 | 212.08 | 325.26 | 322.35 | 97.29 | 101.64 | 20.28 | 20.81 | 0.00 | 0.00 | 0.00 | 0.00 |
| chrysene | 0.02 | 208.45 | 212.77 | 327.02 | 324.19 | 97.39 | 101.77 | 20.50 | 21.02 | 0.00 | 0.00 | 0.00 | 0.00 |
| chrysene | 0.04 | 209.78 | 214.90 | 332.52 | 329.96 | 97.70 | 102.16 | 21.18 | 21.68 | 0.00 | 0.00 | 0.00 | 0.00 |
| chrysene | 0.06 | 212.08 | 218.70 | 342.55 | 340.38 | 98.21 | 102.84 | 22.45 | 22.87 | 0.00 | 0.00 | 0.00 | 0.00 |
| chrysene | 0.08 | 215.52 | 224.69 | 358.94 | 357.06 | 98.95 | 103.82 | 24.53 | 24.76 | 0.00 | 0.00 | 0.00 | 0.00 |
| chrysene | 0.10 | 220.50 | 234.18 | 386.33 | 383.34 | 99.91 | 105.15 | 28.08 | 27.62 | 0.00 | 0.00 | 0.00 | 0.00 |
| benzo[c]picene | 0.00 | 524.12 | 508.53 | 318.08 | 318.98 | 135.29 | 140.66 | 84.42 | 74.21 | 0.00 | 0.00 | 0.00 | 0.00 |
| benzo[c]picene | 0.02 | 527.71 | 512.06 | 319.04 | 320.24 | 135.43 | 140.84 | 85.52 | 75.11 | 0.00 | 0.00 | 0.00 | 0.00 |
| benzo[c]picene | 0.04 | 539.04 | 523.16 | 322.01 | 324.17 | 135.84 | 141.39 | 89.03 | 77.96 | 0.00 | 0.00 | 0.00 | 0.00 |
| benzo[c]picene | 0.06 | 560.15 | 543.63 | 327.35 | 331.30 | 136.55 | 142.32 | 95.68 | 83.25 | 0.00 | 0.00 | 0.00 | 0.00 |
| benzo[c]picene | 0.08 | 595.98 | 577.58 | 335.90 | 342.95 | 137.54 | 143.67 | 107.26 | 92.06 | 0.00 | 0.00 | 0.00 | 0.00 |
| benzo[c]picene | 0.10 | 660.32 | 634.99 | 349.97 | 363.15 | 138.85 | 145.50 | 128.86 | 106.46 | 0.00 | 0.00 | 0.00 | 0.00 |
| benzo[c]naphto[2,1-m]picene | 0.00 | 694.55 | 667.06 | 480.61 | 472.43 | 173.19 | 179.88 | 189.36 | 165.87 | 0.00 | 0.00 | 0.00 | 0.00 |
| benzo[c]naphto[2,1-m]picene | 0.02 | 699.78 | 672.09 | 482.89 | 474.92 | 173.36 | 180.10 | 192.03 | 168.06 | 0.00 | 0.00 | 0.00 | 0.00 |
| benzo[c]naphto[2,1-m]picene | 0.04 | 716.41 | 688.02 | 490.09 | 482.78 | 173.89 | 180.79 | 200.58 | 175.02 | 0.00 | 0.00 | 0.00 | 0.00 |
| benzo[c]naphto[2,1-m]picene | 0.06 | 747.78 | 717.81 | 503.46 | 497.32 | 174.78 | 181.96 | 216.94 | 188.14 | 0.00 | 0.00 | 0.00 | 0.00 |
| benzo[c]naphto[2,1-m]picene | 0.08 | 802.29 | 768.69 | 526.17 | 521.82 | 176.04 | 183.67 | 246.06 | 210.59 | 0.00 | 0.00 | 0.00 | 0.00 |
| benzo[c]naphto[2,1-m]picene | 0.10 | 904.83 | 862.57 | 567.54 | 567.25 | 177.69 | 185.97 | 302.66 | 248.65 | 0.00 | 0.00 | 0.00 | 0.00 |
| tetracene | 0.00 | 386.00 | 373.30 | 196.47 | 197.15 | 98.12 | 102.71 | 0.00 | 0.00 | 0.00 | 0.00 | 0.00 | 0.00 |
| tetracene | 0.02 | 388.79 | 375.88 | 196.83 | 197.75 | 98.22 | 102.84 | 0.00 | 0.00 | 0.00 | 0.00 | 0.00 | 0.00 |

Table 7: Polarizability in au

| | $\omega$ | $\alpha_{xx}$ | | $\alpha_{yy}$ | | $\alpha_{zz}$ | | $\alpha_{xy}$ | | $\alpha_{xz}$ | | $\alpha_{yz}$ | |
|---|---|---|---|---|---|---|---|---|---|---|---|---|---|
| | | Mod. | DFT | Mod. | DFT | Mod. | DFT | Mod. | DFT | Mod. | DFT | Mod. | DFT |
| g(2,2) | 0.00 | 249.08 | 257.69 | 200.20 | 199.56 | 85.64 | 88.99 | -0.00 | 0.00 | 0.00 | 0.00 | 0.00 | 0.00 |
| g(2,2) | 0.02 | 250.06 | 259.12 | 200.70 | 200.26 | 85.73 | 89.10 | -0.00 | 0.00 | 0.00 | 0.00 | 0.00 | 0.00 |
| g(2,2) | 0.04 | 253.07 | 263.63 | 202.23 | 202.39 | 86.00 | 89.45 | -0.00 | 0.00 | 0.00 | 0.00 | 0.00 | 0.00 |
| g(2,2) | 0.06 | 258.40 | 271.94 | 204.89 | 206.17 | 86.46 | 90.03 | -0.00 | 0.00 | 0.00 | 0.00 | 0.00 | 0.00 |
| g(2,2) | 0.08 | 266.60 | 285.88 | 208.95 | 212.02 | 87.10 | 90.88 | -0.00 | 0.00 | 0.00 | 0.00 | 0.00 | 0.00 |
| g(2,2) | 0.10 | 278.80 | 310.60 | 215.13 | 220.80 | 87.96 | 92.02 | -0.00 | 0.00 | 0.00 | 0.00 | 0.00 | 0.00 |
| g(2,3) | 0.00 | 111.56 | 115.26 | 332.67 | 330.18 | 307.87 | 310.92 | 0.00 | 0.00 | 0.00 | 0.00 | -0.00 | 0.00 |
| g(2,3) | 0.02 | 111.67 | 115.40 | 334.00 | 332.01 | 308.90 | 312.37 | 0.00 | 0.00 | 0.00 | 0.00 | -0.00 | 0.00 |
| g(2,3) | 0.04 | 112.01 | 116.56 | 338.11 | 348.70 | 312.05 | 325.18 | 0.00 | 0.00 | 0.00 | 0.00 | -0.00 | 0.00 |
| g(2,3) | 0.06 | 112.59 | 116.56 | 345.48 | 348.70 | 317.60 | 325.18 | 0.00 | 0.00 | 0.00 | 0.00 | -0.00 | 0.00 |
| g(2,3) | 0.08 | 113.41 | 117.62 | 357.20 | 368.01 | 326.14 | 338.68 | 0.00 | 0.00 | 0.00 | 0.00 | 0.00 | 0.00 |
| g(2,3) | 0.10 | 114.48 | 119.04 | 376.10 | 409.11 | 339.10 | 361.49 | 0.00 | 0.00 | 0.00 | 0.00 | 0.00 | 0.00 |
| g(4,2) | 0.00 | 565.70 | 562.28 | 346.03 | 349.57 | 138.19 | 142.92 | 31.01 | 45.53 | 0.00 | 0.00 | 0.00 | 0.00 |
| g(4,2) | 0.02 | 569.52 | 567.52 | 346.97 | 351.46 | 138.33 | 143.09 | 31.41 | 46.81 | 0.00 | 0.00 | 0.00 | 0.00 |
| g(4,2) | 0.04 | 581.49 | 584.86 | 349.85 | 357.74 | 138.75 | 143.61 | 32.65 | 51.40 | 0.00 | 0.00 | 0.00 | 0.00 |
| g(4,2) | 0.06 | 603.45 | 622.14 | 354.92 | 371.57 | 139.46 | 144.50 | 34.95 | 63.42 | 0.00 | 0.00 | 0.00 | 0.00 |
| g(4,2) | 0.08 | 639.55 | 737.47 | 362.77 | 418.95 | 140.47 | 145.77 | 38.74 | 119.57 | 0.00 | 0.00 | 0.00 | 0.00 |
| g(4,2) | 0.10 | 699.59 | 558.16 | 375.10 | 308.25 | 141.79 | 147.47 | 44.84 | -43.88 | 0.00 | 0.00 | 0.00 | 0.00 |
| g(6,2) | 0.00 | 995.21 | 959.29 | 476.82 | 479.41 | 190.38 | 196.10 | 37.69 | 59.13 | 0.00 | 0.00 | 0.00 | 0.00 |
| g(6,2) | 0.02 | 1004.51 | 971.08 | 478.05 | 482.01 | 190.57 | 196.33 | 38.25 | 61.20 | 0.00 | 0.00 | 0.00 | 0.00 |
| g(6,2) | 0.04 | 1034.08 | 1012.41 | 481.82 | 491.42 | 191.13 | 197.03 | 40.04 | 69.93 | 0.00 | 0.00 | 0.00 | 0.00 |
| g(8,2) | 0.00 | 1491.21 | 1408.86 | 606.64 | 608.01 | 242.43 | 249.47 | 42.25 | 67.39 | 0.00 | 0.00 | 0.00 | 0.00 |
| g(8,2) | 0.02 | 1508.20 | 1429.00 | 608.15 | 611.49 | 242.66 | 249.76 | 42.94 | 70.11 | 0.00 | 0.00 | 0.00 | 0.00 |
| g(8,2) | 0.06 | 1667.71 | 1498.45 | 620.90 | 623.96 | 244.59 | 250.63 | 49.43 | 80.83 | 0.00 | 0.00 | 0.00 | 0.00 |
| g(3,3) | 0.00 | 144.51 | 149.07 | 433.14 | 432.79 | 495.22 | 489.85 | 0.00 | 0.00 | 0.00 | 0.00 | -0.00 | 0.00 |
| g(3,3) | 0.02 | 144.66 | 149.25 | 434.76 | 435.74 | 497.59 | 492.94 | 0.00 | 0.00 | 0.00 | 0.00 | -0.00 | 0.00 |
| g(3,3) | 0.04 | 145.09 | 149.78 | 439.81 | 445.56 | 504.99 | 502.74 | 0.00 | 0.00 | 0.00 | 0.00 | -0.00 | 0.00 |
| g(4,3) | 0.00 | 177.27 | 182.47 | 531.58 | 529.83 | 719.27 | 697.34 | 0.00 | 0.00 | 0.00 | 0.00 | 0.00 | 0.00 |
| g(4,3) | 0.02 | 177.44 | 182.69 | 533.49 | 533.71 | 723.72 | 702.76 | 0.00 | 0.00 | 0.00 | 0.00 | 0.00 | 0.00 |
| g(4,3) | 0.04 | 177.96 | 183.32 | 539.42 | 547.12 | 737.67 | 720.17 | 0.00 | 0.00 | 0.00 | 0.00 | 0.00 | 0.00 |
| g(6,3) | 0.00 | 242.47 | 248.85 | 725.36 | 717.63 | 1251.52 | 1179.00 | 0.00 | 0.00 | 0.00 | 0.00 | -0.00 | 0.00 |
| g(6,3) | 0.02 | 242.70 | 249.13 | 727.80 | 722.59 | 1262.16 | 1190.86 | 0.00 | 0.00 | 0.00 | 0.00 | -0.00 | 0.00 |
| g(8,3) | 0.00 | 307.47 | 315.34 | 917.45 | 916.02 | 1867.67 | 1735.26 | 0.00 | 0.00 | 0.00 | 0.00 | 0.00 | 0.00 |
| g(8,3) | 0.02 | 307.76 | 315.69 | 920.41 | 926.18 | 1886.97 | 1756.40 | 0.00 | 0.00 | 0.00 | 0.00 | 0.00 | 0.00 |

Table 8: Polarizability in au

| | $\omega$ | $\alpha_{xx}$ | | $\alpha_{yy}$ | | $\alpha_{zz}$ | | $\alpha_{xy}$ | | $\alpha_{xz}$ | | $\alpha_{yz}$ | |
|---|---|---|---|---|---|---|---|---|---|---|---|---|---|
| | | Mod. | DFT | Mod. | DFT | Mod. | DFT | Mod. | DFT | Mod. | DFT | Mod. | DFT |
| $C_{60}$ fullerene | 0.00 | 479.00 | 496.85 | 479.00 | 496.85 | 479.01 | 496.85 | -0.00 | 0.00 | 0.00 | 0.00 | -0.00 | 0.00 |
| $C_{60}$ fullerene | 0.02 | 480.02 | 498.61 | 480.02 | 498.61 | 480.03 | 498.61 | -0.00 | 0.00 | 0.00 | 0.00 | -0.00 | 0.00 |
| $C_{60}$ fullerene | 0.04 | 483.14 | 504.11 | 483.14 | 504.11 | 483.15 | 504.11 | -0.00 | 0.00 | 0.00 | 0.00 | -0.00 | 0.00 |
| $C_{60}$ fullerene | 0.06 | 488.51 | 514.08 | 488.51 | 514.08 | 488.52 | 514.08 | -0.00 | 0.00 | 0.00 | 0.00 | -0.00 | 0.00 |
| $C_{60}$ fullerene | 0.08 | 496.44 | 530.36 | 496.44 | 530.36 | 496.45 | 530.36 | -0.00 | 0.00 | -0.00 | 0.00 | -0.00 | 0.00 |
| $C_{60}$ fullerene | 0.10 | 507.45 | 558.66 | 507.45 | 558.66 | 507.46 | 558.73 | -0.00 | 0.00 | -0.00 | 0.00 | -0.00 | 0.00 |
| ethyne | 0.00 | 16.97 | 19.01 | 16.97 | 19.01 | 28.10 | 30.47 | 0.00 | 0.00 | 0.00 | 0.00 | 0.00 | 0.00 |
| ethyne | 0.02 | 16.99 | 19.05 | 16.99 | 19.05 | 28.17 | 30.54 | 0.00 | 0.00 | 0.00 | 0.00 | 0.00 | 0.00 |
| ethyne | 0.04 | 17.07 | 19.16 | 17.07 | 19.16 | 28.38 | 30.74 | 0.00 | 0.00 | 0.00 | 0.00 | 0.00 | 0.00 |
| ethyne | 0.06 | 17.21 | 19.35 | 17.21 | 19.35 | 28.75 | 31.07 | 0.00 | 0.00 | 0.00 | 0.00 | 0.00 | 0.00 |
| ethyne | 0.08 | 17.41 | 19.62 | 17.41 | 19.62 | 29.27 | 31.56 | 0.00 | 0.00 | 0.00 | 0.00 | 0.00 | 0.00 |
| ethyne | 0.10 | 17.67 | 20.00 | 17.67 | 20.00 | 29.99 | 32.22 | 0.00 | 0.00 | 0.00 | 0.00 | 0.00 | 0.00 |
| butadiyne | 0.00 | 28.54 | 29.74 | 28.54 | 29.74 | 61.35 | 82.14 | 0.00 | 0.00 | 0.00 | 0.00 | 0.00 | 0.00 |
| butadiyne | 0.02 | 28.59 | 29.79 | 28.59 | 29.79 | 61.60 | 82.45 | 0.00 | 0.00 | 0.00 | 0.00 | 0.00 | 0.00 |
| butadiyne | 0.04 | 28.72 | 29.94 | 28.72 | 29.94 | 62.35 | 83.39 | 0.00 | 0.00 | 0.00 | 0.00 | 0.00 | 0.00 |
| butadiyne | 0.06 | 28.94 | 30.20 | 28.94 | 30.20 | 63.65 | 85.01 | 0.00 | 0.00 | 0.00 | 0.00 | 0.00 | 0.00 |
| butadiyne | 0.08 | 29.26 | 30.57 | 29.26 | 30.57 | 65.60 | 87.43 | 0.00 | 0.00 | 0.00 | 0.00 | 0.00 | 0.00 |
| butadiyne | 0.10 | 29.69 | 31.07 | 29.69 | 31.07 | 68.34 | 90.79 | 0.00 | 0.00 | 0.00 | 0.00 | 0.00 | 0.00 |
| hexatriyne | 0.00 | 39.86 | 40.18 | 39.86 | 40.18 | 127.55 | 160.57 | 0.00 | 0.00 | 0.00 | 0.00 | 0.00 | 0.00 |
| hexatriyne | 0.02 | 39.92 | 40.24 | 39.92 | 40.24 | 128.53 | 161.44 | 0.00 | 0.00 | 0.00 | 0.00 | 0.00 | 0.00 |
| hexatriyne | 0.04 | 40.10 | 40.43 | 40.10 | 40.43 | 131.59 | 164.10 | 0.00 | 0.00 | 0.00 | 0.00 | 0.00 | 0.00 |
| hexatriyne | 0.06 | 40.40 | 40.75 | 40.40 | 40.75 | 137.10 | 168.77 | 0.00 | 0.00 | 0.00 | 0.00 | 0.00 | 0.00 |
| hexatriyne | 0.08 | 40.83 | 41.22 | 40.83 | 41.22 | 145.84 | 175.86 | 0.00 | 0.00 | 0.00 | 0.00 | 0.00 | 0.00 |
| hexatriyne | 0.10 | 41.40 | 41.84 | 41.40 | 41.84 | 159.31 | 186.06 | 0.00 | 0.00 | 0.00 | 0.00 | 0.00 | 0.00 |
| Polyyne($C_8H_2$) | 0.00 | 51.10 | 50.61 | 51.10 | 50.61 | 225.70 | 265.33 | 0.00 | 0.00 | 0.00 | 0.00 | 0.00 | 0.00 |
| Polyyne($C_8H_2$) | 0.02 | 51.18 | 50.68 | 51.18 | 50.68 | 228.38 | 267.20 | 0.00 | 0.00 | 0.00 | 0.00 | 0.00 | 0.00 |
| Polyyne($C_8H_2$) | 0.04 | 51.40 | 50.91 | 51.40 | 50.91 | 236.90 | 273.01 | 0.00 | 0.00 | 0.00 | 0.00 | 0.00 | 0.00 |
| Polyyne($C_8H_2$) | 0.06 | 51.78 | 51.30 | 51.78 | 51.30 | 252.86 | 283.35 | 0.00 | 0.00 | 0.00 | 0.00 | 0.00 | 0.00 |
| Polyyne($C_8H_2$) | 0.08 | 52.32 | 51.86 | 52.32 | 51.86 | 279.93 | 299.43 | 0.00 | 0.00 | 0.00 | 0.00 | 0.00 | 0.00 |
| Polyyne($C_8H_2$) | 0.10 | 53.03 | 52.60 | 53.03 | 52.60 | 326.42 | 323.43 | 0.00 | 0.00 | 0.00 | 0.00 | 0.00 | 0.00 |
| Polyyne($C_{16}H_2$) | 0.00 | 95.87 | 92.44 | 95.87 | 92.44 | 913.12 | 886.72 | 0.00 | 0.00 | 0.00 | 0.00 | 0.00 | 0.00 |
| Polyyne($C_{16}H_2$) | 0.02 | 96.00 | 92.57 | 96.00 | 92.57 | 939.44 | 898.26 | 0.00 | 0.00 | 0.00 | 0.00 | 0.00 | 0.00 |
| Polyyne($C_{16}H_2$) | 0.04 | 96.41 | 92.96 | 96.41 | 92.95 | 1029.19 | 934.99 | 0.00 | 0.00 | 0.00 | 0.00 | 0.00 | 0.00 |
| Polyyne($C_{16}H_2$) | 0.06 | 97.09 | 93.61 | 97.09 | 93.61 | 1228.30 | 1004.32 | 0.00 | 0.00 | 0.00 | 0.00 | 0.00 | 0.00 |
| Polyyne($C_{16}H_2$) | 0.08 | 98.05 | 94.54 | 98.05 | 94.54 | 1702.52 | 1124.12 | 0.00 | 0.00 | 0.00 | 0.00 | 0.00 | 0.00 |
| Polyyne($C_{16}H_2$) | 0.10 | 99.33 | 95.79 | 99.33 | 95.79 | 3522.95 | 1338.92 | 0.00 | 0.00 | 0.00 | 0.00 | 0.00 | 0.00 |
| Polyyne($C_{20}H_2$) | 0.00 | 118.21 | 112.93 | 118.21 | 112.93 | 1397.70 | 1281.13 | 0.00 | 0.00 | 0.00 | 0.00 | 0.00 | 0.00 |

Table 9: Polarizability in au

| | $\omega$ | $\alpha_{xx}$ | | $\alpha_{yy}$ | | $\alpha_{zz}$ | | $\alpha_{xy}$ | | $\alpha_{xz}$ | | $\alpha_{yz}$ | |
|---|---|---|---|---|---|---|---|---|---|---|---|---|---|
| | | Mod. | DFT | Mod. | DFT | Mod. | DFT | Mod. | DFT | Mod. | DFT | Mod. | DFT |
| Polyyne($C_{20}H_2$) | 0.02 | 118.38 | 113.08 | 118.38 | 113.08 | 1448.42 | 1300.87 | 0.00 | 0.00 | 0.00 | 0.00 | 0.00 | 0.00 |
| Polyyne($C_{20}H_2$) | 0.04 | 118.87 | 113.54 | 118.87 | 113.54 | 1627.18 | 1364.45 | 0.00 | 0.00 | 0.00 | 0.00 | 0.00 | 0.00 |
| Polyyne($C_{20}H_2$) | 0.06 | 119.70 | 114.33 | 119.70 | 114.33 | 2058.63 | 1488.10 | 0.00 | 0.00 | 0.00 | 0.00 | 0.00 | 0.00 |
| Polyyne($C_{20}H_2$) | 0.08 | 120.88 | 115.45 | 120.88 | 115.45 | 3333.97 | 1714.98 | 0.00 | 0.00 | 0.00 | 0.00 | 0.00 | 0.00 |
| o-di(1-butadienylmethyl)-benzene | 0.00 | 196.97 | 206.38 | 185.58 | 182.85 | 177.20 | 181.57 | 5.33 | 6.01 | 0.75 | 10.53 | -0.44 | 2.82 |
| p-hexyl-propyl-benzene | 0.00 | 147.20 | 143.90 | 250.53 | 248.63 | 159.15 | 161.25 | 1.01 | 4.37 | 0.00 | 0.00 | -0.00 | 0.00 |
| trans-1.2-(3-vinylpropyl)-(butadienylmethyl)-ethene | 0.00 | 136.18 | 136.41 | 166.33 | 172.95 | 152.09 | 155.78 | -24.27 | -21.57 | -15.49 | -23.01 | 8.46 | 9.73 |
| trans-1-propyl-cis-methyl-decapentaene | 0.00 | 156.92 | 160.54 | 352.59 | 360.44 | 162.20 | 158.66 | 101.43 | 103.14 | 8.46 | 14.05 | 28.59 | 36.57 |
| 2-naphtyl-1-butadienyl-methane | 0.00 | 178.05 | 182.96 | 149.86 | 152.97 | 200.30 | 199.27 | -5.49 | -6.36 | -45.86 | -36.61 | -0.21 | 1.43 |
| 1-octylbenzene | 0.00 | 142.95 | 142.71 | 209.84 | 213.28 | 151.10 | 152.11 | 7.72 | 8.79 | -8.17 | -11.12 | -16.75 | -15.88 |
| 1-penthylbenzene | 0.00 | 99.21 | 98.73 | 166.65 | 168.50 | 121.54 | 124.25 | -4.77 | -2.77 | -0.00 | 0.00 | 0.00 | 0.00 |
| 6-pentyl-undecane | 0.00 | 197.94 | 195.41 | 169.46 | 168.08 | 176.42 | 174.18 | -12.98 | -13.34 | -15.73 | -16.57 | -13.63 | -11.92 |
| tetraphenyl | 0.00 | 133.20 | 139.52 | 500.06 | 532.64 | 250.75 | 258.65 | 0.00 | 0.00 | 0.00 | 0.00 | 0.00 | 0.00 |
| anti-1,3-dibutadienylpropane | 0.00 | 204.66 | 229.01 | 111.98 | 109.89 | 112.67 | 110.85 | -9.35 | -5.63 | -0.00 | 0.00 | -0.00 | 0.00 |
| 1,7-gauche-3-methyl-nonane | 0.00 | 116.03 | 114.52 | 132.09 | 129.42 | 137.89 | 135.85 | 2.30 | 2.05 | -13.53 | -12.43 | -2.87 | -2.08 |
| 6-gauche-2,3,4,5-tetramethylheptane | 0.00 | 130.04 | 128.27 | 136.15 | 132.78 | 152.51 | 148.39 | -4.28 | -3.61 | -4.21 | -3.72 | 12.30 | 11.23 |
| 7-gauche-2,3,4-trimethylheptane | 0.00 | 116.33 | 114.91 | 125.28 | 122.63 | 142.50 | 138.86 | -5.25 | -5.20 | -3.73 | -3.97 | 12.03 | 11.34 |
| 1-(m-ethylphenyl)-2-phenyl-propane | 0.00 | 158.16 | 160.06 | 197.64 | 199.69 | 213.46 | 212.79 | -4.28 | -3.73 | -7.86 | -8.15 | -0.20 | 2.78 |
| 1-phenyl-2-cyclohexyl-ethane | 0.00 | 142.23 | 142.21 | 153.06 | 153.94 | 190.77 | 188.89 | 6.49 | 5.20 | -31.98 | -32.75 | -4.97 | -5.22 |
| cis-1-methyl-decapentaene | 0.00 | 134.01 | 127.37 | 306.50 | 331.53 | 79.67 | 84.14 | 41.76 | 43.55 | 0.00 | 0.00 | -0.00 | 0.00 |
| 1,1-dimethyl-decapentaene | 0.00 | 134.89 | 139.15 | 310.01 | 317.23 | 142.62 | 139.41 | 99.97 | 101.09 | 12.54 | 16.99 | 33.22 | 42.04 |

# Paper 3:

*Interaction model for the argon atom, argon cation and a free electron at moderate separation distances*

Hans S. Smalø and P.-O. Åstrand

J. Chem. Phys.

**Submitted**

# Interaction model for the argon atom, argon cation and a free electron at moderate separation distances

Hans S. Smalø, and Per-Olof Åstrand *

*Department of Chemistry, Norwegian University of Science and Technology (NTNU), N-7491 Trondheim, Norway*

## Abstract

For a plasma with a low degree of ionization, it is natural to assume that doubly ionized molecules are rare, and thus the plasma consists of neutral molecules, cations and free electrons. From a theoretical point of view, monoatomic molecules are relatively simple, and argon is therefore a good model system. Thus a model for the interaction between the argon atom, argon cation and an electron is presented. In addition to electrostatic, polarization and dispersion energies, a model for the exchange based on orbital overlaps is given, and the effects of the size for the electron distribution of argon is discussed. For the electron distribution of argon, both a Gaussian and an exponential distribution are investigated, and it is concluded that for the exchange, a model based on an exponential distribution is preferred.

* Corresponding author: per-olof.aastrand@chem.ntnu.no

## I. INTRODUCTION

In this work, argon is exploited in the quest of understanding a plasma. The goal is to develop a force field capable of simulating a transition from liquid argon to a plasma phase caused by high electric fields. In such a plasma, the degree of ionization is low,[1–3] and under these conditions an argon plasma consist of neutral argon atoms $Ar$, argon cations $Ar^+$ and electrons, $e^-$. Thus the interaction between the species in addition to a description of the transition from $Ar$ to $Ar^+$ and $e^-$ (and vica versa) is needed. In this regard, it is noted that impact ionization of argon has been studied using density function theory and compared to experiments.[4] However, here we focus primarily on the interaction between the species at moderate separation distances.

Argon is well-known for its interatomic van der Waals forces, which often is given in terms of a Lennard-Jones potential[5,6]

$$V = 4\epsilon \left( (\frac{\sigma}{R})^{12} - (\frac{\sigma}{R})^{6} \right) \tag{1}$$

where $\epsilon$ and $\sigma$ are parameters, consisting of a short-range repulsion energy and a dispersion energy. The Pauli principle leads to a repulsive force at short separation distances, which is purely quantum mechanical in nature. Normally, this energy is modelled by adding a short-range repulsive potential, as for example the $R^{-12}$ term in Eq. (1). Argon systems have been studied extensively, and can for example be used as a benchmark calculation to study the speed of molecular dynamics algorithms[7]. Even though Eq (1) may seem trivial today, the study of argon has lead to a detailed understanding of exchange and dispersion forces which are important in intermolecular interactions in general.[8] Dispersion forces are, for example, especially important in non-polar organic liquids.[9]

In the electronic force field (eFF) and similar quantum wave-package models, it is demonstrated that it is possible to include electrons as classical particles in a force field,[10,11] where the electrons are described by Gaussian wave packages, and the dynamics is goverened by Newton's law. The kinetic energy of a Gaussian wave package can be calculated, and has two contributions, one is the kinetic energy of the average speed, and the other is the internal kinetic energy, which is given by the size of the wave package. In addition, based on a harmonic oscillator, a model for the size of the electron is presented.[11] The model introduced here will be similar to the eFF in many ways, however there is one key difference. In eFF, all electrons are treated as independent particles, while here the goal is to include only the

free electrons as independent particles. Thus the nucleus of the argon atom and the bound electrons will be modeled as a single particle, but the free electrons can be treated similarly as in the eFF.[11]

At long and moderate separation distances, the interaction between a neutral argon atom and a charged particle is dominated by electronic polarization. Polarization models can be grouped into two sets, one which is based on the charge transfer between the different atoms and one where each atom is polarized.[12] Because the separation distance between two argon atoms is large compared to normal bond distances, we can primarily focus on the latter contribution. In the point-dipole interaction (PDI) model, each atom is assigned a point-dipole moment, which interact with each other.[13–17] The polarizability of the argon dimer is mostly given by twice the polarizability of the argon atom. However, examining the small deviations from an additive contribution gives insight into how two argon atoms interact, and therefore accurate calculations of the polarizability of the argon and helium dimers have been carried out.[18] Here the deviation from the additive contribution is modeled using the the PDI model.

As demonstrated in this paper, at moderate separation distances, the interaction between the different species ($Ar$, $Ar^+$ and $e^-$) can be calculated using fairly simple models.

## II. THEORY

The theory section will be divided into three subsections, one for electrostatic interactions, one for exchange and finally dispersion forces are discussed. The starting point for this model is our previously published work on the polarizability.[12,19–21]

### A. Electrostatics and polarization

Instead of point charges, Gaussian charge distributions are assumed,[22]

$$\rho_I(r) = q_I \left(\frac{\Phi_I^*}{\pi}\right)^{3/2} e^{-\Phi_I^* r^2} \tag{2}$$

where $q_I$ is the charge of the system and $\Phi_I^*$ is a measure of the size of the particle. The interaction of two such particles, $I$ and $J$, leads to a modified Coulomb's law,[23]

$$V_{IJ}^{qq} = \frac{\mathrm{erf}(\sqrt{a_{IJ}} R_{IJ})}{R_{IJ}} \,, \tag{3}$$

where

$$a_{IJ} = \frac{\Phi_I^* \Phi_J^*}{\Phi_I^* + \Phi_J^*} \tag{4}$$

and $R_{IJ}$ is the distance between the two particles. Eq. (3) can be approximated as[22,24]

$$V_{IJ}^{qq} = \frac{1}{\sqrt{R_{IJ}^2 + \frac{\pi}{4a_{IJ}}}} \, . \tag{5}$$

The electrostatic damping introduced in Eqs. (3) and (5) is based on Gaussian functions, but here we would like to examine the difference between Gaussian orbitals and Slater-type functions,

$$\rho(r) = \frac{k^3}{2\pi} e^{-kr} \, . \tag{6}$$

Similar damping models to Eq. (5) have also been applied to approximate the Coulomb interaction between two Slater-type orbitals.[25–27] Thus, the type of orbital does not seem to be of large importance for the electrostatic interactions. However, it does mean that it is harder to link the parameters for the damping to the parameter $k$ describing $\rho(r)$ in Eq. (6). Thus, if using exponential functions the $\Phi^*$-parameters should be interpreted as damping parameters only, and not a parameter associated with the parameter in Eq. (2). For example, the damping for Slater-type functions has been given as[26]

$$T_{IJ}^{(0)} = \frac{1}{\sqrt{R_{IJ}^2 + d_{IJ}^2}} \tag{7}$$

identical to Eq. (5) with $d_{IJ}^2 = \pi/(4a_{IJ})$. Furthermore, the expression for $T_{IJ,\alpha}^{(1)}$ describing the charge-dipole interaction energy when including the damping term in Eq. (5) becomes

$$T_{IJ,\alpha}^{(1)} = \nabla_\alpha T_{IJ}^{(0)} = -\frac{R_{IJ,\alpha}}{\widetilde{R}_{IJ}^3} \tag{8}$$

where the damped distance, $\widetilde{R}_{IJ} = \sqrt{R_{IJ}^2 + \pi/4a_{IJ}}$, is introduced. Likewise, $T_{IJ,\alpha\beta}^{(2)}$, describing the dipole-dipole interaction energy becomes

$$T_{IJ,\alpha\beta}^{(2)} = \nabla_\beta T_{IJ,\alpha}^{(1)} = \frac{3R_{IJ,\alpha}R_{IJ,\beta}}{\widetilde{R}_{IJ}^5} - \frac{\delta_{\alpha\beta}}{\widetilde{R}_{IJ}^3} \, . \tag{9}$$

### 1. *Atom-electron interaction*

Let an atom consist of a nuclear charge $Z$ and $n$ electrons. The electrostatic interaction between an electron with a damping parameter $\Phi_e^*$ and an atom with parameters $\Phi_I^*$ and

$\Phi_Z^*$ becomes

$$V_{ee}^{qq} + V_{Ze}^{qq} = \frac{n}{\sqrt{R_{Ie}^2 + \frac{\pi}{4a_{Ie}}}} - \frac{Z}{\sqrt{R_{Ie}^2 + \frac{\pi}{4a_{Ze}}}} = \frac{n}{\widetilde{R}_{Ie}} - \frac{Z}{\widetilde{R}_{Ze}} \ . \tag{10}$$

If a point charge is adopted for the free electron, $\Phi_e^* \to \infty$, and $a_{Ie} = \Phi_I^*$. Ideally, the parameter $\Phi_Z^*$ should be extremely large as the nucleus is very small. Since the interactions between the electrons are more damped than the interaction between the electron and the nucleus at short distances, the electrostatic energy becomes attractive at small distances.

If an atom interacts both with an external electric field, $E_\alpha$ and an electron at distance $R_{Ie}$, the induced dipole moment will be given by the linear response to the total electric field,

$$\mu_\alpha^{\text{ind}} = \alpha \left( E_\alpha + \frac{R_{Ie,\alpha}}{\tilde{R}_{Ie}^3} \right) \tag{11}$$

where $\alpha$ is the isotropic polarizability of the atom. The polarization energy $V_{Ie}^{\text{pol}}$ becomes

$$V_{Ie}^{\text{pol}} = -\frac{1}{2}\alpha \left( \frac{R_{Ie,\alpha}}{\tilde{R}_{Ie}^3} + E_\alpha \right)^2 \tag{12}$$

and the total interaction is $V_{Ie} = V_{Ie}^{qq} + V_{Ie}^{pol}$.

*2. Atom-atom interaction*

The charge-charge interaction between two atoms $I$ and $J$, becomes

$$V_{IJ}^{qq} = \frac{Z_I Z_J}{\widetilde{R}_{Z_I Z_J}} - \frac{n_I Z_J}{\widetilde{R}_{n_I Z_J}} - \frac{n_J Z_I}{\widetilde{R}_{Z_I n_I}} + \frac{n_I n_J}{\widetilde{R}_{n_I n_J}} \tag{13}$$

where the $\widetilde{R}$-terms use the appropriate damping parameters. Since the damping for the electron-electron repulsion is larger than the damping of the nucleus-electron attraction at moderate distances, an attractive force is found between two neutral atoms. However, at very short distances the nucleus-nucleus repulsion dominates. To find the atomic dipole moments $\mu_{I,\alpha}$ the two-atom PDI model is solved. Define $E_\alpha^q$ as the electric field at atom $I$ caused by the charge from atom $J$,

$$E_\alpha^q = Z_J \frac{R_{IJ,\alpha}}{\widetilde{R}_{n_I Z_J}^3} - n_J \frac{R_{IJ,\alpha}}{\widetilde{R}_{n_I n_J}^3} \tag{14}$$

where $R_{IJ,\alpha} = R_{J,\alpha} - R_{I,\alpha}$. Assuming two identical systems $I$ and $J$, the PDI model may be written as the following set of equations

$$\frac{\mu_{I,\alpha}}{\alpha} - T^{(2)}_{IJ,\alpha\beta}\mu_{J,\beta} = E_\alpha + E^q_\alpha \tag{15}$$

$$-T^{(2)}_{IJ,\alpha\beta}\mu_{I,\beta} + \frac{\mu_{J,\alpha}}{\alpha} = E_\alpha - E^q_\alpha \tag{16}$$

where $E_\alpha$ is an external electric field. Chosing a coordinate system where $T^{(2)}_{IJ,\alpha\beta}$ is diagonal, simplifies these equations to a two by two matrix problem which has the solutions

$$\mu_{I,\alpha} = \frac{\alpha E_\alpha}{1 - \alpha T^{(2)}_{IJ,\alpha\alpha}} + \frac{\alpha E^q_\alpha}{1 + \alpha T^{(2)}_{IJ,\alpha\alpha}} \tag{17}$$

and

$$\mu_{J,\alpha} = -\frac{\alpha E_\alpha}{1 - \alpha T^{(2)}_{IJ,\alpha\alpha}} - \frac{\alpha E^q_\alpha}{1 + \alpha T^{(2)}_{IJ,\alpha\alpha}} \ . \tag{18}$$

Thus, without an external electric field the atomic dipole moment point towards each other because of the different damping terms for the nuclei and electrons and the dipole-dipole interaction is repulsive, while with a relatively large external electric field, the opposite is true. With the atomic dipole moments given by Eqs. (17) and (18), the total charge-dipole and dipole-dipole interaction energy can be written as

$$V^{q\mu}_{IJ} + V^{\mu\mu}_{IJ} = -\left(\frac{\alpha E^2_\alpha}{1 - \alpha T_{IJ,\alpha\alpha}} + \frac{\alpha (E^q_\alpha)^2}{1 + \alpha T_{IJ,\alpha\alpha}}\right) \tag{19}$$

which includes one contribution from each atom. The total electrostatic and polarization energy is thus

$$V^{el+pol}_{IJ} = V^{qq}_{IJ} + V^{q\mu}_{IJ} + V^{\mu\mu}_{IJ} \tag{20}$$

where the energy terms are given by Eqs. (13) and (19).

Eqs. (17) and (18) give the static polarizability for a diatomic molecule, when charge-transfer contributions are ignored. Introducing a frequency-dependent polarizability model,[20,28] the corresponding frequency-dependent polarizability becomes

$$\alpha_{\alpha\beta} = \frac{2\alpha\delta_{\alpha\beta}}{1 - \alpha T^{(2)}_{IJ,\alpha\beta} - \alpha c^\mu \omega^2} \tag{21}$$

where $c^\mu$ is an atom-type parameter and $\omega$ is the frequency.

### B. Exchange

The exchange energy, $V^{exch}$, is defined as the difference between the energy obtained using a product of non-orthogonal atomic orbitals for the wavefunction and the energy using an anti-symmetric wavefunction (given by a determinant). For two electrons with parallel spin, it may be approximated as[29]

$$V_{IJ}^{exch} = \frac{CS_{IJ}^2}{1 - S_{IJ}^2} \tag{22}$$

where $C$ is a constant and $S_{IJ}$ is the overlap integral given as

$$S_{IJ} = \langle \psi_I | \psi_J \rangle \tag{23}$$

and $\psi_I$ and $\psi_J$ are two normalized, non-orthogonal, one-particle wavefunctions. An expression for the parameter, $C$, may be obtained considering the kinetic energy of two non-orthogonal Gaussian wave packets.[10,11] For $S \ll 1$, a Taylor expansion may be carried out

$$V_{IJ}^{exch} = C_{IJ}S_{IJ}^2 + C'_{IJ}S_{IJ}^4 + \cdots \tag{24}$$

where $C_{IJ}$ and $C'_{IJ}$ are parameters. This expression has been used extensively in the construction of polarizable force fields.[30–32] At moderate separation distances, it is assumed that $S_{IJ}^2$ is small such that only the lowest order term is needed. This is similar to earlier published work,[12] however the constant $C_{IJ}$ obtained there leads to a negative sign for the exchange, since it relied on a Hartree product with orthogonal orbitals. A repulsive form based on non-orthogonal orbitals is however preferred, otherwise an orthogonalization energy has to be included explicitly, see for example Ref. 33.

The exchange energy for two electrons with opposite spin is zero, however it can be argued that if including electron correlation effects, exchange may be modelled as non-zero.[11] Regardless, if one of the systems studied is a closed-shell system, the exchange will be dominated by exchange between electrons with parallel spin, and the total exchange will be given by a sum of such contributions. Furthermore, if one of the systems is a closed-shell system, all exchange contributions will be dominated by the orthogonality requirement and all these contributions will be repulsive.

The interaction between two open-shell systems is more difficult to model. The hydrogen atom has a single electron in its ground state, and thus orthogonality does not necessarily contribute when it interacts with a single electron. However orthogonality does contribute

to the total exchange when it interacts with an electron pair, and thus the total exchange is highly dependent on which two systems that are involved.

For closed-shell systems, the interaction is of the same nature regardless of which system it interacts with. In this case a simple combination, $C_{IJ} = W_I W_J$, has been chosen where $W_I$ and $W_J$ are atom-type parameters. Furthermore, the overlap of orbitals may be approximated by the overlap of charge distribution[34,35]

$$S'^2_{IJ} \approx \frac{1}{2} \int \rho'_1 \rho'_2 d\tau = \frac{n_I n_J}{2} \int \rho_1 \rho_2 d\tau \tag{25}$$

where $\rho_1$ and $\rho_2$ are normalized to one and the factor 1/2 is included because only half of the electrons have the same spin. Thus a model for the exchange is obtained as

$$V^{exch}_{IJ} = W_I W_J S'^2_{IJ} = W_I W_J \frac{n_I n_J}{2} S^2_{IJ} \ . \tag{26}$$

For $S^2_{IJ}$, we investigate two trial functions,

$$S^2_{IJ} = e^{-a^g_{IJ} R^2_{IJ}} \tag{27}$$

and

$$S^2_{IJ} = (1 + a^{exch}_{IJ} R_{IJ}) e^{-a^{exch}_{IJ} R_{IJ}} \tag{28}$$

where $a^g_{IJ}$ and $a^{exch}_{IJ}$ are parameters.,

The first expression can be obtained by examining the overlap given by two Gaussian charge distributions,[12] while the main motivation behind Eq. (28) is to examine the difference between Gaussian and Slater-type orbitals. Figure 1 shows the overlap between two Slater-type charge distributions ($\rho \propto e^{-r}$) calculated numerically, compared both to Eqs. (27) and (28). From Figure 1, it is found that both models can be used to approximate the overlap between two Slater-type orbitals at short separation distances, but Eq. (28) is preferred for longer distances. Thus, one would expect Eq. (28) to perform better than Eq. (27) for the exchange energy.

For the Gaussian charge distribution in Eq. (27), $a^g_{IJ}$ can be linked to the width of the Gaussian described by the $\Phi^*_I$-parameters in Eq. (4). In this work, only argon is studied, and therefore for simplicity we treat both $a^g$ and $a^{exch}$ as separate parameters.

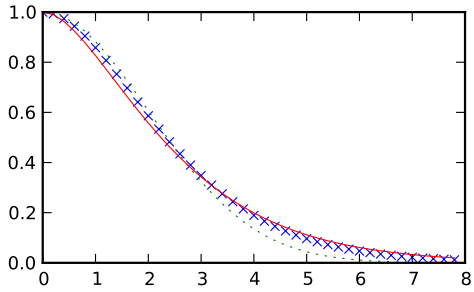


FIG. 1. Numerical integral of the overlap of two exponential functions, $\rho = e^{-r}$ and $\rho' = e^{-r'}$, as a function of separation distance ($\times$), compared to on overlap given Eq. (27) ($\cdots$) and given by Eq. (28) ($-$). Here $a^g = 0.125$ and $a^{exch} = 0.75$.

### C. Dispersion

In the interaction between two unpolar systems, dispersion forces are important. The dispersion energy may be linked to the frequency-dependent polarizability as[32,36]

$$V^{disp} = -\frac{2}{\pi}\int_0^\infty \alpha_{I,\alpha\beta}(i\omega) T^{(2)}_{IJ,\alpha\gamma} T^{(2)}_{IJ,\beta\delta} \alpha_{J,\gamma\delta}(i\omega) d\omega \ . \tag{29}$$

Using our model for the frequency-dependent polarizability,[20,28] the atomic polarizability may be written as

$$\alpha_{I,\alpha\beta}(\omega) = \frac{\alpha_I \delta_{\alpha\beta}}{1 - \alpha_I c^\mu \omega^2} \tag{30}$$

where $\alpha_{I,\alpha\beta} = \alpha_I \delta_{\alpha\beta}$ is the atomic isotropic polarizability and $c^\mu$ is an atom-type parameter. Furthermore, defining $\overline{\omega}_I = 1/\sqrt{\alpha_I c^\mu}$, the regular expression for the Unsöld approximation is obtained[37]

$$\alpha_{\alpha\beta}(\omega) = \alpha_I \delta_{\alpha\beta} \frac{\overline{\omega}^2}{\overline{\omega}^2 - \omega^2} \tag{31}$$

which gives an expression for $V^{disp}$ as

$$V^{disp}_{IJ} = -\frac{1}{4}\frac{\overline{\omega}_I \overline{\omega}_J}{\overline{\omega}_I + \overline{\omega}_J} \alpha_I T^{(2)}_{IJ,\alpha\beta} T^{(2)}_{IJ,\alpha\beta} \alpha_J \ . \tag{32}$$

Including damping by using Eq. (9) for $T^{(2)}_{IJ,\alpha\beta}$ yields three different sums to evaluate, and the final expression for the dispersion energy becomes

$$V^{disp}_{IJ} = -\frac{1}{4}\frac{\overline{w}_I \overline{w}_J}{\overline{w}_I + \overline{w}_J} \alpha_I \alpha_J \left( \frac{9R^4}{\widetilde{R}^{10}} - \frac{6R^2}{\widetilde{R}^8} + \frac{3}{\widetilde{R}^6} \right) \ . \tag{33}$$

TABLE I. Parameters for $Ar$ and $Ar^+$ (in atomic units)

| Parameter | $\alpha$ | $c^\mu$ | $\Phi_I^*$ | $\Phi_Z^*$ | $W_I$ | $a^g$ | $a^{exch}$ |
|---|---|---|---|---|---|---|---|
| Value | 12.35 | 0.21 | 0.50 | 0.55 | 0.60 | 0.25 | 2.1 |

In the long range limit, $\widetilde{R} \to R$ and the expression may be simplified to

$$V_{IJ}^{disp} = -\frac{3}{2}\frac{\overline{\omega}_I\overline{\omega}_J}{\overline{\omega}_I + \overline{\omega}_J}\alpha_I\alpha_J\left(\frac{1}{R^6}\right) \tag{34}$$

so that the familiar $R^{-6}$-dependence of the dispersion energy is obtained.

## III. APPLICATION ON ARGON

All reference data was obtained using density functional theory (DFT) with the BLYP[38,39] functional and the A/TZP[40,41] basis set, using the ADF software.[42–44] For the van der Waals interaction energy, the BLYP-D method was used for an improved description of the dispersion energy.[9] This method gives a binding energy for the *Ar*-*Ar* dimer of about 0.004-0.005 *eV*, or about 0.1 *kcal/mol* which is too low compared to more accurate computations.[45] However, it is sufficient for testing the model.

For $Ar$, an effective nucleus charge $Z^{eff} = 8$ was adopted so that the core electrons are treated together with the nucleus and thus the number of electrons becomes $n = 8$ (or $n = 7$ if $Ar^+$). The parameters are summarized in Table I, and it is noted that the exchange parameters are only used in the *Ar*-*Ar* interaction, since it is difficult to obtaine reference data to test the exchange between a free electron and an argon atom. Here, we have used the same set of parameters for $Ar$ and $Ar^+$, but in general one would expect $Ar$ and $Ar^+$ to behave slightly differently.

The atomic polarizability, $\alpha$, is obtained by a calculation on the isolated atom. Likewise, the $c^\mu$-parameter in the dispersion energy was obtained from calculation of the frequency-dependent polarizability for the atom which in our model is given in Eq. (30). In table II the model is compared to the DFT-polarizability, and a good agreement is noted.

TABLE II. Frequency-dependent polarizability ($\alpha(\omega) - \alpha(0)$ (in atomic units) ) obtained by DFT and our model.

| $\omega$ | $\alpha^{DFT}$ | $\alpha^{Model}$ |
|---|---|---|
| 0.02 | 0.016 | 0.017 |
| 0.04 | 0.064 | 0.065 |
| 0.06 | 0.146 | 0.147 |
| 0.08 | 0.263 | 0.264 |
| 0.10 | 0.418 | 0.418 |

### A. *Ar-Ar* interaction

To obtain reasonable parameters for $\phi_I^*$, the polarizability of the argon dimer was studied (see Figures 2(a) and 2)(b). Except for the shortest separation distances, $\Phi_I^* = 0.5$ gives small deviations from DFT calculations, both for the static and the frequency-dependent polarizability. The deviation between the model and DFT at the shortest separation distance might be explained by a small charge transfer contribution, which is not included in the PDI model. $\Phi_I^* = 0.5$ gives a Gaussian function with a standard deviation of 1 *bohr*, which is a reasonable size for the argon atom. If applying this $\Phi_I^*$ to Eq. (4), a value of $a^g$ exactly to the one used here is obtained, thus separating $a^g$ from $\Phi_I^*$ might not be necessary. Furthermore, with $\alpha$, $c^\mu$ and the $\Phi_I^*$ parameters fixed, all parameters used for calculating the dispersion forces are known, and with the exception of $\Phi_Z^*$, also all parameters describing the electrostatic and polarization energy.

For the *Ar-Ar* interactions, repulsion dominates at short distances and it is therefore an ideal system to investigate in detail a model for exchange effects. In Figures 3(a) and 3(b), the *Ar-Ar* interaction energy as a function of separation distance is shown, both with respect to BLYP-D data, and with exchange models given by Eqs (27) and (28), respectively. Figure 3(a) shows that both trial functions give a reasonable fit and it is difficult to see the difference. However, when changing the scale of the graph (see Figure 3(b)), it is clear that the overlap given by Eq. (28) gives a better fit, while a Gaussian overlap increases too rapidly. This corresponds nicely with the difference between the two functions compared to a numerical integral of two exponentials (see Figure 1).

When applying the model to an argon plasma, where hot electrons easily gain energy

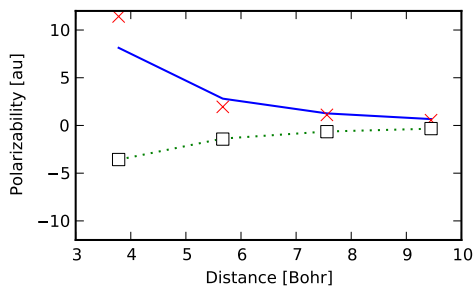


(a)Static polarizability for $Ar_2$

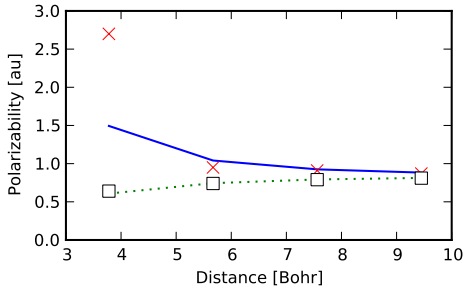


(b)Polarizability at $\omega = 0.1$ *au* for $Ar_2$

FIG. 2. Static and frequency-dependent polarizbility for $Ar_2$. (a) $\alpha_{Ar_2} - 2\alpha_{Ar}$, (b) $\alpha_{Ar_2}(\omega) - \alpha_{Ar_2}(0)$ for $\omega = 0.1$ *au*, as a function of the separation distance. If the $z$-axis is along the $Ar - Ar$ bond, the $xx$ and $yy$ component of the polarizability with respect to DFT is given as $\square$ and the model as $\cdots$ while the $zz$ component of the polarizability with respect DFT is given as $\times$ and the model as $-$.

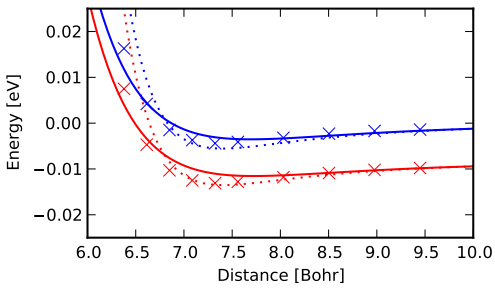


(c)*Ar*-*Ar* interaction energy

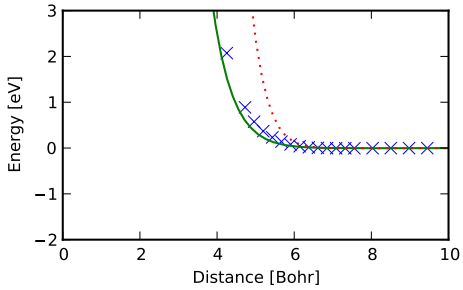


(d)*Ar*-*Ar* interaction energy

FIG. 3. Argon-argon interaction energy, with respect to DFT data ($\times$), model based on overlap given by Eq. (27) ($\cdots$) and given by Eq. (28) ($-$). In figure (a), there are two sets of data, one without external field (the set with highest energy), and the other with an external field along the bond equal to 0.005 au= 25.7 *MV/cm*. In figure (b), the same argon-argon interaction energy (without an external field) is shown in another energy domain.

of the order $eV$, it is of crucial importance to have an overlap function which is capable of describing both what happens at the 0.01 eV energy scale and what happens at the $eV$ range. Therefore it is concluded that an overlap of the form in Eq. (28) is more appropriate

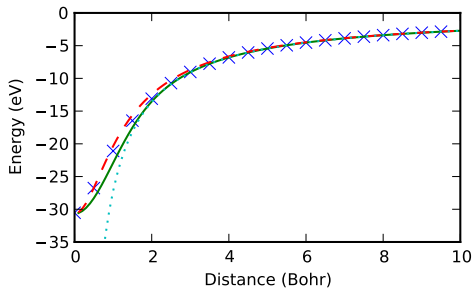


(e)

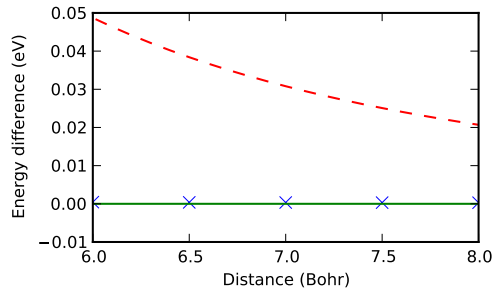


(f)

FIG. 4. (a) The comparison of a 1/R Coulomb potential ($\cdots$), the interaction between a point charge and a Gaussian distribution with $\Phi^* = 1$ using the erf-function ($-$), the damping in Eq. (5) ($--$) and numerical integration using a charge distribution of the form $\rho = e^{-kr}$ ($\times$). Here $k$ was adjusted to give the same result for $R = 0$. (b) The difference between the different damping models and the Coulomb potential, in the range where the Ar-Ar interaction energy is around the minimum.

than a Gaussian overlap as in Eq. (27).

Figure 3(a) also shows the interaction energy of two argon atoms in an electric field. It is noted that the polarizability model correctly describes the reduction in energy caused by the external electric field for $Ar_2$.

Since the electrostatic repulsion between the electrons is more damped compared to the attraction between one nucleus of one atom and the electrons of the other atom, the attraction becomes larger than the repulsion. Thus, the electrostatic attraction in $Ar_2$ is dependent on the damping formula, where a small error in the damping model may lead to large errors in the energy. As seen in figures 4(a) and 4(b), the damping given by Eq. (5) for a Gaussian charge distribution, is slightly too large compared to Eq (3) and especially for moderate distances, where Eq. (3) gives no damping at all. The parameter $\Phi_Z^*$ is needed to correct for the too large damping at moderate distances. Actually, removing all penetration effects by setting $\Phi_Z^* = \Phi_I^*$ yields results which is of the same level of accuracy as the ones presented here. However, a parameter $\Phi_Z^* \neq \Phi_I^*$ was chosen to illustrate how the electrostatic model behaves, which can be seen in Figures 5(a) and 5(b). At 6-10 bohr, the electrostatic energy is negligible, but at short distances, it is interesting to see that a minimum in the

electrostatic energy is obtained. A key point is that the parameters that determines the elctrostatic energy (apart from $\Phi_z^*$) and the dispersion energy have been determined from the polarizability of the atom and the dimer. If only the energy had been parameterized, we had not been able to make this distinction between the distance dependence of the exchange and the electrostatic energies.

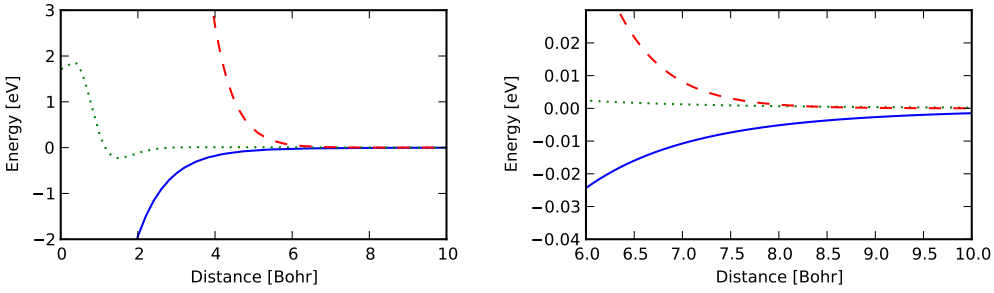


(g) (h)

FIG. 5. *Ar-Ar* interaction energy contributions; dispersion energy ($-$ ), electrostatic energy ($\cdots$) and exchange ($--$). The difference between (a) and (b) is the energy scale. Here Eq. (28) is used for the exchange.

To obtain a more realistic model with the nucleus being a point charge, a more accurate damping model is needed, since for Eq. (5)

$$\lim_{R\to\infty} \frac{1}{R_{IJ}} - \frac{1}{\widetilde{R}_{IJ}} \propto \frac{1}{R_{IJ}^3}, \tag{35}$$

while Eq. (3) reaches Coulomb's law exponentially. For large distances, the damping approaches Coulomb's law exponentially also if considering exponential distributions (see Figure 4(b)). Thus for large distances the electrostatic interaction between two neutral atoms, given by Eq. (13), should decrease exponentially towards zero, but the energy obtained using Eq. (5) is proportional to $R^{-3}$ which is not negligible for example compared to the dispersion forces which is of the order $R^{-6}$. Therefore, even though there is some difference between the damping of an exponential compared to a damping of a Gaussian distribution (see Figure 4(a)), it is better to use the erf-function, instead of a simplified damping model as for example Eq. (5).

Using the erf-function, good results could be obtained using a point charge for the nucleus, however the energies become huge at short separation distances. A minimum in the $V^{qq}$

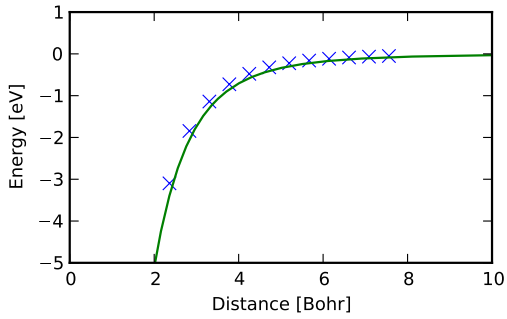


FIG. 6. $Ar$ interaction with a negative point charge with respect to DFT data ($\times$) and model ($-$).

interaction energy between two argon atoms would be of the magnitude $-Zn\sqrt{\Phi_I^*}$, which for $Z^{eff} = n = 8$ and for $\phi_I^* = 0.5$, would be -1200 $eV$, which is completely off the scale. This energy is largely canceled by the exchange, but to model this accurately the exchange model at short separation distances has to be investigated in more detail.

### B. $Ar$-$e^-$ and $Ar^+$-$e^-$ interactions

To test the model for the interaction between $Ar + e^-$ or $Ar^+ + e^-$, DFT calculations (BLYP and A/TZP basis set) were employed with a negative point charge a given distance from the atom. A similar method has been employed recently to study the field dependence of the ionization potential for molecular systems.[46] The interaction between $Ar$ or $Ar^+$ and a negative point charge will not capture the exchange energy which obviously is important for an electron-argon interaction, however, it does capture the electrostatic interaction which dominates at long distances. Since exchange can be turned off also in our model, the results from our model can be compared to DFT.

In Figure 6, the interaction energy between a negative point charge and $Ar$ is shown. In this case, the energy is dominated by the polarization energy $V_{Ie}^{\text{pol}}$, which is an attractive energy contribution. In Figure 7 the interaction energy between an argon cation and a negative point charge is shown. Both with and without an external field, the small difference between DFT and a pure Coulomb attraction is captured by the model.

If an electron is to escape to the right ($R_{Ie} > 0$), a negative permanent electric field is needed. Thus, the polarization due to the free electron and the permanent field has opposite

sign (see Eq. (12)), and at the maximum potential in Figure 7(b), these two effects cancel each other.

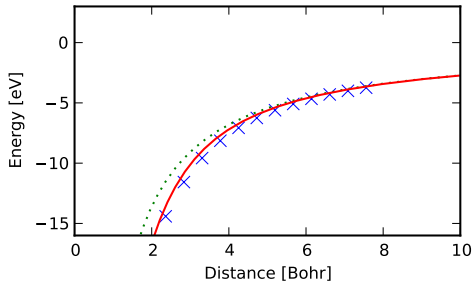


(i)$Ar^+$ and a negative point charge

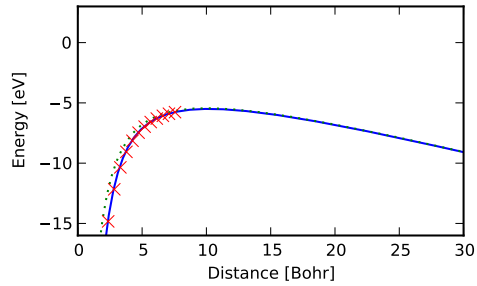


(j)$Ar^+$, a negative point charge and an external electric field

FIG. 7. $Ar^+$ interaction energy with a negative point charge, with respect to a 1/R Coulomb term ($\cdots$), DFT data ($\times$) and model ($-$). (a) without external field. (b) external field of $-0.01$ au= $-51.4$ *MV/cm*.

An external electric field thus leads to a reduction of the barrier needed to ionize a system. In a classical Coulomb potential in an electric field, a maximum potential along the direction of the field is given by $-2\sqrt{E}$, and thus the field-dependent ionization potential may be written as[47]

$$IP = IP_0 - 2\sqrt{E} \tag{36}$$

where $IP_0$ is the ionization potential at zero field. This reduction of the $IP$ is the basis for the classical Poole-Frenkel conduction mechanism.[47] From DFT, it was found that $IP_0$ was $15.7eV$ for argon, while the reduction of the IP was found by the maximum potential along the direction of the field using our model, and has been compared to Eq. (36) in Figure 8. It is concluded that the deviation from the classical result is small. This is because the polarization effects at maximum potential is very small since then the external field and the field from the point charge cancel each other, and the other effects are generally small.

If modeling the interaction between $Ar^+$ and an electron $e^-$, the model at short separation distances is of importance. For future work, it would be possible to divide the atom into three parts, the nucleus $Z$, the core electrons $n^{core}$ and the valence electrons $n^{valence}$. Thus separate damping and exchange parameters for the core and the valence electrons could be

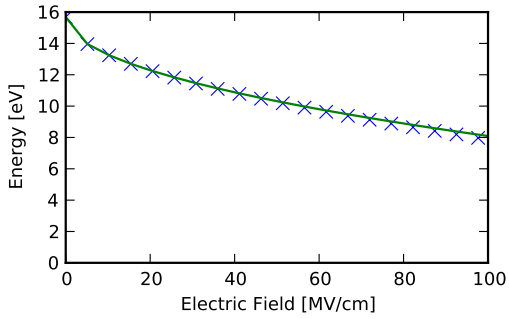


FIG. 8. The ionization potential of Argon as a function of the electric field, both with respect to Eq. (36) (−) and with respect to our model (×).

used to model what happens at short separation distances, and thus a model of the actual ionzation processes would be possible.

## IV. CONCLUSION

The interactions between $Ar$, $Ar^+$ and free electrons $e^-$ at moderate separation distances have been studied. The same set of parameters was used to describe all the different interaction energies as well as both the static and frequency-dependent polarizabilities. The interactions are dominated by polarization effects, dispersion forces and exchange. At moderate distances, the electrostatic effects due to the size of the electron distribution of argon seems to give negligable contributions.

For the electrostatic and polarization energy, the difference between using Gaussian and Slater-type charge distributions does not seem to be important. However for exchange, a model based on Slater-type orbitals is preferred over a model based on Gaussians.

**ACKNOWLEDGMENTS**

Support from the Norwegian Research Council through a Strategic Industry Program (164603/I30), and a grant of computer time are acknowledged.

---

[1] S. Ingebrigsten, N. Bonifaci, A. Denat, and O. Lesaint. J. Phys. D. Appl. Phys., **41**, 235204, (2008).

[2] N. Bonifaci, A. Denat, and P. E. Frayssines. J. Electrostat., **64**, 445-449, (2006).

[3] P. E. Frayssines, N. Bonifaci, A. Denat, and O. Lesaint. J. Phys. D: Appl. Phys., **35**, 369-377, (2002).

[4] D. A. Biava, H. P. Saha, E. Engel, R. M. Dreizler, R. P. McEachran, M. A. Haynes, B. Lohmann, C. T Whelan, and B. H. Madison. J. Phys. B, **35**, 293-307, (2002).

[5] J. E. Lennard-Jones. Proc. Phys. Soc., **43**, 461-482, (1931).

[6] P. W. Atkins. *Physical Chemistry.* Oxford University Press, fifth edition, (1994).

[7] J. Yang, Y. Wang, and Y. Chen. J. Comput. Phys., **221**, 799-894, (2007).

[8] A. D. Buckingham, P. W. Fowler, and J. M. Hutson. Chem. Rev., **88**, 963-988, (1988).

[9] S. Grimme, J. Antony, T. Schwabe, and C. Mück-Lichtenfeld. Org. Biomol. Chem., **5**, 741-758, (2007).

[10] D. Klakow, C. Toepffer, and P. G. Reinhard. J. Chem. Phys, **101**, 10766, (1994).

[11] J. T. Su and W. A. Goddard III. J. Chem. Phys, **131**, 244501, (2009).

[12] H. S. Smalø, P.-O. Åstrand, and L. Jensen. J. Chem. Phys., **131**, 044101, (2009).

[13] L. Silberstein. Phil. Mag., **33**, 92-128, (1917).

[14] L. Silberstein. Phil. Mag., **33**, 215-222, (1917).

[15] L. Silberstein. Phil. Mag., **33**, 521-533, (1917).

[16] J. Applequist, J. R. Carl, and K.-F. Fung. J. Am. Chem. Soc., **94**, 2952-2960, (1972).

[17] J. Applequist. Acc. Chem. Res., **10**, 79-85, (1977).

[18] C. Hättig, H. Larsen, J. Olsen, P. Jørgensen, H. Koch, B. Fernández, and A. Rizzo. J. Chem. Phys., **111**, 10099-10107, (1999).

[19] L. Jensen, P.-O. Åstrand, and K. V. Mikkelsen. Int. J. Quant. Chem., **84**, 513-522, (2001).

[20] A. Mayer, Ph. Lambin, and P.-O. Åstrand. Nanotechnology, **19**, 025203, (2008).

[21] L. Jensen, P.-O. Åstrand, and K. V. Mikkelsen. J. Comput. Theo. Nanosci., **6**, 270-291, (2009).

[22] L. Jensen, P.-O. Åstrand, A. Osted, J. Kongsted, and K. V. Mikkelsen. J. Chem. Phys., **116**, 4001-4010, (2002).

[23] T. Helgaker, P. Jørgensen, and J. Olsen. *Molecular electronic-structure theory.* Wiley, Chichester, (2000).

[24] G. A. van der Velde. A realistic Coulomb potential. In H. J. C. Berendsen, editor, *MD and MC on water. CECAM workshop report*, pages 38–39, Orsay, France, (1972).

[25] P. Bultinck, R. Vanholme, P. L. A. Popelier, F. De Proft, and P. Geerlings. J. Phys. Chem. A, **108**, 10359-10366, (2004).

[26] K. Ohno. Theor. Chim. Acta, **2**, 219-227, (1964).

[27] A. K. Rappé and W. A. Goddard III. J. Phys. Chem., **95**, 3358-3363, (1991).

[28] H. S. Smalø, P.-O. Åstrand, and A. Mayer. (2010). Submitted.

[29] M. Margenau and N. R. Kestner. *Theory of Intermolecular Forces.* Pergamon, Oxford, (1969).

[30] P.-O. Åstrand, A. Wallqvist, G. Karlström, and P. Linse. J. Chem. Phys., **95**, 8419-8429, (1991).

[31] P.-O. Åstrand, A. Wallqvist, and G. Karlström. J. Chem. Phys., **100**, 1262-1273, (1994).

[32] O. Engkvist, P.-O. Åstrand, and G. Karlström. Chem. Rev., **100**, 4087-4108, (2000).

[33] J. N. Murrell and G. Shaw. Mol. Phys., **12**, 475-480, (1967).

[34] R. J. Wheatley and W. J. Meath. Mol. Phys., **79**, 253-275, (1993).

[35] R. J. Wheatley. Chem. Phys. Lett., **294**, 487-492, (1998).

[36] F. London. Z. Phys., **63**, 245-279, (1930).

[37] A. Unsöld. Z. Phys., **43**, 563-574, (1927).

[38] A. D. Becke. Phys. Rev. A, **38**, 3098, (1988).

[39] C. Lee, W. Yang, and R. G. Parr. Phys. Rev. B, **37**, 785, (1988).

[40] E. van Lenthe and E. J. Baerends. J. Comput. Chem., **24**, 1142-1156, (2003).

[41] D. P. Chong. Mol. Phys., **103**, 749-761, (2005).

[42] G. te Velde, F. M. Bickelhaupt, E. J. Baerends, C. Fonseca Guerra, S. J. A. van Gisbergen, J. G. Snijders, and T. Ziegler. J. Comput. Chem., **22**, 931–967, (2001).

[43] C. Fonseca Guerra, J.G. Snijders, G. te Velde, and E.J. Baerends. Theor. Chem. Acc., **99**, 391-401, (1998).

[44] SCM, Theoretical Chemistry, Vrije Universiteit, Amsterdam, The Netherlands. *ADF2008.01.*

[45] S. Tsuzuki and H. P. Lüthi. J. Chem. Phys., **114**, 3949-3957, (2001).

[46] H. S. Smalø, Ø. Hestad, S. Ingebrigtsen, and P.-O. Åstrand. (2010). Submitted.

[47] L. A. Dissado and J. C. Fothergill. *Electrical Degradation and Breakdown in Polymers*. Material and Devices Series 9. The Institution of Engineering and Technology, London, United Kingdom, (1992).

# Paper 4:

*Calculation of Ionization Potentials and Electron Affinities for Molecules Relevant for Streamer Initiation and Propagation*

Hans S. Smalø, S. Ingebrigtsen and P.-O. Åstrand

IEEE Trans. Dielect. Electr. Insul. **17** 733-741 (2010)

# Calculation of Ionization Potentials and Electron Affinities for Molecules Relevant for Streamer Initiation and Propagation

**H. S. Smalø, P.-O. Åstrand**
Department of Chemistry
Norwegian University of Science and Technology (NTNU)
7491 Trondheim, Norway

and **S. Ingebrigtsen,**
Department of Electric Power Technology
SINTEF Energy Research
7465 Trondheim, Norway

## ABSTRACT

**We investigate different quantum chemical methods to compute ionization potentials and electron affinities for various molecules of interest to streamer propagation experiments in liquids. Solvation effects have been studied for the ionization potential using a polarizable continuum model. The ionization potentials can be reasonably well predicted by the methods used, but electron affinities are more problematic. We discuss possible reasons for these problems. Our primary interest in exploiting these calculations is to aid the understanding of discharges in liquids, and to help predict the utility of various additives for insulating liquids.**

Index Terms — **Prebreakdown, streamer, ionization potential, electron affinity, insulating liquid, additives, density functional theory.**

## 1 INTRODUCTION

**THE** ionization potential (IP) and the electron affinity (EA) are two molecular descriptors that qualitatively have been linked to the propagation of streamers in molecular liquids [1-3]. The streamer is a gas/plasma filled channel that initiates and rapidly develops in a region with high electric fields. Shortly before electrical insulating liquids suffer voltage breakdown, these conductive channels of ionized gas propagate through the material and bridge the electrode gap. Their propagation is motored by a continuous liberation and capture of electrons in the liquid phase. Depending on the electronic properties of the molecules comprising the liquid, they may act as sources of electrons in the first stage and later, during impacts, interact with the energetic electrons, resulting in electron capture or multiplication. Interactions of this type, both in the liquid and in the vapor, determine the transfer of energy and to a large degree the propagation behavior of the streamer. A lowering of the IP of the molecules facilitates extraction of electrons from the liquid and thus the development of a plasma channel in high electric fields. For a streamer moving towards a positive electrode, electrons are also supplied to the liquid from within the gas/plasma channel itself, and its continuous formation is determined also by the ability of the liquid to absorb these electrons and their energy. Traditionally molecules are said to have high electron affinity if they effectively capture electrons. Therefore it has been reported that the electron affinity is an important parameter for streamers originating from a negative electrode [4-9]. However, the explicit EA values are seldom reported, and it is not clear if the EA is a suitable observable to describe the ability of a molecule to stop electrons drifting in an electric field.

The IP of molecule $A$ is defined as the energy needed to remove an electron and create a positive ion $A^+$

$$A \rightarrow A^+ + e^- \quad ; \quad IP = E^{A^+} - E^A \tag{1}$$

Similarly, the electron affinity EA is the energy needed to remove an electron from a negatively charged ion $A^-$,

$$A^- \rightarrow A + e \quad ; \quad EA = E^A - E^{A^-} \tag{2}$$

Quantum chemistry provides molecular properties within experimental error bars, and through the advances in methodology and computer power, quantum chemistry can be

*Manuscript received on 17 September 2009, in final form 9 November 2009.*

used for increasingly larger systems. Density functional theory (DFT) has been used to calculate the IP accurately [10-12], and among different functionals (versions of DFT), B3LYP gives results for the IP within experimental error bars [13]. DFT methods have also been used successfully to investigate EA for molecules and molecular radicals (such as OH) where EA > 0 [12, 14, 15].

In this paper we evaluate several quantum chemical approaches for calculating the IP and EA. Even if the IP is more relevant for streamers than the EA, they are two accompanying properties obtained with similar methodology. Our purpose is to demonstrate how quantum chemical methods may be used as screening methods, for example to suggest suitable additives for electrically insulating liquids.

## 2 QUANTUM MECHANICAL METHODS

Koopman's theorem states that the IP of a molecule is equal to minus the energy of the highest occupied molecular orbital (HOMO), while the EA is equal to minus the energy of the lowest unoccupied molecular orbital (LUMO). The main assumption behind Koopman's theorem is that the quantum mechanical states (molecular orbitals) of the system are unmodified when adding or removing one electron. The outer-valence Green function method (OVGF) [16] improves Koopman's theorem applied on the Hartree-Fock orbitals perturbatively, and is available as a standard technique in the Gaussian software package [17]. OVGF is a method which is not only capable of calculating the energy cost to remove an electron in the highest occupied molecular orbital, but the energy cost in removing other electrons in the system as well. Because of this, the OVGF method has been used in connection with spectroscopic studies, see for example reference [18].

DFT is in principle not based on orbitals, but within Kohn-Sham theory, where the electron density is expanded in terms of orbitals, the DFT functional may be regarded as an *ad hoc* correction to the Hartree-Fock approximation. The Kohn-Sham orbitals have thus the same interpretation as in Hartree-Fock theory.

Generally, removing an electron from the HOMO is a smaller perturbation than adding an electron to the LUMO, so it should be expected that the approach works better for the IP than for the EA. It is furthermore expected that the main reason for the limited usefulness of approximating the first excitation energy by the HOMO-LUMO gap is that the perturbation of the LUMO is not small when it becomes occupied.

We have used the OVGF method with the 6-311++G(d,p) basis set. Extra diffuse functions are included in the basis set to improve the description of the EA. For the IP, a smaller basis set would have been sufficient [12, 19], but for consistency we have used the same basis set in all calculations. The molecular geometries have been found by using DFT with the B3LYP functional. The B3LYP functional has been shown to give geometries of high accuracy [20, 21].

To study effects of orbital and geometry relaxation, we have done DFT (B3LYP functional and 6-311++G(d,p) basis set) calculations on $A^+$ and $A^-$ and compared their energies with the energy of the neutral molecule $A$ in line with equations (1) and (2), respectively. When calculating the energies of $A^+$ or $A^-$, we used both the geometry of the neutral molecule and the geometry obtained from separate geometry optimizations of $A^+$ and $A^-$, respectively. For a separate geometry optimization of $A^+$ and $A^-$, the adiabatic IP/EA is obtained, while if the geometry of the neutral molecule is used for the calculation of the energies of $A^-$ and $A^+$ it corresponds to the vertical IP/EA. It is noted that the starting geometry for the geometry optimization of $A^-$ and $A^+$ is the geometry of the neutral molecule $A$. The optimization procedure finds the geometry corresponding to the closest local minimum in energy, but not necessarily the global minimum. The optimized geometry of $A^-$ and $A^+$ should therefore in most cases be close to the geometry of the neutral molecule.

All methods described above give gas phase properties. However, streamer experiments are often performed in liquids, for example in liquid cyclohexane as a base liquid with different molecules added [1, 22-28]. The polarizable continuum model, PCM [29], have been used to estimate how the IP of additives are affected by a surrounding liquid. In PCM, the given molecule is treated by quantum mechanics (B3LYP/6-311++G(d,p) as before) and the surrounding liquid is treated as a dielectric continuum with a given dielectric constant. For the surrounding liquid, cyclohexane is used with a dielectric constant, $\varepsilon$, of 2.023 [30]. To create the molecular cavity, the united atom topology model [31] is used with atomic radii from the UFF [32] force field (UA0 model). Basically, a sphere is placed around each atom which is combined to a molecule-shaped cavity, where the atomic radii are parameters of the PCM.

In vacuum, the energy of a free electron at rest is zero. However in a condensed state, the minimum energy of a quasi-free electron is the energy of the conducting state, $V_0$, which may be positive or negative depending on the liquid. The definition of the IP can be modified according to [33],

$$IP = E^{A+} + V_0 - E^A \qquad (3)$$

However, $V_0$ in liquid cyclohexane is 0.01 eV [28,34] and therefore negligible.

The PCM calculations are done both for the adiabatic and vertical IP, in the same way as for the gas-phase calculations. PCM calculations are not necessarily unproblematic as convergence is not guaranteed [35]. The problem arises mainly from the necessity to discretize the molecular cavity, and that the shape and size of the cavity may change with the geometry of the molecule. PCM calculations have only been carried out for the IP (since as discussed later, gas-phase calculations of the EA is problematic).

Treating the liquid as a dielectric continuum is a crude approximation. Any effects due to the structure of the solvent on a molecular scale cannot be represented in a continuum model. More sophisticated models exist for quantum chemical calculation on molecules in the liquid phase, such as the hybrid quantum mechanical/molecular mechanics (QM/MM) models. These models treat the liquid surrounding with molecular mechanics where each molecule is represented as a classical system, but the molecule or system of greater interest is treated with quantum mechanics [36]. In QM/MM, the structure of the solvent is represented, whereby each individual molecule (or atom) has a given position. These models are about one order of magnitude more time-consuming compared to continuum models.

On a molecular scale, non-polar liquids are less structured as compared to polar liquids like water, and in this respect one may argue that a continuum model should work better for non-polar liquids. On the other hand, standard PCM do not include the van der Waals interaction which are relatively more important for non-polar liquids than for water, in which case electrostatics dominates. The PCM has historically been tested against solvation energies of molecules and ions in water [29], and few accurate experimental data of solvation energies exist for non-polar solvents [37]. The Gaussian software package [17] has been used in all calculations in this work.

The local electrical field is obviously important in streamer processes. Therefore we have considered calculating the IP in an external electrical field in order to simulate conditions closer to those in a streamer. Perturbation theory could be applied to a neutral molecule in order to include the field effect. However, for an ion there is a fundamental problem. The energy of the ion in an electrical field is dependent on the choice of origin of the molecule and cannot be uniquely determined. These effects will be addressed in a future publication.

## 3 RESULTS AND DISCUSSION

We have calculated the IP and EA for a selection of molecules, some of them used as additives or base liquids in streamer propagation experiments [1, 3, 22, 27, 28, 38-44], and compared them with available experimental data. Figure 1 presents a schematic overview of the different molecules considered in this work.

### 3.1 IONIZATION POTENTIAL

From Table 1, we see that all three methods (OVGF, *adiabatic* and *vertical*) give good results for the IP. The adiabatic IPs are only slightly smaller than the vertical IPs, and it is concluded that geometry effects in general are small. However, there are a handful of exceptions: cyclohexane, pentane and tetrakis-dimethylamino-ethylene all have a reduction in IP of around 1 eV due to geometry optimization of the positive ion. In cyclohexane and pentane, two C-C bond lengths have increased from about 1.53 Å in the neutral molecule to about 1.60 Å in the cation, whereas in tetrakis-dimethylamino-ethylene the C=C bond length has increased from 1.34 Å to 1.41 Å. In all these cases, the adiabatic IP is closer to the experimental results compared to the other two methods.

The OVGF method also performs well for the IP, but the calculation does not converge for some molecules (noted as n.c. in Table 1). Although the calculation for dodecane converged, the IP is much higher than the vertical and adiabatic IPs as well as compared to octane. OVGF gives a negative IP for benzil which is non-physical. The OVGF calculations in these cases should thus also be considered as failed calculations.

We conclude that the IP is straightforward to calculate in the gas-phase of molecules of interest to streamer propagation experiments, and that it is required to calculate the adiabatic instead of the vertical IP in a few cases.

There are few experimental data in the literature of the IP of molecules dissolved in liquid cyclohexane. We found experimental data for cyclohexane and p-diaminobenzene [45,46]. For these two cases, the PCM gives a vertical IP close to the experimental value. We included in Table 1 also data for some molecules in other hydrocarbon liquids (n-pentane and neopentane) to demonstrate that the PCM calculations in general gives an IP within the expected range. The PCM reduces the IP by around 1 eV for all molecules when compared to the gas-phase calculations. The energies of the neutral molecules, $E^{A}$, are approximately unchanged while the energy of the positive ions $E^{A+}$ is lowered. In this respect, the main interaction can be interpreted as between a positive point charge and the liquid medium, and it is therefore not unreasonable that the reduction of IP is approximately independent of the molecule of interest. Within the PCM, it is concluded that the IP is straightforward to calculate with good accuracy.

The IP is useful in the interpretation of streamer experiments [28]. The mechanism of streamer propagation from a positive electrode possibly involves an electron avalanche mechanism in the liquid, whereby an exponentially increasing number of electrons is produced by repeated electron impact ionization of neutral molecules

$$e^- + A \rightarrow A^+ + 2e^- \qquad (4)$$

Effects of additives on the positive streamer propagation in liquid cyclohexane are quantitatively in agreement with an electron impact ionization mechanism [28]. If we assume a constant ionization cross-section $\sigma_{ion}$ for incoming electron energies $E(e^-)$ greater than the IP of the molecule, the probability for creating a new electron by the mechanism in equation (4) is proportional to the probability that the electron has an energy above the IP. The probability $P$ for creating an electron by impact ionization, where $f(E)$ is the energy

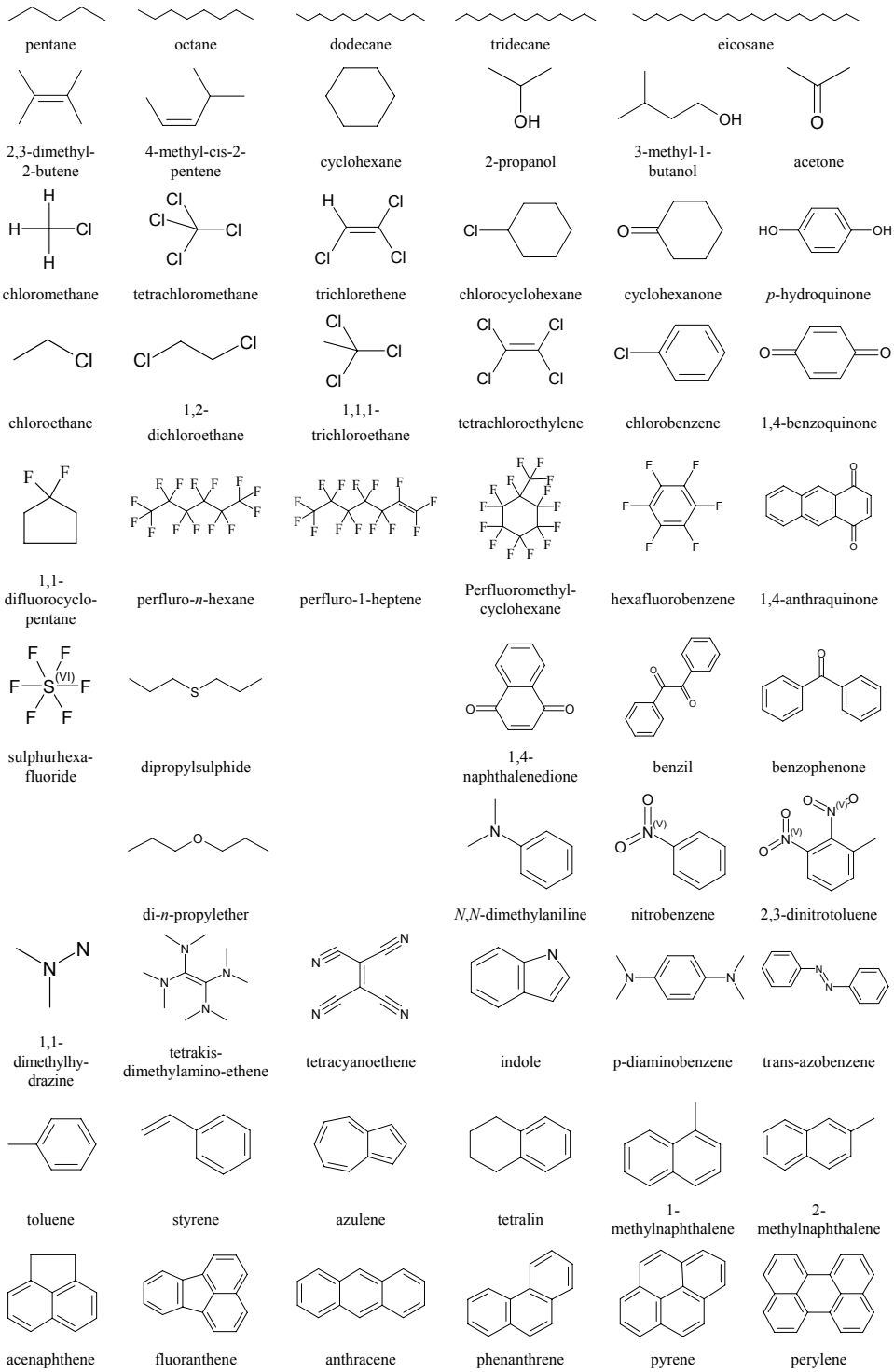


**Figure 1.** Molecules.

**Table 1.** Ionization potentials (eV ).

| Molecule | OVGF | Vertical | Adiabatic | Exp gas phase[1] | PCM Vertical | PCM Adiabatic | Exp IP[2] |
|---|---|---|---|---|---|---|---|
| Sulphurhexafluoride | 16.4 | 15.3 | 15.3 | 15.32 | 14.0 | 14.0 | |
| Perfluoromethylcyclohexane | n.c. | 12.5 | 12.1 | | 11.6 | 11.1 | |
| Perfluro-*n*-hexane | 12.8 | 12.1 | 11.7 | | | | |
| Tetracyanoethene | 11.7 | 11.4 | 11.3 | 11.77 | 10.4 | 10.1 | |
| Chloromethane | 11.1 | 11.3 | 11.3 | 11.22 | 10.0 | 10.0 | |
| Tetrachloromethane | 11.4 | 11.2 | 10.9 | 11.47 | 10.0 | 9.7 | |
| Chloroethane | 10.9 | 11.0 | 10.9 | 10.98 | 9.8 | 9.6 | |
| 1,1,1-Trichloroethane | 11.0 | 10.8 | 10.8 | 11.37 | 9.8 | 9.6 | |
| 1,2-Dichloroethane | 11.1 | 11.0 | 10.7 | 11.04 | 9.7 | 9.6 | |
| Perfluro-1-heptene | n.c. | 10.9 | 10.4 | 10.48[b] | 9.7 | 9.2 | |
| 1,1-Difluorocyclopentane | 11.6 | 11.1 | 10.4 | | 10.2 | 9.4 | |
| 2-Propanol | 10.7 | 10.3 | 9.9 | 10.17 | 9.1 | 8.6 | |
| 1,4-Benzoquinone | 10.9 | 10.0 | 9.9 | 10.01 | 8.8 | 8.8 | |
| Hexafluorobenzene | 9.9 | 10.2 | 9.9 | 9.89 | 9.0 | 8.7 | |
| Nitrobenzene | 10.9 | 10.0 | 9.9 | 9.86 | 9.0 | 8.7 | |
| Chlorocyclohexane | 10.4 | 10.2 | 9.8 | | 9.2 | 8.7 | |
| 2,3-dinitrotoluene | n.c. | 10.0 | 9.8 | | 9.3 | 8.8 | |
| Cyclohexane | 10.6 | 10.7 | 9.7 | 9.86 | 9.2 | 8.6 | 8.41[f] |
| Acetone | 9.7 | 9.6 | 9.5 | 9.7 | 8.5 | 8.4 | |
| 3-Methyl-1-butanol | 10.5 | 10.0 | 9.5 | | 8.9 | 8.3 | |
| 1,4-Naphtalenedione | 9.6 | 9.5 | 9.4 | | 8.7 | 8.4 | |
| Di-*n*-propylether | 10.4 | 9.5 | 9.4 | 9.27 | 8.6 | 8.4 | |
| Trichloroethene | 9.4 | 9.6 | 9.3 | 9.46 | 8.4 | 8.1 | |
| Tetrachloroethene | 9.2 | 9.4 | 9.1 | 9.33 | 8.5 | 8.0 | |
| Cyclohexanone | 9.4 | 9.1 | 9.0 | 9.14 | 8.1 | 7.9 | |
| 1,4-Anthraquinone | n.c. | 9.1 | 9.0 | | 8.4 | 8.2 | |
| Chlorobenzene | 9.0 | 9.1 | 8.9 | 9.07 | 8.0 | 7.8 | |
| Toluene | 8.7 | 8.8 | 8.6 | 9.4 | 7.8 | 7.6 | |
| Benzophenone | 9.1 | 8.9 | 8.7 | 9.08 | 8.0 | 7.9 | |
| 4-Methyl-cis-2-pentene | 9.0 | 8.9 | 8.6 | 8.98 | 7.9 | 7.6 | |
| Benzil | -2.0 | 8.6 | 8.3 | | 7.7 | 7.5 | |
| Styrene | 8.3 | 8.3 | 8.2 | 8.46 | 7.1 | 6.9 | |
| Tetralin | 8.4 | 8.4 | 8.2 | | 7.5 | 7.3 | |
| Acenaphthene | 7.9 | 8.0 | 8.2 | 7.75 | 7.0 | 7.2 | |
| Dipropyl-sulphide | 8.2 | 8.3 | 8.1 | 8.3 | 7.3 | 7.2 | |
| 2,3-dimethyl-2-butene | 8.4 | 8.3 | 8.0 | 8.27 | 7.3 | 7.0 | |
| 1-Methylnaphthalene | 7.8 | 7.8 | 7.7 | 7.97 | 6.9 | 6.7 | 6.20[h] |
| *p*-Hydroquinone | 7.8 | 8.0 | 7.7 | 7.94 | 7.0 | 6.6 | |
| 2-Methylnaphthalene | 7.8 | 7.8 | 7.7 | 7.91 | 6.9 | 6.7 | |
| Trans-Azobenzene | 8.2 | 8.3 | 7.6 | | 7.5 | 6.7 | |
| Fluoranthene | n.c. | 7.7 | 7.6 | 7.9 | 6.9 | 6.7 | |
| Phenanthrene | 7.8 | 7.7 | 7.6 | 7.89 | 6.9 | 6.7 | |
| Indole | 7.7 | 7.7 | 7.6 | 7.76 | 6.7 | 6.5 | |
| Azulene | 7.2 | 7.3 | 7.2 | 7.38 | 6.4 | 6.2 | 6.12[e] |
| Anthracene | n.c. | 7.2 | 7.1 | 7.44 | 6.3 | 6.2 | 6.18[g], 6.54[h] |
| Pyrene | n.c. | 7.2 | 7.1 | 7.43 | 6.4 | 6.2 | 6.20[h] |
| *N,N*-dimethylaniline | 7.1 | 7.2 | 7.0 | 7.12 | 6.3 | 6.1 | |
| 1,1-Dimethylhydrazine | 8.0 | 7.9 | 6.8 | 7.29 | 6.9 | 6.8 | |
| Perylene | n.c. | 6.7 | 6.6 | 6.96 | 6.0 | 5.8 | |
| *p*-diaminobenzene | 6.3 | 6.3 | 5.9 | 6.75[c] | 5.6 | 5.1 | 4.74[d] |
| Tetrakis-dimethylamino-ethylene | 7.0 | 6.9 | 5.7 | 6.11 | 6.0 | 4.7 | |
| Pentane | 11.1 | 11.0 | 10.0 | 10.28 | 9.9 | 8.9 | |
| Octane | 10.5 | 10.0 | 9.4 | 9.8 | 9.1 | 8.5 | |
| Dodecane | 18.1 | 9.5 | 9.1 | | 8.7 | 8.2 | |
| Tridecane | n.c. | 9.4 | 9.0 | | 8.7 | 8.2 | |
| Eicosane | n.c. | 8.9 | 8.7 | | 8.4 | 8.1 | |

n.c: not converged. [1]All experimental data are taken from [49], except [b][50] and [c][51]. [2]Experimental data for ionization potentials in liquid cyclohexane or similar hydrocarbon liquids; in cyclohexane [d][45], [f][46]; in n-pentane [e][52], [g][53]; in neopentane [h][53].

distribution of the quasi-free electrons in the system, then becomes

$$P \propto \int_{IP}^{\infty} f(E)\, dE \qquad (5)$$

This energy distribution is in general unknown, but by assuming that $f(E)$ decreases exponentially in the relevant energy domain (high-energy tail of a Maxwell distribution), a simple expression for the probability $P$ was obtained [28]. Let $P_B$ be the probability for releasing an electron by collisional ionization of the base liquid, and let $P_A$ be the probability for creating an additional electron when an electron collides with the additive. By assuming that the electron energy distribution $f(E)$ is not affected by the additive, we obtain

$$\frac{P_A}{P_B} = e^{-k(IP_A - IP_B)} \qquad (6)$$

where $IP_A$ and $IP_B$ are the IPs of the additive and the base liquid, respectively, and $k$ is a constant. The probabilities $P_A$ and $P_B$ are dependent on the local electrical field, both through the modification of the IP and through the modification of the energy distribution $f(E)$. However, we previously assumed that the ratio between $P_A$ and $P_B$ is field-independent [28]. This enabled us to modify an empirical field-dependence formula for the impact ionization probability in pure cyclohexane to predict the effect of a given additive and calculate streamer propagation voltage thresholds for different additive concentrations [28].

In equation (6), the effect of an additive is determined only by the difference in IP between the additive and the base liquid. By comparing the PCM with gas-phase calculations, the IP relative to cyclohexane (the base liquid in our case) is the same in the gas-phase as for the PCM results for the liquid phase. This indicates that the IP calculated for the gas-phase not only gives a qualitative but also gives a quantitative insight into the processes. For streamers originating from a positive electrode, the IP is experimentally an important molecular descriptor and in this respect, quantum chemical calculations are attractive alternatives for finding the IP when experimental data are missing.

### 3.2 ELECTRON AFFINITY

For the EA (Table 2), the calculations are more problematic compared to the calculation of the IP. Larger differences between the different methods are found, and also between calculated and experimental results. Moreover, there are fewer experimental data available. Experimentally, some molecules have positive EA and create stable anions whereas other have negative EA and create unstable anions. Quantum chemical calculations of these properties are difficult mainly due to instabilities encountered for molecules with negative EA. Even if the anion is stable the electronic states may be very diffuse. It therefore cannot be expected that the EA is as accurate as the calculation of the IP.

**Table 2.** Electron affinities (eV)

| Molecule | OVGF | Vertical | Adiabatic | Exp[1] |
|---|---|---|---|---|
| Tetracyanoethene | 2.4 | 3.4 | 3.5 | 2.2 |
| 1,4-Benzoquinone | 1.0 | 1.9 | 2.2 | 1.91 |
| 1,4-Naphtalenedione | 0.9 | 1.8 | 2.0 | 1.81 |
| 2,3-Dinitrotoluene | n.c. | 1.4 | 1.9 | 1.77 |
| Perfluoromethylcyclohexane | n.c. | -0.1 | 1.6 | 1.07 |
| Sulphurhexafluoride | 0.2 | 1.2 | 3.2 | 1.05 |
| Nitrobenzene | <0.1 | 0.9 | 1.2 | 1.00 |
| Anthracene | n.c. | 0.5 | 0.6 | 0.520 |
| Benzil | 4.2 | 1.5 | 1.7 | |
| 1,4-Anthraquinone | n.c. | 1.6 | 1.8 | |
| Perylene | n.c. | 0.9 | 0.0 | |
| Fluoranthene | n.c. | 0.7 | 0.8 | |
| Pyrene | n.c. | 0.5 | 0.4 | |
| 1,1,1-Trichloroethane | -0.9 | - | - | -0.42[c] |
| Trichlorethene | -1.2 | - | - | >-.065[b,2] |
| Chlorobenzene | -0.8 | - | - | -0.74[c] |
| Tetrachloroethene | -1.3 | - | - | -0.94[a] |
| Perfluro-*n*-hexane | -1.8 | - | - | >-1.1[b,4] |
| 1,2-Dichloroethane | -3.0 | - | - | -1.7[a] |
| Chloromethane | -0.9 | - | - | -3.3[d] |

n.c: not converged. [1]All experimental data are taken from [49] except [a][47], [b][54], [c][55], [d][56] and [c][57]. [2]We have used equation (9) to give an estimate for EA. The following molecules have negative EA within the approaches used here: 1,1-Difluorocyclopentane, 1,1-Dimethylhydrazine, 1-Methylnaphthalene, 2-Methylnaphthalene, *p*-diaminobenzene, 2,3-Dimethyl-2-butene, 2-Propanol, 3-Methyl-1-butanol, 4-Methyl-cis-2-pentene, Acenaphthene, Acetone, Azulene, Benzophenone, Chloro-cyclohexane, Cyclohexane, Cyclohexanone, Di-*n*-propylether, Di-propyl-sulphide, Chloroethane, Hexafluoro-benzene, Indole, *N,N*-dimethylaniline, Perfluro-1-heptene, *p*-Hydro-quinone, Phenanthrene, Styrene, Tetrakis-dimethylamino-ethylene, Tetrachloromethane, Tetralin, Toluene, Trans-Azobenzene, Pentane, Octane, Tridecane and Eicosane.

According to equation (2), one way to calculate the EA is simply to subtract the energy of $A^-$ from the energy of $A$. In quantum chemical calculations, the solution is always the wave function that gives the lowest possible energy. Since it cannot be distinguished between $A^-$ and $A+e^-$, the ground state in a quantum mechanical model could very well be a state described more as $A+e^-$ than as a stable negative ion $A^-$. This is the case if the negative ion $A^-$ is unstable. For an isolated system, the true ground state energy of $A^-$ must therefore be smaller than, or equal to, the energy of the molecule $A+e^-$. The exact ground state energy $E^{A-}$ must therefore obey

$$E^{A^-} \leq E^A \qquad (7)$$

and the EA according to equation (2) always becomes greater than zero. In practice, basis sets are not able to describe a molecule plus a free electron, resulting in $E^{A-} > E^A$ for a limited basis set. The problem is that $E^{A-} \rightarrow E^A$ is obtained in the basis set limit (infinite number of basis functions) and in principle any result may be obtained by improving the basis set incrementally when $E^{A-} > E^A$. In Table 2, DFT results are therefore only included when EA > 0 either experimentally or indicated from our calculations. The molecules with negative

EA are listed in a footnote of Table 2. One may argue that since the molecule is surrounded by a medium the diffuseness of the wave function should be restricted by boundary conditions. This can actually be achieved by carefully choosing a limited basis set that with the chosen quantum chemical method resembles experimental data [15].

For EA > 0, vertical and adiabatic EAs give relatively small differences compared to experimental data, except for perfluoromethylcyclohexane and sulphurhexafluoride. Perfluoromethylcyclohexane is the only case where geometry effects seem to be needed to reproduce experimental data. The main geometrical difference between the geometry of the neutral and the perfluoromethylcyclohexane anion, is that one of the fluorine-carbon distances has increased drastically from 1.37 Å to 2.02 Å, indicating that this molecular ion is not stable. It seems to be a general trend that C-F and C-Cl bond lengths increase, typically around 0.1 Å. However for $SF_6$, the adiabatic EA is much higher than the experimental value, while the vertical EA is close to the experimental value. In $SF_6$, all S-F distances increased from 1.61 Å in the neutral molecule to 1.76 Å in the anion. For the other molecules with experimental EA > 0, the difference between adiabatic EA and vertical EA is around 0.2 eV, thus geometry effects are not substantial.

The OVGF method is not based on a ground state calculation of $A^-$, but rather on a perturbative treatment of the neutral molecule $A$. The method should therefore not have the same limitation as discussed above for methods based on ground state calculations of $A^-$. OVGF predicts the sign of EA (although it gives an EA for nitrobenzene only slightly above zero) and might therefore be useful when the correct sign of the EA is not known. However, the calculations often diverge when EA > 0. This might be understood in terms of the EA being further away from Koopman's theorem, making the perturbation harder to handle.

The same OVGF calculation which gave an unphysical negative IP for benzil also gave a large positive EA. Furthermore, the OVGF method diverged for 1,4-anthraquinone, perylene, fluoranthene and pyrene. With the above argument, this might suggest that the EA could be positive for these molecules. This is in fact in line with DFT calculations giving relatively large positive EA values for these molecules. However there is not a particular good agreement between the values of the EA calculated with OVGF and the experimental values, both for positive and negative EA.

When the EA > 0, the molecular anion is stable and the EA value is indicative of the stability. However it is not clear how a negative EA can be interpreted. In electron-molecule collisions, the probability of creating stable negative ions by, for example, decomposing the molecule into two or more fragments is uniquely determined by different cross-sections. These cross-sections are dependent on the energy of the incoming electron and are not necessarily easy to find or interpret. During streamer propagation, molecules with a negative EA may decompose into fragments as

$$A + e^- \Leftrightarrow A^- \rightarrow B + C^- \tag{8}$$

If $A^-$ is unstable, it is experimentally easier to detect and measure the final products $B$ and $C^-$ than $A^-$. In experiments related to such studies, it is therefore distinguished between the Vertical Attachment Energies (VAE) and Dissociative Electron Attachment (DEA) peaks [45]. VAE is simply the energy difference associated with the first step of equation (8) and is the negative of the EA. DEA denotes the energy of the incoming electron with the highest probability for creating the final product $B + C^-$. Not all collisions creating an unstable state $A^-$ will decompose the molecule into fragments $B$ and $C^-$. The probability for going from $A^-$ all the way to the right in equation (8) will depend on the energy of the incoming electron. Therefore, the DEA peak position will be different from the VAE. The higher the energy of the incoming electron, the higher is the probability for $A^-$ to decompose back into $A+e^-$ and thus [47]

$$| \text{VAE} | = | \text{EA} | > | \text{peak DEA} | \tag{9}$$

The average electron capture per collision is proportional to

$$\int_0^\infty \sigma(E) f(E)\, dE \tag{10}$$

where $f(E)$ is the energy distribution of the quasi-free electrons, and $\sigma(E)$ is the total cross-section associated with the capture of an electron with energy $E$. Because of the integral in equation (10) and since $\sigma(E)$ typically is non-zero even for small energies [47], the entire profile of $\sigma(E)$ as a function of the incoming electron energy is needed. Neither the VAE nor peak DEA reflect the magnitude of the cross-sections or give information about the process at different energies. This situation is in sharp contrast to the simplification in equation (5) where we could use that $\sigma(E)$ is constant for $E >$ IP.

An improved descriptor would be the electron attachment cross-section. To calculate the cross-sections by quantum mechanics is difficult and opposes several challenges. The rotational and vibrational states of the molecule have to be taken into account even when calculating the electronic part of the Hamiltonian, and these states give rise to an almost continuum of possible scattered electronic states [48].

## 4 CONCLUSIONS

The calculations of the IP give accurate and predictive results and the calculations are straightforward. Furthermore, our results indicate that the IP for a molecule placed in liquid

cyclohexane is reduced by around 1 eV, approximately independent of the type of molecule. The IP is a good measure of the barrier to extract an electron from the medium, and also an important descriptor for streamer propagation towards a negative electrode.

DFT methods are useful to calculate molecular EA with positive values. If the sign of the EA is not known, an OVGF calculation can be used to give a useful indication of the sign of the EA. The ability of a liquid to capture electrons drifting in an electric field influences streamer propagation from a negative electrode. For electron capture processes, the EA alone does not describe the processes of interest. Instead, a series of various cross-sections are needed.

## ACKNOWLEDGMENT

Support from the Norwegian Research Council through a Strategic Industry Program (164603/I30) and grants of computer time are acknowledged.

## REFERENCES

[1] S. Ingebrigtsen, L. E. Lundgaard, and P.-O. Åstrand, "Effects of additives on prebreakdown phenomena in liquid cyclohexane: I. streamer initiation", J. phys. D. Appl. Phys., Vol. 40, pp. 5161-5169, 2007.

[2] Y. Nakao, H. Itoh, S. Hoshino, Y. Sakai, and H. Tagashira, "Effects of additives on prebreakdown phenomena in n-hexane", IEEE Trans. Dielect. Electr. Insul., Vol. 1, pp. 383-389, 1994.

[3] J. C. Devins, S. J. Rzad, and R. J. Schwabe, "Breakdown and prebreakdown phenomena in liquids", J. Appl. Phys., Vol. 52, pp. 4531-4545, 1981.

[4] L. Johansson and K. Andersson. "Chemical factors affecting dielectric breakdown in insulating liquids", In Nordic Insulation Symposium, Vaasa, pp. 115-125, 1994.

[5] A. Beroual, M. Zahn, A. Badent, K. Kist, A. J. Schwabe, H. Yamashita, K. Yamazawa, M. Danikas, W. G. Chadband, and Y. Torshin, "Propagation and structure of streamers in liquid dielectrics", IEEE Electr. Insul. Mag., Vol. 14, pp. 6-17, 1998.

[6] R. E. Hebner, E. F. Kelley, E. O. Forster, and G. J. FitzPatrick, "Observation of prebreakdown and breakdown phenomena in liquid hydrocarbons - II: Non-uniform field conditions", IEEE Trans. Electr. Insul., Vol. 20, pp. 281-292, 1985.

[7] H. Yamashita, E. O. Forster, and M. Pompili, "Streamer formation in perfluoropolyether under impulse conditions", IEEE Trans. Electr. Insul., Vol. 28, pp. 324-329, 1993.

[8] E. O. Forster, H. Yamashita, C. Mazzetti, M. Pompili, L. Caroli, and S. Patrissi, "The effect of the electrode gap on breakdown in liquid dielectrics", IEEE Trans. Dielectr. Electr. Insul., Vol. 1, pp. 440-446, 1994.

[9] Y. Nakao, T. Yamazaki, K. Miyagi, Y. Sakai, and H. Tagashira, "The effect of molecular structure on prebreakdown phenomena in dielectric liquids under a nonuniform field", Electrical Engineering in Japan, Vol. 139, pp. 1-8, 2002.

[10] C. Zhan, J. A. Nichols, and D. A. Dixon, "Ionization potential, electron affinity, electronegativity, hardness, and electron excitation energy: Molecular properties from density functional theory orbital energies", J. Phys. Chem. A., Vol. 107, pp. 4184-4194, 2003.

[11] V. Lemierre, A. Chrostowska, A. Dargelos, and H. Chermette, "Calculation of ionization potentials of small molecules: A comparitive study of different methods", J. Phys. Chem. A., Vol. 109, pp. 8348-8355, 2005.

[12] L. A. Curtiss, P. C. Redfern, K. Raghavachari, and J. A. Pople, "Assessment of gaussian-2 and density functional theories for the computation of ionization potentials and electron affinities", J. Chem. Phys., Vol. 109, pp. 42-55, 1998.

[13] A. D. Becke, "Density-functional thermochemistry. III. The role of exact exchange", J. Chem. Phys., Vol. 98, pp. 5648-5652, 1993.

[14] Y. Takahata and D. P. Chong, "Density-functional calculations of molecular electron affinites", J. Braz. Chem. Soz., Vol. 10, pp. 354-358, 1999.

[15] M. Meunier, N. Quirke, and D. Binesti, "The calculation of the electron affinity of atoms and molecules", Mol. Simulat., Vol. 23, pp. 109-125, 1999.

[16] J. V. Ortis, "Electron binding energies of anionic alkali metal atoms from partial fourth order electron propagator theory calculations", J. Chem. Phys., Vol. 89, pp. 6348-6352, 1988.

[17] M. J. Frisch et al. Gaussian 03, Revision C.02, 2004.

[18] M. S. Deleuze, "Valence one-electron and shake-up ionization bands of polycyclic aromatic hydrocarbons. II. Azulene, phenanthrene, pyrene, chrysene, triphenylene, and perylene", J. Chem. Phys., Vol. 116, pp. 7012-7026, 2002.

[19] P. M. W. Gill, B. G. Johnson, and J. A. Pople, "The performance of Becke-Lee-Yang-Parr (B-LYP) density functional theory with various basis sets", Chem. Phys. Lett., Vol. 197, pp. 499-505, 1992.

[20] C. W. Baushlicher Jr., "A comparison of the accuracy of different functionals", Chem. Phys. Lett., Vol. 246, pp. 40-44, 1995.

[21] S. Sigurdsson and R. Strömberg, "Evaluation of several economical computational methods for geometry optimisation of phosphorus acid derivatives", Nucleos. Nucleot. Nucl., Vol. 20, pp. 1381-1384, 2001.

[22] O. Lesaint and M. Jung, "On the relationship between streamer branching and propagation in liquids: influence of pyrene in cyclohexane", J. Phys. D Appl. Phys., Vol. 33, pp. 1360-1368, 2000.

[23] R. Kattan, A. Denat, and O. Lesaint, "Generation, growth, and collapse of vapor bubbles in hydrocarbon liquids under a high divergent electric field", J. Appl. Phys., Vol. 66, pp. 4062-4066, 1989.

[24] H. Yamashita, K. Yamazawa, and Y. S. Wang "Effect of tip curvature on the prebreakdown streamer structure in cyclohexane", IEEE Trans. Dielectr. Electr. Insul., Vol. 5, pp. 396-401, 1998.

[25] L. Dumitrescu, O. Lesaint, N. Bonifaci, A. Denat, and P. Notingher, "Study of streamer inception in cyclohexane with a sensitive charge measurement technique under impulse voltage", J. Electrostat., Vol. 53, pp. 135-146, 2001.

[26] A. Denat, N. Bonifaci, and M. Nur, "Spectral analysis of the light emitted by streamers in hydrocarbon liquids", IEEE Trans. Dielectr. Electr. Insul., Vol. 5, pp. 382-387, 1998.

[27] S. Ingebrigtsen, L. E. Lundgaard, and P.-O. Åstrand, "Effects of additives on prebreakdown phenomena in liquid cyclohexane: II. streamer propagation", J. phys. D. Appl. Phys., Vol. 40, pp. 5624-5634, 2007.

[28] S. Ingebrigtsen, H. S. Smalø, P.-O. Åstrand, and L. E. Lundgaard, "Effects of electron-attaching and electron releasing additives in liquid cyclohexane", IEEE Trans. Dielectr. Electr. Insul., Vol. 16, pp. 1524-1535, 2009.

[29] M. Cossi, G. Scalmani, N. Rega, and V. Barone, "New developments in the polarizable continuum model for quantum mechanical and classical calculations on molecules in solution", J. Chem. Phys., Vol. 117, pp. 43-54, 2002.

[30] C. Wohlfarth and M. D. Lechner, *Static Dielectric Constants of Pure Liquids and Binary Liquid Mixtures*, Vol. 6. Heidelberg: Springer Berlin, 1991.

[31] V. Barone, M. Cossi, and J. Tomasi, "A new definition of cavities for the computation of solvation free energies by the polarizable continuum model", J. Chem. Phys., Vol. 107, pp. 3210-3221, 1997.

[32] A. K. Rappe, C. J. Casewit, K. S. Colwell, W. A. Goddard III, and W. M. Skiff, "UFF, a full periodic table force field for molecular mechanics and molecular dynamics simulations", J. Am. Chem. Soc., Vol. 114, p. 10024, 1992.

[33] W. F. Schmidt, "Charge carrier energetics and dynamics in nonpolar liquids", Nucl. Instrum. Meth. A, Vol. 327, pp. 83-86, 1993.

[34] Y. Tabata and S. Tagawa, *Handbook of Radiation Chemistry*, CRC Press, Boca Raton, 1991.

[35] H. Li and J. H. Jensen, "Improving the efficiency and convergence of geometry optimization with the polarizable continuum model: New energy gradients and molecular surface tessellation", J. Comp. Chem., Vol. 25, pp. 1449-1462, 2004.

[36] M. J. Field, P. A. Bash, and M. Karplus, "A combined quantum mechanical and molecular mechanical potential for molecular dynamics simulations", J. Comp. Chem., Vol. 11, pp. 700-733, 1990.

[37] A. V. Marenich, R. M. Olson, C. P. Kelly, C. J. Cramer, and D. G. Truhlar, "Self-consistent reaction field model for aqueous and nonaqueos solutions based on accurate polarized partial charges", J. Chem. Theory Comput., Vol. 3, pp. 2011-2033, 2007.

[38] A. Beroual, M. Zahn, A. Badent, K. Kist, A. J. Schwabe, H. Yamashita, K. Yamazawa, M. Danikas, W. G. Chadband, and Y. Torshin, "Propagation and structure of streamers in liquid dielectrics", IEEE Electr. Insul. Mag., Vol. 14, pp. 6-17, 1998.

[39] L. Angerer, "Effect of organic additives on electrical breakdown in transformer oil and liquid paraffin", Proc. IEE., Vol. 112, pp. 1025-1034, 1965.

[40] A. Beroual and R. Tobazeon, "Prebreakdown phenomena in liquid dielectrics", IEEE Trans. Dielectr. Electr. Insul., Vol. 21, pp. 613-627, 1986.

[41] T. Schutte, "The influence of the molecular packing on electrical breakdown strength of liquids", In Nordic Insulation Symposium, Vasaa, pp. 147-160, 1994.

[42] E. O. Forster, C. Mazzetti, M. Pompili, and R. Cecere, "The effect of molecular structure on the properties of dielectric fluids", IEEE Trans. Dielectr. Electr. Insul., Vol. 26, pp. 749-754, 1991.

[43] Y. Nakao, H. Itoh, S. Hoshino, Y. Sakai, and H. Tagashira, "Effects of additives on prebreakdown phenomena in n-hexane", IEEE Trans. Dielectr. Electr. Insul., Vol. 1, pp. 383-389, 1994.

[44] W. G. Chadband and T. M. Sufian, "Experimental support for a model of positive streamer propagation in liquid insulation", IEEE Trans. Electr. Insul., Vol. 20, pp. 239-246, 1985.

[45] L. G. Christophorou, *Electron-molecule Interactions and Their Application*, Vol. 1. U.S. Academic Press, San Diego, 1984.

[46] J. Casanovas, R. Grob, D. Delacroix, J. P. Guelfucci, and D. Blanc, "Photoconductivity studies in some nonpolar liquids", J. Chem. Phys., Vol. 75, pp. 4661-4668, 1981.

[47] K. Aflatooni and P. D. Burrow, "Total cross sections for dissociative electron attachment in dichloroalkanes and selected polychloroalkanes: The correlation with vertical attachment energies", J. Chem. Phys., Vol. 113, pp. 1455-1464, 2000.

[48] N. F. Lane, "The theory of electron-molecule collisions", Rev. Mod. Phys., Vol. 52, pp. 29-119, 1980.

[49] D. R. Lide, *Handbook of chemistry and physics*, 84th edition, CRC Press, Boca Raton, 2004.

[50] K. Watanabe, T. Nakayama, and J. Mott, "Ionization potentials of some molecules", J. Quant. Spectrosc. Radiat Transfer., Vol 2, pp. 369-382, 1962.

[51] W. Kaim and M. Bock, "Radikalionen, XXIII: $R_2P$- und $R_2N$-substituierte Benzole: Die Ladungsverteilung in ihren Kationen, Anionen und Trianionen", Chem. Ber., Vol. 111, pp. 3843-3856, 1978.

[52] H. Faidas and L. G. Chrisophorou, "Laser multiphoton ionization of aromatic molecules in nonpolar liquids", Radiat. Phys. and Chem., Vol. 32, pp. 433-438, 1988.

[53] R. A. Holroyd, J. M. Preses, E. H. Böttcher and W. F. Schmidt, "Photoconductivity induced by single-photon excitation of aromatic molecules in liquid hydrocarbons", J. Phys. Chem., Vol. 88, pp. 744-749, 1984.

[54] J. R. Johnson, L. G. Christophorou, and J. G. Carter, "Fragmentation of aliphatic chlorocarbons under low-energy (<10 eV) electron impact", J. Chem. Phys., Vol. 67, pp. 2196-2215, 1977.

[55] G. A. Gallup, K. Aflatooni, and P. D. Burrow, "Dissociative electron attachment near threshold, thermal attachment rates, and vertical attachment energies of chloroalkanes", J. Chem. Phys., Vol. 118, pp. 2562-2574, 2003.

[56] P. D. Burrow, A. Modelli, N. S. Chiu, and K. D. Jordan, "Temporary negative ions in the chloromethanes $CHCl_2F$ and $CCl_2F_2$: Characterization of the sigma* orbitals", J. Chem. Phys., Vol. 77, pp. 2699-2701, 1982.

[57] A. Modelli and M. Venuti, "Temporary $\pi^*$ and $\sigma^*$ anions and dissociative electron attachment in chlorobenzene and related molecules", J. Phys. Chem. A, Vol. 105, pp. 5836-5841, 2001.

**Hans Sverre Smalø** was born in 1978 in and grew up in Trondheim, Norway. In 2002 he obtained the M.Sc. degree in physics at the Norwegian University of Technology (NTNU) in Trondheim. He is currently a Ph.D. student in the Department of Chemistry at NTNU, and is working with computational chemistry and molecular modelling.

**Per-Olof Åstrand**, was born in Sätila, Sweden in 1965. He is Professor in theoretical chemistry at the Department of Chemistry, Norwegian University of Science and Technology, Trondheim, Norway. He received the Ph.D. degree at the University of Lund in 1995 with Prof. Gunnar Karlström as the thesis supervisor, and he spent seven years in Denmark at Aarhus University, University of Copenhagen and Risø National Laboratory before he moved to Norway in 2002. His research interests include the construction of molecular mechanics models for intermolecular forces, reactive force fields and optical properties, with applications in optics, nanoscience, catalysis and electrical breakdown of dielectric liquids.

**Stian Ingebrigtsen** was born in Bergen, Norway in 1978. He received the M.Sc. degree in physics in 2002 and the Ph.D. degree in chemistry in 2008, both from the Norwegian University of Science and Technology (NTNU) in Trondheim, Norway. Since 2002 he has worked with SINTEF Energy Research in Trondheim. His research interests include dielectric performance of materials for electrical insulation purposes.

# Paper 5:

*Field dependence on the molecular ionization potential and excitation energies compared to conductivity models for isolation materials at high electrical fields*

Hans S. Smalø, Ø. Hestad, S. Ingebrigtsen and P.-O. Åstrand

J. Appl. Phys.

**Submitted**

# Field dependence on the molecular ionization potential and excitation energies compared to conductivity models for insulation materials at high electrical fields

Hans S. Smalø[1], Øystein Hestad[1], Stian Ingebrigtsen[2] and Per-Olof Åstrand[1] *

[1] *Department of Chemistry, Norwegian University of Science and Technology (NTNU), N-7491 Trondheim, Norway and*

[2] *Department of Electric Power Technology, SINTEF Energy Research, N-7465 Trondheim, Norway*

## Abstract

The aim of this study is to improve the understanding of high-field phenomena (such as pre-inception currents/conduction, streamer initiation and propagation) in insulating materials in terms of the molecular properties of the substances involved. In high electric fields, ionization is a likely process, and in all such processes, the ionization potential is an important parameter. A fundamental question is how these processes depend on the electric field, and therefore, based on the interaction between a negative point charge and a molecular cation as modelled by density functional theory, a field-dependent model for the ionization potential is developed. In addition, the first excitation energies as a function of the electric field are calculated using time-dependent density functional theory.

It is demonstrated that empirical high-field conduction models for cyclohexane and $n$-tridecane can be explained in terms of the difference between the ionization potential and the first excitation energy. It is also suggested that the reduction of the ionization potential with electric fields, can help explain how fast-mode streamers propagate.

* Corresponding author: per-olof.aastrand@chem.ntnu.no

## I. INTRODUCTION

Pre-breakdown phenomena in liquids and solids have been studied extensively during the last decades to gain insight into the processes responsible for breakdown in dielectric media as a result of high applied voltage. A thorough investigation of pre-breakdown phenomena in cyclohexane and *n*-tridecane stressed by a fast transient in a highly divergent field has been reported.[1–8] With increasing applied voltage, the measured current-voltage characteristics go through three stages[8]:

- Slow increase in recorded current with applied voltage. This is caused by increased conductivity in the high-field region (average currents are in the range up to 1 $\mu$A).
- Large increase in current at a threshold voltage. The average current increases to several $\mu A$ during the formation of a low density region (streamer/electrical tree). This is observed as steps in the charge recordings and a low density/vaporized region can be seen in the liquid phase. For a frozen phase an electrical tree starts to grow in the high-field region, causing lasting damage to the insulation.
- As the voltage is increased further the streamer/electrical tree grows until it traverses the electrode gap at a sufficiently high voltage. This may result in breakdown, resulting in a large step in the recorded current.

This is a simplified description of the phenomena. The conduction current recorded below inception of streamer/electrical trees goes through many stages and the streamer/electrical trees have been observed to go through several stages/modes as well.[4,9] For a more thorough discussion of the pre-breakdown phenomena in liquids and solids, the reader is referred to several review papers on the two topics.[9–11] In this paper, we focus on the currents recorded below the threshold for inception of electrical trees/streamers in the material. These currents are typically referred to as 'pre-inception currents', and can be compared to transient nonlinear finite element method (FEM) simulations based on high-field conduction models.[8,11]

A high electric field induces an increased conductivity which may be caused by[9,12]:

- Increased charge carrier density due to injection of charge from the electrodes in an experimental setup.

- Dissociation of molecules into molecular fragments
- Ionization of molecules creating ion-electron pairs.
- Increased charge mobility.
- Increased ion mobility in a liquid due to electrohydrodynamic (EHD) motion.

The field and temperature-dependent conductivity is important, since the high-field conductivity determines the electric-field distribution and the amount of energy dissipated in the material due to joule heating.[11] Four important high-field conductivity models are given in Table I, where the two first (Schottky and Fowler-Nordheim) describe charge injection from the electrode, and the last two (Hopping conduction and Poole-Frenkel) describe the high-field conductivity in the bulk material. These mechanisms are all based on the lowering of the potential barrier localizing the charge due to an external electric field. If a sufficiently high electric field is applied, the charge can either climb the reduced barrier by thermal excitation (Schottky and Poole-Frenkel) or tunnel through the barrier (Fowler-Nordheim and Hopping conduction).[12–17]

The focus of this paper is mainly on the calculation of the ionization potential, IP, of molecules subjected to a high background field, which is used to interpret current measurements in cyclohexane and *n*-tridecane. The hypothesis is that electrons/holes are the main charge carriers in dielectrics stressed by fast transients (ions are too slow to contribute significantly during the first microseconds). The electrons are localized in molecules prior to the application of the step voltage, and the increase in free electron concentration depends on how much the escape barrier, i.e. the IP, is lowered.

The IP of a molecule $A$ is defined as the energy to remove an electron and create a cation $A^+$,

$$A \rightarrow A^+ + e^- \; ; \; IP = U_{A^+} - U_A \tag{1}$$

where $U_A$ is the energy of molecule $A$ and $U_{A^+}$ is the energy of its cation. Quantum chemistry provides molecular properties (polarizability, dipole moment, excitation energies, ionization potential, etc.) with good accuracy, and through advances in methodology and computer power, quantum chemistry can be used for increasingly larger systems. Density functional theory (DFT) has been used to calculate the IP accurately.[18–20] Earlier work,[21,22] demonstrated how quantum chemistry can be used to calculate the IP, and how the IP is important

Table I. Conductivity models with charge injection from electrodes/bulk

| Name | Equation[a] | Ref. |
|---|---|---|
| Schottky injection | $J(E) = \frac{4\pi emk_B^2(1-R)T^2}{h^3} \cdot e^{-\frac{\Phi}{k_BT}} \cdot e^{\frac{e}{2k_BT}\sqrt{\frac{eE}{\pi\epsilon_0\epsilon_r}}}$ | 12,14,15 |
| Fowler-Nordheim | $J(E) = \frac{e^3E^2}{8\pi h\phi} \cdot e^{-\frac{4}{3}\sqrt{\frac{2m}{\hbar^2}}\frac{\phi^{3/2}}{eE}}$ | 12 |
| Hopping conduction | $\sigma(E) = \frac{2\nu aen}{E} \cdot e^{-\frac{W}{k_BT}} \cdot \sinh(\frac{eEa}{2k_BT})$ | 17 |
| Poole-Frenkel | $\sigma(E) = \sqrt{N_{eff}N_D}e\mu \cdot e^{-\frac{\Phi}{2k_BT}} \cdot e^{\frac{e^{3/2}\cdot\sqrt{E}}{\sqrt{4\pi\epsilon_0\epsilon_r}k_BT}}$ | 12,14,15 |

[a] $\epsilon_0$ is the permittivity of vacuum, $\epsilon_r$ is the relative permittivity, $\mu$ is the charge carrier mobility, $\nu$ is the escape frequency, $\phi$ is the work function, $\Phi$ is the barrier height, $a$ is the distance between traps, $E$ is the electric field, $e$ is the elementary charge, $h$ is Planck's constant, $k_B$ is Boltzmann's constant, $m$ is the electron mass, $n$ is the charge carrier density, $N_{eff}$ is the effective density of states in the conduction band, $N_D$ is the number of potential donors, $R$ is the reflection coefficient, $T$ is the temperature, and $W$ is the trap depth.

for interpreting streamer propagation. However, if the molecule is in an external electric field, the definition of the IP given in Eq. (1) is problematic since the energy of an ion in an electric field is dependent on the choice of origin. Intuitively, a high external electric field should make ionization processes easier, and thus the effect of the external field cannot be neglected. In this paper, the IP is obtained so that it becomes a useful descriptor when the field is different from zero, while Eq. (1) is retained in the limit of zero field. DFT is used to calculate the field dependence of the IP for a few molecules, such as cyclohexane and *n*-tridecane.

The paper is divided into six sections (including this introduction). The next section describes the theoretical foundation for the quantum chemical calculations of the IP and excitation energies when molecules are placed in a high background field. The theory section includes a discussion of how microscopic properties can be linked to conduction models. The third section describes ionization mechanisms. Section four contains the results obtained from the DFT calculations (IP, excitation energies and ground state energies). Section five presents a brief discussion which links the results obtained from DFT with experimental measurements of high-field conduction currents. Finally a conclusion is given.

In this work, atomic units[23] are used in the theory section while $eV$ is used for energies and $MV/cm$ is used for electric fields in the section with the results. It is also noted that the terms *high* and *low* electric fields always depend on a reference field. Intermolecular fields can be an order of magnitude greater than any macroscopic field. Thus even *extremely high* electric fields (100 $MV/cm$) may be small compared to intermolecular fields.

## II. THEORY

### A. Classical system

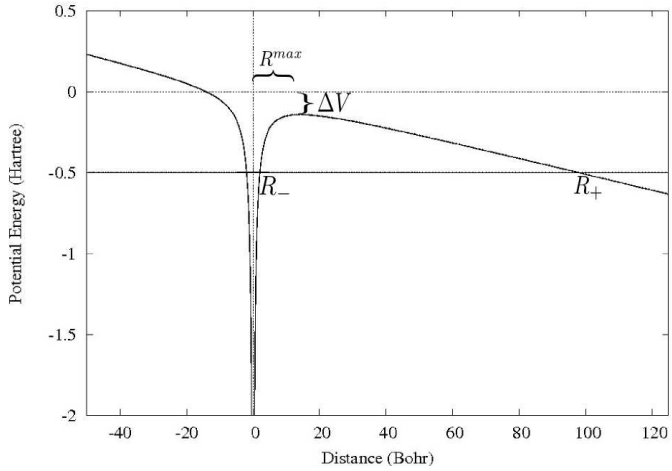


Figure 1. The Coulomb potential energy in an electric field, E=0.005 au, and ground-state energy of the hydrogen atom. In this illustration, the classical turning points, $R_\pm$, the distance to the maximum potential, $R^{max}$, and the maximum potential, $V_e^{max} = \Delta V$, are indicated.

In high electric fields, free electrons can be created by ionization.

A simple quantum-mechanical (QM) system, the hydrogen atom, is considered in the following. In a negative homogeneous external electric field, $-E$, the one-electron potential energy, $V_e$ (illustrated in Figure 1) is

$$V_e = -\frac{1}{|R_e|} - ER_e \tag{2}$$

where $R_e$ is the position of the electron relative to the proton (not distance since the potential is not symmetric about the origin). In this work, we assume that the main effect of the field

is described by a simplified one-dimensional problem along the electric field. This potential has a maximum at

$$R_e^{max} = 1/\sqrt{E} \ , \tag{3}$$

and an electron is bound to the proton only when the total energy of the electron $\varepsilon_e$ is less than the potential at the maximum, $V_e^{max}$. When $E \to 0$, $R_e^{max} \to \infty$ and $V_e^{max} \to 0$. Thus without an electric field the electron is free when $\varepsilon_e \geq 0$. However, when $E \neq 0$, the maximum potential is decreased as

$$V_e^{max} = -\Delta V = -2\sqrt{E} \tag{4}$$

and thus if $\varepsilon_e$ is larger than $V_e^{max}$, the electron is no longer bound by the hydrogen atom. This is true both when the electron is treated quantum mechanically and classically. Eq. (4) represents a reduction of the potential barrier which can release an electron from the hydrogen atom.

A conduction mechanism based on Eq. (4) is the classical Poole-Frenkel mechanism. The barrier between donors is lowered by the external electrical field, thus increasing the number of free charge carriers in the dielectric which increases the conductivity of the material.[12] This mechanism applies to materials with wide band gaps that contain charge donors and/or acceptors. These charge donors and acceptors should require more energy than what is generally available in order to be ionized. In complex materials (i.e. polymers) regions of high or low electronegativity can be created at chemical or physical defects in the material where electrons can be more easily ionized or captured, and these regions will then act as electron donors or acceptors.[12,16]

If one assumes that the source of free electrons are molecules with $IP = IP_0$ at zero field the classical Poole-Frenkel equation is,[12]

$$\sigma(E) = \sqrt{N_{eff} N_d} \cdot \mu \cdot e^{-\frac{IP_0}{2k_B T}} \cdot e^{-\frac{\sqrt{E}}{k_B T \sqrt{\epsilon_r}}} \tag{5}$$

where $N_{eff}$ is the effective density of states in the conduction band, $N_d$ is the number density of donors (molecules), $\mu$ is the mobility of free electrons, and $\epsilon_r$ is the relative permittivity of the material. Eq. (5) assumes that only free electrons contribute to the conductivity. One could also envisage that bound electrons in a molecule can tunnel through the barrier to a neighbouring ionized molecule leaving behind an ionized molecule at the previous location. This is termed hole conduction and also contributes to the overall conductivity.[13] If

one assumes that the mobility of the holes is not field dependent, this contribution to the conductivity can be included in the constant preceding the exponential function in Eq. (5) since the number of holes will be equal to the number of free electrons.

The Poole-Frenkel mechanism assumes that the source of electrons is the bulk material. In a similar mechanism, Schottky injection, the source of electrons is a metal electrode.[12] To a first approximation, the barrier that electrons need to overcome to enter the dielectric can be estimated by the electrostatic attraction between the electron and the electrode, and the contribution from the work function of the metal is thus neglected. The electrostatic attraction can be calculated using the image charge method, and the resulting potential barrier as a function of the distance from the electrode as augmented by the external electric field is given by,[12]

$$V_e = -\frac{1}{4 \cdot |R_e| \epsilon_r} - E R_e \tag{6}$$

Based on a similar analysis as for the Poole-Frenkel model, the current density at the electrode surface as a function of the applied field is[12]

$$J = 4\pi k_B^2 (1-R) T^2 \cdot e^{-\frac{\Phi}{k_B T}} \cdot e^{\frac{\sqrt{E}}{k_B T \sqrt{\epsilon_r}}} \ , \tag{7}$$

where $R$ is the proportion of electrons which are reflected by the surface of the metal, $\Phi$ is the barrier height in the absence of a field, and $T$ is the temperature. Distinguishing between currents caused by the Poole-Frenkel mechanism or Schottky injection is generally difficult, since both are exponential functions which depend on the square root of the field.

Several other conductivity mechanisms giving similar field dependence as the Poole-Frenkel mechanism have been proposed,[24,25] as phonon assisted tunnelling[26] and the Onsager mechanism.[27] For the Onsager mechanism, as for the Poole-Frenkel model, the field dependence stems from the lowering of the Coulomb potential between localized electrons/charges by the external field as in Eq. (4). However the phonon assisted tunnelling model is more involved, since the traps are modelled as dipoles/induced dipoles, and the energetic and spatial distribution of such traps govern the field-dependent mobility.[26] The field dependence of the IP will be important for the Onsager and Poole-Frenkel models, while phonon assisted tunnelling is a pure mobility model that does not require ionization of molecules/traps (it explains the field dependent conductivity by a field dependent mobility, not by creation of more free charge).

### B. Quantum mechanical system

In a hydrogen atom, the lowering of the barrier by an electric field is given by Eq. (4), which is here regarded as a model system for a many-electron system. If the system can be simplified in analogy to the Hartree approximation[28] as an effective one-electron potential for the escaping electron, the electron may escape from the molecule if the energy is above the maximum of this effective one-electron potential. Here, the exchange between the escaping electron and the rest of the electrons is neglected, and the escaping electron is regarded as a negative point charge and not a charge distribution. We assume that

$$U_{A^+ + e^-} = U_{A^+} + V_e \tag{8}$$

such that the one-electron potential $V_e$ (see Figure 1) at position $R_e$ can be calculated from the interaction energy between a negative point charge, $e^-$, placed at $R_e$ and a cation $A^+$. Since the total system $(A^+ + e^-)$ is electrically neutral, the energy in an electric field for the combined system is origin independent. If the electric field is small, $R_e^{max}$ is relatively large such that exchange effects are small. For typical fields (below some tens of MV/cm), a model in terms of effective local one-electron potentials should be a good approximation since for example $R_e^{max} \approx 7$Å for $E = 30 MV/cm$ using Eq. (3). The difference between this QM approach and the classical approach is caused by two effects, a molecular ion is not a point charge, and secondly a molecular ion may be polarized both by the external electric field and by the ionized electron.

In this model, the IP is given as

$$IP = U^*_{A^+ + e^-} - U_A \tag{9}$$

where $U^*_{A^+ + e^-}$ is the total energy of the combined system $A^+ + e^-$ at $R_e^{max}$. A three-dimensional potential is more complicated since the electron has many possible escape paths. The most probable path is in general not a straight line, and $U^*_{A^+ + e^-}$ is a first-order saddle point defined by the maximum of the energy along the simplest escape path. In the present work, only the distance between the point charge and the cation was varied, and a three dimensional search to find $U^*_{A^+ + e^-}$ was not carried out. This is reasonable since the energy $U_{A^+ + e^-}$ depends mostly on the distance between $A^+$ and the point charge along the field direction. At separation distances close to $R_e^{max}$, the potential is necessarily relatively flat

since $dU/dR \approx 0$, and it is thus not critical to find $R_e^{max}$ with high accuracy. The point charge was placed a certain distance along the direction of the field from a given atom chosen more or less at random (test calculations showed that which atom the electron was pulled out of had little influence on the results). For the smallest fields, $E = 0.001$ au $= 5.14$ $MV/cm$ a maximum was generally found between 10 Å and 20 Å from the closest atom, while for the largest fields, $E = 0.02$ au $= 102.8$ $MV/cm$ a similar maximum was found between 1.5 Å and 4 Å from the closest atom. The main objective of this study is to calculate the IP as a function of electric field using Eq. (9), and then compare it to the classical results in Eq. (4) to see if the field dependence of the IP can be used to aid in the interpretation of experimental results.

For the DFT calculations the BLYP[29,30] functional with the augmented TZP basis set[31,32] was used. All calculations were carried out using the ADF software package,[33,34] and the geometries was obtained from a geomtry optimization of the neutral molecules in gas phase. The calculations on the cation were carried out using both the restricted and unrestricted open-shell method. However, only results for the unrestricted open-shell method are presented since the difference between the results of the two methods is small. On a practical note, the interaction energy between the point charges and the external electric field is not included in the energy obtained in ADF and this energy contribution has to be added manually.

To study the effect of the electric field on the neutral molecule in greater detail, excitation energies as a function of electric field were calculated using time-dependent density functional theory[35,36] (TD-DFT) with the same functional and basis set. For these calculations, especially for the high electric fields, a further augmentation of the basis set might have been beneficial, since some excited states may be relatively diffuse, especially in an external electric field. Furthermore, it is noted that TD-DFT is regarded to give accurate excitation energies as long as the excitation is charachterized as local, however for charge-transfer states (which are biradical), or Rydberg states (the excited state is very diffuse) large errors may be obtained for many of the contemporary functionals.[37,38] However, only the lowest singlet-singlet excitation energy whose accuracy is relatively unproblematic is included here.

### C. Effect of a dielectric medium

All calculations in this work were done in the gas phase, however the corresponding experiments have been carried out in the liquid phase,[8] and thus a central question is how gas-phase calculations can be compared to relevant experiments. Representing the medium by a dielectric continuum, the Clausius-Mossotti equation gives the relation between the local field $E_L$ felt by an atom/molecule in a spherical cavity and the average macroscopic field $E_M$ as[39]

$$E_L = \frac{\epsilon_r + 2}{3} E_M \ . \tag{10}$$

The relative permittivity, $\epsilon_r$ of cyclohexane, *n*-tridecane and other non-polar liquids are typically around 2, and thus $E_L \approx 1.3 E_M$. The local field felt by a single molecule is therefore similar to the macroscopic field in an experimental setup. However, using $R_e^{max} = 1/\sqrt{E}$ one obtains $R_e^{max} \approx 7$ Å at $E = 0.005\ au \approx 25\ MV/cm$. Thus, with this model, the escaping electron may be far into the medium before it is released from the attractive potential from the positive ion. Therefore it is not only the local field inside the cavity that is important, but also the field outside. Outside the cavity the medium will screen the cation and thus the escaping electron will feel a smaller field from the cation. Classically in a medium, the reduction of the potential barrier is given by[12]

$$\Delta V = -2\sqrt{\frac{E}{\epsilon_r}} \tag{11}$$

which reduces the IP by a factor of $\sqrt{\epsilon_r}$ in the medium compared to in vacuum (Eq. (4)). Furthermore, by using the polarizable continuum model (PCM) without an electric field, it is found that liquid cyclohexane ($\epsilon_r \approx 2$), reduces the IP by about 1 $eV$ for a large number of molecules.[22]

So, on one hand, without the presence of an electric field, a liquid/solid medium decreases the IP, but on the other hand the electric field reduces the IP less in a medium. The total effect of the medium is not clear and therefore the results of the calculations should only be compared qualitatively with experimental result.

## III. IONIZATION MECHANISMS

For a hydrogen atom in the gas phase, the classical result in Eq. (4) gives

$$IP = IP_0 - 2\frac{e^2}{4\pi\epsilon_0\alpha_0}\sqrt{\frac{4\pi\epsilon_0\alpha_0^2 E}{e}} \tag{12}$$

where $\alpha_0$ is the Bohr radius which is 1 in atomic units. In Eq. (12) the square root is dimensionless and independent of the set of units used. The prefactor is a pure energy term, and it is easy to transform between the different units used. Experimental evidence for a field dependence like the one in Eq. (12) have been reported.[40,41]

The IP is important for all ionization mechanisms, which can be grouped into three main categories, impact ionization, photoionization and field ionization. All are used to explain the various conductivity and streamer propagation mechanisms. Streamers are assumed to have 4 modes of propagation,[42] and different mechanism dominate for the various modes. For example photoionization is believed mainly to be connected to the 4th mode streamers (fast event) but could be of importance also for 2nd and 3rd mode streamers.[43]

### A. Impact ionization

Impact ionization is given by the following reaction

$$e^- + A \rightarrow A^+ + 2e^- \ . \tag{13}$$

For this process to occur, the energy of the incoming electron must be higher than the IP of the molecule. If the IP is high compared to the typical electron energy, the energy of the electrons will be the limiting factor. Thus the probability for such a process to occur can be modelled as being proportional to the number of electrons with energy above the IP,[21]

$$\int_{IP}^{\infty} f_e(\varepsilon)d\varepsilon \tag{14}$$

where $f_e$ is the energy distribution of the electrons. The field dependence of the IP can be estimated by Eq. (4), but to find the field dependence of impact ionization, the field dependence of $f_e$ is also needed, which in general is unknown.

An important type of discharge in gases based on impact ionization is the Townsend discharge,[44,45] which is often used to explain discharges in voids in solid insulation.[12] If

a free electron on average creates more than one new free electron before it releases its energy and is localized, an electron avalanche may be created. Such a mechanism depends on a relatively long mean-free path so that free electrons (accelerated by the electric field) gain sufficient kinetic energy before they collide with a molecule that is ionized by impact ionization. For the discharge to be self-sustained, each electron avalanche must create at least one new avalanche through some form of feedback mechanism. Electron avalanches in condensed phase is controversial due to the higher medium density, and thus lower mean-free path for electrons.[1] Even so, experimental results with negative polarity in cyclohexane under impulse and DC voltage suggests that the onset of streamers in the liquid is caused by an electron avalanche in the liquid phase.[3,46]

### B. Photoionization

In photoionization, a single photon is absorbed by a molecule and an electron is released,

$$h\nu + A \rightarrow A^+ + e^-. \tag{15}$$

This process requires a photon with energy $h\nu$, equal to or higher than the IP of the molecule. If $h\nu$ is higher than the IP of the molecule, the energy conservation may be obtained by either giving the ionized electron more kinetic energy, by allowing the molecule to emit a photon with lower energy, $h\nu'$ or by leaving the cation in an excited state.

Streamers are observed to emit a large amount of visible light,[43] and therefore it is reasonable to assume that the typical photon energies emitted are in the visible light spectrum, which is between 1.8 and 3.1 $eV$. On the other hand, the IP of typical molecules used as electric insulation materials is of the order 10 eV.[22] However, if the molecule interacts with a high electric field in addition to a single high-energetic photon, the IP is predicted to fall according to Eq. (12). Thus, for sufficently strong electric fields, photoionization is plausible, and it has been speculated that photoionization might be responsible for the fast-mode streamer propagation.[43]

For atomic systems, with nonrelativistic energies and without an electric field, the photoionization differential cross-section $\sigma$, per unit solid angle, $\Omega$ is[47]

$$\frac{d\sigma}{d\Omega} \propto \sin\theta_e^2 \tag{16}$$

where $\theta_e$ is the angle between the direction of the photon and the emitted electron. The electron is most probably emitted at an angle around $\theta_e \approx 90°$, which is reasonable since the electric field of an electromagnetic wave is perpendicular to the propagation direction. To find the total ionization cross-section, Eq. (16) is integrated over all angles. However, if a permanent external electric field is applied to the system in addition to an electromagnetic wave, there is only a limited angle which is classically available for ionization (i.e. angles where the kinetic energy of the escaping electron is above the maximum potential in that direction), and it can be assumed that only these angles contribute to ionization. Integrating Eq. (16) over the classically available angles could thus serve as a simplified model for atomic photoionization in the presence of an electric field. The size of the classically available area depends on the energy of the photon, while in what region it lies depends on the direction of the photon compared to the direction of the static electric field. If the photon and the static electric field is parallel, the classically available angles are around $\theta_e = 0°$, while if the photon and the static electric field is perpendicular, the classical available angle is around $\theta_e = 90°$. Thus, one could expect that photoionization is more effective if the external electric field is perpendicular to the photon. This is also reasonable from a classical point of view since in this case the static and the time dependent electric fields are parallel. Streamers are observed as tree structures with various degree of branching, depending on the liquid in which they propagate as well as electrochemical additives in the base liquid.[9,48,49] The angle dependence of photoionization may be important to understand the highly branched structures often observed at high voltages where several of the branches propagate in directions deviating from the direction of the external field. Such branching has been shown to be enhanced by low IP additives in cyclohexane.[49]

### C. Field ionization

The third fundamental mechanism, field ionization, is dependent on tunnelling.[13] It is therefore of interest to study tunnelling with a Coulomb potential in an external electric field. In contrast to impact ionization, which requires the knowledge of the electron energy distribution, $f_e(\varepsilon)$, tunnelling is only dependent on the local electric field and therefore easier to model.

In an electric field, the tunnelling probability, $\tau$, from an electrode has been found to

follow[12,50]

$$\ln \tau \propto \frac{1}{E} \tag{17}$$

both theoretically and experimentally. Eq. (17) assumes that the work function, or potential barrier height is independent of the electric field, but the width of the barrier is reduced when the field increases. This has been found to be a good approximation for removing electrons from metals, field emission, at high fields (20 $MV/cm$).[46] Therefore, if the charge carriers are dominated by electrons donated from a negative electrode, a tunnelling mechanism given by Eq. (17) may describe the conductivity as found for very sharp tips.[46] This mechanism is termed Fowler-Nordheim injection, and is observed for negative electrodes where electrons can tunnel through the barrier and into the dielectric. For positive electrodes a similar phenomena can occur where electrons can tunnel from the liquid to the metal.[13]

However if the barrier height depends on the field, a different field dependence is obtained. Let the potential be given by Eq. (2), $\varepsilon_i$ be the energy of the electron in state $i$, and $\psi_i$ be the corresponding wavefunction. The tunnelling probability $\tau$ is proportional to[28]

$$\tau \propto \frac{\psi_i(R_-)}{\psi_i(R_+)} \tag{18}$$

where $R_\pm$ are the points where the energy of the electron $\varepsilon_i$ is equal to the potential $V(R)$ (Figure 1). For the hydrogen atom $\varepsilon_0 = -1/2$ hartree, and the classical turning points is given when $V(R_\pm) = \varepsilon_i$. When the field is assumed to be small ($E \ll \varepsilon_i$), the classical turning points are given by

$$R_+ = -1/\varepsilon_i \tag{19}$$

and

$$R_- = -\varepsilon_i/E - 1/\varepsilon_i \tag{20}$$

The tunnelling probability as a function of the electric field may be analyzed using the Wentzel-Kramers-Brillouin (WKB) approximation, and the WKB wavefunction is given by[28]

$$\psi_i(R) = \frac{B_\pm}{(\varepsilon_i - V_e(R))^{1/4}} e^{\pm \int \sqrt{2(V_e(R)-\varepsilon_i)} dR} \tag{21}$$

where $B_\pm$ are constants. Since the wavefunction before tunnelling is assumed to be close to the stationary solution, $B_+$ is zero and only $B_-$ is considered. The solution with $B_+$ could be interpreted as important for tunnelling probability into the atom, i.e. the recombination of electrons and positive charged ions. Here we focus on tunnelling out of the Coulomb

barrier, representing a field ionization of a neutral molecule in gas phase, where the electron tunnels out into vacuum.

Exactly at the classical turning points, $R = R_\pm$, the WKB wavefunction has a problem as the prefactor has a singularity at $R = R_\pm$. However, the divergence disappears for $\psi_i(R_-)/\psi_i(R_+)$

$$\frac{\psi_i(R_-)}{\psi_i(R_+)} = \exp\left(-\int_{R_+}^{R_-} \sqrt{2(V_e(R) - \varepsilon_i)}dR\right) \tag{22}$$

As an approximation, the integral is proportional to the length given by $R_- - R_+ = \varepsilon_i/E$, and multiplied by the height given by the maximum of $\sqrt{V_e(R) - \varepsilon_i}$. If this maximum is field independent, the field dependence of the tunnelling probability is given by Eq. (17). However, for the Coulomb potential, $V_e^{max}(r) - \varepsilon_i = -\varepsilon_i - 2\sqrt{E}$, and assuming $\sqrt{E} \ll \varepsilon_i$

$$\int_{R_+}^{R_-} \sqrt{2(V_e(R) - \varepsilon_i)}dR \propto -\frac{\varepsilon_i}{E}\sqrt{-\varepsilon_i - 2\sqrt{E}} = \frac{(-\varepsilon_i)^{3/2}}{E}(1 - \frac{\sqrt{E}}{-\varepsilon_i} + \cdots) \tag{23}$$

$$= \frac{(-\varepsilon_i)^{3/2}}{E} - \sqrt{\frac{-\varepsilon_i}{E}} + \cdots \tag{24}$$

and thus the tunnelling probability, $\tau_i$, given that the electron starts in the electronic state $i$ is

$$\ln \tau_i = -C\left(\frac{(-\varepsilon_i)^{3/2}}{E} - \sqrt{\frac{-\varepsilon_i}{E}}\right) \tag{25}$$

where $C$ is a constant. In very small electric fields the potential is triangular, and thus the first term should be equal to the term obtained from a triangular potential[12,50]

$$\ln \tau_i = -\frac{4\sqrt{2}}{3}\frac{(-\varepsilon_i)^{3/2}}{E} \ . \tag{26}$$

Comparing Eqs (25) and (26) it is seen that $C = 4\sqrt{2}/3$. Another way of obtaining the same result is to assume that the shape of the potential is almost triangular for larger electric field, but the height is given by $\varepsilon_i - 2\sqrt{E}$. The field dependence of the tunnelling probability has also been found elsewhere.[50]

Here it is important to note that $-\varepsilon_0$ can be interpreted as the IP at zero electric field (Koopmann's theorem) while $\varepsilon_0 - \varepsilon_1$ is the first excitation energy. Typically $|\varepsilon_1|$ is much smaller than $|\varepsilon_0|$ such that $\tau_1$ is much larger than $\tau_0$.

### *1. Two-stage process*

In ionization processes by strong low-frequency fields, a tunnelling mechanism may be dominating. However for the hydrogen atom, a pure tunnelling mechanism does not fit

with numerical solutions of the time-dependent Schrödinger equation, and it is indicated that an indirect tunnelling mechanism is important.[51,52] This is in line with the fact that in conductivity models, two-stage processes are often adopted.[12] Thus, first the molecule is excited, then an electron is released by tunnelling. The total tunnelling probability $\tau$ can be modelled as

$$\tau = \sum_i f_i \tau_i \tag{27}$$

where $f_i$ is the probability that the molecule is in excited state $i$, and $\tau_i$ is the probability to tunnel out of state $i$. The probabilities $f_i$ can be modelled by a Boltzmann distribution

$$f_i = \frac{e^{\frac{-\varepsilon_i}{k_b T}}}{\sum e^{\frac{-\varepsilon_i}{k_b T}}} \tag{28}$$

However, these probabilities assume equilibrium, which, depending on the situation, may be questionable. Generally, electrons react faster to changes in for example electric field compared to the heavier protons. Therefore, in the presence of a time-dependent electric field (for example as a step-function), it may not be unreasonable to assume that the number of excited states $f_i$ is far greater than the equilibrium value.

### *2. Hopping*

A series of common conduction models for polymers and dielectrics are termed hopping conduction.[12,17,53] The term hopping refers to a sudden displacement of a charge carrier from one localized site in the dielectric to another nearby site. This can occur either by thermal excitation of the carrier over the barrier or by tunnelling through the barrier between localized sites. In general, a combination is considered the most likely mechanism.[12] First the carrier is excited and then tunnels to a neighbouring site with the same energy level. Thus hopping is in some way a misleading name for this mechanism actually describing thermally assisted tunnelling between two sites, and not hopping over the energy barrier. Hopping is thus best used for the special case where the tunnelling between states can be neglected, and the charge carrier must actually jump over the potential barrier between the two sites/traps.

There are several different flavours of thermally assisted hopping conduction that includes tunnelling through the barrier, two of the most important being variable-range hopping[54]

and the random free-energy barrier model.[55] Hopping is typically viewed as an increase in charge mobility with field, not the charge density as the charge is localized between each jump across the barriers. Thus the average speed/mobility of the carriers is increased with increased field but the average free charge density is not changed. The field dependence of the resulting mobility depends on the distribution of the traps in space and in energy, typically the mobility will increase exponentially with the square root of the field.[24,25]

The hopping model given in Table I is based on hopping from one site to another site over a potential barrier lowered by the electric field. The model is only valid for a single trap depth and uniform distribution of the traps, and it assumes that tunnelling between traps can be neglected. This simple model results in a conductivity that increases exponentially with the field.[24]

However these exponentially increasing mobilities are based on lowering of the barriers between two sites and that it is the crossing of these barriers that limits the mobility. If for example a cyclohexane cation is surrounded by neutral cyclohexane molecules, all neighbouring molecules are potential electron donors. Depending on the distance between the sites and the energy of the electron involved, there might be only a very small barrier or even not a barrier at all. In Figure 2, the potential barrier between two hydrogen atoms is compared to the ground state energy of the hydrogen atom for different separation distances. As seen from the figure, if the distance between two sites is too small, there is no barrier to cross and the mobility must be limited by other factors. Thus in these cases, the hole mobility does not necessarily increase exponentially with the electric field.

## IV. RESULTS

Excitation energies and IPs were calculated for the following molecules: *n*-tridecane, cyclohexane, 2-propanol, p-diaminobenzene, benzene, N,N-dimethylaniline and tetracyanoethene. Benzene was added as a reference molecule, and *n*-tridecane was included because experiments on conduction currents in neat *n*-tridecane have been compared to conductivity models.[8] The rest of the molecules, were chosen based on a previous experimental study on pre-breakdown phenomena in cyclohexane with additives.[5,6,21] Cyclohexane is used as a model liquid for mineral oil, and additives with known electron scavenger properties or low IP were chosen as additives. It was found that the IP of the additives is an impor-

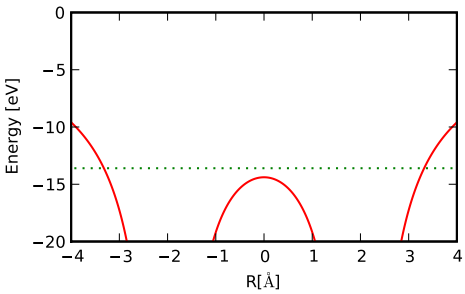


(a) Separation distance: 4.0 Å

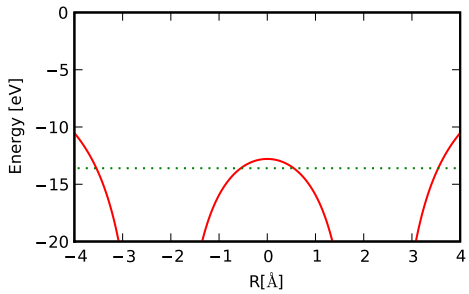


(b) Separation distance: 4.5 Å

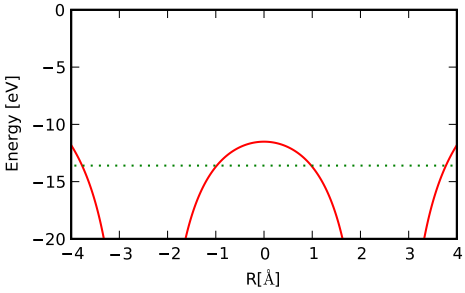


(c) Separation distance: 5.0 Å

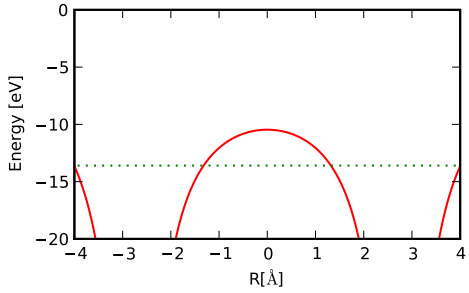


(d) Separation distance: 5.5 Å

Figure 2. Potential (—) between two protons at different separation distance compared to the ground state of the hydrogen atom ($\cdots$) for different separation distances.

tant descriptor for the effect on pre-breakdown phenomena[21]. Based on the Poole-Frenkel mechanism and DFT calculations, it is possible, as is shown in this paper, to compare the experimental results directly to the results obtained from DFT calculations.

The results from the DFT calculations are summarized in Figures 3 and 4. The calculations show that the direction of the electric field is only of minor importance for these properties for most of the molecules (not shown in the figures). The direction of the electric field is therefore only specified in the cases where it was found to be of importance. The ground state energy of the molecules was not significantly altered by the electric field on this energy scale. This is illustrated in Figures 3(c) , 4(c) and 4(d) which shows that the ground state energy is only a relatively weak function of the electric field even for polar molecules like 2-propanol and N,N-dimethylaniline.

The first excitation energy changes very little with the electric field for weak fields

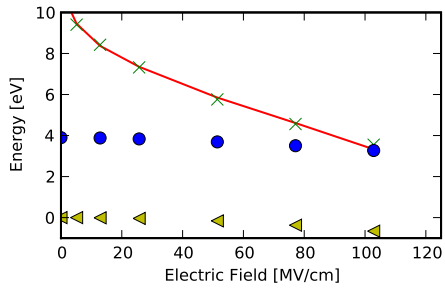


(a) Tetracyanoethene

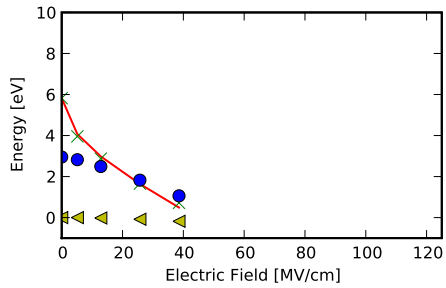


(b) p-diaminobenzene

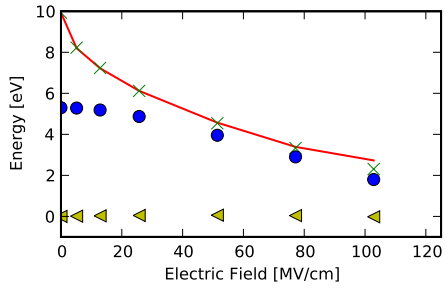


(c) 2-propanol

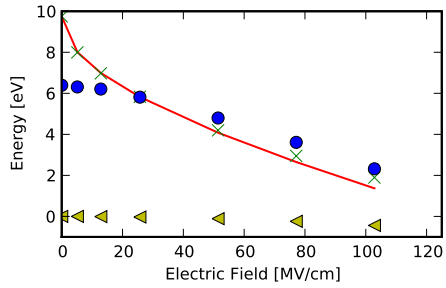


(d) Cyclohexane

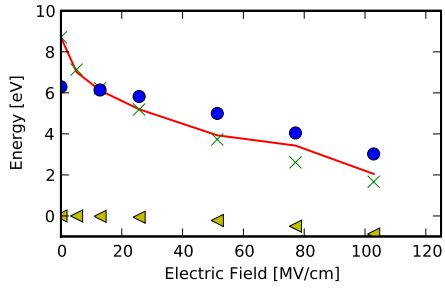


(e) $n$-Tridecane, Electric field perpendicular to chain

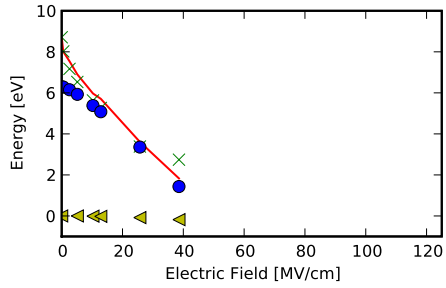


(f) $n$-Tridecane, Electric field parallell to the chain

Figure 3. Ground state energies ($\triangleleft$), lowest singlet-singlet excitation energies ($\bullet$), IP (—) and model IP given by Eq. (29) ($\times$), for different molecules.

($<$20 $MV/cm$) for all molecules included in the study except for $n$-tridecane. The IP on the other hand decreases rapidly even for a relatively small increase in the electric field for all molecules, and above a certain field it approaches the first excitation energy. When the field is increased further the IP and the first excitation energy falls at the same rate. The excita-

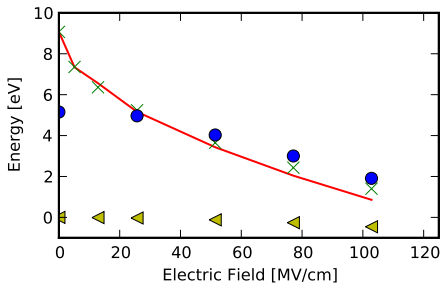


(a) Benzene, Electric field in-plane

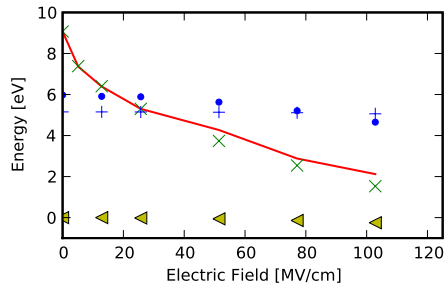


(b) Benzene, Electric field out-of-plane

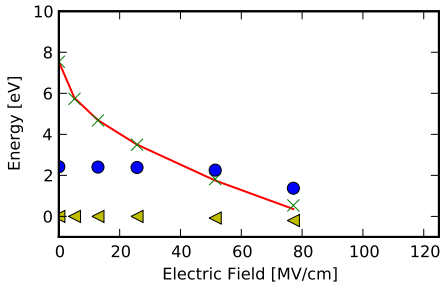


(c) N,N-dimethylaniline, Electric field in-plane

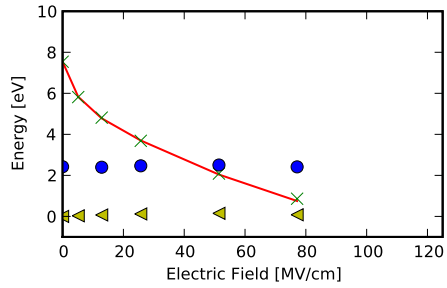


(d) N,N-dimethylaniline, Electric field out of plane

Figure 4. Ground state energies (◁), lowest singlet-singlet excitation energies (•), IP (—) and model IP given by Eq. (29) (×) , for different molecules. In figure (b) the lowest excitation energies for two different symmetry groups (+ and •) are presented.

tion energies for N,N-dimethylaniline and tetracyanoethene are low, but stays constant up to higher electric fields than for the other molecules. Thus larger electric fields are needed to decrease the IP to the first excitation energy (see Figures 3(a) and 4(c)).

It seems to be a general trend that above a certain field strength the first excitation energy as calculated by TD-DFT approaches the IP. Thus above this field the molecule can either be in its ground state or in a state with energy at or above the IP. The basis set used can in principle only describe bound states (states where the wavefunction far from the molecule decreases exponentially with distances). A description of free electrons, which are dependent on $\cos(kx)$ and $\sin(kx)$ functions, are not included in the basis set. Therefore, in theory the basis set limits TD-DFT to bound states only. In practice, however, the basis set may be able to approximate the behavior of a non-bound state locally around the molecule,

but what happens at large separations is unclear. Furthermore, an ionization can be viewed as an excitation to a delocalized state, and therefore the lowest excitation energy should be at the IP or lower. It has been exploited to calculate the IP by adding a very diffuse basis function in coupled-cluster response theory,[56] which is a reasonable approach without an external electric field. For a more detailed discussion on the behavior of TD-DFT at the ionization limit, see Ref 57.

For the planar molecules in this study, the excitation energies are nearly independent of the electric field when the field points out of the plane, as examplified in Figures 4(b) and 4(d) and above a certain electric field, the IP becomes lower than the first excitation energy. In Figure 5, the basis set dependence of the lowest excitation energies of benzene is shown. For the QZ3P-2D basis set, the excitation energies are always smaller than the IP, regardless of field direction. Thus, the reason for the constant excitation energies for planar molecules is a too small basis set to describe the out-of-plane orbitals.

However since the electric field gives an energy term linear in $R_e$, there exist a continuum of delocalized states with energy below the IP (see Figure 1) in addition to the continuum above the IP. Therefore, it is difficult to interpret the excitation energies for high fields when using the large basis sets (see Figure 5). Although in theory the same problem exist for low fields, it is of less importance, since the distance to $R_+$ (see Figure 1) is much higher and the *negative* continuum at large $R$ may be ignored. All basis sets give approximately the same results for low fields (see Figure 5), and qualitatively the same basis set dependence is seen for cyclohexane and $n$-tridecane. Therefore, we restrict our discussion on the excitation energies to fields below 15 $MV/cm$. The IP on the other hand is trivial to interpret, and applying larger basis sets had small effects on the results.

To validate the classical treatment of the IP in Eq. (12), the calculated IP is compared to,

$$IP = IP_0 - \beta_{PF}\sqrt{\gamma E} \tag{29}$$

where $\beta_{PF}$ is treated as a parameter and $\gamma = 4\pi\epsilon_0\alpha_o^2/e$. Linear regression was used to fit the calculated IP to an IP of the form given in Eq. (29) for fields below 30 $MV/cm$. Above this field strength, larger deviations from the classical results are expected and when comparing to pre-inception currents,[8] it is the behaviour below 30 $MV/cm$ which is interesting. For all molecules, an IP of the form in Eq. (29) gives a good fit with an RMSD below 0.1 $eV$, and the value of $\beta_{PF}$ is close to the classical result, see Table II. Neither the type of molecule nor

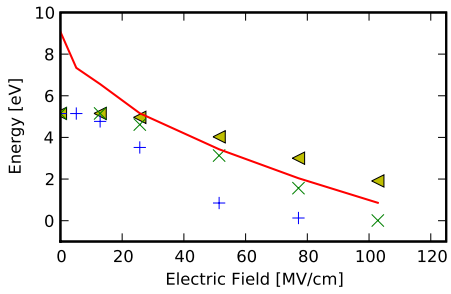


(a) Benzene, Electric field in-plane

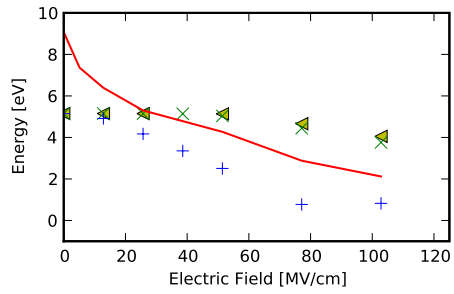


(b) Benzene, Electric field out-of-plane

Figure 5. Basis set dependence of the excitation energy: IP using aug-TZP basis set(−), the lowest excitation energy using aug-TZP (◁), QZ3P-1D (×) and QZ3P-2D (+) basis set.[32]

the direction of the field is important. This supports an assumption that the difference in IP between two different molecules does not depend on the electric field.[21] Above 30 $MV/cm$, the fitted curve typically deviates only slightly from the calculated IP. Since these results are not included in the linear regression, it indicates that the classical result gives the main contribution even for relatively high fields. Thus, even for large fields the monopole is the dominating interaction term. For both $n$-tridecane and cyclohexane, $\epsilon_r \approx 2$, and so to compare these results with experiments, the fitted $\beta_{PF}$ is divided by $\sqrt{\epsilon_r}$ in Table II, following Eq. (11).

For $n$-tridecane, unlike the other molecules studied here, the direction of the electric field is important. Two cases are presented here, one where the field is perpendicular to the chain and one where the field is parallel to the chain. If the electric field is perpendicular to the chain, $n$-tridecane behaves like the other molecules, see Figure 3 (e). The results obtained for an electric field parallel to the chain is more interesting, see Figure 3 (f). Here the excitation energy seems to approach zero at much lower fields than the other molecules. But also in this case, the IP approaches the first excitation energy for fields above 20 $MV/cm$.

$n$-tridecane also differs from the other molecules in terms of the $\beta_{PF}$ coefficients in Table II. An electric field perpendicular to the $n$-tridecane molecule decreases the IP less than the other molecules, but an electric field parallel to $n$-tridecane decreases the IP more. In the latter case, it is also noted that an IP of the form Eq. (29) gives larger deviations, and thus the classical results is not a perfect approximation in this case. The main reason for these

Table II. Field dependence of IP

| Molecule | $\beta_{PF}(eV)$[a] | RMSD[b]$(eV)$ | $\beta_{\epsilon_r=2}$ $(eV)$[c] |
|---|---|---|---|
| Classically | 54.4 | - | 38.5 |
| Cyclohexane[d] | 53.8 | 0.05 | 38.0 |
| $n$-Tridecane[e] | 68.9 | 0.31 | 48.7 |
| $n$-Tridecane[f] | 49.8 | 0.09 | 35.2 |
| Tetracyanoethene[d] | 53.6 | 0.03 | 37.9 |
| 2-propanol[d] | 54.4 | 0.01 | 38,4 |
| N,N-dimethylaniline[d] | 56.1 | 0.03 | 37.7 |
| p-diaminobenzene[d] | 54.5 | 0.06 | 38.5 |
| Benzene[d] | 54.0 | 0.07 | 38.1 |

[a] Eq. (29)

[b] Root mean square deviation (RMSD) between calculated IP and a model IP given in Eq. (29), for fields below 30 $MV/cm$

[c] $\beta_{\epsilon_r=2} = \beta_{PF}/\sqrt{2}$

[d] Averaged over the three different directions of the electric field

[e] Electric field parallell to the chain

[f] Electric field perpendicular to the chain

deviations is the results obtained for the two largest fields, where the $IP$ approaches the excitation energies (Figure 3(f)). If omitting the two highest fields in the linear regression, $\beta_{PF}$ =59.6 $eV$ and an RMSD below 0.1 $eV$ is obtained, which indicates that the classical results fits better for lower fields.

## V. DISCUSSION

Based on symmetry arguments, a natural initial guess for the charge distribution in for example the cyclohexane cation, is to place the positive charge evenly among all carbon atoms. However, as Figure 6 shows, the reduction of the IP with the electric field would be too large for such a charge distribution compared to the IP obtained from a point charge and DFT. The IP would fall to zero at about 30 MV/cm, so that cyclohexane would ionize completely at such fields. Furthermore, Figure 7(a) shows that such a model fails to repro-

duce the interaction energy between a point charge and a cyclohexane cation. On the other hand, a model where only the closest carbon atom is charged, reproduces the interaction energy almost perfectly. A similar plot for $n$-tridecane (Figure 7(b)) shows slightly larger deviations for the one-charge model. However, even for $n$-tridecane, a one-charge model fits rather well. The IP in general fits a one-charge model, even for very high electric fields (see Figures 3 and 4 and Table II).

In quantum chemistry many models exist to obtain atomic charges, and many of them rely on a Mulliken-type of division of the charge distribution.[58] The calculated atomic charges in an electric field could not be used to verify Figures 6 and 7. For example, for cyclohexane these models give an unphysically large charge transfer between the carbon and hydrogen atoms. It has been noted repeatedly that Mulliken charges are highly dependent on the basis set used, see for example Ref 59.

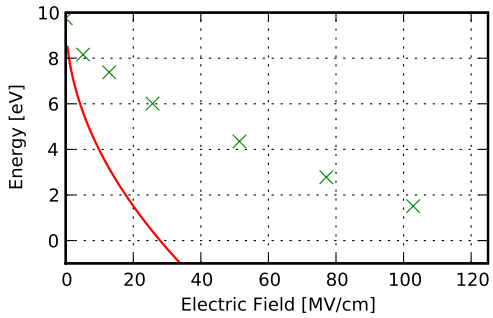


Figure 6. The reduction of IP in cyclohexane as a function of the electric field, both with respect to DFT data (×) and with respect to a model where each carbon gets 1/6 charge (—)

Measurements of high-field conduction currents in cyclohexane have been compared to FEM simulations.[8] The following conductivity model, based on Poole-Frenkel conductivity, was found to fit the experimental data (see Eq. (5)),

$$\sigma(E) = \sigma_0 \cdot e^{\frac{W}{k_B T}} \cdot e^{\frac{\beta_{PF}\sqrt{\gamma E}}{2k_B T}} \tag{30}$$

where $\sigma_0 = 1.3 \cdot 10^{-4}\ S/m$, $W = 0.47\ eV$ is the thermal activation energy,[60] $\beta_{PF} = 40.7\ eV$, and $\gamma = 1.9 \cdot 10^{-12}\ m/V$. The parameter $\beta_{PF}$ and the constant $\gamma$ are introduced in Eq. (29). The proposed high-field conductivity for cyclohexane based on experiments[8] supports an IP of the form given in Eq. (29). There is a good agreement between $\beta_{PF}$ found experimentally

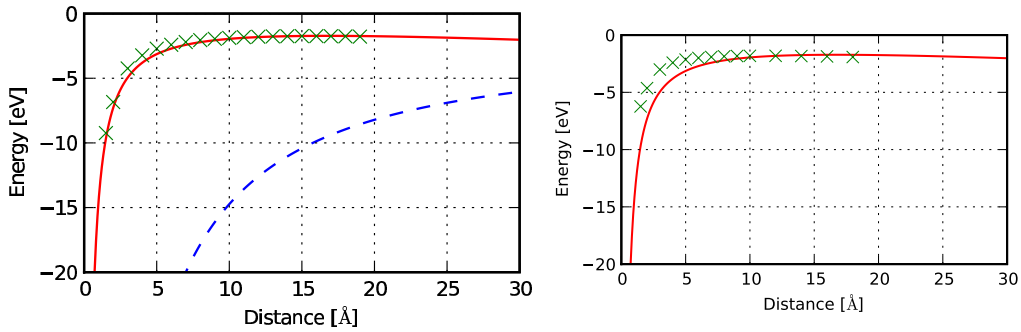


(a) Cyclohexane (b) $n$-Tridecane

Figure 7. The potential energy between a point charge and a cyclohexane/$n$-tridecane cation in an electric field of 0.001 au=5.14 $MV/cm$, as a function of the distance between the point charge and the closest carbon atom, with respect to DFT data (×), a one-charge potential (—) and for cylcohexane a model potential where each carbon atom get 1/6 charge (- -). In (b) the field is parallel to the chain.

of $\beta_{PF} = 40.7\ eV$ and in calculations when the medium is taken into account by dividing the calculated value by $\sqrt{\epsilon_r}$. This suggest that the effect of a medium can be adequately modelled as a dielectric continuum, at least for relative small electric fields ($< 10\ MV/cm$). Thus, the reduction of the IP with increasing fields in liquid cyclohexane with $\epsilon_r \approx 2$, will be lower than in the gas phase.

FEM simulation using the following equations for conductivity,

$$\sigma(E) = \sigma_0 \cdot e^{\frac{\beta_{PF}\sqrt{\gamma E}}{2k_B T}} \tag{31}$$

and

$$\sigma(E) = \sigma_0 \cdot e^{\frac{\beta_{1/3}\sqrt[3]{\gamma E}}{2k_B T}} \tag{32}$$

where $\sigma_0 = 1.0 \cdot 10^{-12}\ S/m$, $\beta_{PF} = 54.3\ eV$, $\beta_{1/3} = 12.4\ eV$, $\gamma = 1.9 \cdot 10^{-12}\ m/V$, have been shown to give pre-inception currents that fits experimental results in neat n-tridecane with needle plane geometry (positive needle).[8] Eq. (31) is similar to a Poole-Frenkel conductivity, but $\beta_{PF}$ is somewhat high. It is interesting to note that the value for $\beta_{PF}$ obtained from DFT calculations is also high compared to the classical result (see Table II). Thus the DFT calculations points in the same direction as the experimental results.

To our knowledge, Eq. (32) is not based on any known conductivity theory, but similar

field dependence for conductivity have previously been reported for polyethylene.[61] Direct comparison of experimental charge recordings and the results from FEM simulations have shown that Eq. (32) fits the measured results better than Eq. (31).[8] The direction of the electric field is important in *n*-tridecane since the IP is reduced more when the electric field is parallel to the chain than when the field is perpendicular to the chain. It is therefore assumed that the parallel component is more important when interpreting experimental data. The DFT results show that the main difference between *n*-tridecane and cyclohexane is in the way the excitation energy depends on the electric field for fields below 20 *MV/cm*. In cyclohexane, the excitation energy is almost constant up to such field strengths (see Figure 3(d)), while it is reduced even at lower fields in *n*-tridecane (see Figure 3(f)). This is probably, as discussed below, why a conductivity given by Eq. (32) fits better than a conductivity given by Eq. (31) for *n*-tridecane.

In order to explain the difference between the experimental conductivity for *n*-tridecane and cyclohexane the difference, $\Delta$, between the first excitation energy, $\varepsilon_1$, and the IP is examined,

$$\Delta(E) = IP(E) - \varepsilon_1(E) \tag{33}$$

Linear regression was used to compare two ansatzes for $\Delta$,

$$\Delta(E) = \Delta(0) - \beta_{PF}\sqrt{\gamma E} \tag{34}$$

and

$$\Delta(E) = \Delta(0) - \beta_{1/3}\sqrt[3]{\gamma E} \tag{35}$$

where $\Delta(0)$ is the energy difference between the first excitation energy and the IP at zero field, $\gamma$ is given by Eq. (29), and $\beta_{PF}$ and $\beta_{1/3}$ are pure energy terms. Fitting the two equations above to the DFT calculations is a way to find the energy terms that can be compared directly to the experimentally obtained conductivity models, $\beta_{1/3}$ in Eq. (32) and $\beta_{PF}$ in Eqs. (31) and (30). For cyclohexane, $\varepsilon_1$ does not depend on the electric field for fields below 30 *MV/cm*. Thus results obtained from linear regression compared to the IP, and compared to $\Delta$ would give the same field dependence, and thus the same value for $\beta_{PF}$ (Table II).

The result for *n*-tridecane, see Figure 8, is interesting as it gives a different dependence on electrical field than what was found for cyclohexane. For *n*-tridecane, a $\Delta$ as in Eq. (35)

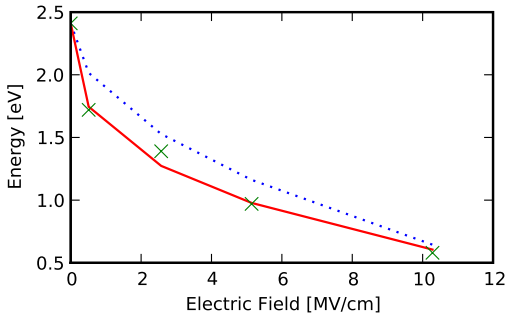


Figure 8. Difference between the IP and the excitation energy for $n$-tridecane, with the electric field parallel to the chain, obtained by DFT ($\times$), model in Eq. (34) (—), and model in Eq. (35) ($\cdots$). With linear regression, the following coefficients are obtained; $\beta_{PF} = 39.5\ eV$ and $\beta_{1/3} = 14.3\ eV$.

fits almost perfectly with the DFT data, while a $\Delta$ as in Eq. (34) (which gives a good fit for cyclohexane) yields a poor fit. The coefficients obtained from linear regression, $\beta_{1/3}$ (see Figure 8) is close to the experimental value,[8] $\beta_{1/3}^{\mathrm{EXP}} = 12.4$ eV, without a modification given by the relative permittivity of the medium. Since the excitation energy is field-dependent even for small fields, it is reasonable to assume that it is also dependent on $\epsilon_r$, and that an increased $\epsilon_r$ will decrease the excitation energy. Therefore the difference between the IP and the excitation energy may be less dependent on the medium compared to the individual properties. For cyclohexane, the excitation energy is not dependent on the electric field for small fields ($<30\ MV/cm$), and thus in this case one can assume that the excitation energy is also less dependent on the dielectric constant. If this is the case only the IP will be dependent on the medium.

A conductivity given by

$$\sigma = \sigma_0 e^{\frac{\Delta}{2K_b T}} \tag{36}$$

similar to the Poole-Frenkel model,[12] explains both a conductivity given by Eq. (31) and (32). This model assumes equilibrium between the first excitation energy and the IP. However, to obtain a conductivity model given by Eq. (36) there cannot be an equilibrium between the ground state and the first excitation energy. If that had been the case, the conductivity would only be dependent on the IP, not $\Delta$. However in the Born-Oppenheimer approximation electron responses are immediate, and thus when electric field is suddenly applied, it is

Table III. The lowest singlet ($S_1$ and $S_2$) and triplet ($T_1$ and $T_2$) excitation energies for $n$-tridecane and N,N-dimethylaniline (in eV)

| Excitation | $n$-tridecane | N,N-dimethylaniline |
|---|---|---|
| $S_1$ | 6.29 | 2.42 |
| $S_2$ | 6.36 | 3.38 |
| $T_1$ | 6.28 | 1.34 |
| $T_2$ | 6.35 | 2.61 |

not unreasonable to assume that the number of exited electrons are far greater than the equilibrium value.

One possible reason for the non-equilibrium between the ground state and the first electronic excitation energy might be impact excitation, where a free electron collides with a molecule and excites it. Experimental evidence indicating that impact excitation is important have been found for negative streamers in $n$-tridecane with N,N-dimethylaniline (DMA),[62] where 0.1 M DMA in $n$-tridecane reduces the injected charge and increases the emission of light for negative first mode streamers. For such streamers, the streamer growth is believed to occur through evaporation of the streamer-liquid interface by inelastic collisions of free electrons created in an ionization region at the needle electrode (glow discharges).[63] These electrons will be slowed down by inelastic collisions with molecules in the streamer and at the streamer-liquid interface. Energy transferred from the electrons by these collisions can either be released as heat or by photon emission. Emission of energy in the form of photons that are transmitted through the liquid or absorbed at safe distances, do not contribute to the phase transition and will thus reduce the streamer growth.

It is important to note that a collision with a free electron may excite the molecule to states which are unlikely through excitation by light. Thus, both the singlet-singlet excitation energies and the singlet-triplet excitation energies may be of importance. In both cases, the free electron will lose a large portion of its energy, but if a molecule is excited to a singlet state, it may relax by emitting a single photon in addition to heat. A molecule excited to a triplet state on the other hand, relaxes in a more complicated way, and the probability for emitting photons is smaller. Thus a larger portion of the energy is released locally as heat.

The lowest singlet state for DMA is as low as 2.42 eV (Table III), and a relaxation from this state would emit photons in the visible range where an optical liquid like $n$-tridecane would not absorb it. Clearly higher energy excitations will also contribute, but energies of that order is probably only available for electrons which lie in the high energy tail of a Maxwell distribution in the region with highest field close to the needle electrode (ionization region). Thermal excitation are unlikely as it requires very high temperatures (at 5000 $K$ 5% of the DMA molecules would be excited to the lowest triplet state, and 0.4% would be in the lowest singlet state using a Boltzmann distribution), thus impact excitation is probably dominant.

Photoionization has been proposed as a possible feedback mechanism during streamer propagation occurring at voltages above the breakdown voltages in liquids.[43] These are the 4th mode streamers propagating with speeds from some tens to above one hundred kilometres per second and are clearly highly field-dependent events. The order of magnitude of the threshold fields may be estimated from threshold voltages reported in the literature.[49] In neat cyclohexane, the 4th mode streamer appears suddenly above 120 kV in a 5 cm point-to-plane gap.[49] By assuming an ideal step voltage and a hyperbolically shaped streamer tip radius of 6 $\mu m$,[49] the corresponding Laplacian field magnitude at the propagating streamer tip is about 40 $MV/cm$. This field magnitude, indicative as it is, lies well within the field range where our calculations show a drastic reduction of the IP, and very close to the typical magnitudes where there are no excitation energies between the IP and the ground state. Thus, through the reduction of the IP, the electric fields in a micrometer region in front of the streamer could significantly aid a photoionization mechanism. Consequently, the study of the field-dependent IP of molecules typically present in insulating liquids can be important to understand the occurrence of fast-mode streamers.

## VI. CONCLUSION

Ionization processes, by impact, photon or tunnelling are not trivial, and it is not necessarily easy to predict probabilities for ionization even though the IP is known. However, for all three types of processes, the IP is the single most important parameter.

The model with the calculation of the interaction energy between a cation and a negative point charge gives a reduction of the IP as a function of the electric field which agrees

qualitatively with experimental results, both with respect to conductivity models for pre-inception currents and for fast-mode streamers. Furthermore, the difference in pre-inception currents for cyclohexane and $n$-tridecane suggest that the field dependence of the first excitation energy is important. Specifically, a conduction which is dependent on the difference between the first excitation energy and the IP, explains both a conduction proportional to $e^{-\beta_{PF}\sqrt{E}/kT}$ and a conduction proportional to $e^{-\beta_{1/3}\sqrt[3]{E}/kT}$, where the first is obtained if the excitation energy is independent of $E$ and the latter is obtained if the excitation energy depends on the electric field.

Furthermore, free electrons will lose energy by exciting molecules electronically, and when an exited molecule relaxes, it may emit light. Thus additives with low excitation energies as N,N-dimethylaniline, can retard 1st mode negative streamer growth by emission of energy in the form of light.

It is a general trend that the difference between the IP calculated by Eq. (9), and the first excitation energy, calculated by TD-DFT, become small above a specific electric field. Thus, above this electric field, the molecules may either be in its ground state or have energy at or above the IP. Furthermore for such high electric fields ($\sim 40\ MV/cm$), a reduction of the IP can significantly aid photoionization, which is believed to be the dominant mechanism for fast streamers.

Thus it is concluded that the IP must be viewed as a field-dependent property, and that the field dependence of the IP is important for all ionization processes in high electric fields and for high-field conduction models.

**ACKNOWLEGEMENTS**

Support from the Norwegian Research Council through a Strategic Industry Program (164603/I30) and grants of computer time are acknowledged. We would also like to thank Steven Boggs and Ramamurthy Ramprasad for helpful feedback, and Anna I. Krylov for fruitful discussions regarding Ref. 57.

---

[1] M. Haidara and A. Denat. IEEE Trans. Elect. Insul., **26**, 592–597, (1991).

[2] A. Denat, N. Bonifaci, and M. Nur. IEEE Trans. Dielect. Elect. Insul., **5**, 382–387, (1998).

[3] L. Dumitrescu, O. Lesaint, N. Bonifaci, A. Denat, and P. Notingher. J. Electrostat., **53**, 135–146, (2001).

[4] P. Gournay and O. Lesaint. J. Phys. D: Appl. Phys., **26**, 1966–74, (1993).

[5] S. Ingebrigtsen, L. E. Lundgaard, and P.-O. Åstrand. J. Phys. D: Appl. Phys., **40**, 5161–5169, (2007).

[6] S. Ingebrigtsen, L. E. Lundgaard, and P.-O. Åstrand. J. Phys. D: Appl. Phys., **40**, 5624–5634, (2007).

[7] Ø. L. Hestad, L. E. Lundgaard, and D. Linhjell. IEEE Trans. Dielect. Elect. Insul., **17**, 767-777, (2010).

[8] Ø. L. Hestad, L. E. Lundgaard, and P.-O. Åstrand. Submitted, (2010).

[9] A. Denat. IEEE Trans. Dielect. Elect. Insul., **13**, 518–525, (2006).

[10] L. A. Dissado. IEEE Trans. Dielect. Elect. Insul., **9**, 483–497, (2002).

[11] S. Boggs. IEEE Trans. Dielect. Elect. Insul., **12**, 929–938, (2005).

[12] L. A. Dissado and J. C. Fothergill. *Electrical Degradation and Breakdown in Polymers*. Material and Devices Series 9. The Institution of Engineering and Technology, London, United Kingdom, (1992).

[13] W. F. Schmidt. *Liquid State Electronics of Insulating Liquids*. CRC Press, (1997).

[14] A. K. Jonscher. Thin Solid Films, **1**, 213–234, (1967).

[15] V. Adamec and J. H. Calderwood. J. Phys. D: Appl. Phys., **8**, 551–560, (1975).

[16] G. Teyssedre and C. Laurent. IEEE Trans. Dielect. Elect. Insul., **12**, 857–875, (2005).

[17] H.J. Wintle. IEEE Trans. Dielect. Elect. Insul., **6**, 1–10, (1999).

[18] C. Zhan, J. A. Nichols, and D. A. Dixon. J. Phys. Chem. A., **107**, 4184-4194, (2003).

[19] V. Lemierre, A. Chrostowska, A. Dargelos, and H. Chermette. J. Phys. Chem. A., **109**, 8348-8355, (2005).

[20] L. A. Curtiss, P. C. Redfern, K. Raghavachari, and J. A. Pople. J. Chem. Phys., **109**, 42-55, (1998).

[21] S. Ingebrigtsen, H. S. Smalø, P.-O. Åstrand, and L. E. Lundgaard. IEEE Trans. Dielect. Electr. Insul., **16**, 1511, (2009).

[22] H. S. Smalø, S. Ingebrigtsen, and P.-O. Åstrand. IEEE Trans. Dielect. Electr. Insul., **17**, 733-741, (2010).

[23] Atomic units (au) are defined by $|e| = 1$, $\hbar = 1$, $m_e = 1$, $1/4\pi\epsilon_0 = 1$. Energy in au is 1 hartree which is given by $E_h = m_e e^4/(4\pi\epsilon_o\hbar)^2 \approx 4.36 \times 10^{-18} J$.

[24] H. J. Wintle. IEEE Trans. Dielect. Elect. Insul., **10**, 826–841, (2003).

[25] D. Braun. J. Polym. Sci. B, **41**, 2622–2629, (2003).

[26] Yu. N. Garstein and E. M. Conwell. Chem. Phys. Lett., **245**, 351–358, (1995).

[27] D. M. Pai. J. Appl. Phys., **46**, 5122–5126, (1975).

[28] A. Messiah. *Quantum Mechanics, two volemes bound as one*. Dover Publications, Inc., (1999).

[29] A. D. Becke. Phys. Rev. A, **38**, 3098, (1988).

[30] C. Lee, W. Yang, and R. G. Parr. Phys. Rev. B, **37**, 785, (1988).

[31] E. van Lenthe and E. J. Baerends. J. Comput. Chem., **24**, 1142-1156, (2003).

[32] D. P. Chong. Mol. Phys., **103**, 749-761, (2005).

[33] G. te Velde, F. M. Bickelhaupt, E. J. Baerends, C. Fonseca Guerra, S. J. A. van Gisbergen, J. G. Snijders, and T. Ziegler. J. Comput. Chem., **22**, 931–967, (2001).

[34] C. Fonseca Guerra, J.G. Snijders, G. te Velde, and E.J. Baerends. Theor. Chem. Acc., **99**, 391-401, (1998).

[35] G. Zhang and C. B. Musgrave. J. Phys. Chem. A, **111**, 1554-1561, (2007).

[36] R. Bauernschmitt and R. Ahlrichs. Chem. Phys. Lett., **256**, 454-464, (1996).

[37] C. Adamo, G. E. Scuseria, and V. Barone. J. Chem. Phys., (1999).

[38] M. J. G. Peach, P. Benfield, T. Helgaker, and D. J. Tozer. J. Chem. Phys., **128**, (2008).

[39] J. D. Jackson. *Classical electrodynamics*. John Wiley & Sons, Inc., (1999).

[40] N. Erdmann, M. Nunnemann, K. Eberhardt, G. Herrmann, G. Huber, S. Köhler, J. V. Kratz, G. Passler, J. R. Peterson, N. Trautmann, and A. Waldek. J. Alloys Compd., **271-273**, 837–840, (1998).

[41] S. Douin, P. Parneix, and P. Brechignac. Z. Phys. D, **21**, 343–348, (1991).

[42] O. Lesaint and G. Massala. IEEE Trans. Dielect. Elect. Insul., **5**, 360–370, (1998).

[43] L. Lundgaard, D. Linhjell, G. Berg, and S. Sigmond. IEEE Trans. Dielect. Elect. Insul., **5**, 388–395, (1998).

[44] J. A. Rees. *Electrical breakdown in gases*. The Macmillan Press LTD, (1973).

[45] J. S. Townsend. *The Theory of Ionization of Gases by Collision*. Constable & Co. Ltd, (1910).

[46] A. Denat, J. P. Gosse, and B. Gosse. IEEE Trans. Elect. Insul., **23**, 545–554, (1988).

[47] D. W. Anderson. *Absorption of Ionizing Radiation*. University Park Press, (1984).

[48] A. Beroual, M. Zahn, A. Badent, K. Kist, A. J. Schwabe, H. Yamashita, K. Yamazawa, M. Danikas, W. D. Chadband, and Y. Torshin. IEEE Electric. Insul. Mag., **14**, 6–17, (1998).

[49] O. Lesaint and M. Jung. J. Phys. D: Appl. Phys., **33**, 1360, (2000).

[50] R. Gomer. *Field emission and field ionization.* American Institute of Physics, (1993).

[51] A. de Bohan, B. Priaux, L. Ponce, R. Taieb, V. Véiard, and A. Maquet. Phys. Rev. Lett., **11**, 113002, (2002).

[52] H. M. Tetchou Nganso, S. Giraud, B. Piraux, Yu. V. Popov, and M. G. Kwato Njock. J. Electron Spectrosc. Rel. Phen., **161**, 178-181, (2007).

[53] J. A. Anta, G. Marcelli, M. Meunier, and N. Quirke. J. Appl. Phys., **92**, 1002–1008, (2002).

[54] N. F. Mott. Phil. Mag., **19**, 835–852, (1969).

[55] J. C. Dyre. J. Appl. Phys., **64**, 2456, (1988).

[56] J. F. Stanton and J. Gauss. J. Chem. Phys., **111**, 8785-8788, (1999).

[57] P. A. Pieniazek, S. A. Arnstein, S. E. Bradforth, A. I. Krylov, and C. D. Sherill. J. Chem. Phys., **127**, 164110, (2007).

[58] R. S. Mulliken. J. Chem. Phys., **23**, 1833-1840, (1955).

[59] P.-O. Åstrand, K. Ruud, K. V. Mikkelsen, and T. Helgaker. J. Phys. Chem. A, **102**, 7686-7691, (1998).

[60] H. Polak and B. Jachym. J. Phys. C: Solid State Phys., **10**, 3811–3818, (1977).

[61] G. Jiang, J. Kuang, and S. Boggs. Evaluation of high field conduction models of polymeric dielectrics. In *Ann. Rep. Conf. Elec. Insul. Diel. Phen. (CEIDP)*, pages 187–190, (2000).

[62] Ø. L. Hestad, S. Ingebrigtsen, H. S. Smalø, P.-O. Åstrand, and L. E. Lundgaard. In preparation, (2010).

[63] N. J. Felici. IEEE Trans. Elect. Insul., **23**, 497–503, (1988).